CHALMERS
UNIVERSITY OF TECHNOLOGY

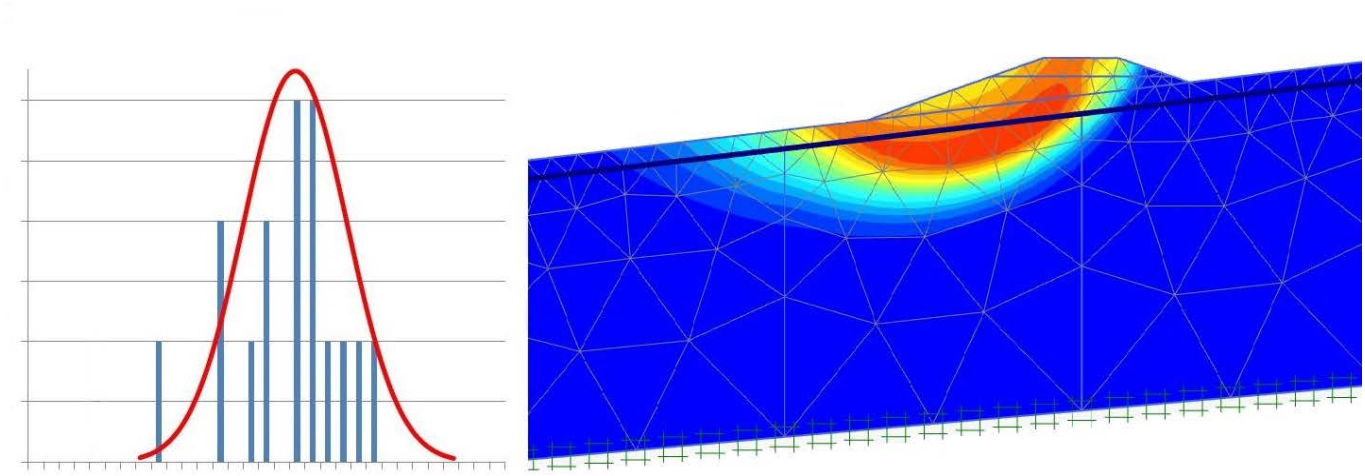

Application of Probabilistic Methods in Slope Stability Calculations

Master's thesis in the Master's Programme Infrastructure and Environmental Engineering

EMIL Cederström

Department of Civil and Environmental Engineering
Division of GeoEngineering
Geotechnical Research Group
CHALMERS UNIVERSITY OF TECHNOLOGY
Gothenburg, Sweden 2014:91

MASTER'S THESIS 2014:91

Application of Probabilistic Methods in Slope Stability Calculations

Master of Science Thesis in the Master's Programme Infrastructure and Environmental Engineering

EMIL CEDERSTRÖM

Department of Civil and Environmental Engineering
Division of GeoEngineering
Geotechnical Research Group
CHALMERS UNIVERSITY OF TECHNOLOGY
Göteborg, Sweden 2014

Application of Probabilistic Methods in Slope Stability Calculations
Master of Science Thesis in the Master's Programme Infrastructure and Environmental Engineering
EMIL CEDERSTRÖM

Examensarbete / Institutionen för bygg- och miljöteknik,
Chalmers tekniska högskola 2014:91

Department of Civil and Environmental Engineering
Division of GeoEngineering
Geotechnical Research Group
Chalmers University of Technology
SE-412 96 Göteborg
Sweden
Telephone: + 46 (0)31-772 1000

Cover:
Normal distribution function with histogram and a slip surface from a Stability Calculation in Plaxis.

Department of Civil and Environmental Engineering
Göteborg, Sweden 2014

Master of Science Thesis in the Master's Programme Infrastructure and Environmental Engineering

EMIL CEDERSTRÖM
Department of Civil and Environmental Engineering
Division of GeoEngineering
Geotechnical Research Group
Chalmers University of Technology

ABSTRACT

A probabilistic approach to slope stability is used in this thesis to evaluate the uncertainties in the input parameters. The case study consist of a comparison between old praxis and new praxis in ground investigation methods. In the case study a road project in Norway at the Rissa area in Sør-Trønderlag is used for the study. The area is famous for the quick clay slide that occurred there in the 1978. The data used in this study is collected from ground investigations in this project. Old praxis in this study is the 54 mm piston sampler and new praxis is Sherbrooke block samples and CPTU. Stability calculation is performed in Plaxis and GEO-Suite mostly utilizing NGI-ADP model. The slope that is modelled consists mostly of clay material and therefore this study is focused on clay material. A First Order Second Moment analysis and Monte Carlo Simulation is used linked to the slope stability calculation. The method gives a probability of failure and a reliability of the calculations. It can also give answers to the impact each of the input parameter have on the result. The analysis shows that the reference value of the shear strength have the largest impact on the results.

The Sherbrooke samples showed higher strength values than the 54 mm samples.

Key words: Anisotropic Shear Strength, FOSM,Quick Clay,Probabilistic model, Plaxis, Block Sample, Piston Sampler, Slope Stability.

Probabilistisk Metoder Applicerade på Släntstabilitets Beräkningar
Examensarbete inom Infrastructure and Environmental Engineering
EMIL CEDERSTRÖM
Institutionen för bygg- och miljöteknik
Avdelningen för Geologi och Geoteknik
Chalmers tekniska högskola

SAMMANFATTNING

En probabilistisk metod för att beräkna släntstabilitet är använd i detta examensarbete för att utvärdera osäkerheterna i indatan. Fallstudien består av en jämförelse mellan gamla och nya metoder av grundundersökningar. Ett vägprojekt i Rissa området i Sør-Trønderlag utgör området för fallstudien. Området är känt för kvicklere skredet som hände här 1978. All data som är använd i denna studien är insamlad ifrån undersökningar i detta området. Gamla grundundersökningsmetoder i denna studien är 54 mm kolvprovtagare och nya metoder är Sheerbrok block prov och CPTU. Den modellerade slänten består mestadels av lera och därför är fokus inriktat på lermaterial. Stabilitetsberäkningarna är utförda i Plaxis och GEO-Suite med material modellen NGI-ADP. Den probabilistiska analysen är gjord med First Order Second Moment metod och Monte Carlo Simulering koppat till släntstabilitetsberäkningarna. Med probabilistiska metoder är det möjligt att bestämma sannolikhet för brott och bestämma pålitligheten i beräkningarna. Det är också möjligt att se vilken påverkan enskilda parametrar har på resultatet. Studien visar att det är skjuvhållfasthets parametrarna som har störst påverkan på resultatet. Sheerbroke block proverna visar på högre skjuvhållfasthetvärden än 54 mm proverna.

Nyckelord: Anisotropi Sjuvhållfasthet FOSM,Kvick Lera,Probabilistic Model, Plaxis, Block Prov, Kolv provtagare, Slänt Stabilitet

Contents

Preface

This MSc-thesis was conducted at Chalmers University of Technology in close cooperation with Norwegian Public Roads Administration. The thesis have been written between 18 January to 10 June.

I would like to thank my supervisor Vikas Thakur at NPRA for all the support and help during the process.

Also Petter Fornes NGI and Maj Gøril Bæverfjord SINTEF for the help.

Trondheim May 2014

Emil Cederström

Notations

Roman upper case letters

FOSM	First Order Second Moment
FORM	First Order Reliability Method
SORM	Second Order Reliability Method
CPTU	Cone Penetration Test Undrained
PEM	Point Estimate Method
Msf	Multiplier safety factor
I_L	Liquidity Index
I_p	Plasticity index
γ	unit weight
COV	Coefficient of Variance
P_d	
R	bearing capacity (resistance)
S	action effect (solicitation)
G_{ur}	unloading/reloading shear modulus

Roman lower case letters

a	attraction
c	cohesion
c'	cohesion intercept
pf	probability of failure
s_u	undrained shear strength
s_{ref}	undrained shear strength reference
s^A	active shear strength undrained
$s^A_{,inc}$	increase of shear strength with depth
s^P	passive shear strength undrained
s^{DSS}	direct simple shear strength
y_{ref}	reference depth
w_L	Liquid limit
w_P	Plastic limit

Greek letters

β	reliability index
μ	mean value
σ	standard deviation
	shear stress
ν’	Poisson’s ratio
φ	Friction angle

1. Introduction

1.1 Background

This master thesis is a part of the national program called Natural Hazards-Infrastructure, Floods and Slides (NIFS). This Government Agency Programme is a partnership project involving. the Norwegian National Rail Administration (JBV), the Norwegian Water Resources and Energy Directorate (NVE) and the Norwegian Public Roads Administration (NPRA). It is also worth mentioning that NPRA and the Chalmers Technical University have a research cooperation and the geotechnical engineering is one of the field of collaborations.

In Scandinavia there is a great concern to investigate areas with sensitive or quick clay. In Norway have 1750 zones with quick clay been identified today and more are expected to be found (NIFS A 2012). In many of these areas there are lots of activities some are built up with houses and roads. Over 150 000 people lives in areas in Norway that is exposed for floods and landslides. These have led to over 1100 casualties in Norway over the time period 1900 to 2010. The damages have cost 6.1 billion NOK in compensations to private interest during 1980 to 2010 and 700 million only in 2011. Many new infrastructure projects are planned in areas with quick clay and this means a great geotechnical challenge. This explains why the field is interesting and necessary to study further.

A model in geotechnics is a mixture of knowledge in mainly three different fields, these are Geotechnical engineering, structural engineering and mathematical science (Alén 1998).

1.2 Probabilistic in Geotechnical Engineering

In geotechnical engineering it often comes down to make a decision in spite of having known uncertainties in the models. This is a difference compared to many other engineering fields where the materials have more well defined material properties unlike soil materials that is formed by natural processes over a long time period. This means that the geotechnical calculations with its uncertainties leads to a form of risk management were a quantification of the uncertainty in the models can be of help when results are evaluated and decisions are to be made.

It is of importance to know which uncertainties that is inherent in models that attempts to simulate reality. Slope stability calculation models contain uncertainties derives from different sources such as the soil material, the ground investigation methods, laboratory methods and calculation models. But data from all these investigations and measurement is used in the same model. Therefore is it important to know what the uncertainties are and what effect will the uncertainty have on the result.

In geotechnics the traditional approach to uncertainties has been to choose parameter values conservative so that the calculation has been on the safe side. This has been made with respect to the uncertainties that always have been known to exist. This means that the design is not optimal solution to a problem since too conservative chosen values will result in expensive and over dimensioned solutions. To introduce probability calculations to the models the result can be refined to get a more optimized design. This was noticed by Engineers like Terzaghi, Peck and Casagrande in the 1930's-1950. By the observational method where a construction where

observed and if the events where not according to the design actions were taken. The observational method was introduced in 1969 by R.B Peck (Peck 1969).

The suggested that approach using the most probable conditions should be used. Probabilistic methods have been used in science for a long time but statistically based methods are not fully implemented in geotechnics. This can have to with that in geotechnics the number of field investigations and laboratory test that can be performed is limited. Therefore the number of data that is low statistically regarded. The probabilistic methods started to develop in the 1950's were materials started to describe with statistics when structure design were made. This was first applied in the 1970's to geotechnical engineering.

The use of probabilistic methods will not eliminate the problem with uncertainties in the calculations but it provides a working method that not ignores the fact that a result is uncertain and importantly it gives a consistent working method that deals with the uncertainties. To introduce a probabilistic approach to the calculations will also provide a base for the decision that the engineer has to do.

Current state of Knowledge

The use of methods with reliability and probabilistic analysis has increased in the recent years (Beacher and Christian 2003), (Christian 2004). Since the start of probabilistics a lot of research in the field has been made. Probabilistic approach to describe the uncertainties in soil properties and the variability in the soil material have been made by (Lumb 1966), (Vanmarcke 1977), (Beacher 1986), (Lacasse 1996), (Alén 1998), (Phoon 1999) Today research of uncertainties in input parameters, and how they can be modelled probabilistically (Christian 1994), the calculation algorithms; numerical (Griffiths 2004) (Low 2006) and analytical have been made (Ang and Tang 1984), (Griffiths 2007).

Research on how to apply a probabilistic approach to geotechnical problems have been made by (Vanmarcke 1980), (Thoft-Christensen and Baker 1982), (Madsen 1989), (Paice 1997) (Griffiths 2004), (Ang 2006), (Müller 2013), and (Benjamin 2014) This includes also Bayesian statistics applied to geotechnics that gives a method to deal with the limited number of observations. This has also given information of how correlation of variables and previous knowledge of a variable shall be treated. Since geotechnical studies often have a small amount of data available, statistically regarded, model updating is suited for geotechnical engineering. This means that Bayesian statics is suited to apply to the calculations. This topic have been researched by (Zhang 2004, 2009), (Cao and Wang 2013). Table 1 gives a summary of the literature used for the theoretical framework of the thesis.

Table 1 overview of literature for theoretical framework on probabilistics in geotechnics.

Topic	Brief summary	References
Uncertainties in soil material	Characterization of uncertainties in soil material. Aleatory and Epistemic uncertainties. Determination of variability in soil properties.	(Lumb 1966), (Vanmarcke 1977), (Beacher 1986), (Lacasse 1996)
Probabilistic approach to Geotechnical problem	Probabilistic methods of level 1, 2 and 3 applied to Geotechnical problems such as slope stability, ground superstructure interaction, dams and settlements. Structural reliability methods. FOSM,FORM,SORM, Monte Carlo Simulation	(Vanmarcke 1980), (Thoft-Christensen and Baker 1982), (Madsen 1989), (Paice 1997), (Alén 1998) (Griffiths 2004) (Ang 2006), (Müller 2013) (Benjamin 2014)
Numerical and analytical analysis	Probabilistic analysis and Reliability analysis based on FEM	(Griffiths 2004) (Low 2006) (Ang and Tang 1984), (Griffiths 2007), (Zhang 2004, 2009), (Cao and Wang 2013)

Variations in soil material properties

Lumb was one of the earliest to describing the random variations in soil material with a trend function based on a distribution. This approach provided a rational basis for making decision when choosing design parameter values. Thereby it also became possible to determine the probability that the value was less or more than the value meaning it is possible to determine risk.

The earlier stages of probabilistic analysis in geotechnics focused much on determine and make models to treat the uncertainties in the geotechnical problems. To do that the sources of uncertainties first had to be evaluated. Vanmarcke was one of the earliest to make models of how to treat the uncertainties in a soil property.

Lacasse and Nadims research how to describe the characteristics of the uncertainties in the soil properties. They clearly state the benefits of knowing about the uncertainties in the geotechnical problems and how to document and make them explicit to make the calculations less uncertain. To quantify the uncertainties in the sources firstly have to be reviewed and treated statistically. The sources of uncertainties are mainly categorized as Aleatory and Epistemic. Natural variability or randomness of a property and lack of knowledge. They introduce methods to use

when geotechnical data with the spatial variability is to be handled. A review of methods such as Short-cut estimates by Bascher and Snedecor and Cochran, Mean, variance, histogram and probability density by Ang and Tang. Geostatics by Matheron and Nadim is made. The review concludes for what type of cases the methods are applicable together with recommendations. This gives guidance to engineers when setting up a reliability analysis. Nadim later developed the previous research and applied the theories to FOSM, FORM, SORM and Monte Carlo simulation and how this can be linked to event probabilities.

Probabilistic approach

The probabilistic approach to geotechnical problems has developed from the knowledge of the uncertainties in the soil materials properties. The uncertainties have been treated statistically as the input parameters to the calculations. Therefore it became possible to state probability for failure or certain outcomes and the reliability of the results. The structural reliability concepts of different levels of methods where developed for other fields of engineering but where then applied to geotechnics. The basic idea is to check the structural strength against a limit state (Madsen and Egeland 1989). Madsen was one of the earliest in this field and applied structural reliability to geotechnical calculations. The models in the different levels that where applied to geotechnics where FOSM, FORM, SORM and Monte Carlo Simulations to mention some. Ang and Tang applied the first order second moment approach to geotechnical problems in 1984. This gave an analytical way to treat the parameters as functions of mean and standard deviation in the input parameters. Swedish research by Claes Alén applied the probabilistic approach can be applied to geotechnical. The research weaves the fields of mathematical statistics, geotechnics and structural engineering together. To subject in geotechnical engineering, Slope stability and interaction between ground and superstructure is made where probabilistic models of level 1,2 and 3 is applied to the cases. Phoon and Kulhawy made models to handle the geotechnical variability that derives from different sources into a model. They describe soil properties as functions of depth with terms to cover the uncertainties. These terms is based on the coefficient of variance of the property regarding, transformation and measurement errors. In geotechnical engineering Fenton and Griffiths work are well recognized. They have researched on numerical modelling with random variables. Both with thoroughgoing background on statistics to appliance of probabilistic models in design.

Geotechnical calculations are today often performed in FEM software like PLAXIS. It is possible to link this software to reliability programs so the input variables are changed for each simulation run in PLAXIS and the result is evaluated against a convergence criterion. Research on this topic have been made by (Schwecikendiek 2006) and (Wolters 2012).

The calculations today are governed by regulations and standards. Eurocode is a widely implemented system that forms the basis for the Norwegian regulation TEK 10 and the Swedish TK Geo11. These regulating codes are based on reliability when the partial factors are set. Therefore it is an advantage to know how to deal with reliability and statistics in the calculations when decision is depending on quantify risks and benefits. The load and resistance factor used in AASHTO system in North America is also based on reliability design.

This summary of the probabilistic approach and its history is not complete summary of the work and research in the field but it is a selection used for the literature review for this thesis.

Introduction to statistics

In this report there will be statistical and probability theory involved. To get more insight to these theories Fenton and Griffiths "Review of Probability Theory, Random Variables, and Random Fields" is recommended to be read for basic knowledge.

1.3 Purpose of the thesis

To investigate the uncertainties in the relevant input data to slope stability calculations in quick clay and sensitive clay. To identify the sources of uncertainties in the ground investigation. To implement a probabilistic approach to slope stability calculations and to investigate how old praxis in ground investigations and laboratory test and new praxis affects the uncertainties in the calculations.

1.4 Limitations

The thesis will look into the uncertainties related to the input parameters such as ground conditions, topography and external loading. This thesis will not incorporate a probabilistic analysis of the calculation models that are used today. The thesis will only treat clay material.

1.5 Method

Literature study with a review of important subjects for the thesis should be done in the initiating phase. These subjects are geology, quick clay and sensitive clay material, ground investigation methods, laboratory investigation methods, applied probability and statistics in geotechnics, slope stability calculation.

Compilation of material from ground investigations and laboratory testing material from the area. This material shall then be investigated and evaluates to quantify the uncertainties and determine input parameters to stability calculations. This will be done with statistic and probability methods.

This data should then be used in slope stability calculation models in case study. Two different scenarios shall be investigated to determine the difference in results for the slope stability when input data is collected from ground investigations from old praxis compared to new praxis.

2. Theory

The theory chapter is intended to introduce necessary background information about the different fields that the case study is within. This chapter is gathered from the literature review and includes an introduction to statistics and uncertainties in geotechnics.

2.1 Introduction to statistics

In order to understand the statistical and probabilistic calculations in the report this chapter will introduce the necessary theories.

Event probability

The probability of a certain event to occur is by definition between zero and one or 0% it will not happened and 100% it will happened. This gives equation 2.1:

$$0 \leq P[A] \leq 1 \quad (2.1)$$

Where $P[A]$ denotes the probability of an event A.

The complementary event is the probability that an event don't occur this gives equation 2.2:

$$P[A^c] = 1 - P[A] \quad (2.2)$$

A^c is called the complementary event to A.

If there are more than one event that is compared and the have a relationship this can be illustrated by the Venn-diagram, See figure 1.

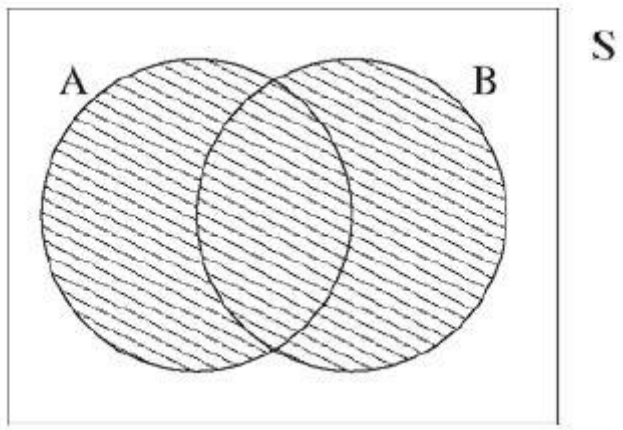

Figure 1 the Venn-diagram illustrates the union of two events A and B (Griffiths 2007).

To calculate the probabilities the additive rules applies, see equation 2.3:

$$P[A \cup B] = P[A] + P[B] - P[A \cap B] \quad (2.3)$$

$P[A \cup B]$ is the union for both event A and B occurs.

$P[A \cap B]$ is the intersecting area in the Venn-diagram.

Conditional Probability

If the probability of an event is affected by another event there is a conditional probability. The definition of this is:

$$[A|B] = \frac{P[A \cap B]}{P[A]} \quad (2.4)$$

The equation 2.4 gives the conditional probability for event B given that event A has already occurred.

Bayesian statistics

Bayesian statistics describes how empirical observations change the knowledge of parameters. Bayesian statistics is a method where the inference is used when models are updated (Stevens 2009).

Bayes theorem

Bayes theorem is used to determine conditional probabilities. It was discovered by Thomas Bayes (1702-1761). The equation for Bayes theorem in general form is:

$$P(A|B) = \frac{P(A \cap B)}{P(B)} = \frac{P(B|A) \cdot P(A)}{P(B)} = \frac{P(B|A) \cdot P(A)}{P(B|A) \cdot P(A) + P(B|\ddot{A}) \cdot P(\ddot{A})} \quad (2.5)$$

What the Bayes theorem is saying is the probability for event A to occur given that event B occurs, that is P(A|B). P(A∩B) is the probability that both event A and B occurs, the intersect in Venn diagram. The denotation $P(\ddot{A})$ is the complement event to A, that is event A not occurs.

Bayesian updating

To reduce the uncertainties in the variables in the calculations the updating is done Bayesian, this means that the correlation is considered when the probability distributions is updated (Ching 2010).

Random variable

Random variable is used to identify events so they can be treated numerical in calculations. A definition made by Fenton and Griffiths is:

*Consider a sample space **S** consisting of a set of outcomes {s_1,s_2…}. If **X** is a function that assigns a real number **X(**s) to every outcome sε**S**, then X is a Random variable.*

2.1.2 Distributions

There exist several numbers of distributions that are suitable to use when describing a geotechnical parameter. Which one to choose depends on the specific parameter and its nature. Here follows a summary of distributions often used in geotechnical engineering.

Normal Distribution

The normal distribution is the most used distribution. It is sometimes referred to as Gaussian distribution. The normal distribution is largely used today because sums of random variables tend to a normal distribution. This is proven by the central limit theorem (Griffiths 2007). Another reason that the normal distribution is widely used is

due to its simplicity and availability, this has led to that the normal distribution has been used even when it fits the physical property poor (Alén 1998). The density function of the normal distribution is expressed in equation 2.6:

$$f(x) = \frac{1}{\sigma\sqrt{2\pi}} e^{-\frac{1}{2}(\frac{x-\mu}{\sigma})^2} \; for -\infty < x < \infty \qquad (2.6)$$

As can be seen from the density function the normal distribution is open. The properties of the normal distribution that it is symmetric about the mean value, μ, therefor the median is equal to the mean. The mode of the distribution function is at the mean value, see figure 2. The characteristics of the normal distribution E[X]=μ and VAR[X]=σ^2, where X is a random variable gives the notation $X \sim N(\mu, \sigma^2)$.

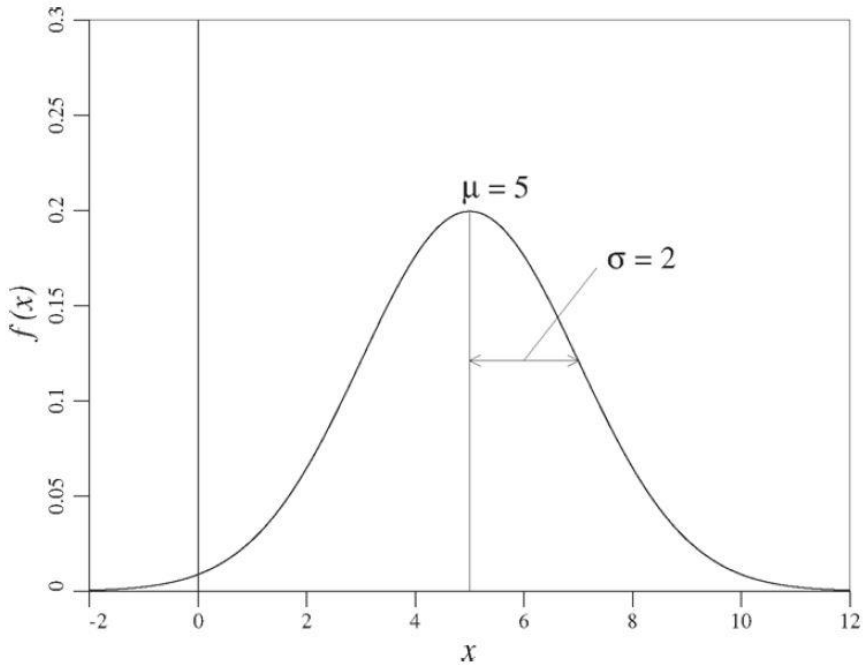

Figure 2 the normal Distribution with mean 5 and standard deviation 2 (Griffiths 2007).

The standard normal distribution is a case of the normal distribution. The standard normal distributions density function is equal to one and its mean value zero and the standard deviation is 1. Normal distribution values can be transformed into standard normal distribution with equation 2.7:

$$Z = \frac{X-\mu}{\sigma} \qquad (2.7)$$

B-distribution

The β-distribution is a general type of distribution that is often used. The β-distribution is defined on the closed interval 0 to 1. The beta distributions can be defined by the mean value, standard deviation, maximum value and minimum value (Alén 1998). The beta distribution has two free shape parameters denoted α and β.

The mean and variance is given by:

$$\mu = \frac{\alpha}{\alpha+\beta} \qquad (2.8)$$

$$\sigma^2 = \frac{\alpha\beta}{(\alpha+\beta)^2(\alpha+\beta+1)} \qquad (2.9)$$

The distribution function β (α, β) is

$$\hat{x} = \frac{\alpha-1}{\alpha+\beta-2} \quad (2.10)$$

Lognormal

The Lognormal distribution have the property that it is always positive unlike the normal distribution see figure 3. This is good for engineering problems which seldom deals with negative values, like loads or soil modulus. The Lognormal distribution have a random variable with a logarithm is normally distributed. The properties, mean and variance, in a Lognormal is defined as:

$$\mu_{lnx} = E[X] \quad (2.11)$$

$$\sigma_X^2 = Var[lnX] \quad (2.12)$$

Where X is a Random variable.

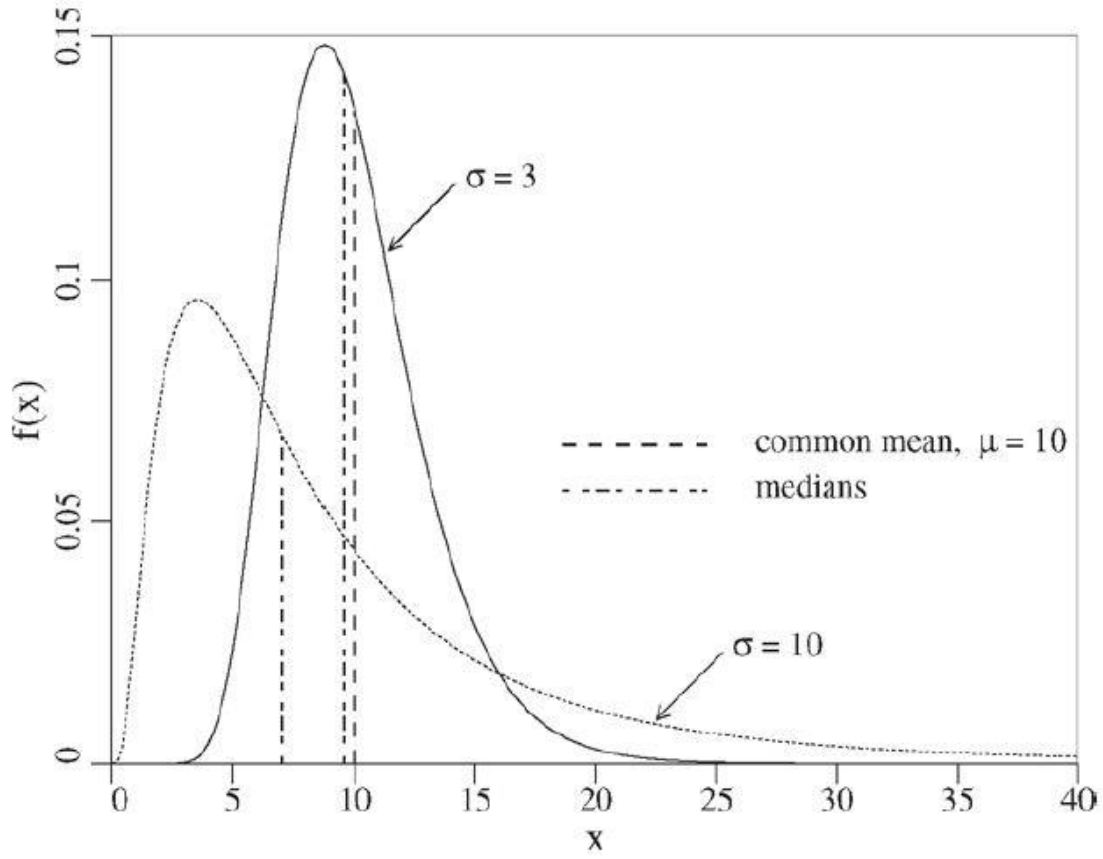

Figure 3 the Lognormal distributions, the figure shows the effect of changing variance (Griffiths 2007)

Extreme value distribution

The extreme value distribution is an interesting distribution in engineering. When modelling engineering problems it is often the maximum or minimum values that are of interest. Examples of this are structures evaluated for the maximum loads exercised on the structure. The Gumbel distribution is related to the extreme value distribution.

Gumbel distribution is a special case of extreme value distribution. The Gumbel distribution is also referred to as type I distribution.

2.2 Uncertainties

To be able to quantify the uncertainties is preferable, they first have to be identified. The input parameters to an analysis have to be collected from investigations, measurements and evaluations. This leads to various sources of uncertainties. The uncertainties associated with a geotechnical problem can be divided into two categories, Aleatory uncertainty and Epistemic uncertainty (Nadim 2007).

Aleatory uncertainties are the natural randomness that is in a parameter. A good example in geotechnics is the inherent variation in a soil parameter that leads to an uncertainty in the properties. The aleatory uncertainties cannot be eliminated or reduced.

Epimistic uncertainty is related to the knowledge of a parameter. Lack of knowledge on a variable can be from measurement uncertainties, model uncertainties and statistical uncertainties (Nadim 2007). Measurement uncertainties come from how the testing is performed and this comes done both to the method and the person performing the measurement. Model uncertainties relates to idealizations and physical problems that is made. Statistical information is due to the limited number of data that is obtained in a geotechnical survey.

The total uncertainty in a soil property is both aleatory uncertainties and epistemic uncertainties is put into the same model and is contributing to a total uncertainty. From this sources uncertainties the total uncertainty can be described mathematically according to (Baecher 1997) like equation 2.13.

$$V(x) \cong V_{sp}(x) + V_e(x) + V_{stat}(x) + V_{bias}(x) \quad (2.13)$$

Where

$V(x)$ is the variance of total uncertainty in the property x

$V_{sp}(x)$ is the variance of the spatial variability of x

$V_e(x)$ is the variance of the measurement noise in x

$V_{stat}(x)$ is the variance of the statistical error in the expected value of x

$V_{bias}(x)$ is the variance of the measurement or the model bias in the procedures used to measure x

All these uncertainties that a soil property is illustrated in the figure 4.

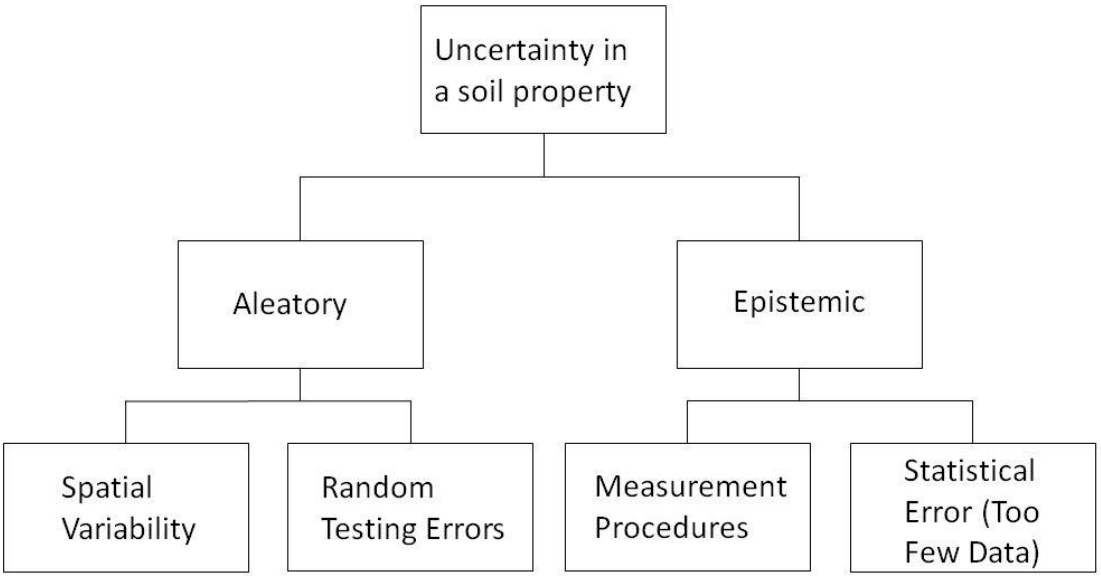

Figure 4 Sources of uncertainty in geotechnical soil properties (Jones 2002).

2.2.1 Sources of uncertainties

Uncertainties in a soil parameter are derived from several sources. This chapter brings them up a shows means of how they can be treated.

2.2.2 Natural variation

Soil material is not a homogenous material and therefore there can be differences in soil properties. The soil properties is said to be varying 10-1000 times more than more well defined materials that is used in building construction (Sällfors 2009). This variation is called natural variation and it is due to the geological conditions that the soil has been exposed for historically. Geological processes are the reason for the soil material is not homogenous material and properties may vary in an area that is determined to be of same material (NIFS B 2012).

Many soil parameters are varying both vertical and horizontal direction with the depth. Therefore to describe a soil parameter a function of the depth can be established (Phoon 1999). This function, see equation 2.14, can be used to model the natural variation in the soil profile.

$$\xi(z) = t(z) + w(z) \qquad (2.14)$$

ξ represents an in situ value of a soil parameter that is varying with the depth. t (z) is a trend function and w(z) represents the fluctuating component. The fluctuating component is the inherent variation in the soil material. Figure 5 shows the inherent soil variability varying with the depth.

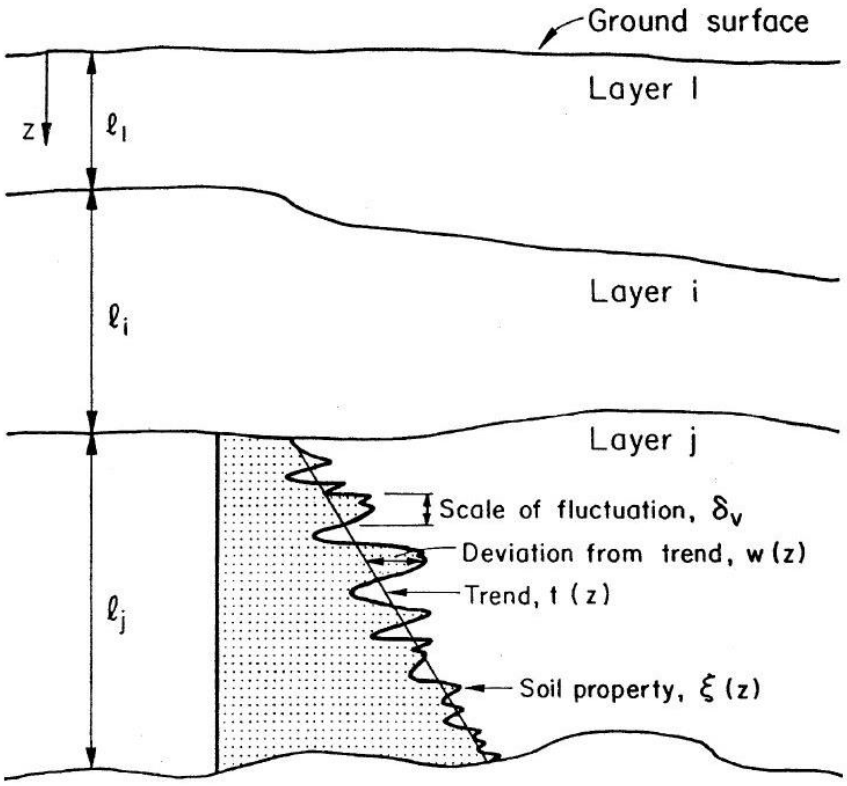

Figure 5 the inherent soil variability (Phoon 1999a)

There are two conditions that w has to fulfill in order to be used in this model (Phoon 1999). The functions mean value and the variance shall not vary with the depth, this is also called statistically homogenous. The other term is that the correlation of the deviation between two depths is a function of the distances and not the absolute positions (Phoon 1999).

If the above mentioned requirements are fulfilled the functions for the inherent soil variability can be evaluated with equation 2.15 for standard deviation:

$$\sigma_w = \sqrt{\frac{1}{n-1}\sum_{i=1}^{n}[w(z_i)]^2} \qquad (2.15)$$

The coefficient of variance of for σ_w is can be used to normalize it regarding to the trend, t, mean value, see equation 2.16.

$$COV_w = \frac{\sigma_w}{t} \qquad (2.16)$$

It is also necessary to see the correlation of the parameter value. This is done when the vertical fluctuation is evaluated equation 2.17 (Vanmarcke 1977). This is illustrated in figure 5.

$$\delta_v = 0.8\bar{d} \qquad (2.17)$$

The $\bar{d}$ denotes the "average distance between the intersections of the fluctuating property and its trend function" (Phoon 1999).

Table 2 shows empirical values of the COV for different soil parameters. These parameter values are determined both from laboratory methods and field methods. It gives a hint of how large the variations can be in a soil property.

Table 2 Inherent variability for soil parameters (Phoon 1995)

Test type	Property	Soil type	Mean	COV(%)
Lab strength	s_u(UC)	Clay	10–400 kN/m^2	20–55
	s_u(UU)	Clay	10–350 kN/m^2	10–30
	s_u(CIUC)	Clay	150–700 kN/m^2	20–40
	$\overline{\phi}$	Clay and sand	20–40°	5–15
CPT	q_T	Clay	0.5–2.5 MN/m^2	<20
	q_c	Clay	0.5–2.0 MN/m^2	20–40
	q_c	Sand	0.5–30.0 MN/m^2	20–60
VST	s_u(VST)	Clay	5–400 kN/m^2	10–40
SPT	N	Clay and sand	10–70 blows/ft	25–50
DMT	A	Clay	100–450 kN/m^2	10–35
	A	Sand	60–1300 kN/m^2	20–50
	B	Clay	500–880 kN/m^2	10–35
	B	Sand	350–2400 kN/m^2	20–50
	I_D	Sand	1–8	20–60
	K_D	Sand	2–30	20–60
	E_D	Sand	10–50 MN/m^2	15–65
PMT	p_L	Clay	400–2800 kN/m^2	10–35
	p_L	Sand	1600–3500 kN/m^2	20–50
	E_{PMT}	Sand	5–15 MN/m^2	15–65
Lab index	w_n	Clay and silt	13–100%	8–30
	w_L	Clay and silt	30–90%	6–30
	w_p	Clay and silt	15–25%	6–30
	PI	Clay and silt	10–40%	—[a]
	LI	Clay and silt	10%	—[a]
	γ, γ_d	Clay and silt	13–20 kN/m^3	<10
	D_r	Sand	30–70%	10–40; 50–70[b]

[a]COV = (3–12%)/mean.
[b]The first range of values gives the total variability for the direct method of determination, and the second range of values the total variability for the indirect determination using SPT values.

2.2.3 Measurement uncertainties

Since the soil properties have to be evaluated by doing measurement there is also a risk for measurement errors in the input data. To cover measurement errors in the in situ soil property a variable e has to be introduced to the equation, see equation 2.18. This variable is also depending on the depth z and is normally uncorrelated to w (Phoon 1999). The source of measurement errors are the equipment, how the measurement is performed and random testing effects.

$$\xi_m(z) = \xi(z) + e(z) \quad (2.18a)$$

$$\xi_m(z) = t(z) + w(z) + e(z) \quad (2.18b)$$

m is for measurement.

2.2.4 Uncertainties from testing methods

All soil parameters are derived from testing. The testing will introduce uncertainties into the models if the measurements or the interpretation are not performed in a correct and scientific manner (NIFS B 2012).

In the uncertainties from testing methods there are mainly three categories of errors that are common. Systematic errors in the testing method, Random errors in the testing method and Errors due to the limited number of tests. (Alén 1998).

Systematic errors come from how high the precision of the test method is. If the method is calibrated well systematic errors can be avoided.

Random errors can come from low accuracy of the method or the person that is performing the test is not handled it in a correct way.

2.2.5 Errors due to the limited number of tests

The numbers of test that can be done are limited due to many factors including economy. This means that the test results are not characteristic for the soil even if the testing methods are performed correct. The number of testes that can be done is low in a statistical point of view even if it is considered as extensive for a geotechnical survey in a certain project.

The Random errors and the errors from limited number of test can be called statistical uncertainties.

2.2.6 Transformation uncertainties

The geotechnical measurements do seldom give the design parameter that is required in the model and therefore a transformation often has to be done in order to get the searched design parameter. In the transformation the measured value have to be transformed into to a suitable design parameter. When doing so an uncertainty, transformation uncertainty, is added. The figure 6 below shows the transformation in a probabilistic character.

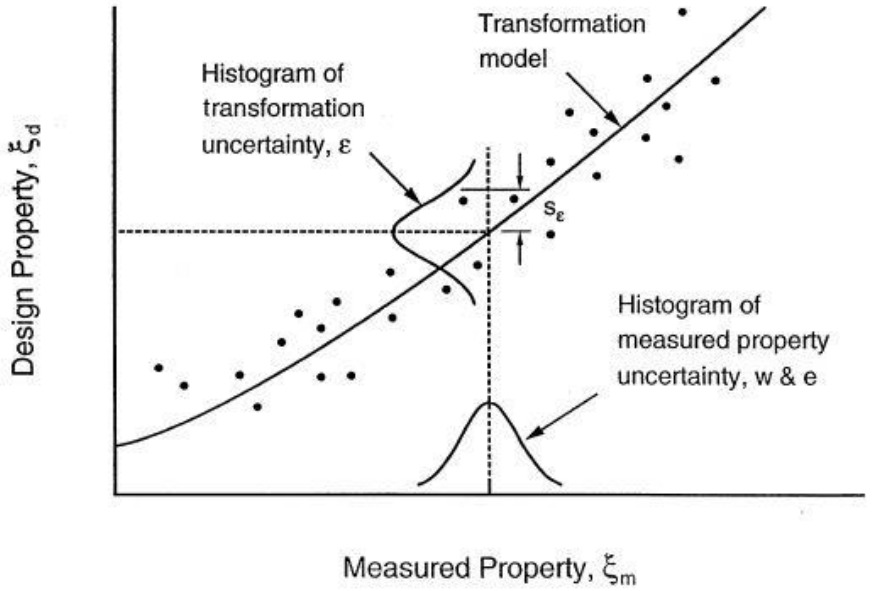

Figure 6 Show the transformation uncertainty when transformation from measurement to design property (Phoon 1999).

2.3 Calculation Models (Statistic and probability modelling)

The traditional concept of factor of safety and safety margin do not give any indications of how much the different parameters affect the stability neither does they give any clue how representative the value is in terms of reliability. The idea of establish a reliability model to the calculation models will give a working process where the uncertainties will be taken into consideration and quantified in order to check how reliable is the result.

The probability analysis can give answers to the probability that a failure in a slope will occur. The probability of failure, p_f, can then be combined in the reliability index, β, which is a function of p_f. The parameters in the input data can also be evaluated to see which combinations are most probable when a slope is failing and how much the total uncertainties are affected by the each parameter in the calculation models.

A concept that is important to about a calculation is whether the calculation has accuracy and precision. These two properties is not correlated so one doesn't give the other (Alén 1998). This is illustrated in figure 7.

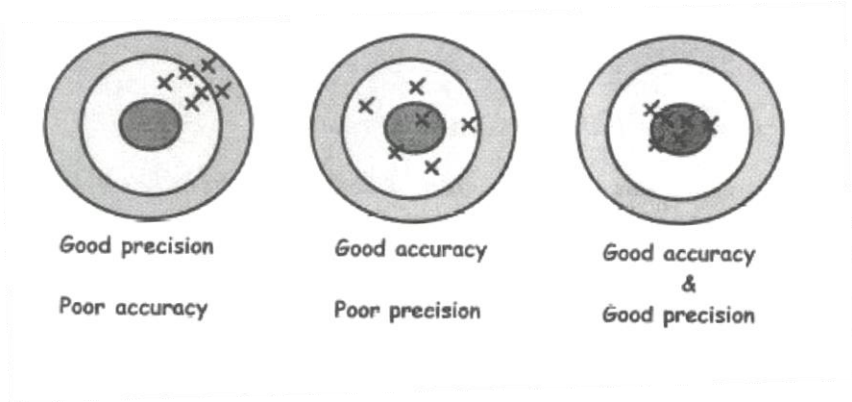

Figure 7 Precision and accuracy (Alén 1998).

To have the calculation to be of both good accurate and good precision is of course preferable. But this does not necessarily say that models that don't fulfill this are worse (Alén 1998).

Reliability Analysis

A reliability analysis shall give answer to how reliable a result from a model is. For slope stability problems the interesting result to evaluate is the probability for a failure, p_f, of a slope. In general the probability of failure is the relationship of action effects and the resistance that the slope can mobilize. This can be expressed as equation 2.19.

$$p_f = P(R \leq S) \tag{2.19}$$

The limit state is the border between safe state and failure state. When the failure in the slope occurs this border, limit state, is crossed and the critical state of failure is reach. In this limit state several variables is critical. A limit state function Z(**X**) can be used in the probability of failure expression, see equation 2.20.

$$p_f = P(Z(\boldsymbol{X})) \tag{2.20}$$

X is a function of several variable i.e. like geometry of a slope, unit weights of material, shear strength, internal friction angle etc. The limit state function needs to be defined so that failure or stable behavior is stated. If Z(**X**)> 0 the slope is stable and Z(**X**) <0 failure occurs. What the limit state function says is (Schwecikendiek 2006):

Z > 0 no failure as is the desired state

Z=0 limit state

Z<0 failure as is the unwanted state

Reliability models can be done in different levels of complexity. The different levels are made from how much information that is provided used to solve the problem (Madsen 1989)

Level 1

Deterministic reliability models with characteristic values. Only one characteristic value is assigned to the parameter that is uncertain. For a slope stability problem can an equilibrium models based on Resistance and Load be an example of a level 1 method. The level 1 methods is sometimes referred to as semi-probabilistic. For these methods it is necessary to have previous knowledge about the variables. Level 1 methods is the method that is applied when the partial safety factors is used. Example of this is a failure criterion when partial factors are applied to the characteristic values, see equation 2.21.

$$\frac{R_k}{\gamma_k} > \gamma_S \cdot S_k \qquad (2.21)$$

Where R_k is a characteristic strength value, γ_k is a partial factor, S_k is the characteristic value of the load and γ_s is a partial factor.

From this is then the reliability index for the case calculated.

Level 2

In Level 2 methods two values are assigned to the uncertain parameters. Normally this is done by a mean value and a variance. To check correlation of the parameters the covariance can be used. Example of a level 2 method is First Order Second Moment, FOSM, reliability index method, First Order Reliability Method, FORM and Second Order Reliability Method, SORM and Point Estimate Method.

First Order Second Moment (FOSM)

The First Order Second Moment method is giving an analytical approach to make an approximation of parameters. The parameters are treated as functions of mean value and the standard deviation of the various input factors and their correlations (Nadim 2007). FOSM means that the first order of the Taylor approximation terms is used (Christian 2004). So for the assessment of mean, μ_Y equation 2.22, and standard deviation, σ_Y, equation 2.23, the input variables are treated as:

$$\mu_Y \approx Y(\mu_{x1} + \mu_{x2} + \ldots \mu_{xn}) \qquad (2.22)$$

$$\sigma_Y^2 \approx \sum_{i=1}^{n} \sum_{j=1}^{n} \rho_{xi} x_j \sigma_{xi} \sigma_{xj} \frac{\partial Y}{\partial xi} \frac{\partial Y}{xj} \qquad (2.23)$$

Where μ_{xi} is the mean value if X_i; $\rho_{xi} x_j$ is the coefficient between X_i and X_j; and σ_{xi} is the standard deviation of X_i (Muller 2013). If the variables are uncorrelated the equation can be simplified as equation 2.24.

$$\sigma_Y^2 \approx \sum_{i=1}^{n} \sigma_{Xi}^2 \left(\frac{\delta Y}{\delta Xi}\right)^2 \quad (2.24)$$

First Order Reliability Method (FORM)

FORM means First Order Reliability Method where first order means that the limit state function is linear (Alén 1998). The limit state function is meeting the linearization at the design point where the limit state function is zero, this is also the highest probability, see figure 8 (Schwecikendiek 2006).

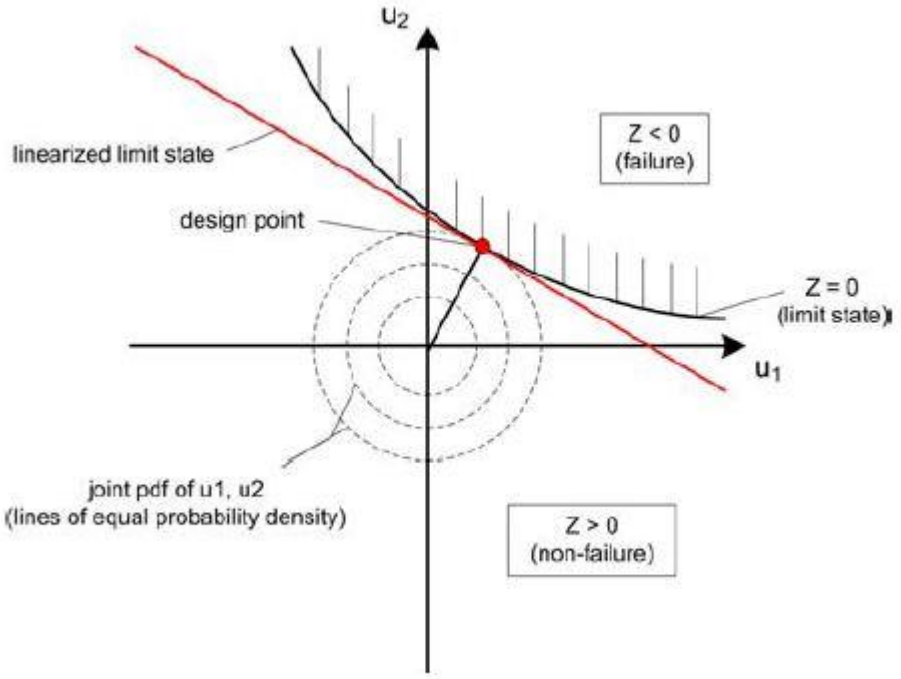

Figure 8 the design point and linearized limit state for two dimensions in U-Space (Schwecikendiek 2006).

Second Order Reliability Method (SORM)

In second order reliability methods are the failure function not linear as it is in FORM. In SORM the second order approximation of the function is established. So if the limit state function is not linear it will improve the result by including the second derivate of the failure function when the design value is determined. This is only if the limit state function is smooth if it on the other side is rough the result might also be worse (Schwecikendiek 2006).

Point Estimate Method (PEM)

Point Estimate Methods can be to model parameters in a statistical approach. This is desirable in geotechnical engineering where the parameters are associated with uncertainties. With PEM it is possible to approximate lower order moments of functions of random variables (Lu 2008). Normally an interval of the distribution of a parameter is made as estimation to capture the parameter value (Alén 1998). The

PEM method is a weighted average method where the mean value, standard deviation and skewness are the central elements used, this is illustrated in figure 9.

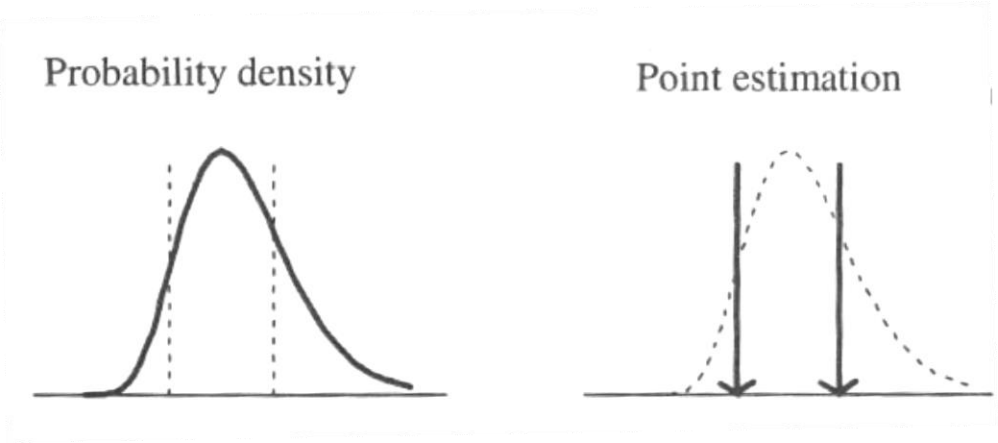

Figure 9 the principle for describing random variable with Point Estimate Method (Alén 1998).

Level 3

In level 3 methods no idealizations are made so the probability of failure can be seen as a measure. Therefore this method demands high knowledge of distributions of uncertain parameters. Level 3 methods are fully probabilistic. Methods in this category are First Order Reliability Method FORM, Second Order Reliability Method SORM, Monte Carlo Simulation, Directional Sampling and other sampling methods.

Monte Carlo simulation

The Monte Carlo simulation is a method that can be used to simulate input data to a geotechnical calculation. The method is a stochastic method and when the simulation is made a random value is often used to generate values. A large number of simulations are run. A common approach when doing a Monte Carlo Simulation will be to first assign distributions for variables, simulate sample values of variables by using a random number generator in the simulation and then use the values in calculations. By using a random number generator all numbers have the same probability. The accuracy of the method is directed by how many simulations that is made but to cover the tails of the distributions many iterations are necessary.

2.3.1 Deterministic models

Deterministic is when a behavior of something is determined by some known parameters, this is a common and traditional approach in geotechnics. The traditional method to calculate slope stability is based on equilibrium of resistance and action effect and modern methods is element analysis methods. Both of these deterministic models can be combined with a reliability analysis but the options have to be carefully evaluated.

Reliability index β

The reliability index gives an indication of the uncertainties in the input data as well as the probability of failure. The reliability index is suited where small probabilities of failure are calculated. In these cases it is more suited than PEM and Monte Carlo methods (Alén 1998). The reliability index where originally based on the equilibrium relationship of the safety margin concept. This is the quotient of the mean value and the standard deviation of the safety margin. The probability of failure can be calculated from the beta index with equation 2.25. To use this formula the safety margin must be normally distributed (Alén 1998).

$$\beta = \frac{\mu_M}{\sigma_M} \tag{2.25}$$

The relationship between the probability of failure is expressed in equation 2.26a and b.

$$p_f = \Phi(-\beta) \tag{2.26a}$$

$$\beta = -\Phi^{-1}(p_f) \tag{2.26b}$$

The probability of failure corresponds to a value in the beta table. The probability of failure is standard normal distributed. The reliability index can also be related to time perspective. This is done in the standards like Eurocode 7 where there is different *Reliability Class*. Reliability class 1 have a reference time of a 50 years and the probability of failure is$5 \cdot 10^{-4}$. This is a Beta value of 3.3. The annual probability of failure is10^{-5}, a beta value of 4.3 (Alén 2012).

To calculate the reliability index (Baecher and Christian 2003) is giving this work procedure:

- Identify all variables that affect the mechanism that is researched.
- Determine the best estimate of each variable and use these to calculate the best estimate of the function.
- Estimate the uncertainty in each variable and its variance
- Perform sensitivity analysis by calculating the partial derivate of the function with respect to each of the uncertain variables or by approximating each derivate by the divided difference.
- Use the equation of the variance to obtain the variance of the function.
- Calculate the reliability index.

2.3.2 Random models

In a traditional calculation models the input data can be determined for each case, therefore it is called a deterministic model. This means that every equation gives a unique solution depending on the input data. To be able to get a perception of the range of the results from such models the calculations have to be done many times. To overcome this problem a random model can be used instead. In a random model the uncertainties in the input data is described by using random variables (Alén 1998). By doing this the interval of parameter values can be covered together with the probability.

The input parameters have to be described in a distribution that is suited for the problem that is to be solved and the nature of the parameter. One problem in geotechnics when choosing distributions to describe parameters in is the low number, statistically regarded, of test that can be performed in for example a ground investigation due to economic limitations.

2.3.3 Algorithms

The calculation algorithms are set up to be able to calculate the probability outcome of different events. In the algorithms statistical methods can be incorporated. The probabilities that is of certain interest is if the limit values if ultimate limit state or serviceability limit is exceeded (Alén 1998). What method that shall be used is a choice that have to be made for the specific case that shall be studied.

2.3.1 Mathematical analysis

Mathematical analysis is one tool that can be used in a probabilistic analysis. The mathematical analysis is often restricted to problems that are not too complicated. Therefore numerical and approximate methods often have to be used. But for some basic cases explicit solutions can be obtained, these cases can be divided into four groups (Alén 1998):

- Exact solutions which gives the unknown parameters of a distribution.
- Exact solutions which give both the type and parameters of an unknown distribution.
- Approximate solutions which give the unknown parameters of a distribution
- Approximate solutions which give both the type and the parameters of an unknown distribution.

2.4 Modelling of soil properties

Soil is a material with large variations in properties due to the natural in the processes that forms the material and the state the soil is in the ground. Therefore there are several sources of uncertainties involved in the process of evaluating a soil parameter, See figure 10 below.

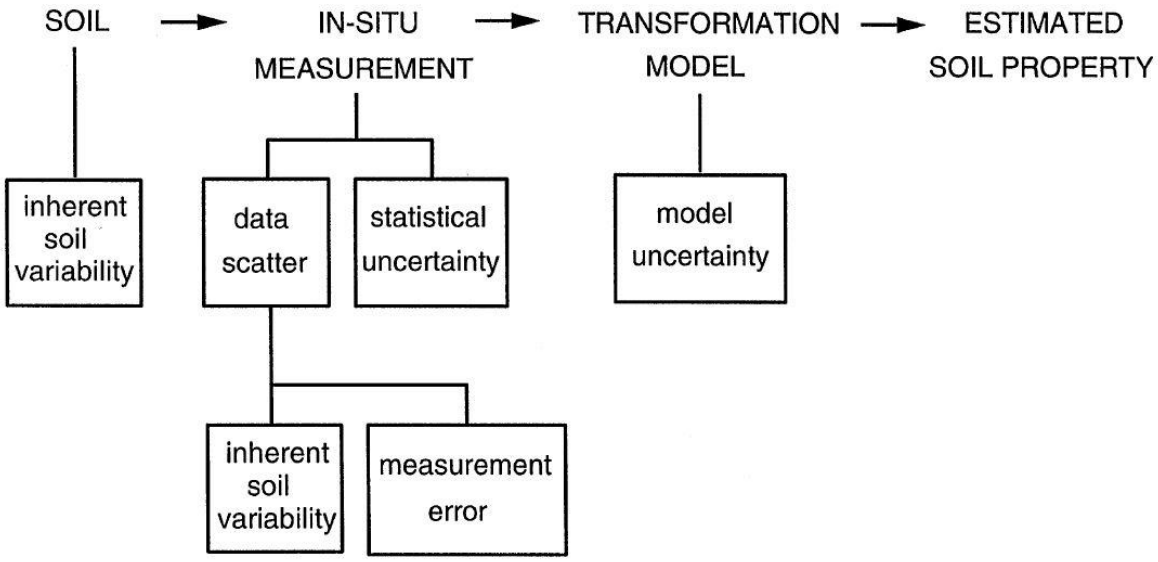

Figure 10 uncertainties in estimating a soil parameter (Phoon 1999).

2.4.1 Reality versus model

When probabilistic modelling is performed the input parameters must be represented in a statistical manner. This brings up several questions that is related to the uncertainties. Questions in this field can for example be (NIFS B 2012):

- Shall the material parameter be as representative as possible or shall they be chosen with caution?
- How is brittle material treated?
- How is representative mean values, standard deviation and correlation established for the material parameter?
- Is it always valuable to have as many observations as possible?
- How is the most reliable observations determined?
- How is the different data weighted?
- What says the traditional plots with gathering plots of measured shear strength values for one borehole, regardless of the quality of the samples and the uncertainties in the measurement methods?
- What can the models be used for?
- Is the data correlated?

This is all questions that the geotechnical engineer has to consider when the representation is made. When the uncertainties in the material parameter is evaluated is important to know that the data set is consistent. To know this will prevent us of non-consistent data, this can be when soil parameters from different layers is compared. This means that the parameter value will not be representative since the state in the soil is different due to different stress history and therefor further uncertainties is added to the analysis (Lacasse 1997).

2.4.2 Various soil properties

This part is about how certain parameters that is of interest in stability calculations can be treated.

Soil unit weight

The soil unit weight is an important property when slope stability is calculated. Soil unit weight is the density times the gravity, meaning that the unit weight is acting in direction towards the earth center. The unit weight of the soil is often regarded as an action effect in the slope stability. This is because the weight of the soil is a load and therefore the higher weight the larger load the soil is representing.

$$\gamma = \rho \cdot g \tag{2.27}$$

Where ρ is the density and g is the gravity.

The unit weight is recommended to be treated as a normal distributed property (Lacasse 1997). This is due to that the soil unit weight can be looked upon as a sum of small particles (Alén 1998). The soils unit weight is affecting the stress conditions in the soil meaning that it also effect other soil properties such as shear strength.

Pore water pressure

The pore water pressure determines how high the effective stress is in a material. High pore pressure will often imply reduced shear strength so it is a clear link between these parameters in the material and this need to be considered. The pore water pressure shifts during the year due to variations in the seasons. When pore pressure is to be modelled in a statistical analysis a gumbel distribution is suitable (Alén 1998).

Shear strength

One of the important parameters in slope stability is the shear strength. In a Mohr-Coulomb model the shear stress at failure $\tau_{f,}$ the stress when soil element reaches failure envelope, defined as function of the cohesion intercept, c', together with the effective stress in the soil, σ', and the angle of shearing resistance, φ' (Craig 2012).This level also corresponds to the shear strength ,c, see equation 2.28.

$$c = \tau_f = c' + \sigma' \tan(\varphi') \tag{2.28}$$

The failure in the soil element occurs when the critical combination of shear stress an effective stress is apparent in the soil.

Because of the low permeability in cohesion soils it is important to differentiate the undrained shear strength from the drained shear strength.

The shear strength of the soil material is varying with the depth and when a depth profile from several investigations are compiled these can be clearly seen. The shear strength can be seen as a function of depth like equation 2.29.

$$s_u(z) = s_{u0} + \Delta s_u \cdot z \quad (2.29)$$

To model the shear strength statistically the equation for soil properties X can be applied.

Evaluate shear strength from CPTU

The shear strength can be directly evaluated from the CPTU investigation data. This can be done either by the cone resistance, q_t, or from the pore water pressure (NIFS B 2012). Equation 2.30 and 2.31 gives the shear strength directly from the cone resistance and the pore water pressure.

$$s_u = \frac{q_t - \sigma_{v0}}{N_{kt}} = \frac{q_n}{N_{kt}} \quad (2.30)$$

$$s_u = \frac{u_2 - u_0}{N_{\Delta u}} = \frac{\Delta u}{N_{\Delta u}} \quad (2.31)$$

Where N_{kt} is the calibration factor for determine s_u from CPTU data and is defined as equation 2.32.

$$N_{kt} = 7.2(B_q)^{-0.77} \quad (2.32)$$

A good approximation for starting values of N_{kt} is 15 (Craig 2012).

B_q is a function of the pore pressure defined as equation 2.33.

$$B_q = \frac{u_2 - u_0}{q_t - \sigma_{v0}} \quad (2.33)$$

Post peak shear strength

It is common that when the peak shear strength of a geomaterial is reached the strength is reduced. This behaviour is known as strain softening (Thakur 2014). When strain softening is occurring this is characterized by a decrease if the shear strength after the peak shear strength is reach. This behaviour is happening in two states. First fully softened post-peak or post-rupture state for strain levels of 10 to 20 %. The second state is residual state when the strains are very large.

Early research where suggesting that the post-peak reduction in shear strength for clay was associated with friction angle and cohesion. New research on the phenomena have found out that post-peak shear strength reduction in soft sensitive clays is controlled by shear induced pore pressure ratio (Thakur 2014A).

Figure 11 is from a laboratory study when idealization of undrained strain softening in soft sensitive clay is excessed for strains up to 20%. The shear stress at peak and the shear stress after post-peak are occurring between 10 to 20 % strain. The relation to the shear induced pore pressure can be seen when effective stress is decreasing.

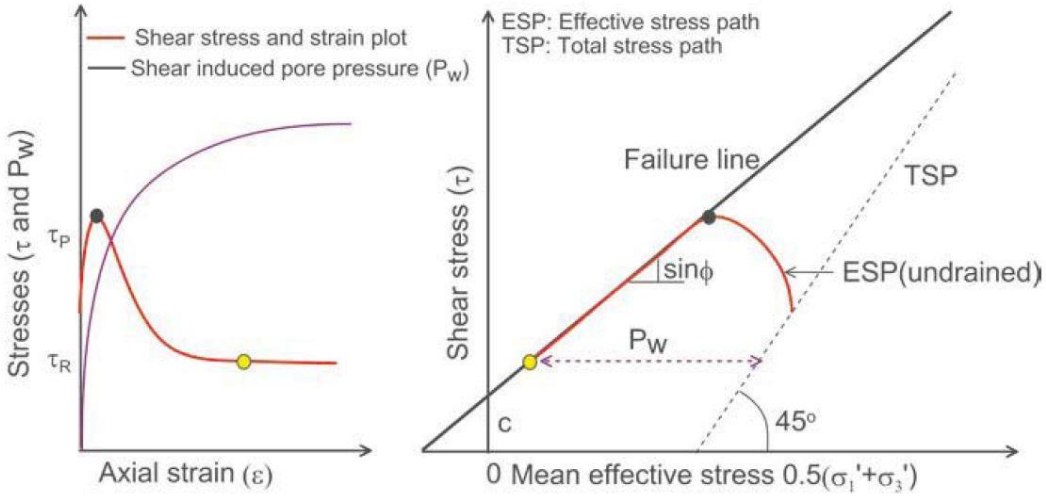

Figure 11 Idealization of undrained strain softening in soft sensitive clays seen at the laboratory strain levels up to 20 %

SHANSEP

Stress History And Normalized Soil Engineering Properties, SHANSEP is a concept used for determine undrained shear strength for soil material through the relation of over consolidation ratio, OCR, and the effective vertical stress σ'_{v0}.
OCR is the numerical parameter that is quantifying the stress history of a soil and is defined as the ratio of the maximum vertical stress, preconsolidation pressure, over the current effective vertical stress, see equation 2.34.

$$OCR = \frac{\sigma'_{max}}{\sigma'_{v0}} \quad (2.34)$$

If the OCR=1 the soil is normally consolidated, OCR>1 it is over consolidated. The OCR cannot be less than 1.

Figure 12 is from test on block samples and is showing the relation of undrained active shear strength and effective vertical stress and OCR. The correlation is defined as equation 2.35.

$$\frac{s_{ua}}{\sigma'_{v0}} = \alpha OCR^m \quad (2.35)$$

Where α=s_{ua}/σ'_{v0} for OCR=1.0 as is corresponding to a normal consolidated clay that have not developed any preconsolidation pressure.

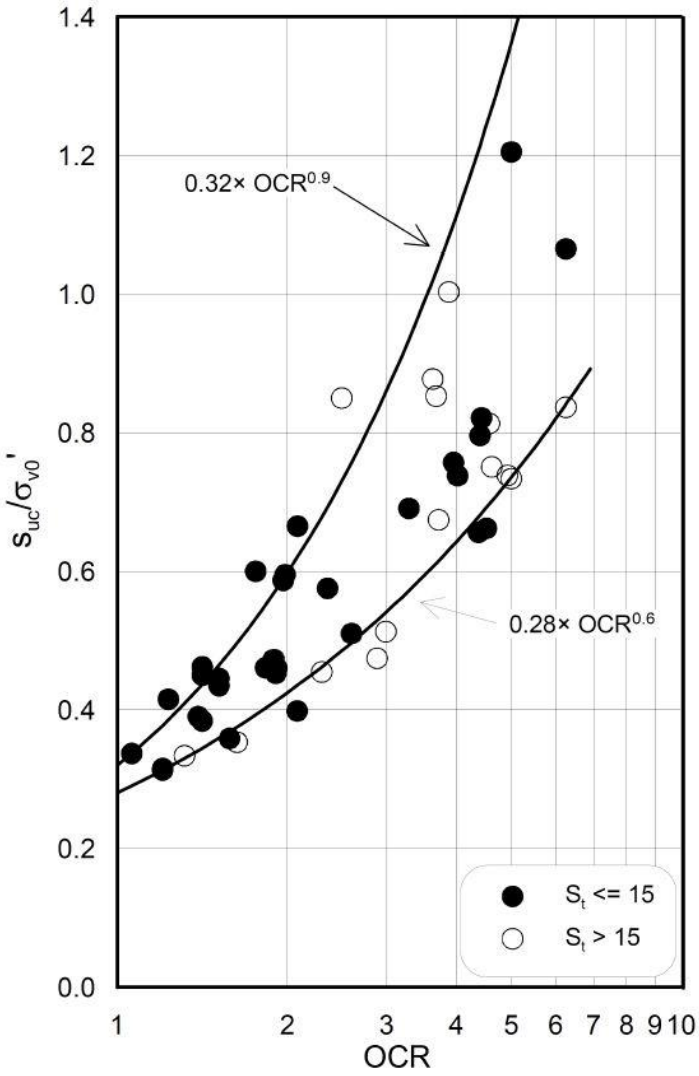

Figure 12 relation between $s_{ua}/\sigma_{v0}^{'}$ and OCR (Kornbrekke 2013)

3 Slope Stability

3.1 Introduction

The slope stability calculations can be performed in many different ways, but the main issue when a slope is evaluated is to answer on the question: Is it safe? And if it is How safe? With a probabilistic approach it is possible to answer to both these questions and state reliability to the answer. The answer to how safe the slope is the probability of failure in a probabilistic analysis.

3.2 Concept of safety

In slope stability there are mainly two concepts that is used to describe the safety, stability of a slope and they are Factor of safety also referred to as safety factor and safety margin.

3.2.1 Factor of Safety

The factor of safety is used to describe the stability of a slope. There are many definitions of the factor of safety but in general terms they all involve the shear strength of the soil and the shear stress that is required for equilibrium see equation 3.1 (Duncan 2005).

$$F=\frac{shear\ strength\ of\ the\ soil}{shear\ stress\ required\ for\ equilibrium} \quad (3.1)$$

The factor of safety is often used to find the critical slip surface of slope by evaluate a slope in order to find the slip surface that got the lowest factor of safety. The definition of the factor of safety, F, with respect to shear strength is expressed in equation 3.2, this is illustrated in figure 13 (Sällfors 2009).

$$F = \frac{\tau_f}{\tau_{mob}} \quad (3.2)$$

Where τ_f is the available shear strength and τ_{mob} is the mobilized shear stress. Equilibrium shear stress is the shear stress required to maintain a just-stable slope (Duncan 2005).

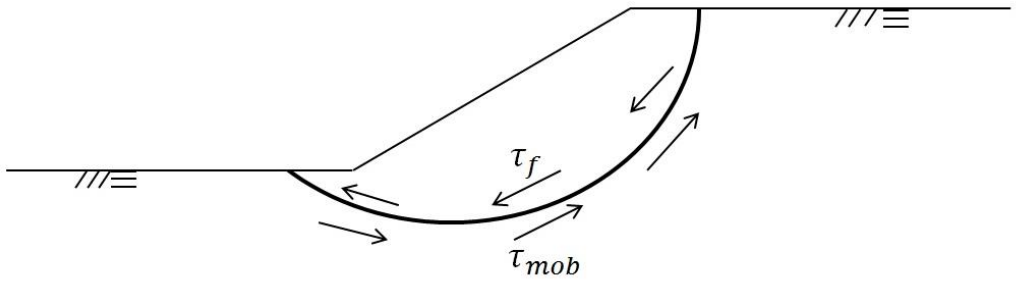

Figure 13 the mobilized shear stress and the available shear stress along a slip surface

τ_f is the maximum shear stress can take before failure and therefore it is directly coupled to the Mohr-Coulomb failure criterion see equation 3.3 (Craig 2012). Here it is in terms of effective stresses.

$$\tau_f = c' + \sigma' \cdot \tan(\varphi') \quad (3.3)$$

Equation 3.3 form the failure envelope, red line in figure 14 below, when the soil conditions reaches this state failure occurs.

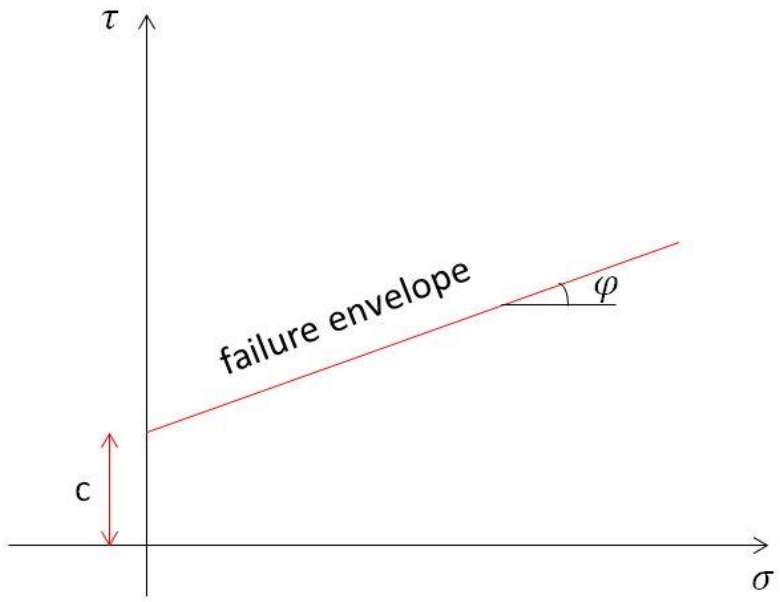

Figure 14 failure envelope which is the maximum shear stress the soil can take before failure

There exist several definitions of factor of safety and the reason for that is what use or purpose the calculation shall be of.9 The safety factor can also be defined as the quotient of the bearing capacity of a slope, R, and the action effect, S (Alén 1998) See equation 3.4.

$$F = \frac{R}{S} \tag{3.4}$$

This equation says that F>1 to be a stable slope and unstable if F<1. F=1 is the point of failure.

The factor of safety concept is analogue with the concept of the degree of mobilization (Alén 1998). That is a ratio of shear stress and shear strength like equation 3.5.

$$f = \frac{\tau}{c} = \frac{1}{F} \tag{3.5}$$

To make a probability model with the factor of safety the criterion can be set to p(F<1).

3.2.2 Safety Margin

The safety margin of slope is a way to describe how stabile a slope is and it is derived from the relation between the bearing capacity and action effect. There are several definitions to describe the safety margin. A suitable way for slope stability problems develops from equation 3.6.

$$M = c - \tau \tag{3.6}$$

If the critical slip surface shall be found using safety margin and with a probabilistic approach a dimensionless safety margin, m, is an option (Alén 1998).

$$m = \frac{R-S}{R} = \left(\frac{c-\tau}{c}\right) = 1 - f = 1 - \frac{1}{F} \tag{3.7}$$

This equation 3.7 also shows how the dimension less safety margin relates to the factor of safety.

3.2.3Factor of safety in practice

The factor of safety is often used as a design criterion. The standards in different parts of the world have somewhat different values on the factors of safety that have to be obtained for ensuring a safe design. Often are these values based on experience (Duncan 2005). Table 3 is showing recommendations that the safety factor have to meet in designs according to the U.S. Army Corps of Engineers' slope manual. The required factors of safety is for slopes of dams, levees, dikes, embankments and excavation slopes.

Table 3 Factor of safety criteria from U.S Army Corps of Engineers' slope stability manual.

Types of slopes	Required factors of safety[a]		
	For end of construction[b]	For long-term steady seepage	For rapid drawdown[c]
Slopes of dams, levees, and dikes, and other embankment and excavation slopes[c]	1.3	1.5	1.0–1.2

[a]For slopes where either sliding or large deformations have occurred, and back analyses have been performed to establish design shear strengths, lower factors of safety may be used. In such cases probabilistic analyses may be useful in supporting the use of lower factors of safety for design. Lower factors of safety may also be justified when the consequences of failure are small.

[b]Temporary excavated slopes are sometimes designed only for short-term stability, with knowledge that long-term stability would be inadequate. Special care, and possibly higher factors of safety, should be used in such cases.

[c]$F = 1.0$ applies to drawdown from maximum surcharge pool, for conditions where these water levels are unlikely to persist for long enough to establish steady seepage. $F = 1.2$ applies to maximum storage pool level, likely to persist for long periods prior to drawdown. For slopes in pumped storage projects, where rapid drawdown is a normal operating condition, higher factors of safety (e.g., 1.3 to 1.4) should be used.

3.3 Calculation methods for slope stability

3.3.1 General

Traditional methods for slope stability calculations are based on the equilibrium of the resistance and action effects in the slope. The equilibrium models have some simplifications that is made to handle the calculations that often were made by hand easier. This means that it is harder to treat them in statistics. One assumption that is made is same degree of mobilization of the shear strength along the whole slip surface.

More advanced method is such as it is possible to calculate the deformations in the slope. These models are normally finite element based methods. In a finite element based method it is possible to model elastic and plastic behavior of the soil. An advantage of these methods is that it is possible to describe the slope in detail both at failure and before failure. But if the results shall be trusted the knowledge of the input parameters also have to be detailed (Alén 1998).

It is normal to make a slope stability analysis in to different cases drained conditions and undrained conditions. These two cases are extreme cases where there are no consolidation in the undrained analysis and full consolidation in drained analysis (Alén 1998). These conditions have a great importance of the mechanical behavior of the soil.

3.3.2 Drained analysis Effective Stresses

Drained analysis is the long term case often the whole design life of a construction. This means that the effective stresses is used in the analysis. Drained in this situations do not mean that there is no water in the soil pores, it means that there are no excess pore water pressure. This means that the shear strength is different in drained conditions compared to undrained conditions (Craig 2012). In the drained conditions the water will flow in or out of the soil mass during the time that the soil is exposed for a load change. This means that the pore water pressure will not change when the volume of the voids is affected by the load (Duncan 2005). The drained analysis is characterized by the use of:

- Total unit weights
- Effective stress shear strength parameters
- Pore pressure determined from hydrostatic water levels or steady seepage analyses

Effective stresses is the stress that is transmitted only through the soils particles, the soil skeleton (Craig 2012). The effective normal stress, σ', is the total stress minus the pore water pressure, see equation 3.8

$$\sigma' = \sigma - u \qquad (3.8)$$

Where u is the pore water pressure. From equation 3.8 can the relation between total and effective stress be seen.

Since drained analysis is the long term case it means that the drained shear strength applies to the strength of the soil when it is loaded slowly enough so excess pore water pressure is dissipating when the loads are applied. In laboratory test drained conditions is performed just so that the test specimens are slowly loaded so that pore pressure is not built up. In field this is the result of loads applied to the soil mass during a long enough time so the soil can drain.

3.3.3 Undrained analysis Total Stresses

Undrained analysis is the case in fully saturated clay immediately after the construction. This means that the total stresses is used when the equilibrium analysis is done. Undrained shear strength can be determined with relatively simple and less time consuming laboratory methods. However time dependency and volume changes must be considered when using these results (Sällfors 2009). In the undrained conditions the water cannot flow in or out of the soil mass during the time that the soil is exposed for a load change. This means that the pore water pressure will response to the volume change of the voids in the soil material created by the load change (Duncan 2005). The undrained analysis is conducted with:

- Total unit weights
- Total stress shear strength parameters

The total normal stress, σ, is the sum of the forces that is being transmitted in through the particles in the soil material and through the water pressure divided by the total area (Duncan 2005). This is expressed in equation 3.9.

$$\sigma = \frac{P}{A} \tag{3.9}$$

Where P is a force that is applied on the area A.

The undrained shear strength is the strength that the soil upholds when it is loaded until failure under undrained conditions. This can be simulated in laboratory by loading a test specimen so fast that it do not drain or seal the specimen with impermeable membranes (Duncan 2005). In field undrained conditions is reach when the soil is loaded so fast that the soil mass don't have time to drain.

Figure 15 concludes the difference of the drained and undrained shear strength. The failure envelope of effective stress is controlled by the effective stress and density. The failure envelope for the total stress reflects the pore water pressure that is developed during the undrained shear. The total stress failure envelope is horizontal meaning that that it is independent of the magnitude of total stress.

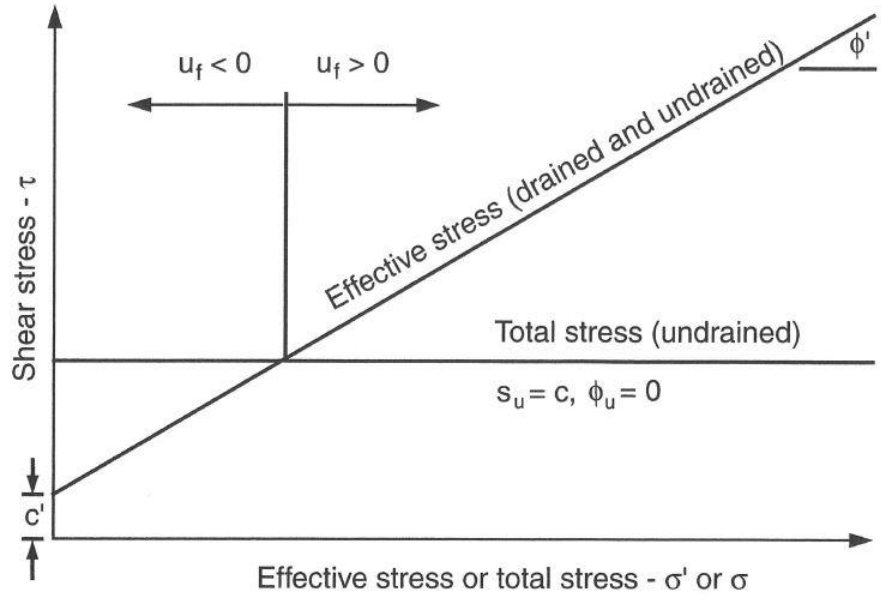

Figure 15 Drained and undrained strength envelopes for saturated clay (Duncan 2005)

3.3.4 Reliability analysis by random models Slope Stability

The factor of safety is giving a way of quantifying the slope stability. Because the input parameters contain uncertainties the value of the factor of safety is never absolute. If the safety factor is 1.0 it means by definition that the slope is just stable on the border of stabile and unstable. To link this to reliability of a slope, R, a simple definition can be made, see equation 3.10.

$$R = 1 - p_f \tag{3.10}$$

Where p_f is the probability of failure. This gives the reliability or probability of no failure.

The reliability model of the slope stability can be made by application of the theory of different level given by the complexity of the model (Madsen 1989). Applicated to a slope stability problem the levels can be (Alén 1998):

Level 1. The slope stability given by a simple formula.

A simple formula is good for using a random model approach on. The uncertainties in the calculation model can be covered by random variable applied to model the input data.

Factor of safety is a level 1 method where the formula for slope stability, undrained analysis, is given by (Janbu 1954). It can be defined as equation 3.11.

$$F = \frac{N(\theta,d)\cdot s_u}{\gamma \cdot H} \tag{3.11}$$

N is the stability number of the slope and is dependent on the inclination of the slope, Θ, and the depth of the slip surface, d. In the denominator γ is the density of the soil and H is the height of the slope. The stability number is given from a charter see Figure 16.

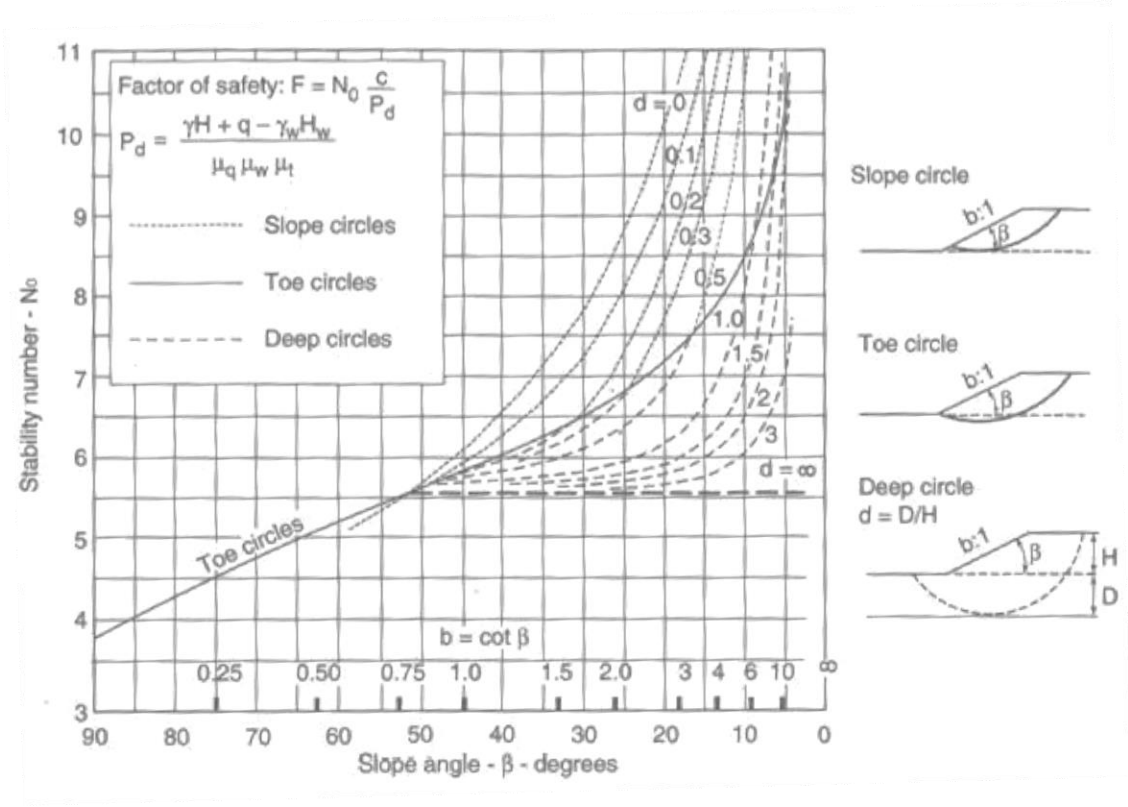

Figure 16 design charter where the stability number N is obtained (Duncan 2005)

A more general notation of the same formula is equation 3.12.

$$F = \frac{N \cdot s_u}{P_d} \tag{3.12}$$

Where P_d is the notation for denominator.

So the probabilistic approach to check p(F<1), meaning the probability of failure, needs the variables to be treated as independent.

ln(F) is a sum of the random variables see equation 3.13.

$$\ln(F) = \ln(N) + \ln(s_u) - \ln(P_d) \quad (3.13)$$

To use this formula the variables must be treated as independent, lognormal random factors.

Since the input parameters is given in distributions the factor of safety is like equation 3.14.

$$\ln(F) = N(\mu_{lnF}, \sigma_{ln\,F}) \quad (3.14)$$

N stands for normal distribution with mean value and standard deviation. So the mean value of ln(F) is equation 3.15.

$$_{lnF} = \ _{lnN} + \ _{lns_u} - \ _{lnP_d} \quad (3.15)$$

And standard deviation is equation 3.16.

$$\sigma_{\ln(F)} = \sqrt{\sigma^2_{\ln(N)} + \sigma^2_{\ln(s_u)} + \sigma^2_{\ln(P_d)}} \quad (3.16)$$

If the coefficient of coefficient of variance is low, less than 25-30%, the formulations can be approximated to (Alén 1998) like equation 3.17 for mean.

$$_{lnF} \approx \ln(\mu_N) + \ln(\mu_{s_u}) - \ln(\mu_{P_d}) \quad (3.17)$$

And equation 3.18 for standard deviation.

$$\sigma_{\ln(F)} \approx \sqrt{V_N^2 + V_{s_u}^2 + V_{P_d}^2} \quad (3.18)$$

Then can the safety margin be obtained as *m*=ln(F). The reliability index beta is defined as mean value over standard deviation so for the normal distributed factor of safety it becomes equation 3.19.

$$\beta = \frac{\mu_{lnF}}{\sigma_{lnF}} \quad (3.19)$$

Level 2. The slope stability given by limit equilibrium methods or limit analysis. Most of the stability calculations are made with level 2 methods (Alén 1998).

Level 3. The deformation of the soil is considered in level 3 methods. This is hard to simulate in limit equilibrium methods. Therefore level 3 methods in FEM is interesting when progressive failure is evaluated.

3.3.6 Anisotropy Active Direct Passive shear zone

Soil is an anisotropic material that has different properties in different directions. In a slope stability problem this is manifested in the different types of shear modes that is occurring in a slope, see figure 17. The slope can be divided into three different zones for the type of shear (Nylander and Ekstrand 2013). The zones are named after the shear stresses, Active shear zone, Direct shear zone and Passive shear zone. The anisotropy is taken into account in many calculations and strength relationship based on mean values in Norwegian soft clays can be seen in NGI: s database, see equation 3.20 and 3.21 (Lunne 2006).

$$\frac{S_{uDSS}}{S_{uCAU}} = 0.69 \quad (3.20)$$

$$\frac{S_{uCAUp}}{S_{uCAUa}} = 0.42 \quad (3.21)$$

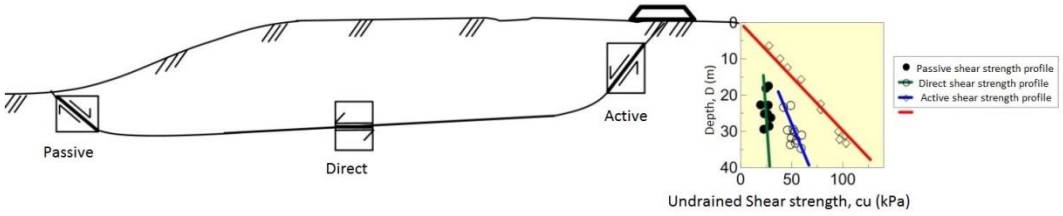

Figure 17 the figure also illustrates how the shear stress is affecting a soil element in the different zones (Thakur 2014)

The shear strength is one important parameter that governs the slope stability is different in the three zones. Therefore it is important to consider anisotropy in the calculations. This will of course require testing methods that evaluates this. This can be done with Triaxial test. There are also ways to calculate values for active and direct shear strength from direct shear test, vane shear stress and fall cone test if they are correlated to the liquid limit.

3.4 Software used for slope stability analysis

Slope stability analysis is today mostly done in geotechnical software. The programs that are based on limit equilibrium have been used for many years. More modern programs are utilizing finite element methods.

Plaxis

PLAXIS is finite element method based software. In this study it is Plaxis 2D that is used, but there exists version that is in 3D, Plaxis 3D. The software was developed 1987 at Delft University of Technology. The modelling in Plaxis is basically done in four steps input, calculations, output/result and evaluations of output in form of plots.

In the set-up of the model the user has to decide if a 6-node or 15-node mesh. The more nodes that is used the more shape functions and the higher polynomial there will be used. This improves accuracy but will also increase computation time.

The principle of describing the global safety factor in Plaxis is the Multiplier Safety Factor that is derived from φ-c-reduction. The φ-c-reduction is representing the ultimate limit state. In Plaxis M_{sf} smaller than 1 means failure (Plaxis 2012). This will be used to define the limit state function in the case study. The calculation procedure in Plaxis is so that the load is kept constant and φ and c, that is the strength parameters, is lowered incrementally (Plaxis 2011). M_{sf} is calculated in Plaxis like, equation 3.22.

$$\sum Msf = \frac{c}{c_r} = \frac{tan\varphi}{tan\varphi_r} \quad (3.22)$$

Where c and φ is the input strength parameters and c_r and φ_r is the reduced strength parameters.

If M_{sf} is used as the evaluation criteria the use need to take notice if there is other mechanism than the soils strength parameters that is triggering the failure (Schweckendiek 2006).

Material Models

To describe the different mechanical behavior of different soils it is possible to choose soil model in Plaxis. There are several models available in the program but those who will be used in this thesis is the Mohr-Coulomb Model and NGI-ADP Model.

Mohr-Coulomb Model

The material model that is used is the Mohr-Coulomb model. This model is a linear elastic perfectly plastic model, meaning that it is associated with irreversible strains (Plaxis 2011). The failure criteria, f, is a defined as function of stress and strain where the yield criterion is f=0. The full Mohr Coulomb yield criterion used in Plaxis is consisting of six functions when all terms is formulated, see equation 3.23 a-f (Plaxis 2011). Figure 18 is the failure envelope for the undrained and undrained case.

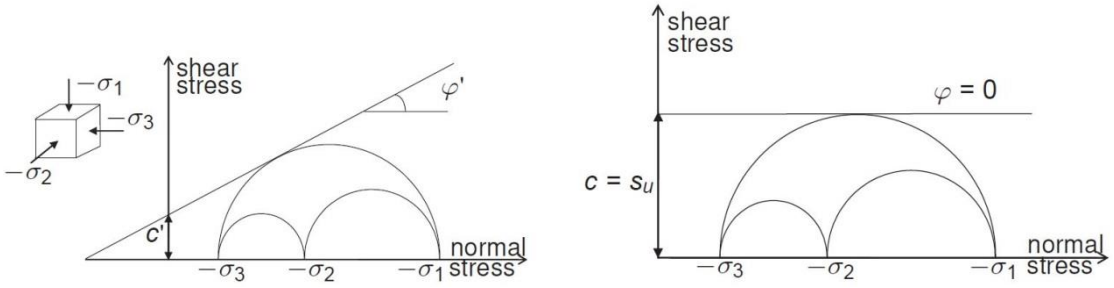

Figure 18 failure envelope effective strength parameters b. failure envelope undrained strength parameters

$$f_{1a} = \frac{1}{2}(\sigma_2' - \sigma_3') + \frac{1}{2}(\sigma_2' + \sigma_3')sin\varphi - cos\varphi \leq 0 \quad (3.23a)$$

$$f_{1b} = \frac{1}{2}(\sigma_3' - \sigma_2') + \frac{1}{2}(\sigma_3' + \sigma_2')sin\varphi - cos\varphi \leq 0 \quad (3.23b)$$

$$f_{2a} = \frac{1}{2}(\sigma_3' - \sigma_1') + \frac{1}{2}(\sigma_3' + \sigma_1')sin\varphi - cos\varphi \leq 0 \quad (3.23c)$$

$$f_{2b} = \frac{1}{2}(\sigma_1' - \sigma_3') + \frac{1}{2}(\sigma_1' + \sigma_3')sin\varphi - cos\varphi \leq 0 \quad (3.23d)$$

$$f_{3a} = \frac{1}{2}(\sigma_1' - \sigma_2') + \frac{1}{2}(\sigma_1' + \sigma_2')sin\varphi - cos\varphi \leq 0 \quad (3.23e)$$

$$f_{3b} = \frac{1}{2}(\sigma_2' - \sigma_1') + \frac{1}{2}(\sigma_2' + \sigma_1')sin\varphi - cos\varphi \leq 0 \quad (3.23f)$$

Where σ_i' is the effective stress and φ is friction angle.

The yield surface given by equation 3.15a-f form a yield surface in three dimensions, see figure 19.

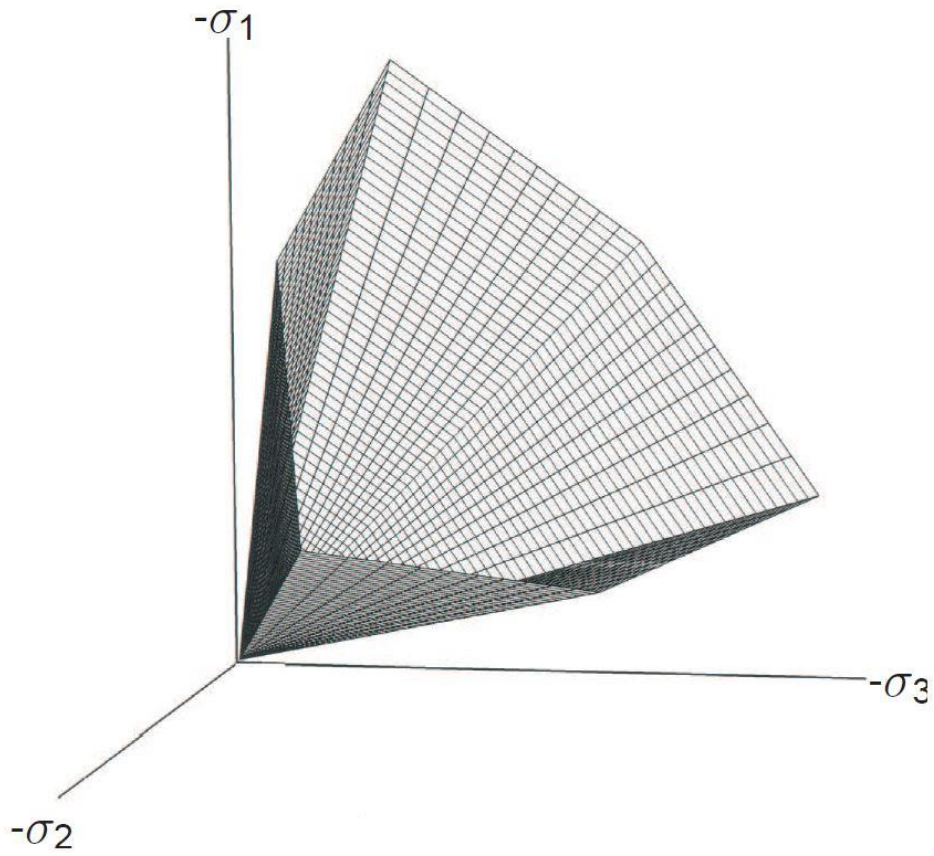

Figure 19 Mohr Coulomb yield surface in principal stress space (Plaxis 2011)

The Mohr- Coulomb model requires 5 input parameters (PLAXIS 2011).These are presented in table 4 below. All parameters can be obtained from standard test of samples.

Table 4 input parameters to the Mohr- Coulomb model in PLAXIS

Input parameter		Unit
E	Young's modulus	kN/m^2
v	Poisson's ratio	-
C	Cohesion	kN/m^2
ϕ	Friction angle	°
ψ	Dilatancy angle	°

NGI-ADP Model

The other material model used in the Plaxis analysis is NGI-ADP model. The name stands Norwegian Geotechnical Institute Active Direct Passive. The basics for the material model is input parameters for shear strength for three different stress paths, Active, Direct simple shear, Passive. Yield criterion is based on a translated Tresca Criterion. Elliptical interpolation functions for plastic failure strains for shear strengths in arbitrary stress paths, Isotropic elasticity, given by the unloading/reloading shear modulus, G_{ur} (Plaxis 2011).

The triaxial test is giving compressional and extensional results. This is corresponding to active and passive conditions in the soil material. This can be seen in figure 20 where the stress and strain from a compressional and extension results from a triaxial test is plotted. This is the same as the anisotropic conditions that is in the slope that is going to be evaluated.

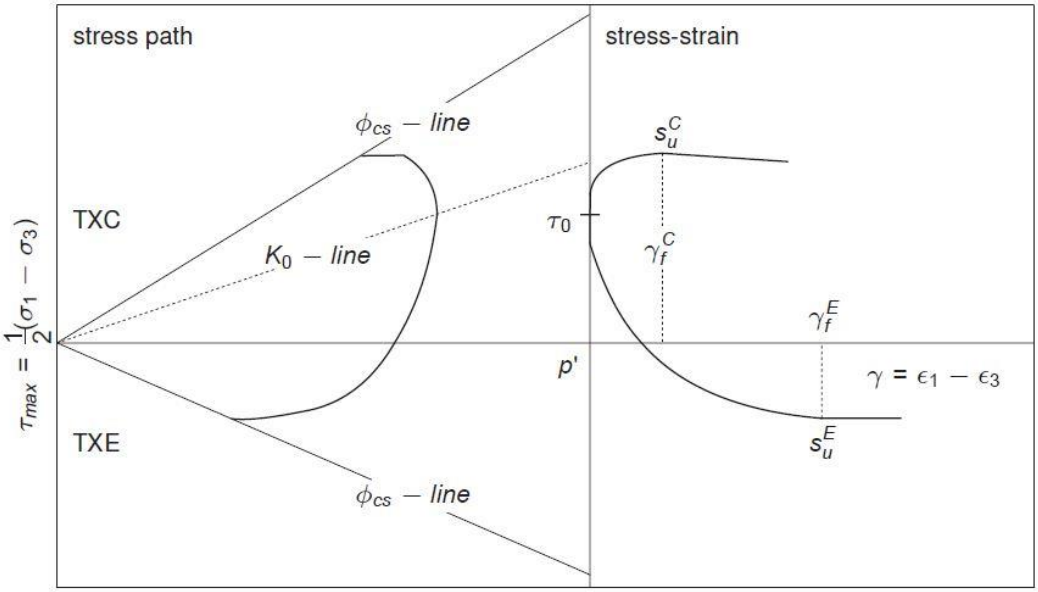

Figure 20 Stress paths and stress strain curves from triaxial test compression and extension showing active and passive conditions (Plaxis 2011)

The yield criterion in the NGI-ADP model is based on Tresca failure criterion. In plane strain the failure criterion is defined as equation 3.24.

$$f = \sqrt{\left(\frac{\sigma_{yy}-\sigma_{xx}}{2} - (1-\kappa)\tau_0 - \kappa\frac{s_u^A - s_u^P}{2}\right)^2 + \left(\tau_{xy}\frac{s_u^A + s_u^P}{2s_u^{DSS}}\right)^2} - \kappa\frac{s_u^A + s_u^P}{2} = 0 \qquad (3.24)$$

Where κ is defined as equation 3.25 for $\gamma^p < \gamma_f^p$ else κ=1.

$$\kappa = 2\frac{\sqrt{\gamma^p/\gamma_f^p}}{1+\gamma^p/\gamma_f^p} \qquad (3.25)$$

The strength parameters in the NGI-ADP Model are presented in table 5 below.

Table 5 the input parameters for NGI-ADP model with description and unit.

Parameters	Description	Unit
$s_{u,ref}^{A}$	Reference active shear strength	kN/m^2/m
$\frac{s_u^{C,TX}}{s_u^A}$	Ratio triaxial compressive shear strength over active shear strength	-
$s_{u,inc}^{A}$	Increase of shear strength with depth	kN/m^2/m
$\frac{s_u^P}{s_u^A}$	Ratio of passive shear strength over active shear strength	-
$\frac{\tau_0}{s_u^A}$	Initial mobilization	-
$\frac{s_u^{DSS}}{s_u^A}$	Ratio of direct simple shear strength over active shear strength	-
ν'	Poisson's ratio	-

GeoSuite

GeoSuite is a geotechnical software for calculate stability. The program utilizes BEAST methods to calculate stability, bearing capacity and earthy pressure problems. The analysis can be undrained, drained or combined and the slip surface can be non-circular, circular or combined. The BEAST methods include equilibrium, Bishops simplified and modified method. The program determines the critical slip surface by calculating several different surfaces and finding the most critical, the one with lowest F.

GeoSuite will be used in this report as alternative to check the Plaxis result. The program is not suited to make calculations were input parameters have to be varied. So the calculations will be used to confirm the Plaxis results so they are reasonable.

4 Benchmark Case

In this chapter two examples of how probabilistic models can be set up to show the theory in practice. Example 1 is a level 1 model of a slope stability problem and example 2 is a benchmark case utilizing a level 2 method where the programs Plaxis is used for the analysis.

4.1 Level 1 Example

This example is a slope stability problem that will be treated with a probabilistic approach. The example will be made with idealized conditions to keep it simple and focus on the probabilistic calculation method. Figure 21 is showing a principal idealization of the problem.

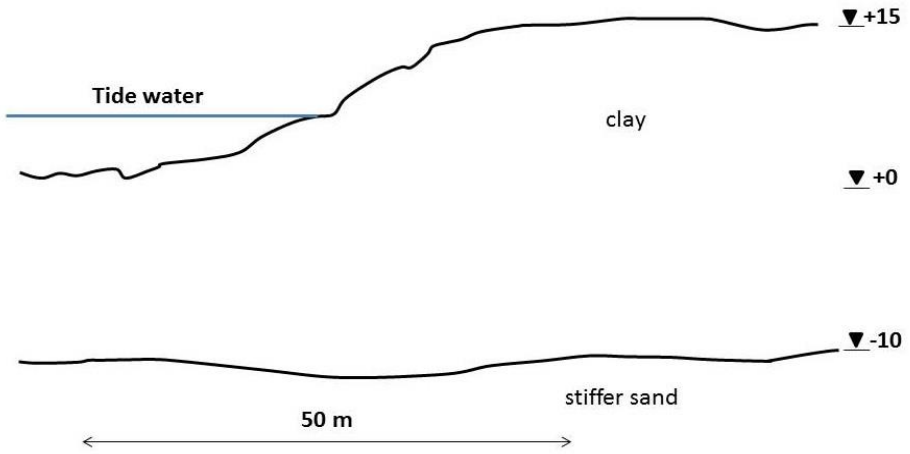

Figure 21 showing the geometry of the slope

Description

A long natural slope shall be evaluated for the risk of landslide. The slope is situated along a shoreline so that there is water on the toe of the slope. Predictions say that tide water levels on the slope may change in the future and this may affect the slope stability. The slope consists of soft clay on top of a stiffer sand material layer. The clay has a unit weight of γ=16 kN/m^3 and the water γ_w=10 kN/m^3.

In this example the factor of safety for the natural slope is to be evaluated. This is a traditional way to describe the safety for slope stability. In the probabilistic calculations the probability of failure is the criterion that is to be evaluated. This means p(F<1).

The slope is considered to be in a geologically active area with erosion by the sea bottom and therefore undrained analysis is made. Normally a drained analysis would be used when long term conditions are evaluated.

Conceptual model

To calculate the slope stability and the probability of failure a conceptual model must be set up. In this case the concept factor of safety can be chosen to idealize the case. The safety factor, see equation 4.1, is defined so that failure occurs if it is lower than

1. This was proposed by Janbu for undrained analysis. See chapter 3 for theory about the method.

$$F = \frac{N \cdot S_u}{P_d} \quad (4.1)$$

Where

N is the stability number given by the slope geometry.

S_u is the undrained shear strength.

P_d is describing the driving forces acting on the slope, see equation 4.2.

P_d, see equation 4.2, is taking loads on the slope, cracks in dry crust and the tide water levels acting on the toe of the slope into consideration. In this case there are no load only a natural slope therefore q is zero and μ_q is one. No cracks in the dry crust are considered in this case therefore μ_t is one. The low slope angle together with the ratio between slope height and tide water levels gives μ_w values of 0.99 to 1.0 for the varying tide water levels. Therefore this factor is set to one.

$$P_d = \frac{\gamma \cdot H + q - \gamma_w \cdot H_w}{\mu_q \cdot \mu_w \cdot \mu_t} \quad (4.2)$$

The chosen method will evaluate circular slip surface in the homogenous clay layer.

Now that the conceptual model is established the parameters in the model have to be set. In this particular case there is water pressure on the toe, therefore the denominator term have to include this meaning the equation looks like equation 4.3:

$$F = \frac{N \cdot s_u}{\frac{\gamma \cdot H - \gamma_w \cdot H_w}{\mu_w}} \quad (4.3)$$

Where γ_w is the water density and H_w is the water depth. The factors in the equation are treated as independent, lognormal random variables. Therefore the factor of safety is a sum of normal random variables

$$\ln(F) = \ln(N) + \ln(s_u) - \ln(P_d) \quad (4.4)$$

LnF is normal distributed with mean, equation 4.5, and standard deviation, equation 4.6.

$$lnF = lnN + lnsu - lnPd \quad (4.5)$$

$$\sigma_{\ln(F)} = \sqrt{\sigma^2_{\ln(N)} + \sigma^2_{\ln(su)} + \sigma^2_{\ln(Pd)}} \quad (4.6)$$

So the analytical solution will be to evaluate the safety margin in order to get a reliability index. The safety margin can be expressed as equation 4.7.

$$m = \ln(F) < 0 \quad (4.7)$$

Reliability Index β

In this case the beta index, β, is saying how many standard deviations there are until failure. See equation 4.8a and b.

$$\beta = \frac{\mu_{lnF}}{\sigma_{lnF}} \quad (4.8a)$$

The reliability index, β_F, based on the factor of safety

$$\beta_F = \frac{\mu_F - 1}{\sigma_F} \quad (4.8b)$$

Slope geometry

A geometry of the slope have to be decided, to cover the variations of how the geometry can be interpreted two different slopes is drawn. So N is a function of the angle of the slope, α, and the ratio between height of the slope, H, and depth to firm bottom, D, see equation 4.9 and figure 22.

$$N = f(\frac{D}{H}, \alpha) \quad (4.9)$$

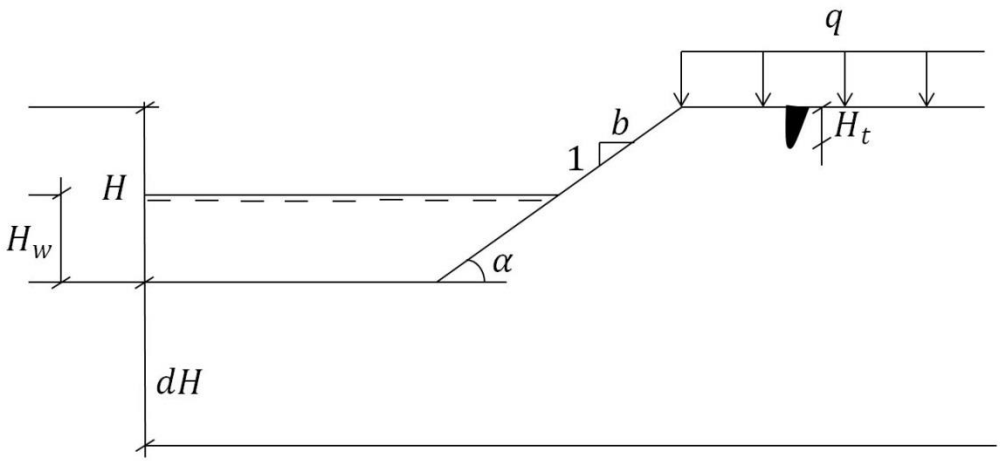

Figure 22 schematic figure describing the geometry of the slope when using Janbu's direct method

The height of the slope is the same, 12.9 m, the difference is the angle of the slope. The level of the slopes toe or bottom is also the same for both slopes. Slope number one has an angle of 14.8 degrees and slope number two 24.7 degrees. From this it is possible to go into the design chart to obtain the stability number, N. The stability numbers for this geometry is presented in table 6.

Table 6 stability number for the two slopes

Slope	H [m]	α [°]	D [m]	Stability number N
1	12.9	14.8	8.75	7.3
2	12.9	24.7	8.75	6.1

Variations of tide water levels

The water acts as a load on the toe of the slope and is therefore a force that is stabilizing the slope, so the future water levels are crucial to the slope stability. The predictions of the future water levels can be seen in table 7. The future water levels are modelled with the low water value as a mean and standard deviation is calculated with a 99 % confidence interval. The low value is chosen since it is the low levels that govern the risk for slide.

Table 7 the future predicted water levels.

Tide Level	[m]
High High Water	+11,5
High Water	+11
Medium Water	+10
Low Water	+9
Low Low Water	+8,5

Undrained Shear strength

In the clay deposit the average value of the undrained shear strength where found to be 25 kPa with a variance of 10 %, see table 8. An assumption to get a good coverage of the undrained shear strength from the samples is to take the average plus minus the standard deviation. This will cover 70% of the values (Alén 2013).

Table 8 average value of the undrained shear strength and variance

Undrained Shear strength	[-]
Average value	25 kPa
Variance	10%

Monte Carlo simulation

The uncertainties are modelled with a Monte Carlo Simulation to obtain the factor of safety. The parameters that will be simulated is water levels, stability number and shear strength. The simulation is made with 10 000 runs or iterations. The simulation is a little different for each parameter depending on the nature of a certain parameter. The water levels simulations are made so that a random variable that only can have values between zero and one is multiplied with normal inverse function of the parameter that is to be modelled in each run. The normal inverse function is giving the cumulative normal distribution for a set mean value and standard deviation. The different water levels will return a new P_d for each iteration run.

To model the shear strength an upper and lower strength is determined with a confidence interval of 70%. The upper and lower S_u is calculated with first take the average value from the site investigation and determine the low and high value with the 70% confidence interval. The high and low value is calculated with equation 4.10 and the standard deviation is calculated with equation 4.11.

$$S_{u,HI,Lo} = S_{u,Average} + (S_{u,Average} \cdot VAR)^2 \quad (4.10)$$

$$Standard\ deviation = \sqrt{(S_{u,HI} - S_{u,Average})^2} \quad (4.11)$$

The Monte Carlo Simulation returns a S_u that is iterated from the High and Low S_u for each simulation.

The geometry uncertainties are treated in the simulation by calculating a High and Low N value and take the average of these for every simulation run.

The factor of safety is then calculated with equation 4.3. A new F is given for each simulation run with the uncertainties modelled. The probability of failure is the obtained by check the probability that F mean from the 10 000 runs together with the standard deviation is smaller than one.

To validate the simulation 50 values of F from the simulations where taken out and mean value where taken.

Results

The factor of safety was determined to be 1.26 from the simulations. This can be compared with 1.21 if only mean values is used in the calculations. This was done to illustrate a set of parameters that is conservatively chosen. The probability of failure, meaning that F is smaller than 1 for the population in the 10000 simulation runs is 3.78%.

The safety margin and safety factor with corresponding standard deviation is shown in table 9. The reliability index corresponds $\varphi(-\beta) \approx 7.68\%$.

Table 9 mean, standard deviation and reliability index for the safety margin

	μ	σ	β
F	1.259	0.083	3.122
m	0.230	0.066	3.455

To check the effect of the factor of safety of each modelled parameter, N, S_u and P_d, a sensitivity analysis was carried out. In this analysis all parameters but one was kept fixed to the mean value to obtain a factor of safety.

All calculations can be seen in Appendix 1 where the Excel sheet is also provided.

Discussion

Probability of failure is said to be 3.78 % in this study. A failure of a slope does not necessary meaning a catastrophic failure, that should be remembered what a failure can be. What is interesting to consider is the reliability index as an evaluation of the factor of safety. A high factor of safety does not necessary mean that the slope is safe, just as a low factor of safety is not saying that it is near a failure. This argument can be showed graphic, see figure 23, the probabilities of failure is plotted against the factor of safety and the coefficient of variance of the safety factor is the lines. This figure is for a lognormal distribution of F.

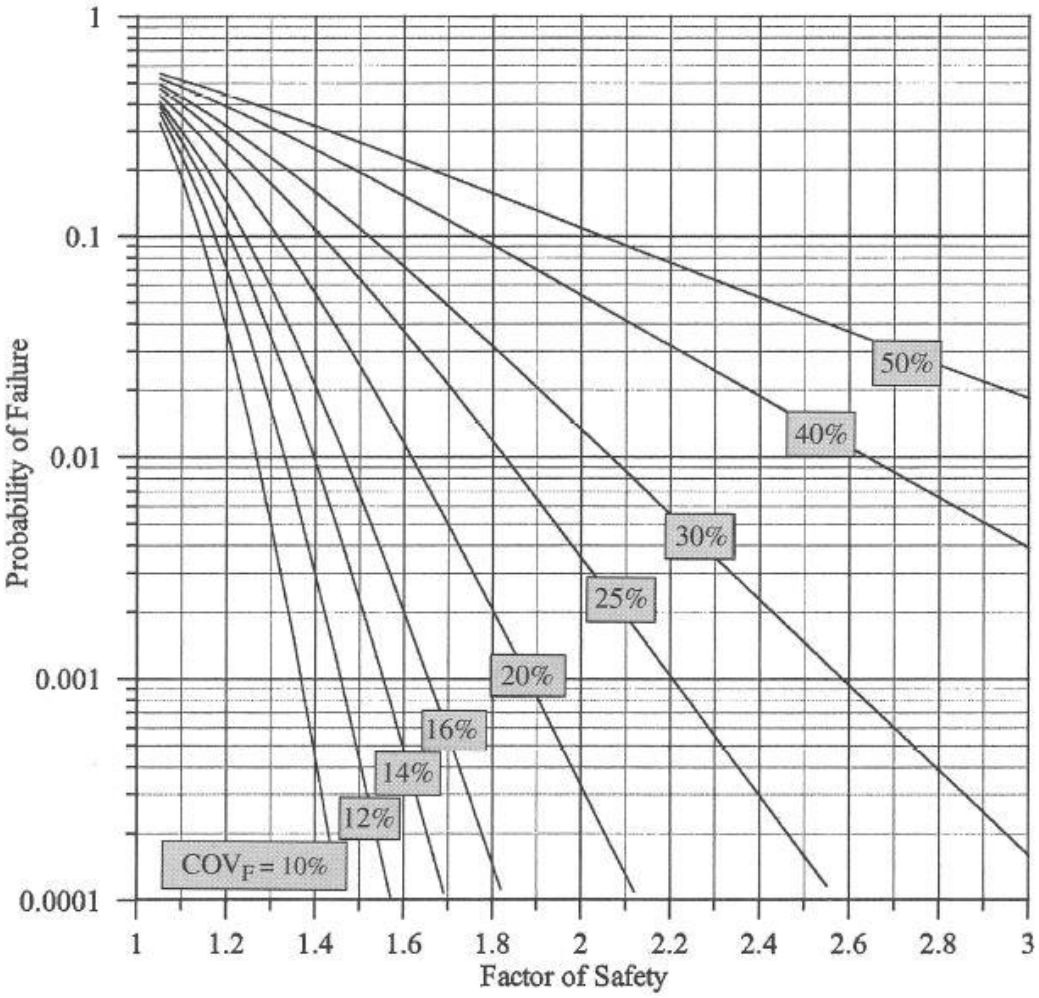

Figure 23 Probabilities of failure based on lognormal distribution of F

4.2 Example Level 2Plaxis model Benchmark case

The finite element method program Plaxis 2D is used to make an analysis to perform a benchmark case. The statistic calculations of input parameters are performed in Excel. This benchmark case is using ground investigation, laboratory test and geometry from a real case. This example will have simplified geometry since its purpose is to introduce the probabilistic approach to stability calculations and a more extensive analysis will be done in the case study. This also applies for the evaluation of data to the input parameters. Figure 24 is showing the idealization of the problem.

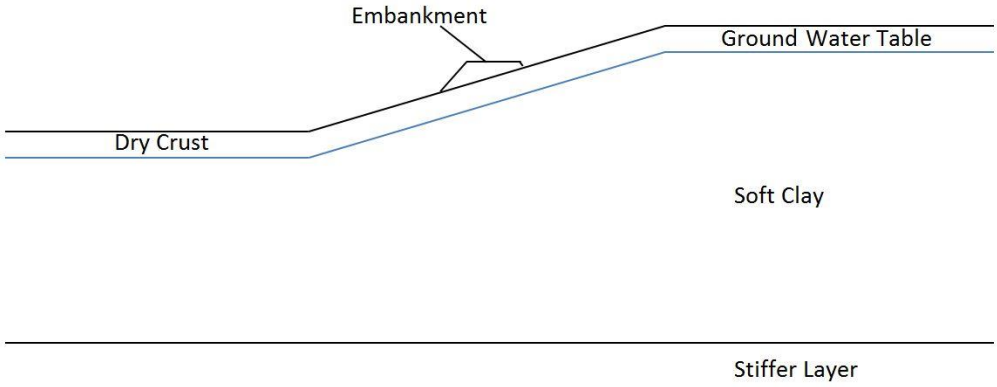

Figure 24 principal scheme of the problem

Set up

The Plaxis analysis is done with 3953 15-nodes elements. The model is divided into 9 clusters or zones to obtain realistic shear strength profile on the whole section. To calculate the initial stress conditions gravity loading has been used in Plaxis.

The numbers of steps used when the multiplier Msf is iterated have been set to 70. This is done to lower the time. The effect on Msf is not considered to be significant, when 90 steps where used Msf was 1.283 and 70 steps Msf was 1.284. This was with mean values on all variables.

The First Order Second Moment method is used for the statistical calculations of the input parameters. The method is described in chapter 2.3. In the FOSM the parameters for stiffness will be set to deterministic values since they will not affect the calculate stability.

Geometry

The profile is divided into nine different clusters. This is done to have a continuous shear strength profile through the whole model. The shear strength is in reality varying with the depth this is possible to simulate in Plaxis by using the $s_{u,inc}$ function, see equation 4.12.

$$s_u^A(y) = s_{u\,ref}^A + (y_{ref} - y) \cdot s_{u\,inc}^A \qquad (4.12)$$

Where y_{ref} is the reference depth for the inclination term of the shear strength. The clusters in the slope section have the reference depth set to the mid value of the height in the cluster. Therefore the more clusters a slope section is divided into the more realistic shear strength profile is obtained. However there is also a practical side to this, after a certain number of clusters the effect on the result is not so large that it is

motivated to make more, so this is a reason for limit the number of clusters. It is also possible to divide the geometry into horizontal clusters to further optimize the model. Down to the reference depth the shear strength is constant with depth.

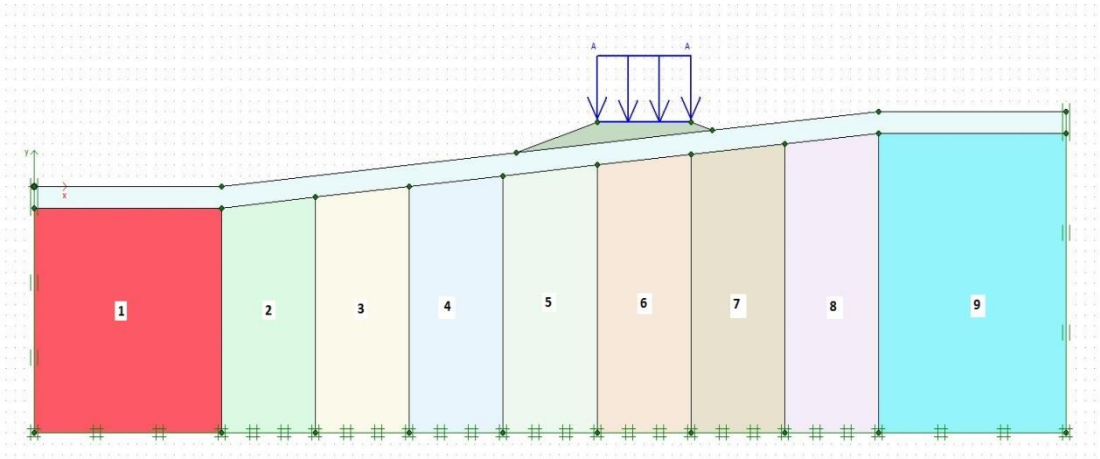

Figure 25 the geometry of the slope used in the Plaxis analysis showing the 9 clusters, dry crust, embankment and distributed load system.

The idealised slope profile is divided into nine clusters, two with flat top and seven in the slope section see figure 25. The bottom border is representing the rock surface and is impermeable and the inclination is zero. The slope inclination is 1:10. The top of cluster one is $\pm$0m and bottom is -23m. The top of the slope is at +7m. In the slope there is an embankment. The embankment is 2m as highest and the shoulder is 10m wide. On top of the embankment there is a distributed load of 13 kPa that is representing traffic load.

The top 2 m is dry crust, this was found out in from the CPTU investigations. The ground water surface level begins from the bottom of the dry crust and is hydrostatic all the way down to the rock surface.

Material model NGI-ADP Model

The material model used in the Plaxis analysis is NGI-ADP model. The name stands Norwegian Geotechnical Institute Active Direct Passive. The basics for the material model is input parameters for undrained shear strength for three different stress paths, Active, Direct simple shear, Passive. Yield criterion is based on a translated Tresca Criterion. Elliptical interpolation functions for plastic failure strains for shear strengths in arbitrary stress paths. Isotropic elasticity, given by the unloading/reloading shear modulus, G_{ur} (Plaxis 2011). More about anisotropy can be read in chapter 3.3.6. More about NGI-ADP model can be read in chapter 3.4

This model was chosen before Mohr-Coulomb model since NGI-ADP Model is considering anisotropy that is prevailing in Norway.

The strength parameters in the NGI-ADP are presented in table 10 below.

Table 10 the input parameters for NGI-ADP model with description and unit.

Parameters	Description	Unit
$s_{u,ref}^{A}$	Reference active shear strength	kN/m^2/m
$\frac{s_u^{C,TX}}{s_u^A}$	Ratio triaxial compressive shear strength over active shear strength	-
$s_{u,inc}^{A}$	Increase of shear strength with depth	kN/m^2/m
$\frac{s_u^P}{s_u^A}$	Ratio of passive shear strength over active shear strength	-
$\frac{\tau_0}{s_u^A}$	Initial mobilization	-
$\frac{s_u^{DSS}}{s_u^A}$	Ratio of direct simple shear strength over active shear strength	-
v′	Poisson's ratio	-

Input Parameters

The input parameters are evaluated from CPTU, 54mm samples and active triaxial test see table 11.

Table 11 input parameters with mean value and standard deviation.

Material	Parameter	Mean value	Standard Deviation
Clay	$s_{u,ref}^{A}$	24	4.8
Clay	$s_{u,inc}^{A}$	1.5	0.08
Clay	$\frac{s_u^P}{s_u^A}$	0.359	0.106
Clay	$\frac{s_u^{DSS}}{s_u^A}$	0.623	0.058
Clay	γ	19.5	0.68

Undrained shear strength profile

The shear strength profile is based on fourteen CPTU tests and 54 mm samples see figure 26. To determine $s_{u\,ref}^{A}$ the triax results are considered to be more trustworthy and the inclination in shear strength profile is given from evaluation of CPTU. The values in the top meters, see figure 26, is spread and this is most likely due to that there is a dry crust in the levels meters. Therefore y_{ref} is set to consider this. The data from the ground investigation gives y_{ref} values around 1,5m below the dry crust.

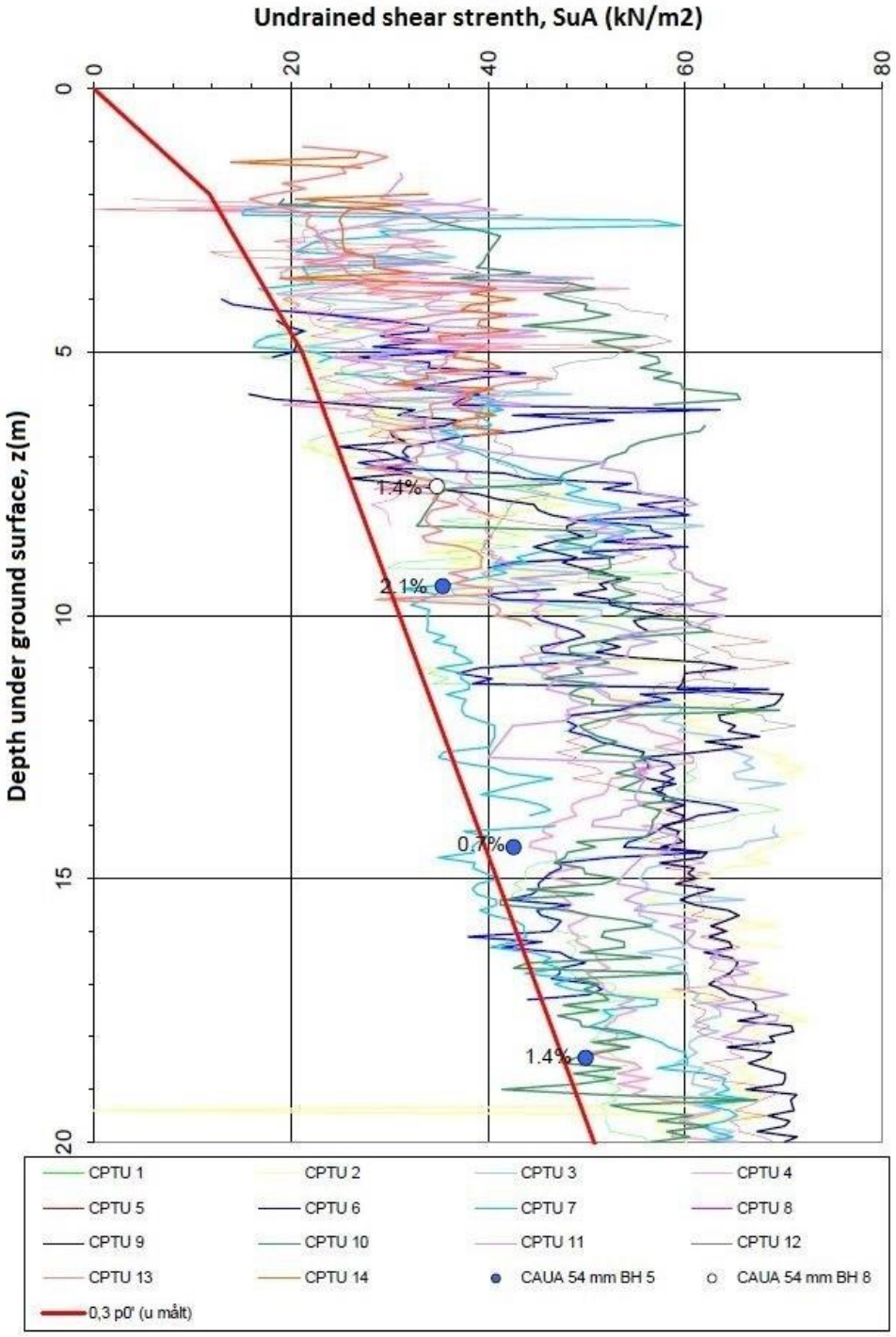

Figure 26 the results from the CPTU and active triaxial test on 54 mm samples (NIFS B 2012).

FOSM

In the analysis is each variable treated as independent of each other and normal distributed. The stability calculation is performed deterministic in Plaxis with mean values for all variables and for each run is one variable increased or reduced with one tenth of the standard deviation. The c/φ-reduction in Plaxis with Msf multiplier is used to obtain the global safety factor F. For each calculation a safety factor is obtained and a mean value and a standard deviation of the safety factor. The probability of failure is the checked as the probability of F is lower than 1. The variables can be seen in table 12.

To get the standard deviation of safety factor the equation 4.13 is used:

$$\sigma_F = \sum \sqrt{\left(\frac{\Delta F}{\Delta X}\right)^2 \cdot \sigma^2} \qquad (4.13)$$

Table 12 FOSM Analysis.

Material	Parameter	X*	std.dev	Dx	X*+DX	X*-DX	F+	F-	dF/dX	(dF/dX)^2xσ^2
Clay	Su,ref	24	4,8	0,48	24,48	23,52	1,301	1,266	0,035	0,0282
Clay	Su,inc	1,5	0,08	0,008	1,508	1,492	1,285	1,281	0,004	1,02E-07
Clay	Su,DSS/SuA	0,623	0,058	0,0058	0,6288	0,6172	1,289	1,279	0,01	3,364E-07
Clay	SuP/suA	0,359	0,106	0,0106	0,3696	0,3484	1,286	1,282	0,004	1,798E-07
Clay	γ	19,5	0,68	0,068	19,568	19,432	1,281	1,288	-0,007	2,266E-05
										0,0282
									σF	**0,1681**
									pf	0,0456
									pf %	4,56 %
									Beta-index	1,689

Results

The results are a probability of failure of 4.56 % and a beta index of 1.689. The beta index is defined as mean value of F minus 1 over standard deviation of F.

The parameter that got the largest effect on the safety factor is S_{uref} The difference in safety factor where 0.035.

Discussion

From this benchmark case it can be seen that the parameter that have the greatest influence on the factor of safety is Su,ref. The effect on the factor of safety for the variation input values can be seen in table 13.

Table 13 variation of factor of safety from the simulation

Parameter	X*±ΔX	F
Su,up	24,48	1,301
Su,low	23,52	1,266
Su,inc UP	1,51	1,285
Su,inc LOW	1,49	1,281
SuDSS/SuA Up	0,629	1,289
SuDSS/SuA Low	0,617	1,279
SuP/SuA Up	0,3696	1,286
SuP/SuA Low	0,3484	1,282
γ_low	19,432	1,288
γ_Up	19,568	1,281
	Mean F	**1,284**

The mean value for the safety factor is 1.284 from the simulations and this is too low for many standards to meet the recommendations. But what can be seen is that the standard deviation of the safety factor is rather low and that gives a high beta index.

5. Case study

The case study will be done to evaluate the slope stability depending on the methods used when the ground investigation and the laboratory test to determine the input parameters. The case study is based on material from a real case. The different methods used in the old praxis will be compared to the new praxis, the differences will lead to differences in the uncertainties in the parameters. In the case study the uncertainties in the geotechnical parameters for different levels of investigations will be coupled to reliability and the uncertainties is quantified. The probability of failure will for the slope will be calculated with input parameters from old and new praxis that is defining the two scenarios used in the case study.

5.1 Description of Rissa area

The Rissa area is a very interesting area from a Geotechnical perspective. The ground conditions are very complex with sensitive clay and quick clay. In 1978 there was a big landslide here known as *The quick clay landslide in Rissa* (Gregersen 1981). The slide area covered 330 000 m^2 and the masses were 5-6 million m^3. After the slide have a lot of research been done in the area to study the event.

The Norwegian Road Public Roads Administration plans to build a new road, FV.717, between Sund and Bradden at Rein Kirke in the Rissa Area northwest of Trondheim in Sør-Trønderlag County. The land stretch is located between the lake Botn, to the east, and the sea in the west. The planning works started in 2009 but where halted due to the geotechnical challenges of the project. The planned road is passing a slope long slope of low inclination, which consists of clay material. The analysis that was done indicated very low slope stability and therefore it was decided that new investigations of high quality had to be made to evaluate the slope. In the new investigations 54 mm Sherbrook samples were used together with the previous investigation and laboratory material.

The ground investigation methods that is used is CPTU, 54mm piston samples, and block samples. There were also electrical resistivity measurements, R-CPTU, to evaluate the layer structure.

5.1.2 Regional geology

The regional geology in Sør-Trøndelag County is strongly characterized by the last glaciation period, Weichsel, that had its maximum extension for 22 000 years ago (Andréasson 2009). The glacial did cover large parts of Scandinavia and the major part of Norway. When the glacial started to melt and draw back the glacial till where formed at the ice front. These deposits where formed along the Norwegian cost.

The glacial moved in north west direction in Sør-Trøndelag until the thickness made the glacial movement be governed by the topography. Then the glacial where left in the fjords and large valleys in the area. The Sør-Trøndelag coast were free from ice 12 500 years ago but the melting process where halted and the glacial front stood still end moraine where formed along the whole coast stretch of the area. By 11 000 years ago it was glacial on both sides of the Trondheim fjord. The glacial front moved back and forward between year 11-10 000 this can be seen from the end moraine formed during this time period. The deglaciation in Sør-Trønderlag was finished 9000 years ago. When the burden of the ice disappeared the land heave started. Today the heave is 2-3 mm per year.

The soil materials in the area are characterized by the processes and circumstances that formed them. The moraine was formed under the ice and the glacial till was out washed in the ice rivers where the fluid was decreasing. Large parts of the Trondheim area are old seabed that is land today due to the land heave that is around 200 m in the area. The layer structure is related to how strong the currents have been in the area. Where the currents have been higher like the narrower fjords the layer structure is more mixed and in the more opened areas the layers aren't so mixed. Clay silt is varying with thin layers of silty sand. These fractions where formed during periods of high fluids of melting water. In the Trondheim region the clay thicknesses is often more than 50 m and contains elements of sand, stones and block. This might indicate that it was formed close to the glacial front.

The most of the sea and fjord deposits in the area is composed of 25 to 50% clay and locally over 50%. The content of silt is varying between 30 to 70%, the remaining material is sand, small amount of gravel, stones and block (Reference 33 Kornbrekke).

5.1.3 Rissa quaternary geology

The area around Lake Botn is covered by a thick layer of sea deposits, see figure 27. These sea deposits sit directly on the rock surface. The other dominating soil type is the marine deposits who cover the western parts of the area, the whole stretch from north to south. The marine deposits where formed when the glacial where retreating approximately 12 500 years ago. The Rein monastery is situated directly on the rock surface. There are some areas with peat and bog in the areas with sea deposits.

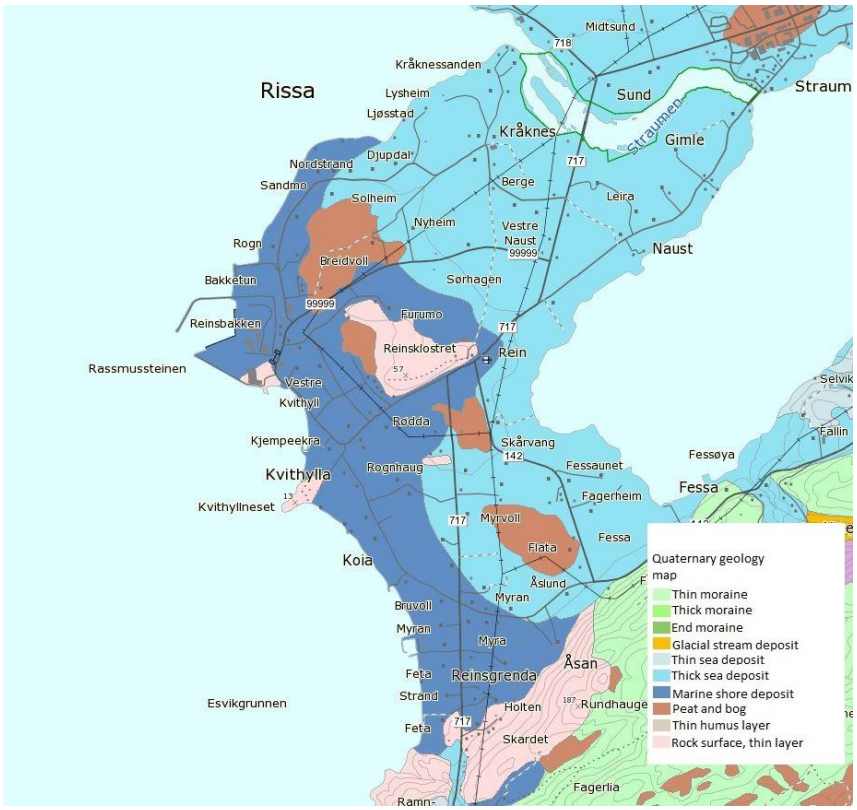

Figure 27 Quaternary map of the area (NGU 2014)

The Glacial had melted in the Rissa area around 9000 years ago. After that the land heaved around 158 m over the former coastal line. The land heave has exposed the marine clay for fresh water that have washed out the salt and lowered strength. This have led to that quick clay has been formed in some parts of the area.

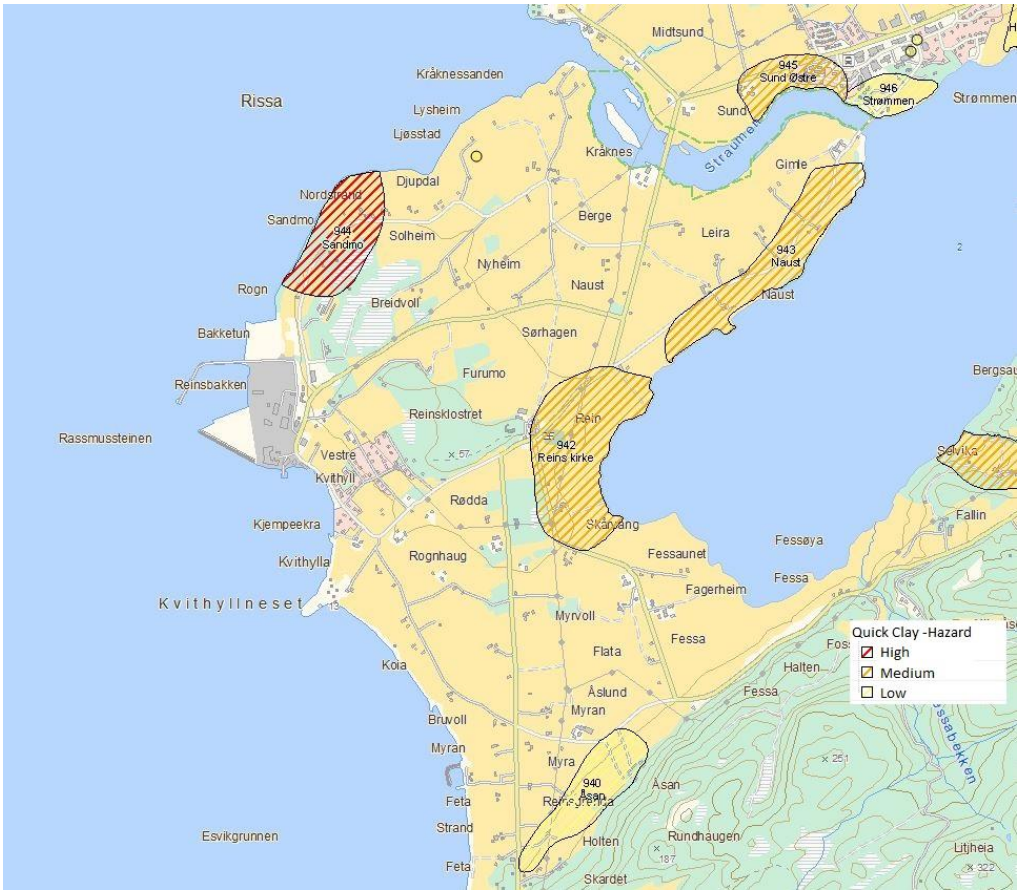

Figure 28 the quick clay areas is evaluated risk for landslide (NVE 2014).

Figure 28 above shows zones where there is risk for landslides in quick clay. The levels of hazards are representing the probability for a landslide from high to low. The risk levels is based the conditions of topography, geotechnical and hydrologic. The area of the case is situated in the medium risk level area. Medium level means that the topography is not so beneficial, there are active erosion in the shoreline and considerable landslide activity.

5.1.4 Quick and sensitive clay

Quick clays is forming when the sedimentation of particles is done in saltwater. The clay particles are of small grain size and is of a flat shape and form a structure with large pore space between the grains (Nelson 2012). Grain sizes for clay particles is less than 0.002 mm (Sällfors 2009). When the clay particles is exposed for saltwater the clay particles becomes electrical charged. This charge makes the particles form bindings in a structure that is referred to as a house of cards structure (Kornbrekke 2012). Since the sedimentation process is under water the pore space is filled with saltwater. The structure is stabile as long as the pores are filled by saltwater. But during the land heave in the area the clay has been exposed for erosion and saltwater

was washed out. When the salt content is lowered in the clay the structure in the clay is becoming more unstable.

Quick clay can take stresses in vertical direction but it is weak in taking shear stresses.

5.1.5 Sensitivity

The clay material in the Rissa is a sensitive clay. This means that if the structure of the clay particles is changed it will lose much of its strength. "The sensitivity of a soil is defined as the ratio of the undrained strength in the undisturbed state to the undrained strength, at the same water content, in the remolded state"(Craig 2012). To be a sensitive clay the sensitivity, S_t, have to be higher than 4. Quick clays can have a value of 100. There are no end of the scale for sensitivity value but higher number than 100 is rare. The sensitivity of a clay have a correlation with the liquidity index, I_L, can be calculated with equation 5.1 (Bjernum 1960). This equation is derived from test data where the sensitivity is checked against the liquidity index. The plot indicates a linear correlation, See figure 29.

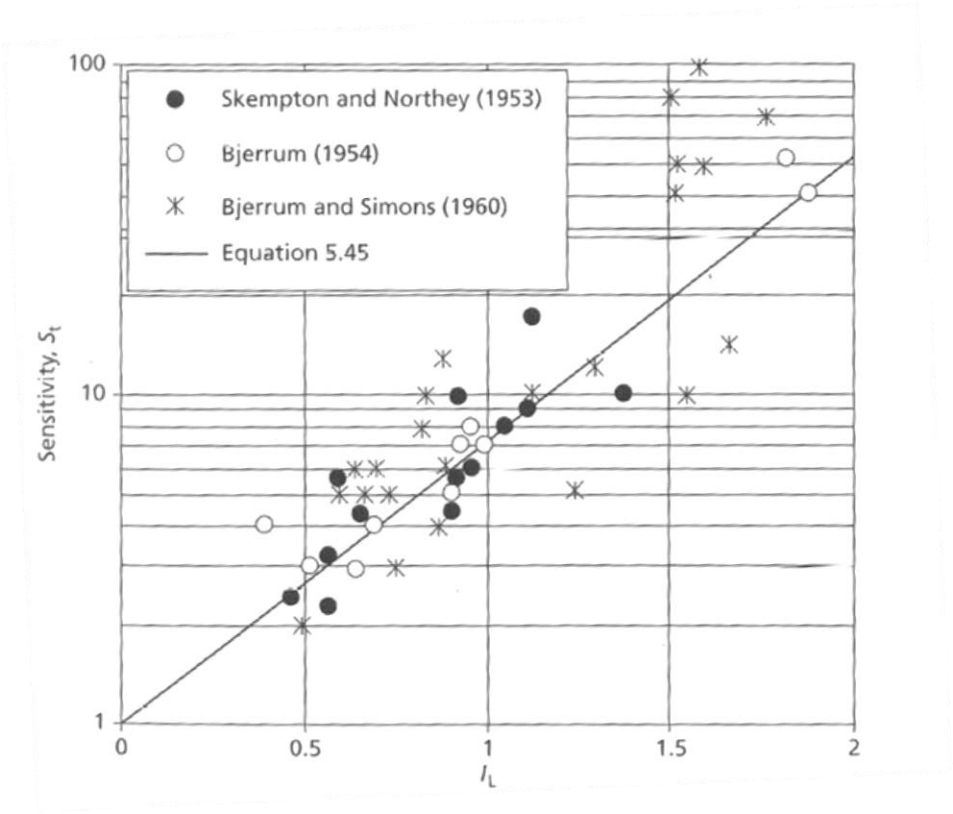

Figure 29 Correlation of sensitivity S_t with index properties (Craig 2012).

$$S_t \approx 100^{0.43 I_L} \quad (5.1)$$

The classification system according to Craig have limits by sensitivity 4, 8 and 16, see table 14, but there exist several definitions on where the limit between the different classes shall be.

Table 14 Sensitivity classes for clays (Craig 2012).

Clay	S_t
Normal Clay	1-4
Sensitive Clay	4-8
Extra sensitive Clay	8-16
Quick Clay	16->100

5.1.6 Quick clay slides

The behavior of a quick clay slide is different from normal clay. The failure modes in quick clay are retrogressively slide or flake-type slide (Gregersen 1981).

A retrogressive slide starts with an initial slide occurring and the shear stresses behind increasing and trigger new slides that is moving backwards from the front of the initial slide.

The slip surface in a Flake type slide is a thin layer of clay where the sliding plane is formed. Flake type slides can have several sliding planes (Solberg 2007). So there exists a critical slip surface that needs to be evaluated.

5.1.7 Brittle material

Brittle failure in clay is when the shear strength is reduced during deformation in undrained conditions after a failure (NPRA 2010). Material that is classified as brittle material have this characteristics that the shear strength is much reduced when it is exposed for deformations. Soil types that have this behavior is both clays and silt material. This materials have a sensitivity of 15 and remolded shear strength less than 2 kPa. Quick clay is a type of brittle material with remolded shear strength less than 0.5 kPa.

When the peak value in shear stresses is reach the reduction is started, this is also referred to as strain softening see figure 30.

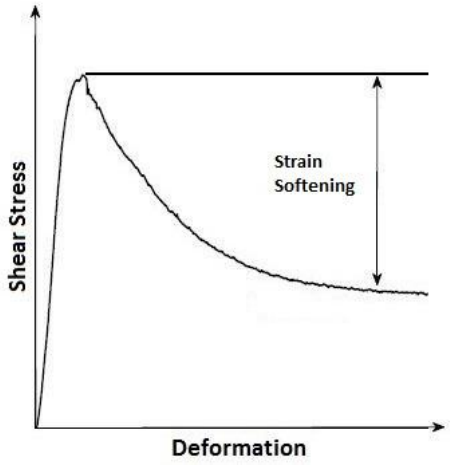

Figure 30 reduction in shear strength of brittle material when deforming.

5.2. Geotechnical investigations

In this chapter the geotechnical ground investigation methods and the laboratory test that is used in the case study is described. The field investigation methods are CPTU, piston sample, Sherbrook block sample and electrical resistivity, the laboratory test are block tests, oedometer test and triaxial test. These investigations have been previously used in a master thesis, *Slope stability at Rein Kirke based on results from Sherbrooke block samples* by Helene Alexandra Kornbrekke. In her thesis the characteristics of the ground investigation can be read more detailed. Figure 30 shows where the samples were taken. The results from the ground investigations can be seen in table 19 -22.

5.2.1. Ground investigations

The ground investigations have been performed by different times. NGI made the first ground investigations in 2007 in connection with the first detail planning of the project. Additional investigations were made by NGI 2009.

The NGI ground investigations showed that there was much quick clay in the area. Therefore NGI performed an analysis of the degree of risk for landslide in 2011 based on data from their own investigations and ground investigations that NPRA have made 1974 to 2009. The areas with the highest risk are at Reinsalléen by Åsen. The road construction where planned to pass Reins kirke but where halted due to the risk levels that were exceeding the regulations.

NGU in cooperation with a master student from NTNU made electrical resistivity measurement in 2009 to 2010. From these eight 2-D resistivity profiles where made. In 2011 NGU continued the geophysical investigations and made a seismic refraction measurement where the Lake Botn was mapped. In 2012 NGU performed complementing resistivity measurements by Rein kirke and made twelve new 2D profiles.

In 2011 Geo-Vest Haugland and Multiconsult performed extensive ground investigations in the area between Rein Kirke and Lake Botn. In 2011 there were taken 4 block samples by Botn from depths between 3 to 4 m, 3 of the samples contained clay material.

NGI 2007-2009

The ground investigations that were performed were CPTU, total sounding and samples were taken. Due to the difficult conditions additional investigations were made in 2009 with 72 mm samples to reduce the effect of disturbed samples.

CPTU results were in general of poor quality. Application class for friction was 4, cone resistance varied between class 2 and 4 and pore pressure varied between class 1 and 4. The response of the pore pressure was in general useable, but many test had poor response. The inclination was not measured. See table 21 for summary of test results.

Based on eight oedometer test from the area the conclusion that the soil material was approximately normally consolidated. Three triaxial test were conducted in the area and they showed somewhat lower values than SHANSEP based test with α=0.3 an m=0.8 that was determined from test in the vicinity at Rein tunnel. It is assumed that the deposits at Rein is the same as the ones at Reins tunnel. The anisotropy conditions

used was $Su_D/Su_A=0.67$ and $Su_P/Su_A=0.33$. Table 15 is a summary of parameter values used by NGI.

Table 15 summary of the routine investigation made by NGI 2007-2009 (NGI 2009 A)

		Sensitive Clay	Non-Sensitive Clay
S_t	[-]	19.86	5.6
I_p	[%]	8.9	13.4
γ	[kN/m^3]	19.7	
a	[kPa]	1	
ϕ	[^{o}]	29	

Based on these parameter values where the slope stability by Rein church calculated. The critical safety factor at profile 3-3 was 1.04 and 1.01 at 5-5, see figure 30.

In 2011 was an evaluation of the geotechnical difficulties based on earlier made investigations made in the area by NGI and NPRA 1974 to 2009. The area that have the highest degree difficulty was at Reinsalléen by Åsen. In an area by Rein Church it was found out that the stability was so low according to regulations that road construction is not allowed. This led to that the project was halted.

NTNU 2009-2010

NTNU together with the NPRA have made several ground investigations in the Rissa area together with masters students of NTNU. One of the students where Kristoffer Kåsin that conducted several CPTU's and test series. His conclusions were that the area was more over consolidated than previously assumed. Values for undrained shear strength were also found to be higher than the former values.

The CPTU results were of higher quality than previous tests made by NGI and are therefore used together with newer ground investigations. The survey included CPTU, 73 mm and 54 mm cylinder samples, that was judged to be of good quality. The CPTU graphs can be seen in appendix 2 named KK1, KK3 and KK4.

The sample quality was conservatively estimated based on earlier available results. The quality was reconsidered and sample disturbance was taken into account later. A summary of the results can be seen in table 21 and 22.

2011

NPRA commissioned Geo- Vest Haugland to take CPTU sounding and 54 mm cylinder samples in a new ground investigation where the critical areas had been identified from previous investigations. These were profile 3-3 and 5-5 that can be seen in figure 30. The CPTU results were of high quality and was used as basis for correlations. Multiconsult made special tests on some of the 54 mm samples but some of the samples were disturbed and were judged to be less trustworthy.

By the autumn of 2011 were four Sherbrooke block samples taken by C3 in figure 31. Three of them contained clay the four block samples that were taken three contained clay.

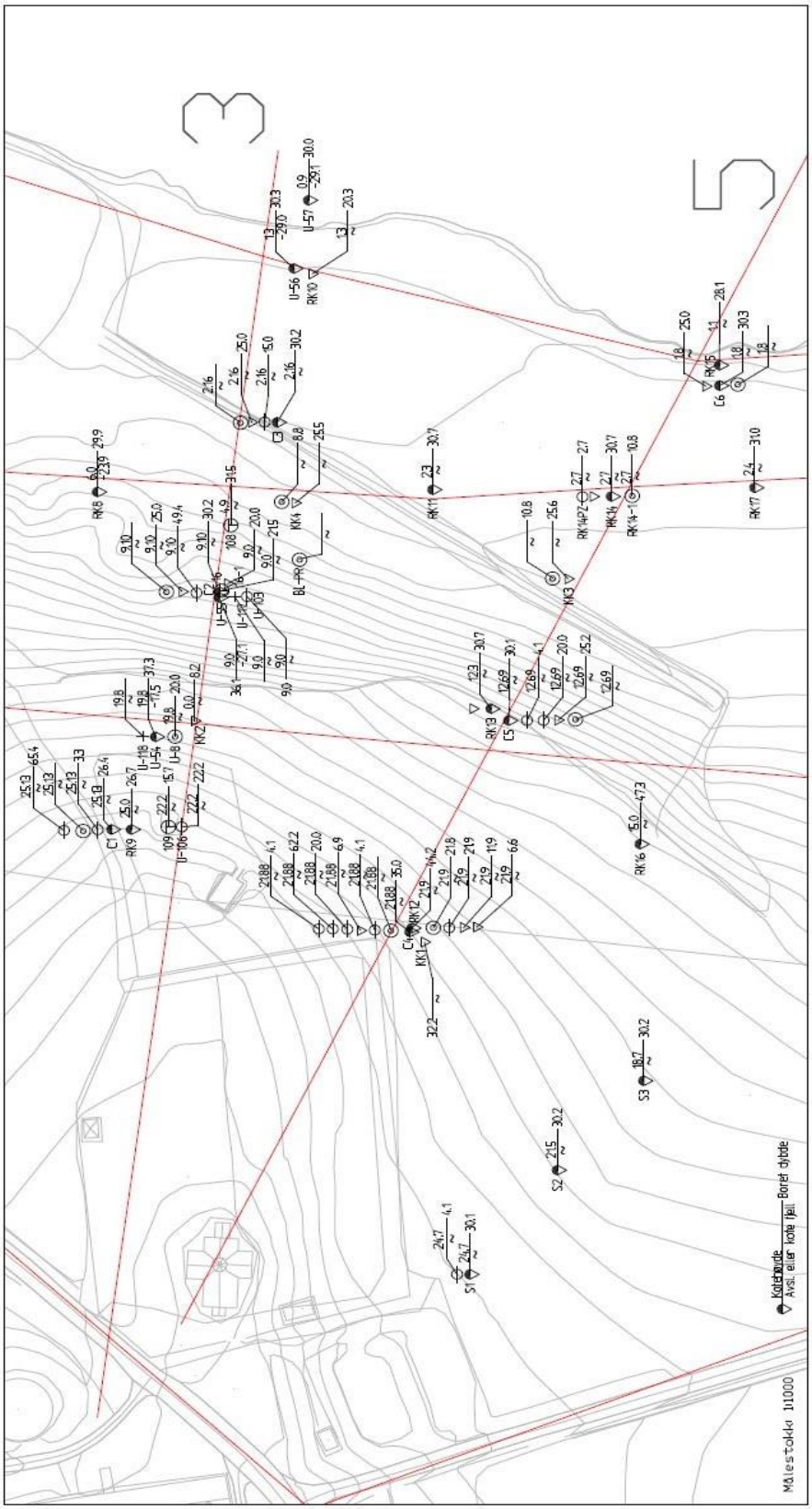

Figure 31 map showing where the samples were taken at the site (NPRA 2012)

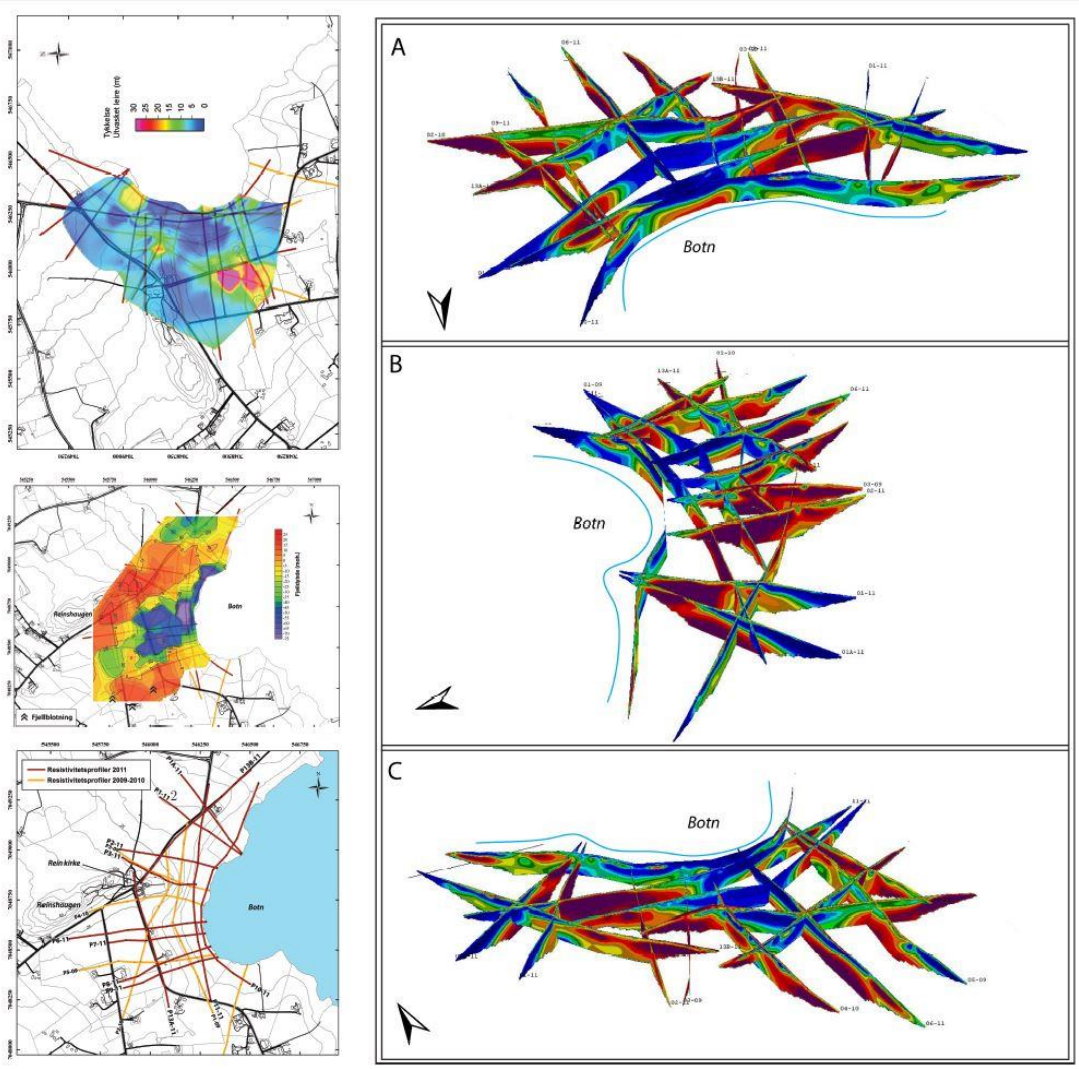

Figure 32 view of the area showing where the resistivity measurements made by NGU and 3D representation of results by Rein church (NGU 2012).

The first resistivity measurements at Rissa were made 2009-2010 by NGU in collaboration with a master's student from NTNU. The made 8 2D resistivity profiles 5 of them were by Rein Church, see figure 32. In 2011 were a number of new profiles made in the same area. In total there existing 17 resistivity profiles in the area that is less than 1 km^2, this is the most extensive resistivity investigation ever made in Norway to map quick clay (NGU 2009).
The investigations concludes that electrical earthing conditions are in general good with exceptions were the profiles is crossing roads and the data quality is consistently very high. Table 16 is showing the base for classification of the soil from resistivity values.

Table 16 Basis for classification of material from resistivity values (NGU 2012).

Resistivity value	Material	Color	Description
1-10 Ωm	Non-out washed marine clay deposits	Blue	The clay has been little exposed for out washing after the deposition. Pore water is still containing large quantities of ions that stabilize the structure and gives good conductivity and thereby low resistivity. Minerals with high conductivity as sulphides, graphite and other sediments saturated with water rich of ions can also give low resistivity values
10-100 Ωm	Out washed marine deposits	Green, Yellow	Out washing of clay leads to fewer ions in the pore water and with salt content lower than about 5g/l can quick clay be formed. Resistivity values are still low but higher than non-quick clay, clay moraine and silty sediments can also be in this interval.
100+ Ωm 50-150 Ωm 150+ Ωm 1000 + Ωm	Dry crust Silty soils Sand, Gravel Rock	(Yellow),Orange Yellow, Orange Orange, red, red to purple	Dry crust, clay that has been in a landslide, sand and gravel will have higher resistivity values. Water content in the sediment will be of importance for conductivity. Rock have in general resistivity values of many thousands of Ωm, but fractured rock and rock types with high content of ore may have significantly lower resistivity.

Figure 32 is a 3D visualization of the resistivity profiles by Rein Church. In the investigated area a clay deposit in a rock depression with sand of some meter thickness on top of the slope. The blue color is representing marine clay that have not been out washed and as can be seen in figure 32 it is large quantities of this soil in the middle of the rock depression. Yellow and green color is out washed clay that have a salt content about 5g/l and could be quick clay. This layer is in the border between clay and rock, which is common since the rock surface is acting as a drain on the clay.

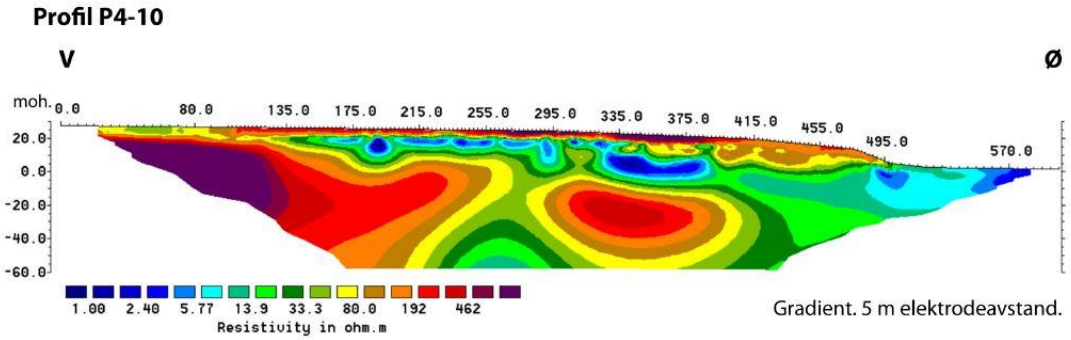

Figure 33 resistivity profile P4-10 geotechnical profile 5-5 (NGU 2011)

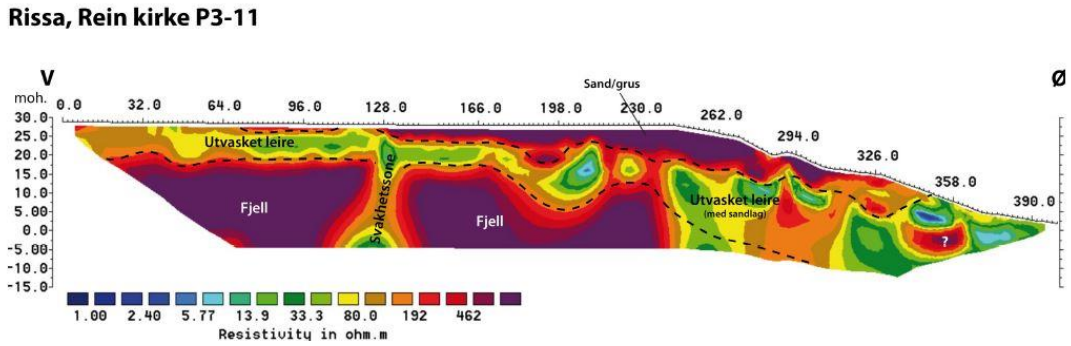

Figure 34 resistivity profile P3-11 geotechnical profile 3-3 (NGU 2011)

Profile P2-11 is situated 40-125 m away from profile P3, see figure 33. The rock is close to the surface with large amount of out washed clay on top of the slope and about 5 m of dry crust on top. There are some sand and gravel closer to the lake Botn and large amount of quick clay close to the waterside. It looks like the rock has a fractured zone with soil material that have the same inclination in all profiles. Profile P3-11 is situated by Rein Church and corresponds to profile 3-3 in figure 31. The rock has the same position here as in profile P2-11. This profile contains more sand, gravel and out washed clay. Soundings indicate clay next to Botn contains sand layers and that some of the clay is classified as quick clay. The profile is also showing pockets of clay containing salt. Profile P4-10 is also situated by Rein church but on the other side related to profileP3-11. This is corresponding to profile 5-5 in figure 31. It shows same conditions as in p3-11 without washed clay over the rock surface and a sand layer of some meters in thickness on the top of the slope. Between these layers there are several pockets of salt containing clay. It is also salt containing clay on the surface of Botn but this is more out washed with depth and closer to the rock surface.

Figure 32 shows the top layer of the out washed clay. It is about 20 m in the middle of the slope between Rein church and Botn but there is also a layer of out washed clay between salt containing quick clay and more coarse material. Out washed is mostly over the level of Botn that have the level ±0 in this study. The reason for this could be the rock surfaces topography under the deposits have importance for ground water and pore pressure conditions in the area.

There are large deposits of thickness up to 1 m of sand and gravel in the middle of the slope between Rein church and Botn, about the same place where the top layers of out washed clay is. There are large sand and gravel deposits in this are that might have acted so that the clay is more out washed right here. The clay contains much sand.

This is not shown in the resistivity profile but this can give higher resistivity values. Figure 32 is also giving guidance in the depth to the rock. The local geology is complex with undulated rock surface with varying rock types (NGU 2010). Two parallel rock ridges were interpreted in North East to South West direction and the depression between them is up to 75 m. The depth to the rock have great uncertainties depending on varying resistivity and deformed rock and therefore shall this depth not be regarded as absolute (NGU 2012).

In 2010 have NGU carried out mapping of the lake bed with high resolution and has collected 2D reflection seismic profiles in Botn as research and development project to map slides in shorelines. There are traces of earth slides under the water level in the lake along most of the water front around the lake. This can be seen due to the characteristic bowl like shapes left from the landslide.

The southern part of Botn is characteristic by the thick sea and fjord deposits. There are also registered quick clay zones by Rein church and by Naust. The slopes in the shore area are 150 to 400 m long and 20 to 25 m high. The reflection seismic shows that the lake bed is governed by the rock surfaces topography with NE-SW oriented ridges. The slope angel is smaller than 15° (NGU 2011).
In the Ryl bay there traces of a 20 m wide and 1 m deep canal shape that is over 250 m long. This could have been formed erosion from the stream Rylbekkens mouth but it is not certain that it is active.
The top outside Hestrøa is the top of the slope even the first 100 to 130 m and thereafter is the lake bed sloping steeper with an inclination up to 25°. By the toe of the slope there are several pocket marks that is circular depressions that is formed when flow of gas or liquids are coming out from the underground for a short time period. This corresponds with the pore pressure that where measured by NGI in 2009 and can be related to ground water flow to the lake (NGI 2009B). The sediments are of a thickness up to 25 m over the rock at Hestrøa were 7m is glacial marine deposits, sediments that have been deposited of the melting glacier during the last glaciation of the area. Over this layer there are a mixture of sea and fjord deposits and soil exposed for landslides. It can also be traces of a stream mouth that was here for 2000 to 3000 years ago (NGU 2011).

5.2.2 54 mm samples Standard piston sampler

The 54 mm cylinder samples are a common method used in Geotechnical investigations in Norway. The sampler was developed by NGI in the late 1970's. It takes cylindrical samples soil samples that later is analyzed in laboratory to get the soil parameters. The sampler is made of a composite piston sampler with plastic inner tubes (Long et al 2009).

There are also cylinder sampler in larger dimensions, 76 mm, 95 mm, and 120 mm, but the 54 mm is the most used. The larger dimensions can be used when there is a certain need for samples of higher quality.

5.2.3 Sherbrooke Block Samples

The method was developing by Quebec University between 1975 to 1978. A Sherbrooke sampler is shown in figure 35. It functions so that a cylindrical sample with a diameter of 250 mm and height of 350 mm is taken from the ground. When this is done the borehole must be of 450 mm in diameter and filled with water for ensure the stability. When the borehole is made a planer is used to smooth the surface before the Sherbrooke sampler is put down. The Sherbrooke is cutting the sample and lifts it up to surface level. The sample is the wrapped in plastic to conserve the material properties and taken to the laboratory. The sample is divided at the laboratory into different sizes depending on what test that shall be performed (Kornbrekke 2012).

Figure 35 from left to right, Sherbrooke samples, planer, a sample at laboratory (Kornbrekke 2012).

The block samples were taken from different depths and the laboratory test are divided into three rounds. 3.50 to 3.85 m, 3.85 to 4.20m and 4.20 to 4.50 m.

The summary of the block sample test results can be seen in appendix 3 and in table 23 and 24.

5.2.4 CPTU

The Cone Penetration Test Undrained (CPTU) is common test in a geotechnical survey. The gives many necessary parameters direct from field investigation. The CPTU is more suited to use in more fine grained soils like clay since it can also measure the excess pore water pressure behind the cone (u_2), see figure 36. So the cone resistance, q_t, can be calculated more accurate with the refined CPTU with equation 5.2. Where a is denoting the area relation of the cone.

$$q_t = q_c + u_2(1 - a) \quad (5.2)$$

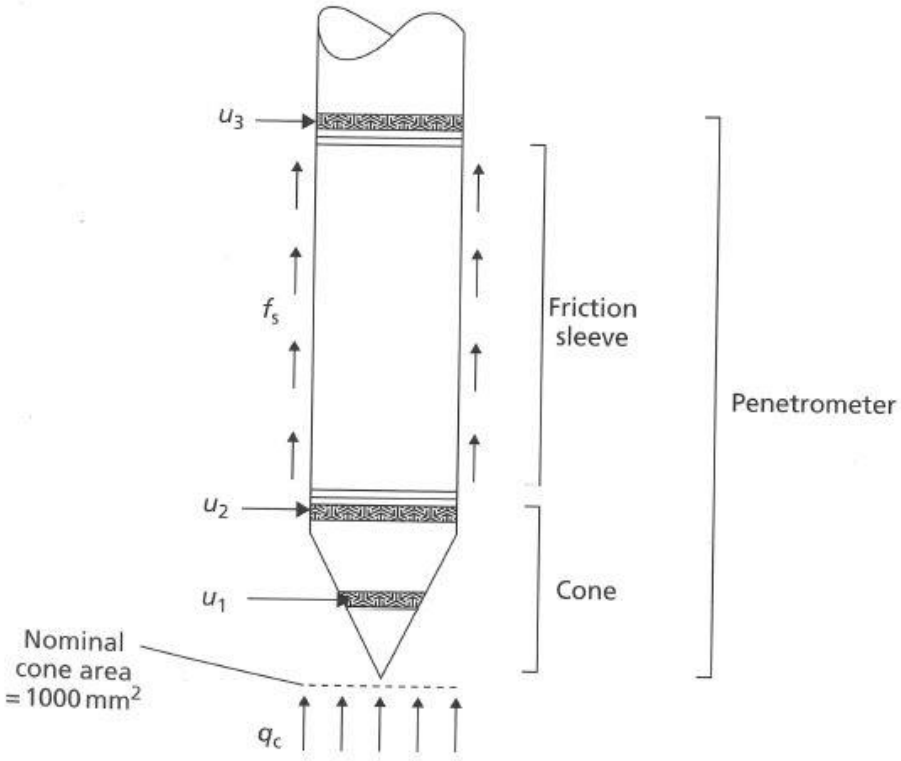

Figure 36 schematic of piezocone (CPTU) (Craig 2012)

Layer structure and detection of quick clay

CPTU sounding is a good method to determine occurrence of quick and sensitive clay material since all measurements is done directly in the cone (SINTEF-Multiconsult 2012). Therefore will the measurements not be effected by the accumulation of side friction. The measurement gives the mechanical resistance at the cones head, the sleeve friction and the pore pressure that can detect collapse mechanisms in the material when the sounding is done.
There are mainly three parameters given from CPTU used for detection of quick clay. These are net cone resistance, sleeve friction and pore pressure ratio.

Net cone resistance

Net value of the cone tip resistance, q_n. That is the corrected cone resistance minus the vertical total stress, see equation 5.3.

$$q_n = q_t - \sigma_{v0} \quad (5.3)$$

In the ideal case the q_n is constant or equally decreasing with depth. This may not be as obvious as in a dynamic sounding method when the rod is turned.

Sleeve friction

Sleeve friction or the interface shearing resistance f_s is one parameter that can be used when analyzing CPTU results for detecting quick clay. Low values on the sleeve friction are normally an indicator of quick clay. The friction conditions that is obtained from the sleeve friction can also be an evaluation criteria. This is calculated with equation 5.4.

$$R_f = \frac{f_s \cdot 100\%}{q_t} - z \qquad (5.4)$$

Where q_t is obtained by equation 5.4 and z is the sounding depth.

Quick clays have a remolded shear strength that is lower than 0.5 kPa and when the clay is in this state it acts as a thick liquid. If the clay would be in this state the sleeve friction would be very low. But CPTU results show quick clay with relatively high sleeve friction values and much higher sleeve friction than zero. This often occurs when the clay is mixed with silt and coarser clay so that the material need more than one stir to show the fully remolded shear strength. Testing have been done to exemplify this behavior by doing the sounding in the same place 5 to 10 times and then the clay where going from stabile to liquid in the remolded state.

Pore pressure conditions

High pore pressure values is also an indicator of quick and sensitive clays. The pore pressure parameter from CPTU, B_q, see equation 2.33.

$$B_q > 1.0$$

The limit value is B_q larger than one.

The sounding will displace material around the cone and create large tensions around cone tip. The tension and strain changes will result in changes in the pore pressure around the cone. These changes is measure by the pore pressure measurements by the back of the cone, see figure 36.

In normal consolidated clays and clays with high water content the B_q values can be between 1 to 1.5 when measured by the back of the cone. If it is so the clay is classified as quick clay in the classification charts based on normalized CPTU data, see figure 37.

In stiffer over consolidated quick clays is the B_q often significant lower, between 0.6 to 0.9, depending on the degree of pre consolidation (SINTEF-Multiconsult 2012). This is due to the pore pressure is measured behind the conic part and therefore it will not contribute so much to the shear strength induced pore pressure as in a normally consolidated clay (Sandven 1990). The dilatancy properties is an evaluation parameters linked to this. Therefore it can be possible for quick clay to be outside zone 1 in the chart, figure 37, even if it is quick clay. This means that B_q cannot be used single handedly as a detection parameter for quick clay.

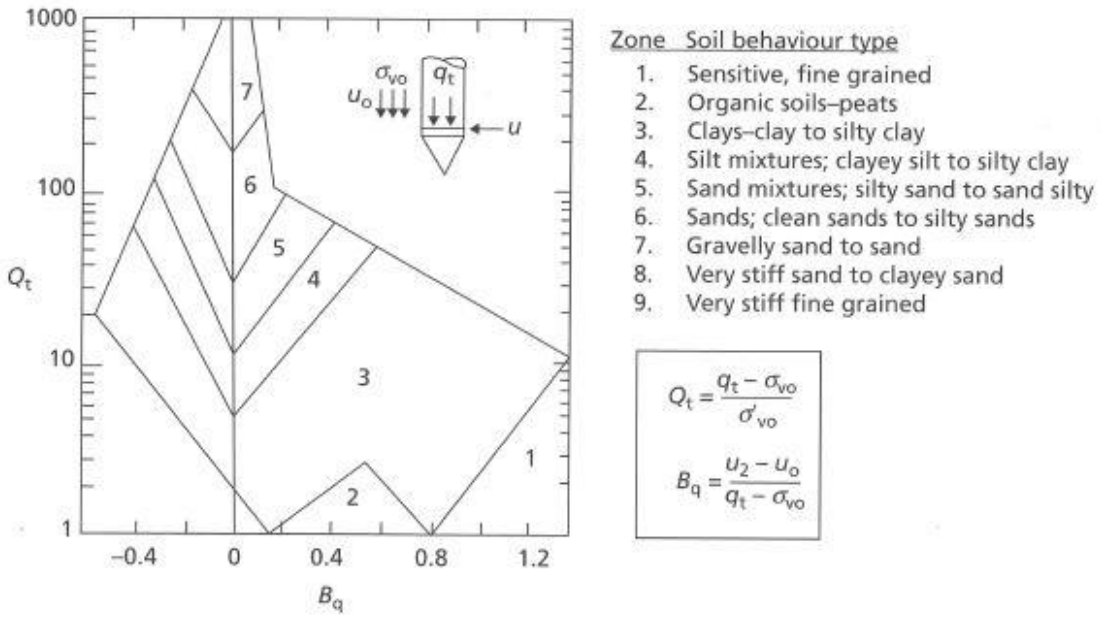

Figure 37 Soil behaviour type classification chart based on normalized CPTU data (Craig 2012)

Figure 38 shows the test results from a CPTU sounding in Møllenberg in Trondheim Norway. Quick clay where detected between 5 to 22 m, the layer is represented by the pink area in the figure. As can be seen the net cone resistance is somewhat decreasing with depth but the B_q<1.0 and the sleeve friction is relatively low with R_f about 0.4 %.

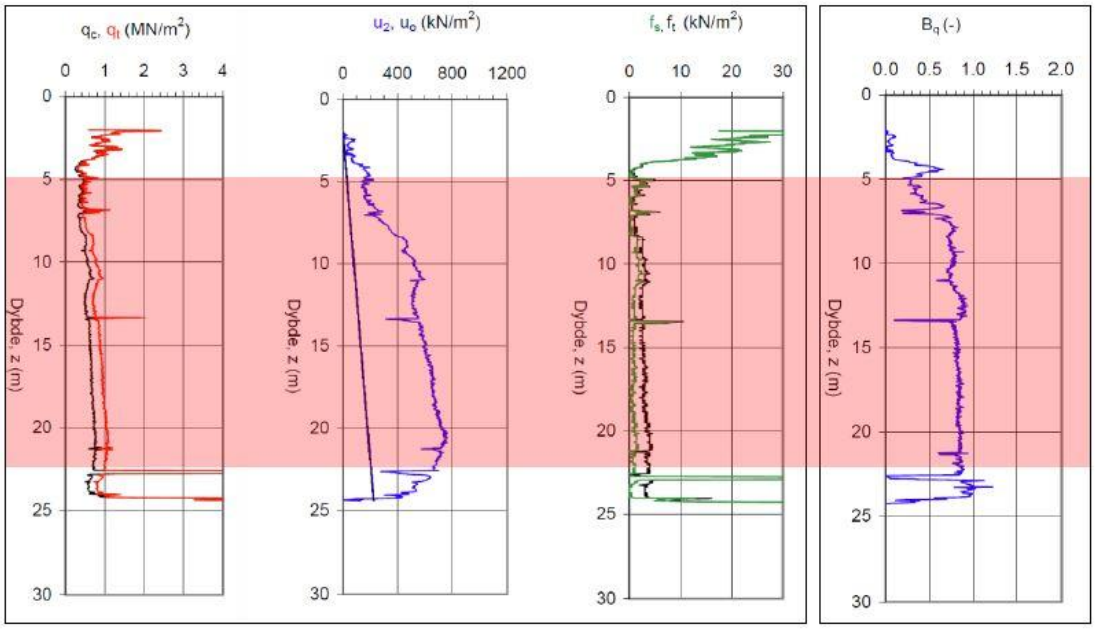

Figure 38 CPTU test results from Møllenberg in Trondheim Norway.

Application classes

The application classes for CPTU test are giving guidance on selecting the CPTU to get the right accuracy. The existing ground conditions shall be reflected by the choice of application class. The application classes are summarized in Table 17.

Table 17 Application classes (ISO 2012)

Class	Test type	Parameter	Accepted accuracy	Recommended ground conditions
1	TE2:q_c, f_s, u, inclinometer	Cone resistance Sleeve friction Pore pressure Inclination	35 kPa or 5% 5 kPa or 10% 10 kPa or 2% 2°	Soft to very soft soil deposits. Normally not apt for mixed bedded profiles with soft to dense layers (q_c<3 MPa)
2	TE2:q_c, f_s, u TE1: q_c, f_s, Inclinometer	Cone resistance Sleeve friction Pore pressure Inclination	100 kPa or 5% 15 kPa or 15% 25kPa or 3% 2°	Mixed bedded profiles with soft to dense soils. Profiling and material identification, indicative interpretation in soft layers.
3	TE2:q_c, f_s, u TE1: q_c, f_s, Inclinometer	Cone resistance Sleeve friction Pore pressure Inclination	200 kPa or 5% 25 kPa or 15% 50kPa or 5% 5°	Mixed bedded profiles with soft to dense soils. Profiling and material identification, interpretation in stiff to very stiff soils.
4	TE1: q_c, f_s	Cone resistance Sleeve friction	500 kPa or 5% 50 kPa or 20%	Mixed bedded profiles with soft (loose) to very stiff (dense) layers. Indicative profiling and material identification. No interpretation of engineering parameters.

5.3 Laboratory tests

The laboratory test was conducted at the laboratory facilities at NTNU in 2012. The block samples were taken 30 th of November 2011 and were sealed in kept in a cold storage room that kept 6°. The block samples covered depth between 3.5 to 4.6 m. The laboratory tests used where Oedometer and Triaxial test summary of these tests can be seen in table 22 and 23. All test series can be seen in Appendix 4.

5.3.1 Oedometer test

In the Oedometer the specimen is put into a cylinder where it is excessed for a one dimensional load. Often this test is made to determine consolidation and swelling properties of the soil. The oedometer tests have been performed with constant rate of strain. The parameters given from oedometer test are coefficient of consolidation, total stresses, pore pressure and material Modulus. A summary of the test results can be seen in table 23.

5.3.2 Triaxial test

The triaxial test is a commonly used laboratory test that is used to determine the shear strength of soil sample. An advantage in using triaxial test is that the drainage conditions can be controlled so both drained and undrained conditions can be tested (Craig 2012). The test is suitable for all types of soils. The triaxial test evaluates the anisotropy in the material so that active, direct and passive shear strength can be obtained. The test apparatus used is set up for 54 mm samples and therefore tests where samples are larger have to be trimmed down into the right size. Test results can be seen in table 22.

For a slope stability problem the strength parameters is the most important. The manner that the laboratory tests is made may affect the value given from the investigation. In figure 38 are all triaxial test for the block samples plotted and table 18 is showing what rate the samples where tested with. The color scheme in figure 38 is telling what rate the tests where run at. It shows that the samples that where tested with a speed over 3 % is giving the largest values of undrained shear strength. Test CAUa016 that got the largest shear strength value after CAUa015 was run at 1%/hour. These two tests were from the same test specimen and were tested shortly after it was opened and came from a place in the area with horizontal layer structures. Samples with lower values where from places with sloping layer structure and with some mixing in the layer structure.

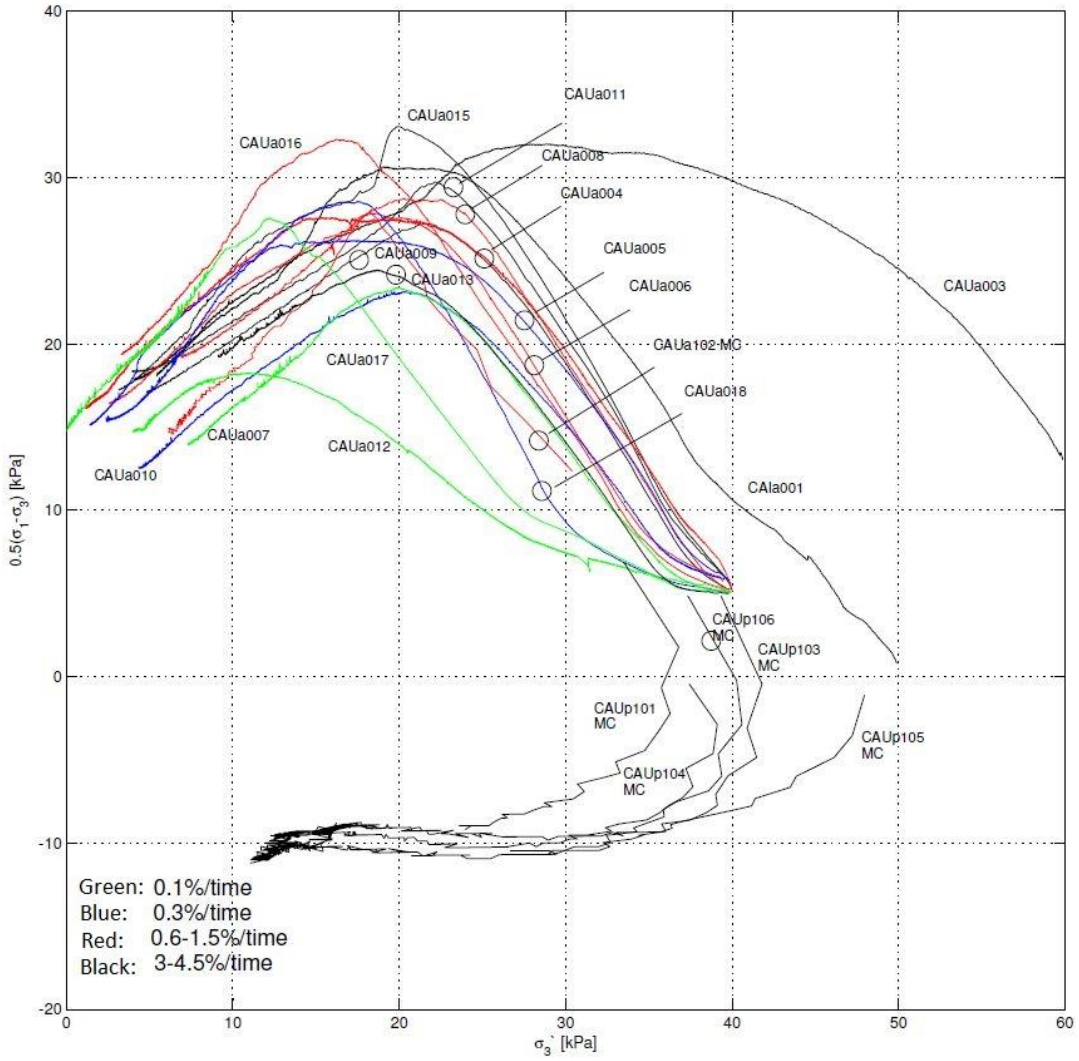

Figure 38 summary of the triaxial test on block samples, see table 18 for more information(Kornbrekke 2012)

Table 18 strain rates used for triaxial tests

[%/hour]	Sample	[%/hour]	Sample	[%/hour]	Sample
4.5	CAUa011	1.5	CAUa008	0.3	CAUa005
3.0	ClUa001	1.2	CAUa102		CAUa010
	CAUa003	1.0	CAUa006		CAUa018
	CAUa009		CAUa016	0.1	CAUa007
	CAUa015	0.6	CAUa004		CAUa012
					CAUa017

The test results show that the undrained shear strength values is depending on the rate that the specimen it loaded at. Figure 39 shows the relation of undrained shear strength and the rate that the test is run in. The undrained shear strength is normalized

to a reference test run in 4.5%/hour. The black line at the bottom is a test is for block test from 3.5-3.85 m. The testing were mad with speeds from 0.1 to 4.5 %/hour.

The undrained shear strength is increased with about 30 % for the for strain rates on 0.1 to 3 %/hour. This observation is for samples from the same depth or same test specimen.

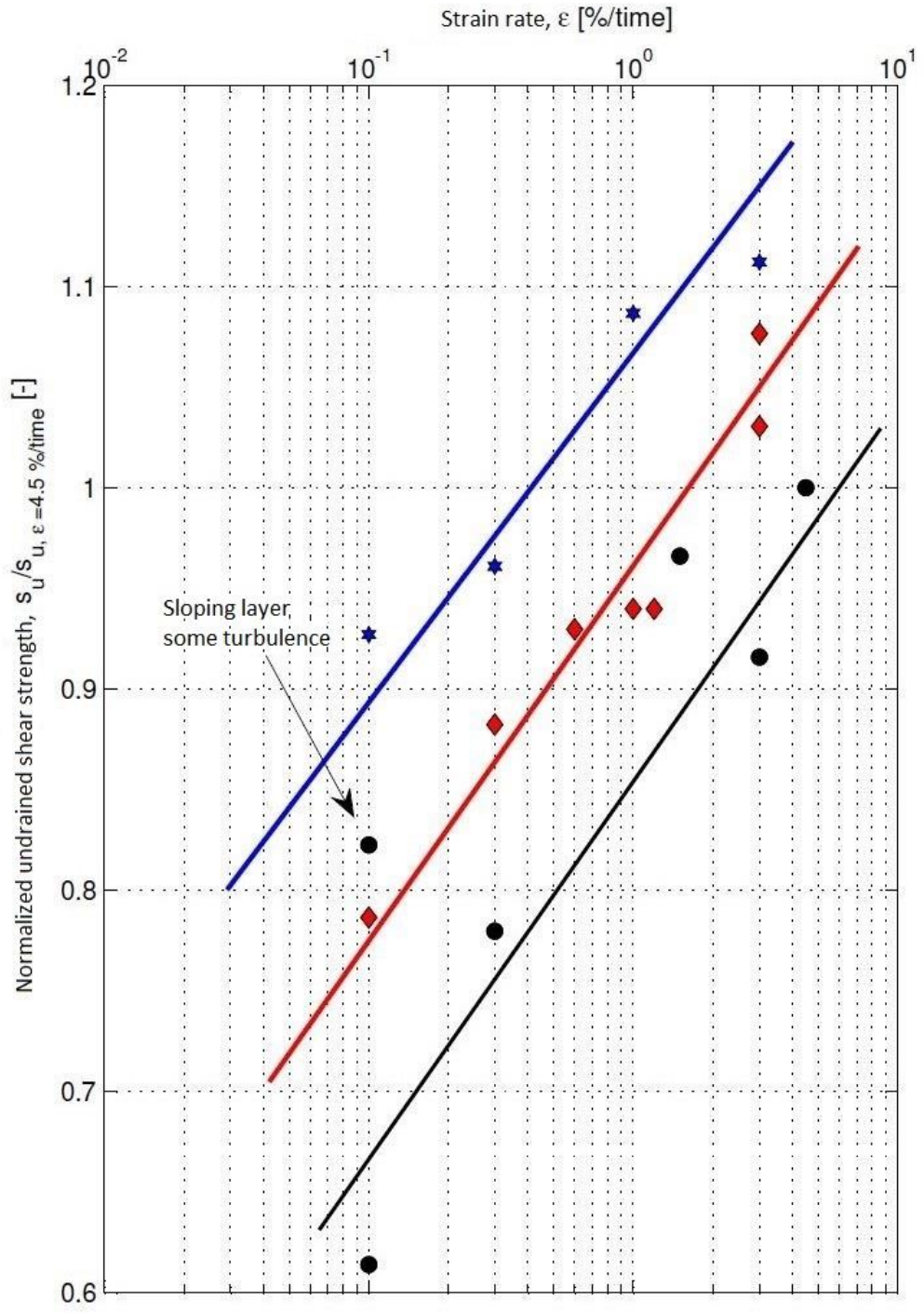

Figure 39 effect of strain rate in Rissa clay (Kornbrekke 2012)

5.4 Layer profile

The 54 mm piston samples are analyzed to see what material they contain. The samples from different levels give a picture of what the layer structure looks like. The old praxis has been to only use 54 mm samples to determine the structures.

The results from the 54 mm samples can be complemented with CPTU soundings. CPTU soundings give a continuous result with depth. To determine the layers the CPTU results are put together with 54 mm samples to get a complete picture of the area.

The layer profile that will be used in this case study can be seen in the map in figure 31. The profile is 3-3 is the modelled profile.

5.5 Summary of Ground investigation and Laboratory results

This is a summary of earlier made laboratory tests as triaxial test and Oedometer test. Only test with good or acceptable quality is listed. CPTU results together with new ground investigation are summarized in table 21 and 22.

Table 19 summary of 54 mm piston samples with acceptable/good quality (Kornbrekke 2012)

Sample	$d\epsilon/dt$ [%/hr]	Depth Level [m]	[m]	σ'_{vo} [kPa]	w [%]	γ [kN/m^3]	c_u [kPa]	a [kPa]	$tan\phi$ [-]	D [-]	ϵ_f [%]	ΔV [cm^3]	ϵ_v [%]	σ'_c [kPa]	OCR [-]	$\Delta e/e_o$ [-]	q_t [kPa]	u_o [kPa]	$u2$ [kPa]	f_s [kPa]	I_p [%]	S_t [-]
CAUaC3	5.0	10.40	-8.20	108.8	28.5	19.8	34.5	5	0.50	-0.14	0.65	6.97	3.04	166.5	1.53	0.05	587	499	94	5.8	11.5	12.0
CIUaKK4	3.0	5.40	-1.90	61.3	33.0	18.6	33.0	10	0.51	-0.08	1.76	5.04	2.20	141.1	2.30	0.04	358	280	44	1.5	16.4	7.6
CIUaKK4	3.0	3.40	0.10	42.3	36.0	19.9	30.0	10	0.51	-0.12	1.70	3.66	1.60	122.2	2.89	0.03	311	265	24	2.0	8.7	11.7
CIUaKK3	3.0	6.35	-2.85	70.3	31.0	19.7	36.0	10	0.51	0.13	1.90	6.41	2.80	150.1	2.13	0.05	358	331	54	1.8	11.9	5.1
CIUaKK3	3.0	6.50	-3.00	71.8	29.0	19.7	42.0	17	0.51	0.00	1.50	7.10	3.10	151.5	2.11	0.05	472	308	55	1.9	11.9	5.1
CIUaKK3	3.0	7.45	-3.95	80.8	33.0	19.8	42.0	11	0.51	0.05	1.75	5.27	2.30	160.5	1.99	0.04	437	374	65	2.0	13.8	6.9
CIUaKK3	3.0	9.40	-5.90	99.3	32.0	19.9	48.0	18	0.51	-0.01	1.80	7.56	3.30	178.9	1.80	0.06	609	444	84	2.2	14.4	5.4

Table 20 Summary of oedometer test (Kornbrekke 2012)

Borhole	Type of test	$d\epsilon/dt$	Depth	Level	σ'_{vo}	w	γ	σ_c	OCR	M	m	c_v	ϵ_v	$\Delta e/e_o$
	[kPa]	[%/hr]	[m]	[m]	[kPa]	[%]	[kN/m^3]	[kPa]	[-]	[MPa]	[-]	[m^2/år]	[%]	[-]
RK12	CRS		13.44	8.46	121.0	27.8	20.3	200	1.65	4	17	31.5	3.92	0.06
RK12	CRS		21.26	0.64	191.3	27.8	20.6	275	1.44	10	11	31.5	2.33	0.04
RK14	CRS		6.43	-3.73	57.6	41.1	19.3	150	2.60	6	17	37.8	0.98	0.02
KK3	CRS	1.50	2.35	1.15	24.2	42.1	18.4	110	4.55				1.50	0.03
KK3	CRS	1.50	7.60	-4.10	71.0	32.1	19.8	163	2.30				3.00	0.05
KK4	CRS	1.50	3.60	-0.10	35.0	36.0	19.9	130	3.71				1.50	0.03
KK4	CRS	1.50	6.25	-2.75	59.0	34.0	18.6	153	2.59				4.00	0.07
C2	CRS		12.35	-3.15	143.3	25.0	21.0	300	2.09	8	21	8.2	2.20	0.03
C3	CRS	0.80	5.25	-3.08	59.9	30.2	19.6	105	1.75	1	20	26.0	3.10	0.05
C3	CRS	0.72	5.50	-3.33	62.3	33.2	19.6	105	1.69	2	20	22.0	2.00	0.03
C3	CRS	0.60	15.50	-13.33	157.3	30.3	19.6	225	1.43	8	20	39.0	2.10	0.03
C4	CRS	0.72	10.40	11.50	105.6	36.4	19.4	150	1.42	4	17	6.0	3.25	0.06
C5	CRS	0.66	9.30	3.40	95.7	33.5	19.4	150	1.57	2	18	8.0	4.05	0.07
C6	CRS	0.46	17.50	-16.31	175.3	27.7	20.1	150	0.86	5	20	18.0	4.31	0.07

Not specifiedvalues was not stated or where not calculated in reviewed reports

Table 21 new ground investigations 2010 (Kornbrekke 2012)

	Measurement Accuracy						Application Class		
CPTU id.	Zero point q Change NA [kPa]	Zero point u Change NC [kPa]	Zero point f Change NB [kPa]	Max. inclination [o]	Pore Pressure	Other	Coneresistance	Pore pressure	Friction
C2	-7	-0.3	-0.5	5.9	Very good response		1	1	1
C3	26.7	0.1	-0.2	3.4	Very good response		1	1	1
C4	-9.1	-1	0	3.9	Very good response		1	1	1
C5	4.8	-0.6	-0.2	3.5	Very good response		1	1	1
C6	-15.2	-0.8	-0.5	3	Very good response		1	1	1
C3, 2 mm/s	4.3	-0.7	-0.3	3.8	Very good response		1	1	1
C3, 200 mm/s	-21.2	0.1	-0.2	4.2	Very good response		1	1	1

Table 22 Summary of earlier made ground investigations (Multiconsult 2012)

	Measurement Accuracy						Application Class		
CPTU id.	Zero point q Change NA [kPa]	Zero point u Change NC [kPa]	Zero point f Change NB [kPa]	Max. Inclination [o]	Pore pressure	Other	Coneresistance	Pore pressure	Friction
16	78	34	-35	Not meas.	OK, usable response		4	4	4
17	-251	126	-34	Not meas.	Poor response OK,		4	4	4
106	-485	160	-158	Not meas.	usable response OK,		4	4	4
110	-90	-15	23	Not meas.	usable response OK,		4	2	4
111	-94	-59	54	Not meas.	usable response OK,		4	4	4
112	-16	-65	74	Not meas.	usable response OK,		3	4	4
RK4	126	-4	20	Not meas.	usable response OK,		3	1	4
RK10	58	-3	-14	Not meas.	usable response OK,		3	1	4
RK12	76	-3	8	Not meas.	usable response OK,		3	1	4
RK13	90	-4	28	Not meas.	usable response OK,		3	1	4
RK14	54	13	-103	Not meas.	usable response OK,		3	2	4
RK18	44	16	-2	Not meas.	usable response		3	2	4
RT1	106	23	-4	12	Poor response		3	3	4
RT2	68	13	-3	22	Poor response		2	2	4
RT3	82	13	-3	16	OK, usable response	Error in meas.	2	2	4
RT4	-62	13	-1	33	Poor response	Error in meas.	3	2	4
RT5	524	-13	-2	11	OK, usable response under 6 m		4	2	4
RT6	52	23	-2	11	OK, usable response		2	3	4
RT7	-12	61	-3	Not meas.	Poor response		2	4	4
RT8	-106	47	-4	11	Poor response		3	3	4
RT9	-106	24	-4	21	Poor response		3	3	4
RT9-2	88	-15	-3	Not meas.	Poor response		3	2	4
S3	66	12	-5	Not meas.	OK, usable response		3	2	4
S6	84	10	-4	Not meas.	Uncertain measurment		3	2	4

Table 23 Summary, block sample results, triaxial test (Kornbrekke 2012)

Test	$d\varepsilon/dt$	Depth	Level	σ'_{vo}	w	γ	s_u	a	$tan\phi$	E_0	D	ε_f	ΔV	ε_v	σ'_c	OCR	$\Delta e/e_o$	q_t	u_2	u_0	f_s
Block sample	[%/hr]	[m]	[m]	[kPa]	[%]	[kN/m^3]	[kPa]	[kPa]	[-]	[MPa]	[-]	[%]	[cm^3]	[%]	[kPa]	[-]	[-]	[kPa]	[kPa]	[kPa]	[kPa]
CAUa001	3.0	3.96	-1.76	45.6	35.9	19.5	30.7	15	0.54	5.7	-0.03	1.75	5.13	2.21	101.2	2.22	0.04	368.9	251.6	29.6	0.1
CAUa102*	1.2	3.96	-1.76	45.6	34.8	19.2	28.0	8	0.59	11.3	-0.04	0.73	3.63	1.56	101.2	2.22	0.03	368.9	251.6	29.6	0.1
CAUa003	3.0	3.96	-1.76	45.6	37.3	0.0	32.0	23	0.43	6.6	-0.15	1.42	5.16	2.23	101.2	2.22	0.04	368.9	251.6	29.6	0.1
CAUa004	0.6	4.07	-1.87	46.6	36.3	19.5	27.7	16	0.56	5.2	-0.04	1.80	4.45	1.92	102.4	2.20	0.04	349.4	244.1	30.7	0.2
CAUa005	0.3	4.07	-1.87	46.6	36.5	19.8	26.2	10	0.69	5.2	-0.05	1.61	3.45	1.49	102.4	2.20	0.03	349.4	244.1	30.7	0.2
CAUa006	1.0	4.07	-1.87	46.6	35.8	19.8	27.9	21	0.46	4.7	0.00	1.51	3.26	1.40	102.4	2.20	0.03	349.4	244.1	30.7	0.2
CAUa007	0.1	4.07	-1.87	46.6	36.0	19.8	23.4	10	0.51	5.4	-0.06	1.21	4.31	1.86	102.4	2.20	0.03	349.4	244.1	30.7	0.2
CAUa008	1.5	3.64	-1.44	42.8	31.3	19.8	28.7	19	0.47	6.6	0.01	1.40	3.12	1.35	97.8	2.29	0.02	402.6	257.2	26.4	0.2
CAUa009	3.0	3.75	-1.55	43.8	34.1	19.5	27.2	22	0.43	7.1	-0.01	1.07	3.28	1.41	99.0	2.26	0.02	374.5	248.8	27.5	0.1
CAUa010	0.3	3.64	-1.44	42.8	32.1	19.3	23.2	12	0.48	5.4	-0.09	1.22	4.01	1.73	97.8	2.29	0.03	402.6	257.2	26.4	0.2
CAUa011	4.5	3.64	-1.44	42.8	35.4	19.4	29.7	25	0.41	7.4	0.01	0.96	3.64	1.57	97.8	2.29	0.03	402.6	257.2	26.4	0.2
CAUa012	0.1	3.75	-1.55	43.8	32.4	19.4	18.3	15	0.49	3.3	-0.34	1.69	4.87	2.10	99.0	2.26	0.04	374.5	248.8	27.5	0.1
CAUa013	0.1	3.75	-1.55	43.8	32.7	19.3	24.5	22	0.42	6.9	-0.07	1.17	4.08	1.76	99.0	2.26	0.03	374.5	248.8	27.5	0.1
CAUa014	0.01	3.75	-1.55	43.8	37.4	19.3	13.7	10	0.55	14.7	-1.34	0.29	4.40	1.90	99.0	2.26	0.04	374.5	248.8	27.5	0.1
CAUa015	3.0	4.37	-2.17	49.3	37.7	19.3	33.1	15	0.56	6.4	0.02	1.35	3.44	1.48	105.6	2.14	0.03	374.5	258.8	33.7	0.1
CAUa016	1.0	4.37	-2.17	49.3	37.5	19.3	32.3	14	0.62	6.3	-0.01	1.47	4.63	2.00	105.6	2.14	0.04	374.5	258.8	33.7	0.1
CAUa017	0.1	4.37	-2.17	49.3	37.4	19.3	27.6	14	0.60	7.8	-0.05	1.01	3.54	1.52	105.6	2.14	0.03	374.5	258.8	33.7	0.1
CAUa018	0.3	4.37	-2.17	49.3	35.5	19.3	28.6	11	0.63	7.3	0.04	0.93	4.00	1.73	105.6	2.14	0.03	374.5	258.8	33.7	0.1
CAUp101*	-1.2	3.96	-1.76	45.6	33.8	19.3	9.4			0.6		1.21	5.88	2.53	101.2	2.22	0.05	368.9	251.6	29.6	0.1
CAUp103*	-1.2	4.07	-1.87	46.6	33.4	19.1	10.2			17.0		0.58	3.77	1.63	102.4	2.20	0.03	349.4	244.1	30.7	0.2
CAUp104*	-1.2	3.66	-1.46	42.9	26.6	19.2	10.3			13.1		1.35	3.44	1.48	98.0	2.28	0.02	378	206.6	26.6	0.2
CAUp105*	-1.2	3.75	-1.55	43.8	32.5	19.4	9.8			14.9		0.84	4.94	2.13	99.0	2.26	0.04	374.5	248.8	27.5	0.1
CAUp106*	-2.4	4.37	-2.17	49.3	37.1	19.3	11.2			5.3		1.01	4.36	1.88	105.6	2.14	0.04	374.5	258.8	33.7	0.1

*Made by Multiconsult

Table 24 Summary block sample, oedometer test (Kornbrekke 2012)

Block sample	Type of test	Load [kPa]	$d\varepsilon/dt$ [%/hr]	Depth [m]	Level [m]	σ'_{vo} [kPa]	w [%]	γ [kN/m^3]	σ'_c [kPa]	OCR [-]	M [MPa]	m [-]	c_v [m^2/year]	ε_v [%]	$\Delta e/e_o$ [-]
CRS001	CRS: $5\mu m/min$		1.5	3.92	-1.72	45.3	37.3	19.50	95.00	2.10	4.00	25.00	13.50	2.17	0.04
CRS002	Creep test A* σ_v=150			3.96	-1.76	45.6	37.2	19.50	100	2.19	2.50	23.00	8.00	2.63	0.05
CRS003	Creep test B	150	1.5	3.99	-1.79	45.9	35.4	19.50	100	2.18	2.50	23.00	8.00	2.27	0.04
CRS004	CRS: $5\mu m/min$		1.5	4.02	-1.82	46.2	35.8	19.30	100	2.17	3.50	26.00	18.50	1.72	0.03
IL001	Step wise			4.07	-1.87	46.6	36.8	19.80	90	1.93					
CRS006	Triple Creep test A	80-90-150		4.10	-1.90	46.9	35.7	19.90	100	2.13		22.00		3.21	0.06
CRS007	CRS: $5\mu m/min$		1.5	3.64	-1.44	42.8	32.0	19.40	Destroyed during testing						
CRS008	CRS: $5\mu m/min$		1.5	3.66	-1.46	42.9	32.8	19.4	Destroyed during testing						
CRS009	CRS: $5\mu m/min$		1.5	3.62	-1.42	42.6	36.5	19.4	100	2.47	2.35	24	10	3.39	0.06
CRS010	Triple Creep test B	80-90-150	1.5	3.64	-1.44	42.8	35.5	19.4	100	2.34		25		2.81	0.05
CRS011	CRS: $5\mu m/min$		1.5	3.66	-1.46	42.9	34.8	19.5	95	2.21	3.2	24	14.1	2.26	0.04
CRS012	Triple Creep test C	80-90-150	1.5	3.62	-1.42	42.6	33.3	19.4	100	2.35		24		2.99	0.05
CRS013	Triple Creep test F	60-80-120	1.5	3.64	-1.44	42.8	33.2	19.5	100	2.34		25		2.91	0.05
CRS014	CRS: $4\mu m/min$		1.2	3.66	-1.46	42.9	33.4	19.4	100	2.33	3	24	10.9	2.09	0.04
CRS015			1.5	3.71	-1.51	43.4	33.6	19.5	Destroyed during testing						
CRS016	CRS: $3\mu m/min$		0.9	3.74	-1.54	43.7	33.5	19.3	100	2.29	3.3	26	80	2.57	0.04
CRS017	CRS: $2\mu m/min$		0.6	3.77	-1.57	43.9	32.8	19.3	160	3.64	2	26	6	3.45	0.06
CRS018	Triple Creep test E	50-80-120	1.5	3.8	-1.6	44.2	31.7	19.6	100	2.26		24		2.31	0.04
CRS019	CRS: $5\mu m/min$		1.5	4.33	-2.13	49.0	37.3	19.1	100	2.04	3.1	24	13.9	2.20	0.04
CRS020	Triple Creep test D	80-90-150	1.5	4.37	-2.17	49.3	37.0	19.3	100	2.03		24		2.53	0.05
IL002	Step wise			4.41	-2.21	49.7	38.3	19.1	90	1.81					
IL003	Step wise			4.32	-2.12	48.9	34.4	19.3	90	1.84					
IL004	Step wise			4.35	-2.15	49.2	35.9	1.9	90	1.83					
IL005	Step wise			4.38	-2.18	49.4	35.5	1.92	90	1.82					

5.6 Scenario 1

The old approach to ground investigations has been to take 54 mm samples to evaluate soil parameters from and determine a layer structure in the profile. The 54 mm sample is the most common method used in the geotechnical ground survey in Norway today. In this study data from 5 different 54 mm samples will be used. The parameter values in the study are peak values therefore strain softening is not considered.

Routine investigations

The routine investigations from the 54 mm samples are presented for the two types of clay that is identified, sensitive and not sensitive clay. The routine test is sensitivity, plasticity index, density, attraction and friction angle, see table 25.

Table 25 routine investigations results.

	Sensitive Clay	Not Sensitive Clay
S_t [-]	19.86	5.6
I_p [%]	8.9	13.4
γ [kN/m^3]	19.7	19.7
a [kPa]	1	1
Φ [°]	29	29

Parameter evaluation

The parameters that is used in the model is chosen to be analysed based the importance they have on slope stability. They also have to be with the material model NGI-ADP used in Plaxis.

Shear strength

In the NGI-ADP the anisotropy in the material is taken into consideration. Therefore the shear strength is evaluated for Active, Direct and Passive mode. The reference shear strength, $S_{U,ref}^{A}$, is determined from the 54 mm samples. The reference value is given by the equation of depth. Figure 40 shows the shear strength profile evaluated from 54mm piston sample at borehole C3.

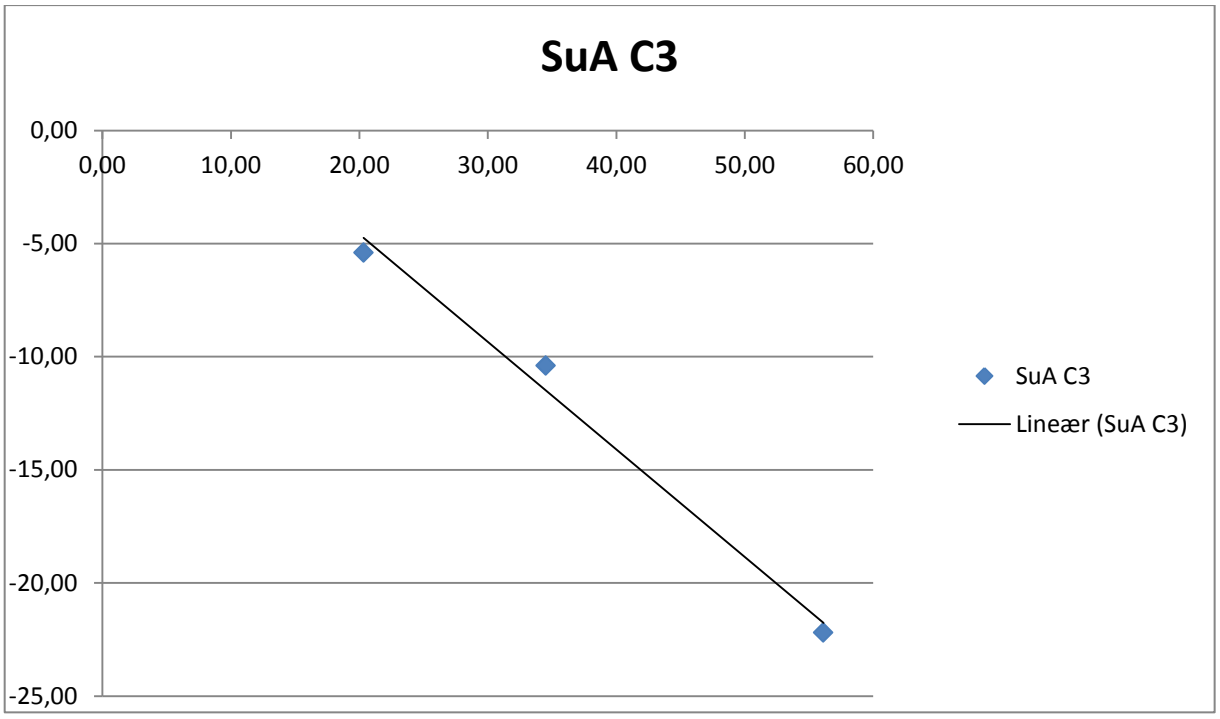

Figure 40 SuA profile from borehole C3 evaluated from 54mm piston sample

Table 26 is showing values for the reference shear strength and the increasing term from the 54 mm samples. They are all correlated so they are from the top of the clay layer. The shear strength profiler is increasing with depth and the term that is governing this is the$s_{U,inc}^{A}$. These functions have been made into one that is used in the modelling. The mean value together with the standard deviation is used in the model. Standard deviation is evaluated with the simplified method.

Table 26 Values for SuA,ref and SuA, inc based on data from 54 mm samples. The mean value and standard deviation for both parameters is also shown.

Sample	SuA,ref	SuA,inc
C2	27.19	2.35
C3	21.03	2.1
C4	36.31	2.06
C6	20.85	2.06
K3	27.54	3.56
Range	15.46	1.51
Mean	26.58	2.42
n=5	0.43	0.43
Std.dev	6.65	0.65

The Shear strength profile for the clay layers, se equation 5.3, this is plotted with depth in figure 40 with the whole standard deviation for the upper and lower limit. Su

ref is considered to be normal distributed. This is shown in figure 41 where the frequency histogram and bell function is plotted for three standard deviations.

$$s_u^A(y) = 26.58 + 2.42 \cdot y \qquad (5.3)$$

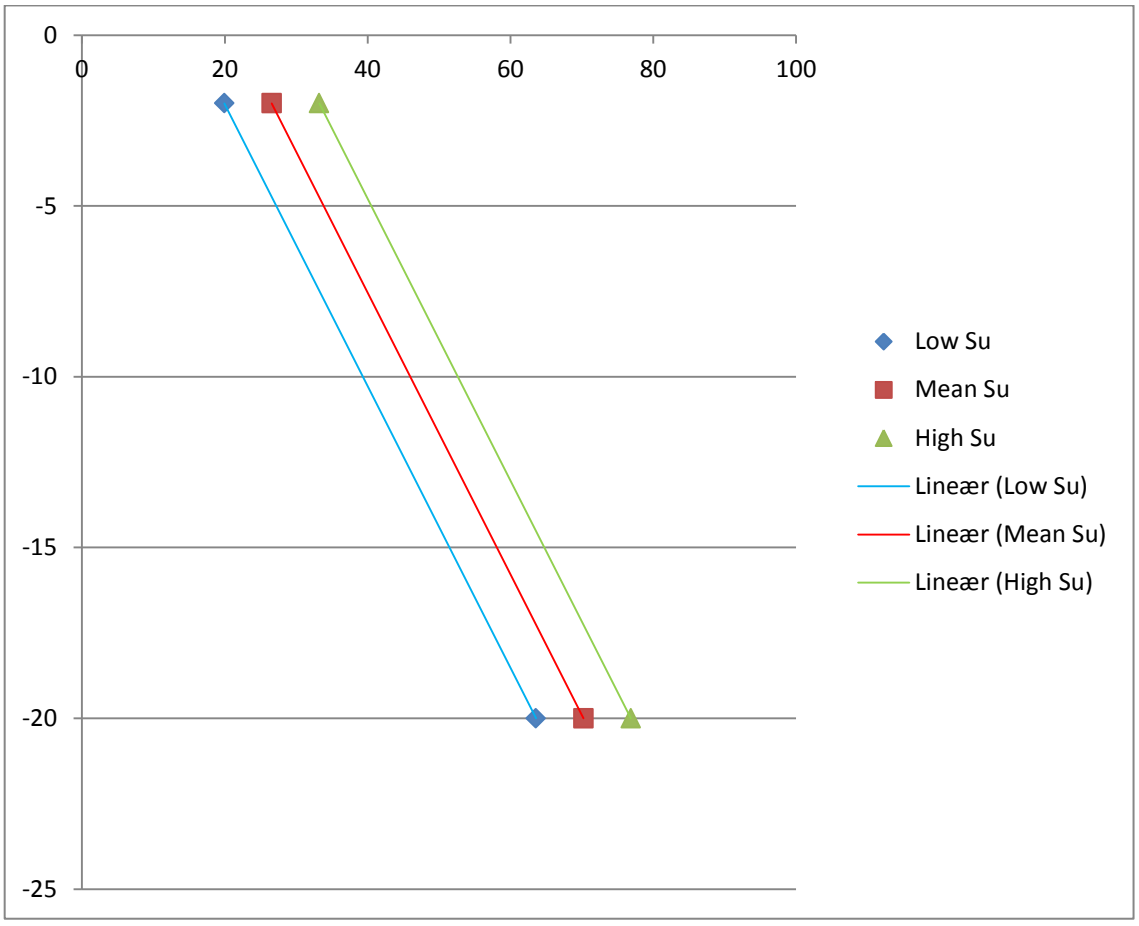

Figure 40 shear strength profile used in model with mean value and low and high value with the whole standard deviation.

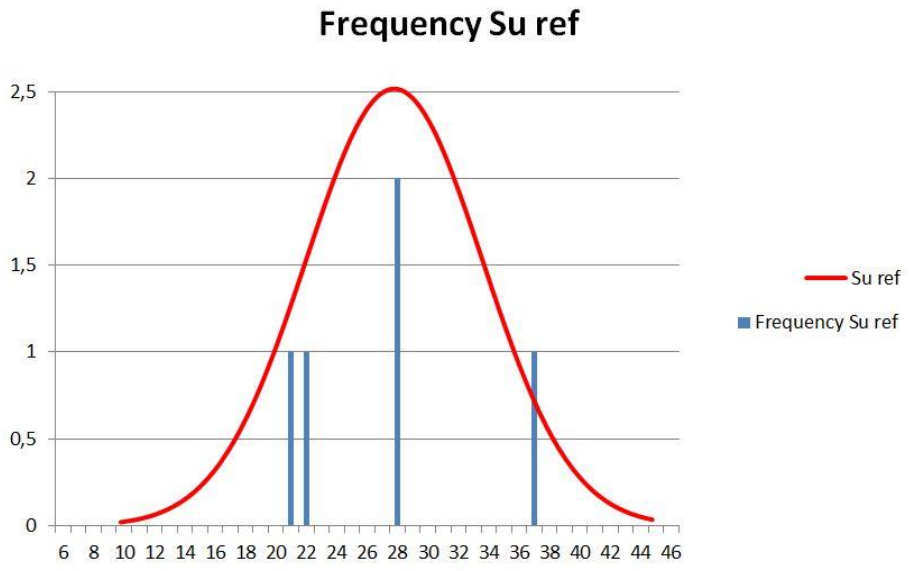

Figure 41 Su ref normal distributed and Su ref frequency histogram

The data from triaxial test gives values for active and passive shear strength. It is the quotient between them that is used in the soil model so it is important to have values from same depth levels to get correct values. If test is from different levels they can be calculated with the function of depth that they are so that they fit. There are more test done for active mode than passive in the data set, see Table 27.

Table 27 values for active and passive shear strength.

Sample	Type of Test:	Depth [m]:	S_u [kPa]
C2	CAUa	-2.45	27.19
C2	CAUa	-21.45	76.17
C2	CAUp	-12.50	17.75
C3	CAUa	-5.40	20.33
C3	CAUa	-10.40	34.52
C3	CAUa	-22.2	56.12
C3	CAUp	-5.60	7.63
C3	CAUp	-10.60	11.64
C4	CAUa	-10.25	36.31
C4	CAUa	-16.30	48.78
C5	CAUa	-9.40	30.98
C5	CAUp	-15.40	18.90
C6	CAUa	-3.30	20.85
C6	CAUa	-17.40	49.82
C6	CAUp	-3.40	9.57
C6	CAUp	-17.70	19.52

Values can also be obtained by the correlation of the plasticity index as is recommended to be used in future praxis (Thakur et.al 2014). The limit value is a plasticity index of 10 %. The formulas can be seen in table 28. Plasticity index is the range of water content that the soil exhibits plasticity (Craig 2012).

Table 28 ADP-factors where Ip shall be in %.

Ip	SuDSS/SuA	SuP/SuA
Ip≤ 10 %	0.63	0.35
Ip > 10 %	0.63+0.00425(Ip-10)	0.35+0.00375(Ip-10)

The anisotropy factors used in the case study will be evaluated according to these new recommendations. The samples evaluated with these formulas gives values presented in table 29.

Table 29 ADP shear strength evaluated from plasticity index.

Sample	Depth [m]	Ip [%]	SuDSS/SuA	SuP/SuA
C2	-6.35	10.00	0.63	0.35
C3	-3.35	6.30	0.63	0.35
C3	-4.35	5.20	0.63	0.35
C3	-8.35	11.50	0.64	0.36
C3	-20.35	12.00	0.64	0.36
C3	-21.45	9.40	0.63	0.35
C4	-13.35	4.60	0.63	0.35
C4	-17.35	12.30	0.64	0.36
C5	-8.35	4.90	0.63	0.35
C5	-20.35	14.70	0.65	0.37
C6	-2.35	16.70	0.66	0.38
C6	-4.35	9.20	0.63	0.35
C6	-10.35	10.20	0.63	0.35
K3	-2.33	13.77	0.65	0.36
K3	-4.69	11.81	0.64	0.36
K3	-5.4	13.91	0.65	0.36
K3	-6.69	11.86	0.64	0.36
K3	-7.63	13.77	0.65	0.36
K3	-8.12	8.53	0.63	0.35
K3	-9.43	14.41	0.65	0.37
K3	-10.38	11.74	0.64	0.36

The parameter values, see table 30, is obtained from this data and is input to the modelling with mean values and standard deviation:

Table 30 mean value and standard deviation for SuDSS/SuA and SuP/SuA.

Value	SuDSS/SuA	SuP/SuA
Mean	0.64	0.36
Std.dev	0.01	0.01

Density

The unit weight is evaluated as a mean value and a standard deviation. The unit weight in the clay layer is 19.87 kN/m^3 with a standard deviation of 0.524 kN/m^3.

Case study modelling

The input parameters are evaluated from the ground investigation 54 mm samples. The stability calculations will be performed in Plaxis and FOSM method is used to evaluate probability of failure and reliability index.

Set up

The Plaxis analysis is made with 10 385 15-nodes element. The number of steps used when the multiplier Msf is calculated is set to 50. This is done to decrease the calculation time. It is checked that the function is stabile so this makes is possible to make this.

The First Order Second Moment method is used for the statistical calculations of the input parameters. The method is described in chapter 2.3. In the FOSM the parameters for stiffness will be set to deterministic values since they will not affect the calculate stability.

Geometry

The geometry used in the model is a idealization of the real slope at Rein Kirke, Sund-Bradden see figure 42.

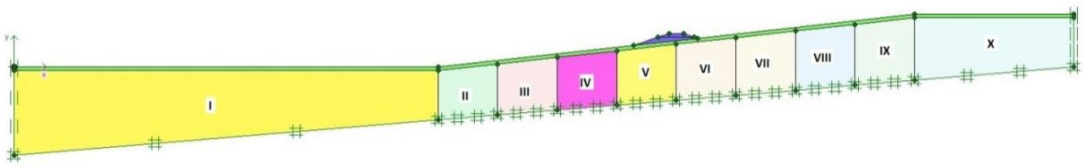

Figure 42 the geometry used Plaxis.

The lower boundary is the rock surface. This is sloping 1:12 and is a closed hydraulic boundary. The toe of the slope is at +0 and the top is at +30. The slope is divided into 10 different clusters. The sloping section into 8 clusters of the same length and the surface inclination is 1:9. These have a reference depth that is shifting for each cluster to get a realistic behaviour of the inclination of the shear strength with depth like equation 5.4.

$$s_u(y) = s_{u,ref} + (y_{ref} - y) \cdot s_{u,inc} \quad (5.4)$$

The dry crust is 2 m thick and this has been estimated from the ground investigation material. The groundwater table is directly under the dry crust 2 m below the surface. The ground water is hydrostatic down to the rock surface. In the slope an embankment is constructed as planned in the project of the new FV. 717. The Embankment has an 8.4 m wide road shoulder according to the standard for this type of road (NPRA 2013).

Material Model

The material model that is used in the analysis is NGI-ADP for the clay layer and Mohr-Coulomb Model for the Embankment and dry crust.

Calculation Steps

The calculation steps starts with the initial phase, see table 31. The initial phase is used to generate the initial ground water conditions, the initial geometry and the initial effective stress state. Gravity loading is used to as calculation in initial phase. Gravity loading is chosen above K_0 procedure since it is a slope that is to be simulated and for non-horizontal layer gravity loading more appropriate than K_0 procedure. In this phase the embankment is deactivated so that the stress conditions are correctly generated. The construction of the embankment is simulated with staged construction. The embankment is constructed in two phases, first is the lower part activated in phase 1 and in phase 2 is the top part of the embankment built. Both these is plastic calculations. In Phase 3 is a load applied on top of the embankment to simulate traffic, this is also a plastic calculation.

The safety calculations are performed to evaluate the stability of the slope. The safety factor given in these phases is given by evaluating the reduction in the strength parameters that is controlled by the incremental multiplier Msf. The safety factor is checked for the natural slope after initial phase, after the construction of the embankment and after traffic load is applied on the embankment.

Table 31 calculation steps used in the Plaxis analysis

Identification	**Phase no.**	**Start from**	**Calculation**	**Loading input**
Initial phase	0	N/A	Gravity loading	Staged construction
Embankment 1	1	0	Plastic	Staged construction
Embankment 2	2	1	Plastic	Staged construction
Load	3	2	Plastic	Staged construction
Initial Safety	4	0	Safety	Incremental multipliers
Embankment Safety	5	2	Safety	Incremental multipliers
Load Safety	6	3	Safety	Incremental multipliers

Results stability calculations

In the natural state the critical slip surface is deep along the rock surface as can be seen in figure 43. When the embankment is built the critical slip surface is beneath the embankment. The figure shows the incremental deviatoric strain. The safety factor for

the simulation is shown in figure 44. Both this figures corresponds to simulation with only mean values.

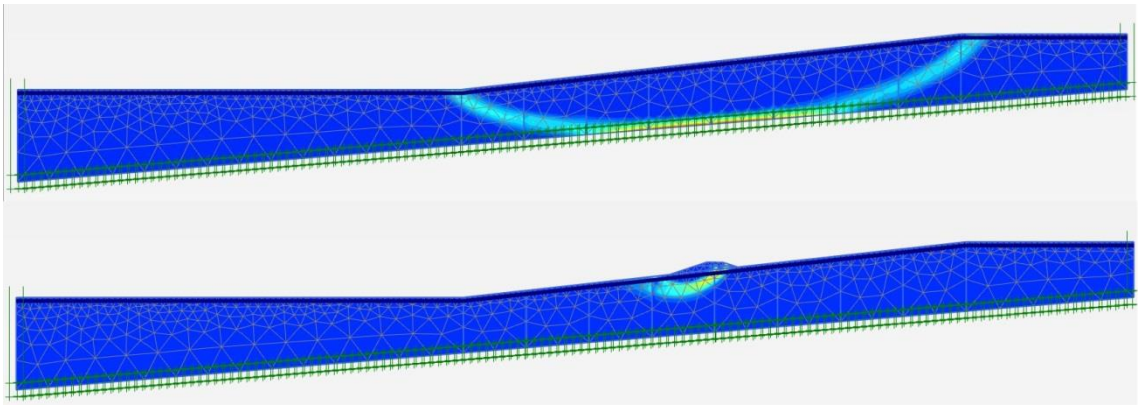

Figure 43 slip surface in the natural state and after construction of the embankment incremental deviatoric strain

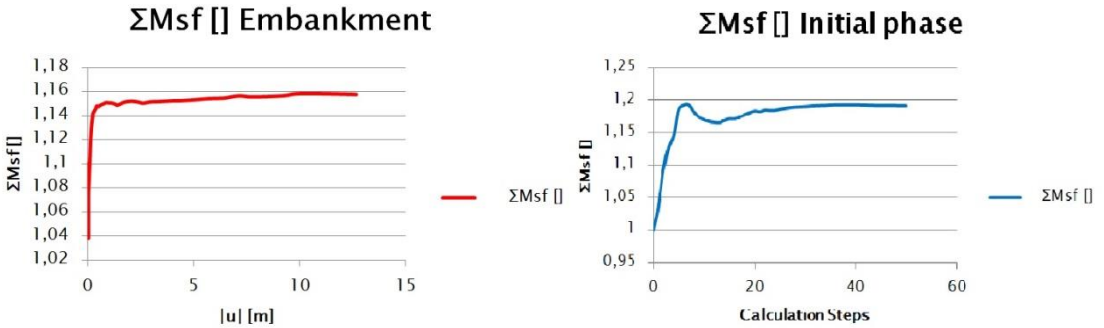

Figure 44 Msf from the Plaxis analysis shows the safety factor before and after construction of embankment

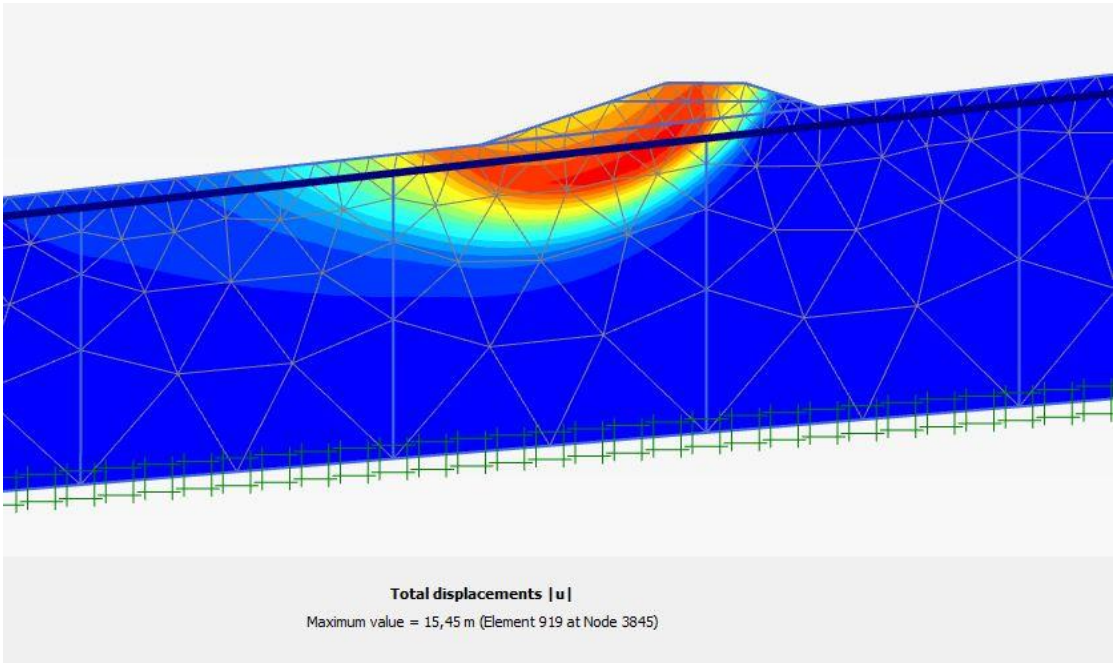

Figure 45 failure mechanisms for scenario 1 with mean values

The failure mechanisms for scenario 1 with mean values calculated from c-φ reduction is shown in figure 45.

FOSM

In the analysis each variable is treated as independent of each other is normal distributed. For the stability calculation Plaxis is used to make a deterministic calculation. The parameters are varied so that all parameters are set to the mean value and only one parameter is changed for each calculation run. The c/φ-reduction in Plaxis gives the factor of safety from the Msf multiplier. This is used as the failure criterion F<1. The factor of safety that is used is the obtained safety factor after the construction of the embankment. The parameters that govern the stiffness are fixed to a deterministic value since they do not have an effect on the calculated slope stability.

To each independent variable mean value and standard deviation has been estimated from data of ground investigations by Sund-Bradden, see table 32. All parameters are considered to be normal distributed from consultation with experts and testing.

Table 32 input parameters with distributions scenario 1

Variable	Mean value μ	Standard Deviation σ	Distribution	μ based on	σ based on
Su ref	26.584	6.648	Normal	54,A	T,f
Su inc	2.425	0.647	Normal	54, A	f
SuP/SuA	0.355	0.008	Normal	Ip, A	f
SuDSS/SuA	0.635	0.009	Normal	Ip, A	f
γ	19.87	0.524	Normal	54,A	s

μ and σ based on:

Type of test: 54-54mm piston sample T-Triax test Ip-Plasticity Index

Method: f- simplified method s-standard deviation A-Average

The standard deviation of the safety factors is calculated as equation 5.5.

$$\sigma_F = \sum \sqrt{\left(\frac{\Delta F}{\Delta X}\right)^2 \cdot \sigma^2} \qquad (5.5)$$

The parameter is varied in this study with 10%, 30%, and 50% of the standard deviation. The analysis done with different magnitude of the standard deviation can be seen in table 33, 34 and 35.

Table 33 FOSM with 10% of standard deviation

Material	Parameter	X*	std.dev	Dx	X*+DX	X*-DX	F+	F-	dF/dX	(dF/dX)^2xσ^2
Clay	Su,ref	26,584	6,648	0,665	27,249	25,919	1,136	1,108	0,028	0,0346
Clay	Su,inc	2,425	0,647	0,065	2,489	2,360	1,127	1,109	0,018	1,36E-04
Clay	Su,DSS/SuA	0,635	0,009	0,0009	0,636	0,635	1,118	1,117	0,001	7,64E-11
Clay	SuP/suA	0,355	0,008	0,0008	0,356	0,354	1,118	1,116	0,002	2,38E-10
Clay	γ	19,87	0,524	0,052	19,926	19,821	1,118	1,115	0,003	2,47E-06
										0,0348
									σF	**0,1865**
									pf	0,2631
									pf %	26,31 %
									β	0,847

Table 34 FOSM with 30 % of the standard deviation

Material	Parameter	X*	std.dev	Dx	X*+DX	X*-DX	F+	F-	dF/dX	(dF/dX)^2xσ^2
Clay	Su,ref	26,584	6,648	1,994	28,578	24,590	1,207	1,107	0,100	0,442
Clay	Su,inc	2,425	0,647	0,194	2,619	2,230	1,193	1,140	0,053	0,001
Clay	Su,DSS/SuA	0,635	0,009	0,003	0,638	0,633	1,161	1,156	0,005	1,91E-09
Clay	SuP/suA	0,355	0,008	0,002	0,357	0,352	1,159	1,158	0,001	5,95E-11
Clay	γ	19,87	0,524	0,157	20,031	19,716	1,161	1,154	0,007	1,34E-05
										0,443
									σF	**0,666**
									pf	0,405
									pf %	40,53 %
									β	0,240

Table 35 FOSM with 50 % of the standard deviation.

Material	Parameter	X*	std.dev	Dx	X*+DX	X*-DX	F+	F-	dF/dX	(dF/dX)^2xσ^2
Clay	Su,ref	26,584	6,6478	3,3239	29,908	23,260	1,236	1,071	0,165	1,203
Clay	Su,inc	2,4246	0,64715	0,323575	2,748	2,101	1,203	1,087	0,116	0,006
Clay	Su,DSS/SuA	0,635454	0,008742	0,004371	0,640	0,631	1,163	1,156	0,007	3,74E-09
Clay	SuP/suA	0,354813	0,007713	0,003857	0,359	0,351	1,159	1,159	0	0,00E+00
Clay	γ	19,87	0,523608	0,261804	20,135	19,612	1,165	1,151	0,014	5,37E-05
										1,209
									σF	**1,099**
									pf	0,444
									pf %	44,39 %
									β	0,141

Monte Carlo Simulation

A Monte Carlo simulation has been run on the safety factor. The simulation have been made with 1000 runs. A high and low safety factor is calculated by taking the mean value of the safety factor from the FOSM and subtract and add the standard deviation from the FOSM multiplied by a random number between zero and one se equation 5.6. The mean value of High and Low safety factor is then calculated together with the standard deviation and is then tested for the probability that F is lower than 1.

$$F_{High,Low} = \mp\sigma_F \cdot Random\ number \qquad (5.6)$$

Results

The slope stability is very low at the natural state the factor if safety is 1.191. The results from all FOSM in Scenario 1 is presented in table 36, 37 and 38.

Table 36 FOSM results with 10 % of standard deviation.

Parameter	Value
F mean	1.158
σF	0.187
pf	26.31 %
Beta index	0.847

Table 37 FOSM results with 30 % of standard deviation.

Parameter	Value
F mean	1.160
σF	0.666
pf	40.53 %
Beta index	0.240

Table 38 FOSM results with 50 % of standard deviation.

Parameter	Value
F mean	1.155
σF	1.099
pf	44.39 %
Beta index	0.141

In table 39 the result from the Monte Carlo Simulation is presented. This is after 1000 simulations runs. The frequency plot for the safety factor from the Monte Carlo Simulation with 10% of the standard deviation is shown in figure 46.

Table 39 Monte Carlo simulation results Scenario 1 for the different variation of standard deviations

	σ 10%	σ 30%	σ 50%
μF	1.157	1.153	1.164
σF	0.039	0.133	0.230
pf(F<1)	0.003 %	12.48 %	23.74 %
β	4.019	1.152	0.715

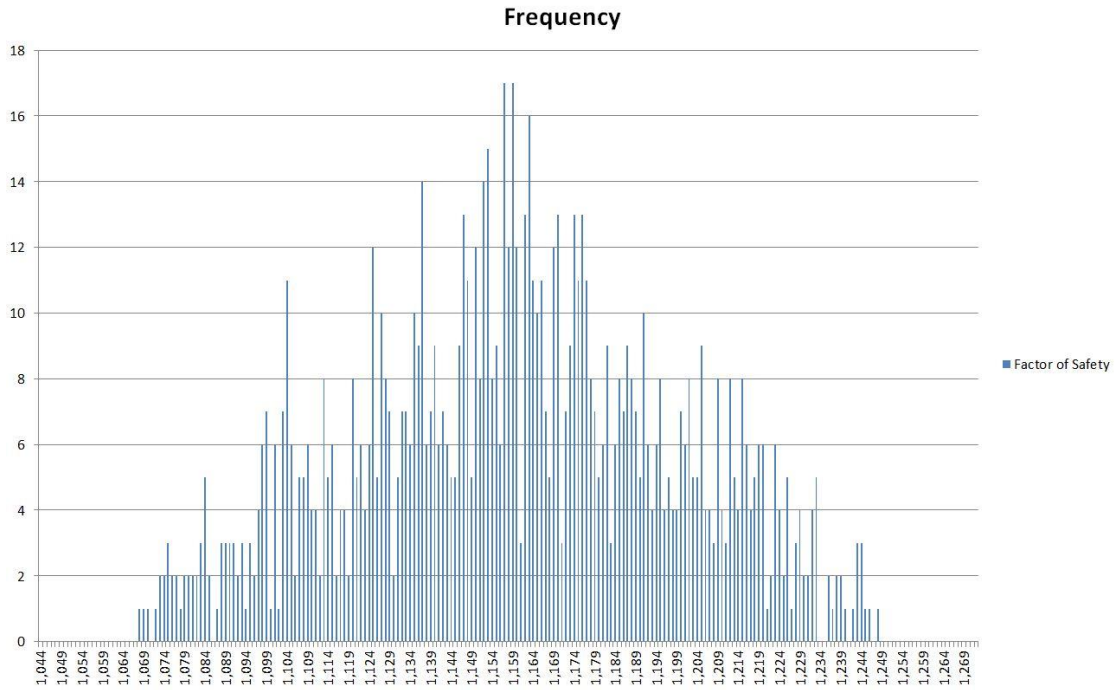

Figure 46 frequency plot of safety factor from the Monte Carlo simulation with 10% standard deviation

Comment

The coefficient of variance is very low for $\frac{s_u^{DSS}}{s_u^A}$ and$\frac{s_u^P}{s_u^A}$, 1.5% and 2.3%. According to Phoon the liquid limit that the relation is developed from with the equations in table 2 is varying with 3 to 20 %. These equations are saying 0.63 for $\frac{s_u^{DSS}}{s_u^A}$ and 0.35 for $\frac{s_u^P}{s_u^A}$ if the plasticity index is lower than 10 and the test results shows that is the case. A test run with 10 % CoV on these parameters were done and it showed that it had low impact on the result. The difference is on the fourth decimal on Msf.

5.7 Scenario 2

In scenario 2 the analysis will be carried out with input parameters evaluated from new praxis. That is CPTU and Sherbrooke samples with triaxial test. The parameter values in the study is peak values therefore strain softening is not considered.

The setup is for FOSM and stability calculations are the same as in scenario 1. It is the input parameters that is alternated based on the new investigation methods that is used.

Sherbrooke block samples

The samples are from depths between3.64 to 4.07 m depth and they are all thought to be from the same layer. This layer was identified as quick clay in the early stages by NGI and that is the reason for the block samples were taken here.

Routine Investigations

The sensitivity is lower than the criterion for quick clay but it shows that it is in the region extra sensitive clay to quick clay. The plasticity index was also here mostly beneath 10 % see table 40.

Table 40 routine investigations of the Sherbrooke samples (Kornbrekke 2012)

Block sample:		3.50-3.85 m	3.85-4.20 m	4.20-4.60 m
s_u (konus)	[kPa]	13.70	18.60	13.70
s_r	[kPa]	0.69	1.45	0.69
S_t	[-]	19.86	13.36	19.86
γ	[kN/m^3]	19.43	19.58	19.3
w	[%]	33.68	36.57	37.7
w_p	[%]	18.08	16.48	19.37
w_l	[%]	26.24	25.22	29.72
I_p	[%]	8.16	8.74	10.35
I_f	[%]	3.30	2.30	4.30
n	[%]	47.73	48.43	49.55
S_r	[%]	85.56	96.45	98.64
e	[-]	1.09	1.05	1.06
S	[g/l]	6.00	4.00	2.00

CPTU

The undrained active shear strength is interpreted from the CPTU test. The CPTU curves are plotted for each 10 cm in depth that is the reason for the look of their graphs see figure 47.

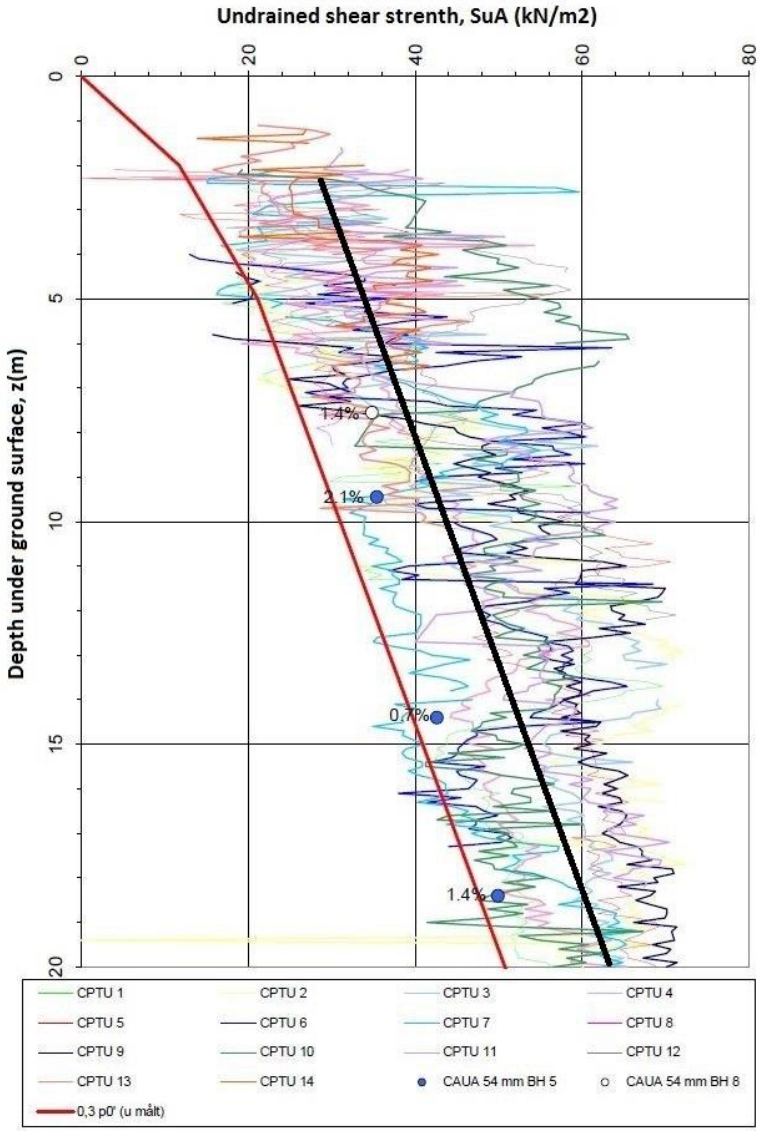

Figure 47 CPTU test undrained shear strength plotted with depth.

The CPTU graphs have been used to evaluate the increase of shear strength with depth, the $s_{u\ inc}$ term. A function is adapted to the different values where the reference shear strength is taken from the block samples. The CPTU implies a little lower increase with depth than the 54 mm samples where suggesting. The shear strength is increasing with 2.77 kPa per m. This is evaluated from the CPTU graphs and the standard deviation is calculated with the simplified method to be 0.28kPa.

Su ref

The shear strength is evaluated from the triaxial test performed on the Sherbrooke samples see table 41. The mean value where 28.86 kPa with a standard deviation of 4.98, this was determined with simplified method. Su ref is considered to be normal distributed. This is shown in figure 48 where the frequency histogram and bell function is plotted for three standard deviations.

Table 41 block sample shear strength

Depth [m]	S_u [kPa]:
3.96	33.48
3.96	31.16
4.07	30.26
4.07	28.97
4.07	30.25
4.07	25.8
3.64	31.22
3.75	28.95
3.64	25.44
3.64	32.36
3.75	21.28
3.75	27.32
3.75	17.08
4.37	35.39
4.37	34.68
4.37	30.32
4.37	31.27

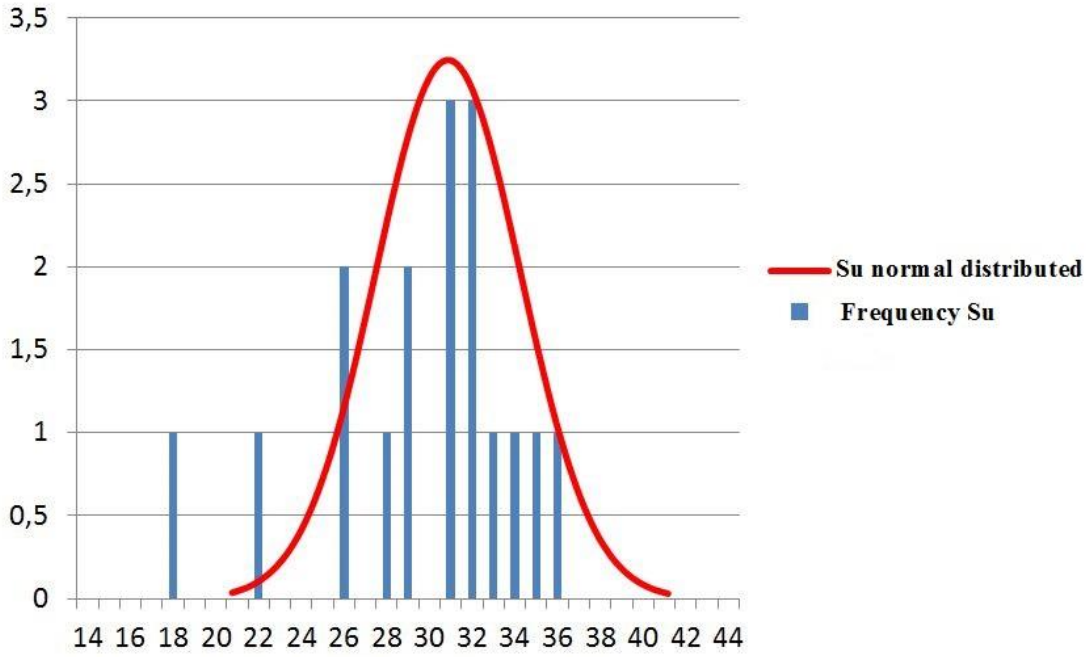

Figure 48 Su ref normal distributed and frequency histogram

The ADP parameters where determined with the same method as in scenario 1 with correlation to the plasticity index. Only three samples where available and two of them had Ip under 10 %. The result is shown in table 42.

Table 42 mean value and standard deviation for SuDSS/SuA and SuP/SuA.

Value	SuDSS/SuA	SuP/SuA
Mean	0.63	0.35
Std.dev	0.01	0.01

Material Model

The material model that is used in the analysis is NGI-ADP for the clay layer and Mohr-Coulomb Model for the Embankment and dry crust.

Calculation Steps

The same calculation procedure as in scenario 1 is used in the analysis for scenario 2. See table 31 for the calculation steps.

Results stability calculations

The behaviour is similar to scenario 1, in the natural state the slip surface goes deep down to the boundary and when embankment is constructed the slip surface is beneath the embankment. Figure 49 shows the slip surface as the incremental deviatoric strain and 50 the multiplier for safety facto both is taken from scenario 2 with mean values on all parameters.

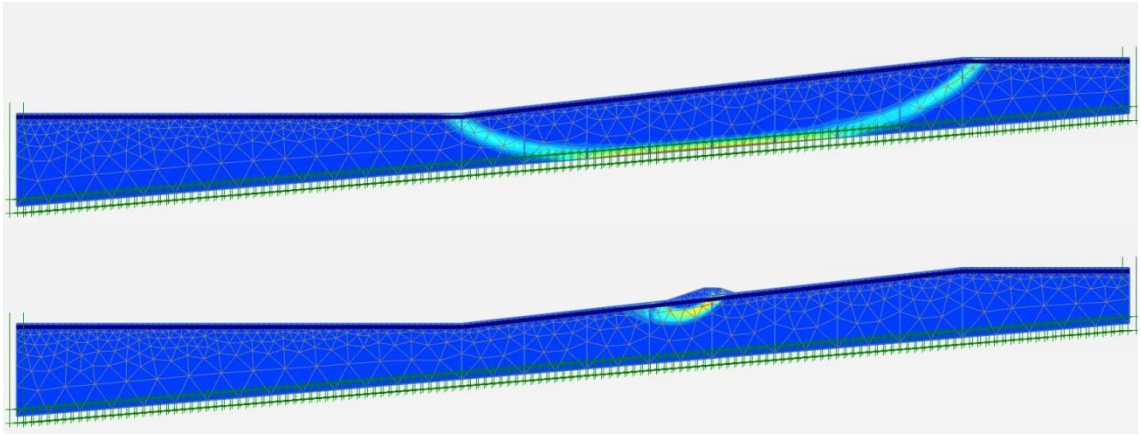

Figure 49 slip surface in the natural state and after construction of the embankment incremental deviatoric strain

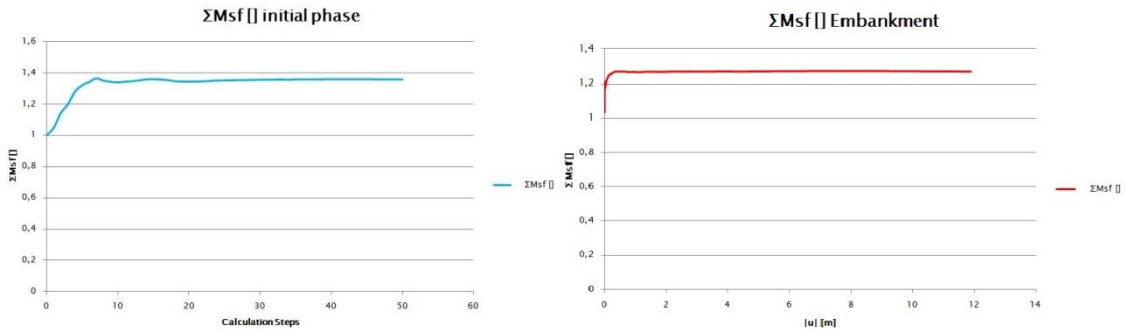

Figure 50 Msf from the Plaxis analysis shows the safety factor before and after construction of embankment

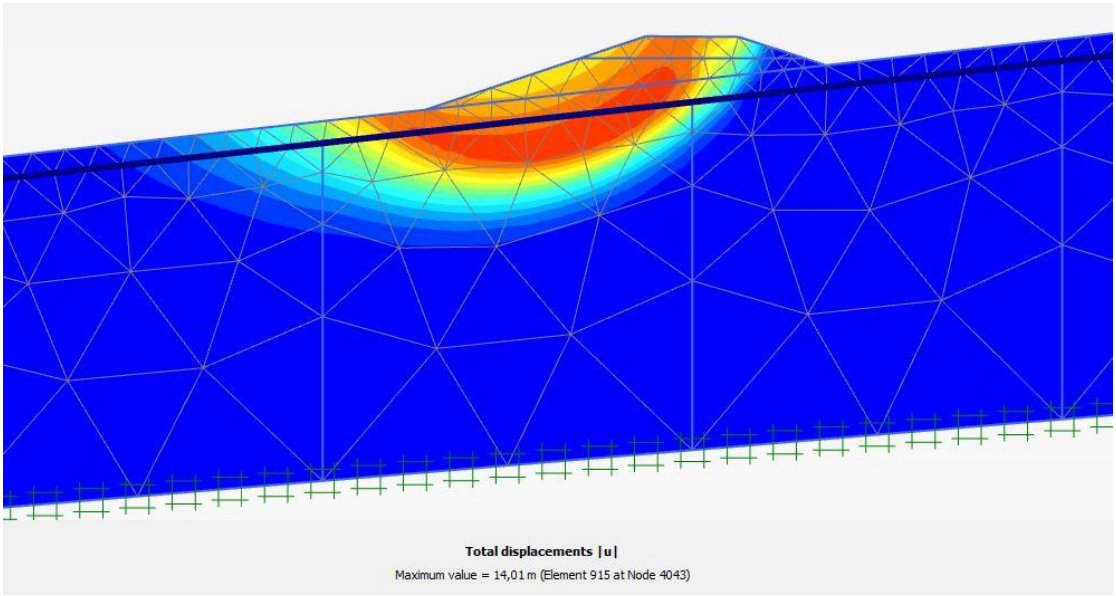

Figure 51 failure mechanisms for scenario 2 with mean values

The failure mechanisms for scenario 2 with mean values calculated from c-φ reduction is shown in figure 51.

FOSM

The set up for FOSM in scenario 2 is the same as in scenario 1. The analysis is done with 10 %, 30% and 50 % of the standard deviation as variation. To each independent variable mean value and standard deviation has been estimated from data of ground investigations by Sund-Bradden, see table 43. All parameters are considered to be normal distributed.

Table 43 input parameters with distributions scenario 2.

Variable	Mean value μ	Standard Deviation σ	Distribution	μ based on	σ based on
Su ref	28.86	4.981	Normal	B,A	T, f
Su inc	2.77	0.300	Normal	C, A	f
SuP/SuA	0.350	0.001	Normal	Ip, A	f
SuDSS/SuA	0.630	0.001	Normal	Ip, A	f
γ	19.38	0.248	Normal	B,A	s

μ and σ based on:

Type of test: B- Block Sample; C-CPTU; T-Triax test; Ip-Plasticity Index

Method: f- simplified method; s-standard deviation; A-Average

The FOSM analysis in scenario 2 is presented in table 44, 45 and 46.

Table 44 FOSM with 10 % of the standard deviation

Material	Parameter	X*	std.dev	Dx	X*+DX	X*-DX	F+	F-	dF/dX	(dF/dX)^2xσ^2
Clay	Su,ref	28,86	4,498	0,450	29,310	28,410	1,287	1,258	0,029	0,017
Clay	Su,inc	2,770	0,277	0,028	2,798	2,742	1,276	1,271	0,005	1,92E-06
Clay	Su,DSS/SuA	0,630	0,001	0,0001	0,630	0,630	1,274	1,272	0,002	4,00E-12
Clay	SuP/suA	0,350	0,001	0,0001	0,350	0,350	1,275	1,272	0,003	9,00E-12
Clay	γ	19,38	0,248	0,025	19,405	19,355	1,273	1,272	0,001	6,15E-08
										0,0170
									σF	**0,1304**
									pf	0,0182
									pf %	1,82 %
									β	2,084

Table 45 FOSM with 30 % of the standard deviation

Material	Parameter	X*	std.dev	Dx	X*+DX	X*-DX	F+	F-	dF/dX	(dF/dX)^2xσ^2
Clay	Su,ref	28,86	4,498	1,349	30,209	27,511	1,317	1,235	0,082	0,136
Clay	Su,inc	2,770	0,277	0,083	2,853	2,687	1,282	1,264	0,018	2,49E-05
Clay	Su,DSS/SuA	0,630	0,001	0,000	0,630	0,630	1,274	1,272	0,002	4,00E-12
Clay	SuP/suA	0,350	0,001	0,000	0,350	0,350	1,275	1,272	0,003	9,00E-12
Clay	γ	19,38	0,248	0,074	19,454	19,306	1,276	1,271	0,005	1,54E-06
										0,136
									σF	**0,369**
									pf	0,229
									pf %	22,90 %
									β	0,743

Table 46 FOSM with 50 % of standard deviation

Material	Parameter	X*	std.dev	Dx	X*+DX	X*-DX	F+	F-	dF/dX	(dF/dX)^2xσ^2
Clay	Su,ref	28,86	4,498	2,249	31,109	26,611	1,337	1,212	0,125	0,316
Clay	Su,inc	2,770	0,277	0,139	2,909	2,632	1,288	1,258	0,03	6,91E-05
Clay	Su,DSS/SuA	0,630	0,001	0,001	0,631	0,630	1,274	1,272	0,002	4,00E-12
Clay	SuP/suA	0,350	0,001	0,001	0,351	0,350	1,275	1,272	0,003	9,00E-12
Clay	γ	19,38	0,248	0,124	19,504	19,256	1,274	1,272	0,002	2,46E-07
										0,316
									σF	**0,562**
									pf	0,313
									pf %	31,34 %
									β	0,486

Monte Carlo Simulation

The Monte Carlo simulation is made in the same manner as in scenario 1.

Results

The global factor of safety in the natural slope is 1.36. When the embankment is built the safety factor is 1.27 in all cases. If larger variation of safety factor is used in the model the standard deviation of safety factor is greater and also the probability of failure gets higher. The analysis with 10 % standard deviation, see table 47, got the lowest probability of failure of all analyses that are made.

Table 47 FOSM results with 10 % of standard deviation.

Parameter	Value
F mean	1.273
σF	0.131
pf	1.82 %
Beta index	2.084

The probability of failure and reliability index is changing for the worse if larger variation in standard deviation is used see table 48 and 49. This is naturally a direct consequence of statistic calculations.

Table 48 FOSM results with 30 % of standard deviation.

Parameter	Value
F mean	1.274
σF	0.369
pf	22.9 %
Beta index	0.743

Table 49 FOSM results with 50 % of standard deviation.

Parameter	Value
F mean	1.273
σF	0.562
pf	31.34 %
Beta index	0.486

The results from the Monte Carlo simulation in scenario to have all probability of failure lower than 1 % see table 50. The distribution of the factors of safety from the Monte Carlo Simulation is plotted in Figure 52, this is for the case with 30 % standard deviation.

Table 50 Monte Carlo simulation results Scenario 2 for the different variation of standard deviations

	σ 10%	σ 30%	σ 50%
μF	1.273	1.272	1.273
σF	0.026	0.077	0.114
pf(F<1)	0.000 %	0.022 %	0.852 %
β	10.507	3.510	2.386

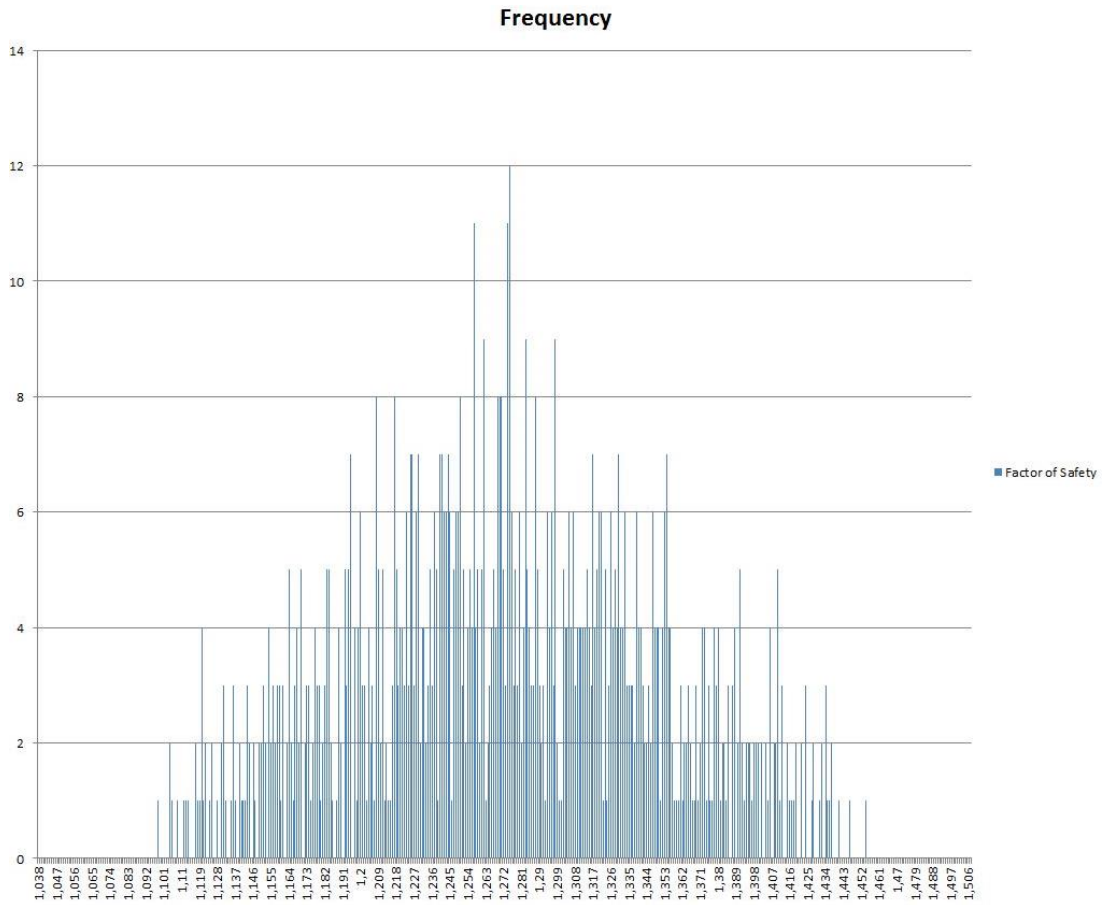

Figure 52 distribution of the factor of safety from Monte Carlo simulation using 30 % standard deviation

The probability of failure from the analysis is adapted to a probability distribution. Normal distribution is assumed to match the data well, see figure 53. The curve parameters for normal distribution is obtained by taking the difference of the accumulated factor of safety and the cumulative normal distribution.

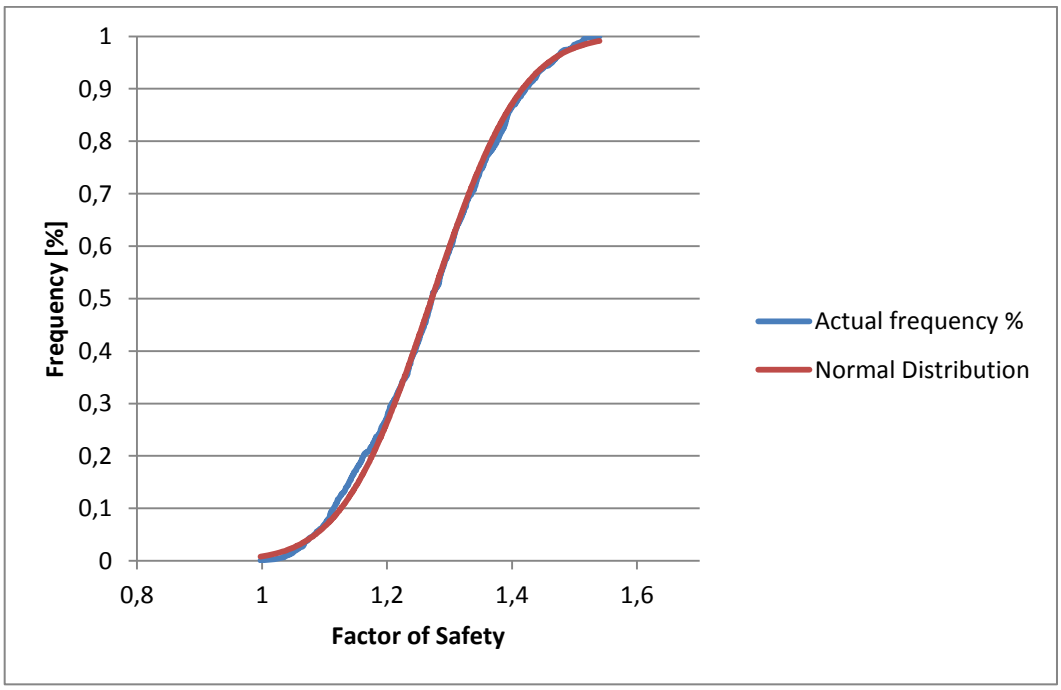

Figure 53 cumulative adaption for factor of safety with normal distribution for 50 % standard deviation

5.8 Comparison between Scenarios

The higher shear strength from the Sherbrooke samples and the higher inclination term led to higher safety factor in Scenario 2, 1.36 compared to 1.191 in the slopes natural state.

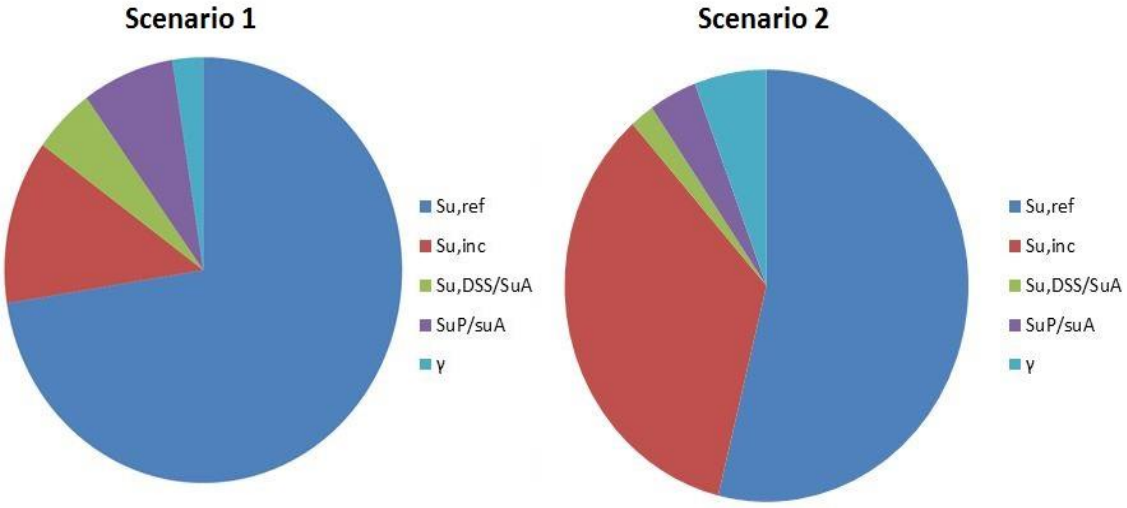

Figure 54 pie chart showing the effect each modelled parameter has on the safety factor in the 10 % trial.

In both scenarios Su ref and Su inc have the largest effect on safety factor see figure 54. These two parameters clearly govern the stability. The variation in the anisotropy parameters are were very low. This is due to the way they are calculated, when the plasticity index is lower than 10 they are fixed. The probability of failure is based on that the factor of safety is normal distributed. The reliability index gives a measurement on how many standard deviations there are until failure. Table 51 gives a summary of probability of failure and reliability index from scenario 1 and 2.

Table 51 probability of failure and beta index results from the analysis.

		pf	β
Scenario 1	10% σ	26.31 %	1.158
	30% σ	40.53 %	1.742
	50% σ	44.4 %	1.05
Scenario 2	10% σ	1.82 %	9.759
	30% σ	22.9 %	3.453
	50% σ	31.34 %	1.273

5.9 GeoSuite Calculations

The stability calculations in GeoSuite are used as a compliment to give a validation to the stability calculations in Plaxis. The geometry is made by NGI from ground investigation in the area (NGI 2009 B). Both scenarios are analyzed in GeoSuite to with same terrain model but with different layer profile. The different layer profile in the section is due to the new methods found out that the old praxis methods suggested inaccurate layer structure.

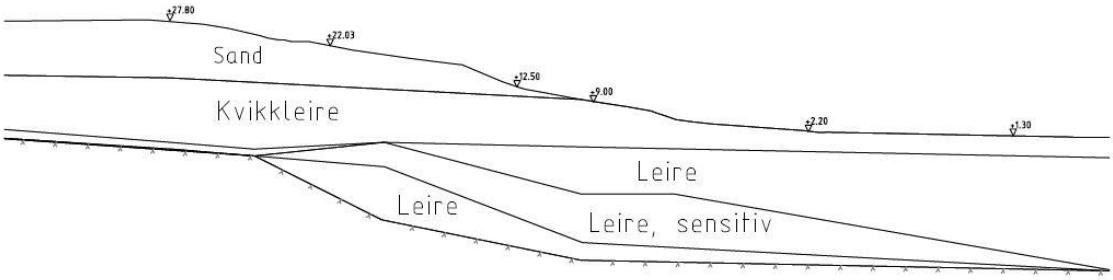

Figure 55 profile from Old Praxis methods.

The quick clay material that were assumed to be on top in the old profile were found out in the new testing to be a sensitive clay see figure 55 and 56.

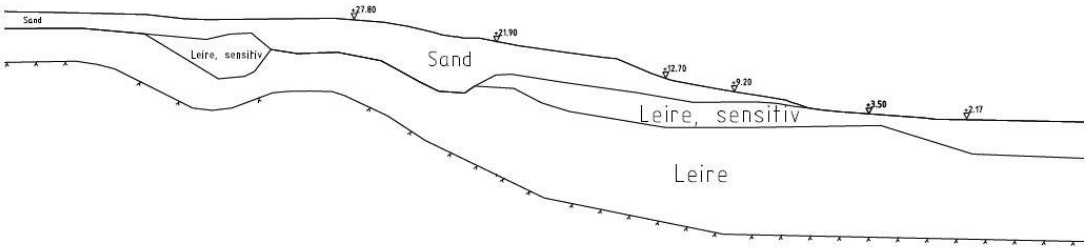

Figure 56 profile from new praxis methods.

The safety factor calculated for same situation as scenario 1 where between 1.03 to 1.14 in the natural state, see figure 57. The most critical slip surface where found in the slope most likely to the layer that was thought to be quick clay. The results from new praxis methods were a safety factor between 1.28 to 1.35 see figure 58.

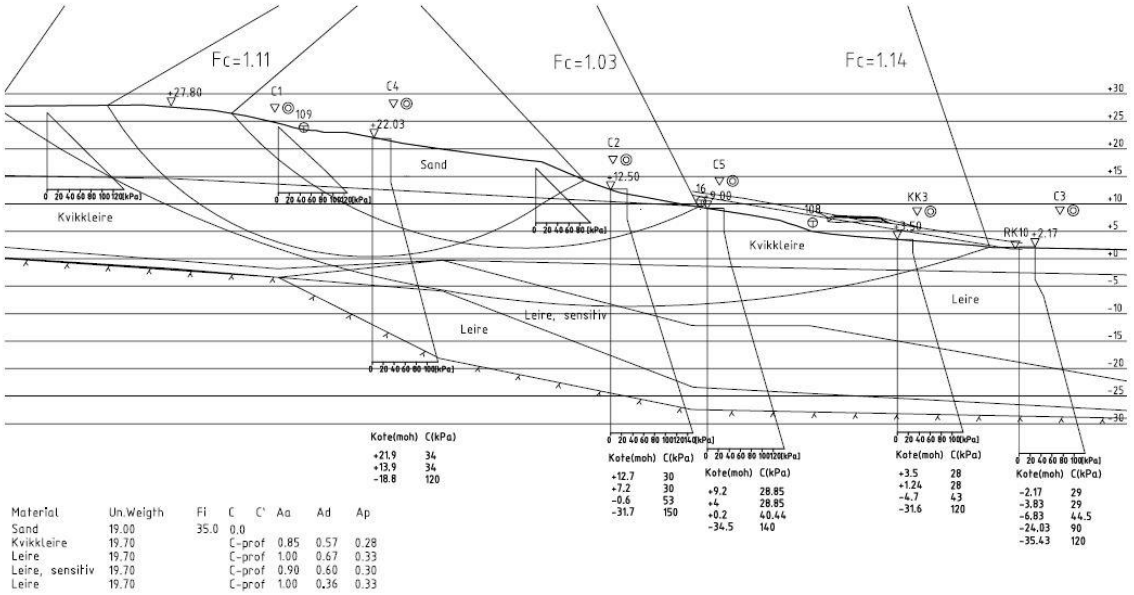

Figure 57 GeoSuite stability calculations scenario 1.

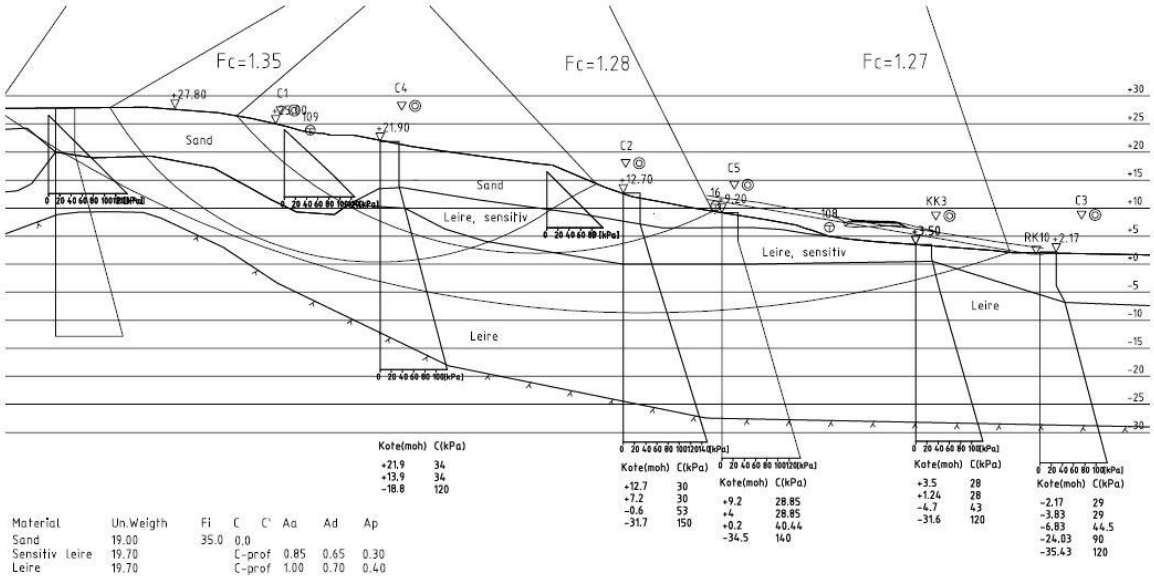

Figure 58 GeoSuite stability calculations scenario 2.

6 Discussion

In this chapter the model is discussed, assumptions and uncertainties and what effect they have on the result. Similarities and differences in results in this thesis compared to others are discussed.

6.1 Model

The Plaxis analysis tries to represent the reality and perform numerical analysis to get a value on the slope stability in the form of safety factor. This model contains many simplifications and assumptions. The geometry is simplified so that topographic variations are not fully taken into the geometry and in the thesis Plaxis 2d is used. The layers in the model is treated as a homogenous clay layer even though it is classified as different layers from ground investigations. This is considered in the GeoSuite calculations but the results are similar between the programs.

FOSM is a relatively simple method to estimate the probability function to the safety factor of the slope. More advanced method can be used but that will require more work to perform manually and will require computer programs to perform the reliability analysis. The probability of failure that is given from the FOSM shall not be regarded as a design value more as a validation parameter in the calculations. The probability of failure is dependent on how the definition of the safety factor or safety margin is made. In this report the Msf in the Plaxis have been the benchmark. To get annual probability of failure trigger mechanisms must be introduced and that require a more advanced model. The more of the standard deviation that is used when parameter values are changed in the analysis the larger the standard deviation of the safety factor is. Therefore the choice that the user does will have a large impact on the result.

The reliability index is defined as mean value over standard deviation in this report other definitions are possible to use. This gives a measurement of how many standard deviations there are until failure.

The FOSM is a transparent method that can easily be applied to stability calculations in geotechnics. It gives results so that comparisons can be made and uncertainties can be treated in it without unreasonable workload for the engineer.

6.2 Input Parameters

In the case study extensive amount of ground investigation and laboratory material from the site were available. Even though to that the amount of data is more extensive than in a normal project it is not so much statistically regarded. Often the simplified method developed by Snedecor and Cochran have been used to calculate standard deviations but this have been tested and it was confirmed that it gives accurate values. In this study have the peak value for the strength parameters been used so strain softening have not been considered. This is due to that the method how these values is determined is under review. The effect on this study would not have an impact since the scope is to look upon the differences between old and new praxis.

This study with different magnitude of the standard deviation used in the FOSM shows how much the probability of failure is changing. When determine parameter values from 54 mm samples or CPTU 1 kPa more or less can easily be chosen but it will have a great impact on the result.

$s_{u\,ref}^{A}$

The reference value of the shear strength is the parameter that has the greatest effect on the safety factor. The new praxis is resulting in a higher shear strength profile compared to old praxis methods. This may be to the higher quality of the samples that Sherbrooke gives compared to 54 mm piston sample.

The shear strength parameters can be affected by many things when they are determined. When sensitive clay is analyzed it is especially important to be sure that the sample is not disturbed when the laboratory test are performed. The strain rate that the triaxial tests are made can also have an impact on the value of the undrained shear strength. For samples of same specimen or ground level an increase of about 30 % in undrained shear strength where obtained. In scenario 2 where Block samples is used they are treated in laboratory as if they have perfect quality from standards used but in fact they also have disturbance. But the study is showing that higher quality of the samples gives higher shear strength and thereby also higher slope stability. The closer to the real values that is current in the soil the better can the result be regarded to be.

$s_{u\,inc}^{A}$

The increase of shear strength with depth where also found to be higher when CPTU curves were evaluated compared to the results from the 54 mm piston samples. The estimation of the increase from CPTU is considered to be more certain though it gives data continuously for many levels plotted with depth. The 54 mm piston samples give only values from the levels where samples are taken and between these a function have to be estimated. The CPTU will also providing a continuous profile with the depth not only single points as the 54 mm samples will only give a value at the level that the samples is taken at. This means that an approximation of the values in between the tested levels have to be made and changes in layer structure can be missed.

ADP-factors

In the calculations the new recommendations stated in Report 14 2014 from NIFS have been used. These recommendations is based on the plasticity index that comes from the difference between liquid limit and plasticity limit. These values have low variation within layers and with depth and therefore this are valid. It is the active shear strength that have the largest importance to the result.

The ADP conditions are directly incorporated in the soil model used in this project.

Results

The results say that the stability is low in the slope. This confirms that concerns NPRA had when the project was halted. The stability was lower in scenario 1 than 2 this is also reflected in the probability of failure and reliability index. Calculations made by others with data from old praxis methods have come up with results of a safety factor between 1.03 to 1.14 in natural state. With new praxis method results where F between 1.16 to 1.53. The results in this study is in the same region as the results from NGI previous investigations of the area.

The probability of failure and reliability index can give a complement to the calculation so that the result can be interpreted more but they shall not be used as a design value.

7 Conclusions

The literature study on the probabilistic methods applied to slope stability concludes that probabilistic methods applied to slope stability and geotechnical engineering can give new insights and understanding of the calculations. In praxis today a probabilistic approach are however these methods not in use. To transform the theory of available probabilistic methods into practice is a very time consuming process this is due to that there are relatively few real project where probabilistic methods have been applied. So the few earlier projects that have been made have had a scientific element and not a practical so a clear framework for example a slope stability calculation does not exist. This means that it will be difficult to use a probabilistic method as a design tool today because of the many analyses that have to be made. But for research purposes and for evaluation of slope stability it can help to get a better understanding and provide a good understanding of the concepts of standards based on probabilities. It is also important to remember that the answers from a probabilistic method is not an absolute truth it is still a model of the reality but it will give more tools to geotechnical engineering.

The literature study is showing different practices in the Norway and Sweden. Both countries have a standard based on Eurocode but it has been interpreted with some differences. Determination of dimensioning values and the working procedures is not the same in the both countries. The normal field investigation methods are also different. Norwegian projects often utilize total sounding with rotary pressure sounding and 54mm piston sampler compared to 50 mm piston sampler and total sounding in Sweden. In Norway quick clay is a well-known phenomenon that has been in focus for geotechnical engineering, therefore have the methods been developed to detect clay and especially presence of quick clay. In situ parameters are determined with CPT in both countries however does not one evaluation standard exist in Norway as Sweden's Conrad. Every firm has their own program often Excel based. The laboratory testing is made with the same methods. The routine investigations are the same but in Sweden they are often complemented with CRS-test and in Norway Triaxial test. Laboratories in Norway have often high work load so that waiting time for testing can be several months, meaning that samples have to be stored. The definition of quick clay in Norway is remolded undrained shear strength less than 0.5 kPa and in Sweden less than 0.4 kPa. Stability calculations is made different, in general calculations with effective stresses is performed more in Norway, meaning that more advanced laboratory testing have to be made. FEM programs are more in use in Norway. In Sweden total stresses analysis and combined analysis is used in calculations and in Norway either total- or effective stresses analysis is made separately. In total stresses analyses is ADP analysis used in Norway. In Sweden the direct shear strength is in general used as a mean value along the whole slip surface. Therefor is the Swedish calculation more conservative since considering anisotropy will give higher safety factor in cohesion soils. Total stresses is also used in Norway for cases with short or rapid load changes ab effective stresses analysis is used for drained long term conditions. Meaning that that bearing capacity calculation is made with effective stresses analysis, which is rare in Sweden.

The first benchmark case is showing that a probabilistic approach do not have to be very advanced and can be very useful when a problem with an element of future predictions is to be analyzed. The further develop this model an event tree should be made to see the event probabilities.

One important conclusion from the benchmark cases is that a high safety factor is not necessarily saying that a slope is safe. The benchmark cases is showing that the variations of the safety factor can be larger so that a slope with a safety factor well over 1 can have a standard deviation so that probability of failure is higher for a slope with a high safety factor than a slope with a lower safety factor with smaller standard deviation of the safety factor.

Both benchmark cases are demonstrating that a probabilistic analysis doesn't have to involve a calculation effort that is extremely high.

The case study has been made from a real case in Norway in the light of the available data from laboratory and field investigations. The information given from a reliability analysis is providing useful information of the problem and can also be used for further development of a probabilistic design concept. What also is shown in the case study is how a reliability analysis can be incorporated with a FEM program.

The comparison between the scenarios shows that higher quality in ground investigation results increases the reliability in the stability calculations. In this study between old and new praxis the uncertainties in the ground investigation material are also made visible.

New praxis Sherbrooke samples correlated with CPTU results leads to higher shear strength profiles. Both Su ref and Su inc is higher and this affects the safety factor since these two parameters have the largest impact as can be seen in the sensitivity analysis.

The results from the slope stability calculations performed in Plaxis are assessed to be credible since they are showing results similar to the GeoSuite calculations. If a probabilistic method shall be used a deterministic calculation shall also be made to validate the result.

The parameter study shows which parameters that have the greatest effect on the safety factor. s_u^A is the parameter with the largest effect on the factor of safety. Therefore effort to get good investigations on the shear strength parameters and conclude how they should be evaluated and what is influencing them in field and laboratory. This can also give guidance on what ground investigations in field and in laboratory that shall be made.

Statistical evaluation in geotechnical parameters are hard to made since the data available from ground investigations are limited. Even though in this case study much data were available it is a small number to perform statistical calculations on and in a normal project the data available will be even less.

Probabilistic methods is a rational approach to approach the uncertainties involved in geotechnical engineering. It will give an assessment of the calculation and give a measurement of the reliability of the results from the calculation. Probabilistic methods can be of interests to look upon to know how site and laboratory investigations are set up in the planning phase.

8 Further studies

A study with the material model NGI-ADP softening could be of interests to evaluate and also evaluate the effect of progressive landslide development in cohesion material. If softening is to be used more input parameters is used and therefore a more automated calculation method are recommended to be used.

A systematic approach to evaluate ground investigation methods with a probabilistic method. So that it becomes possible to determine the correct shear strength profile in projects that have many investigations in the same area. Statistical methods such as Geostatics can be evaluated.

Make an evaluation of the slope stability in the area of the case study with Plaxis 3d.

A more sophisticated level 3 method applied to the same case study.

Can probabilistic approach be a widely used method in Geotechnics and how shall a model be? Can the probabilistic methods be used to evaluate and choose partial factors?

9 References

Abrahamson, L.W., Lee T.S., Sharma, S. and Boyce, G.M. (2002). Slope stability and stabilization methods second edition. John Wiley & Sons, Inc., New York

Andréasson, P-G. (2009) *Geobiosfären en introduktion.* Lund: Studentlitteratur AB

Ang, A. H.S and Tang W. H. (2006) *Probability concepts in engineering planning & design, 2nd edition* John Wiley Sons, New York first edition 1984.

Alén, C. (1998), *ON PROBABILITY IN GEOTECHNICS -Random calculation models exemplified on slope stability analysis and ground-superstructure interaction* Department of Geotechnical Engineering. Chalmers University of Technology. Gothenburg.

Alén, C. (2012) *Säkerheten för befintliga slänter* Presentation at Teknologidagene – Trondheim 10-11 oktober 2012

Alén, C. (2013) *Lecture in Risk Analysis and. Decision Support in Engineering at Chalmers 2013.*

Beaecher, G.B. (1986) *Geotechnical Error Analysis* Transportation Research Record Issue 1105 p.23-31

Baecher, G.B. and Christian, J.T (2003) *Reliability and Statistics in Geotechnical Engineering* John Wiley & Sons Ltd, The Atrium, Southern Gate, Chichester, West Sussex PO19 8SQ, England.

Benjamin, J. R. and Cornell, C. A., (2014) Probability, Statistics, and Decision for Civil Engineers 1970 edition, Doover Publications, New York, USA

Bjernum, L. Simons, N.E. (1960). Comparison of shear strength characteristics of normally consolidated clays, in Proceedings of research conference on shear strength of cohesive soils, Boulder Colorado

Cao, Z. and Wang, Y. (2013) *Bayesian Approach for Probabilistic Site Characterization Using Cone Penetration Tests* Journal of Geotechnical and Geoenvironmental Engineering (139 p.267-276.

Ching, J., Phoon, K.-K., Chen, Y.-Y. (2010). *Reducing shear strength uncertainties in clays by multivariate correlations* Canadian Geotech. Journal. 47: 16-33.

Christian, J. (2004). ”Geotechnical Engineering Reliability: How Well Do We Know What We Are Doing?.” *J. Geotech. Geoenviron. Eng.*, 130(10), 985–1003.

Christian, J.T. Ladd, C. Baecher, G.B. (1994) Reliability applied to slope stability analysis. Journal of geotechnical engineering, Vol. 120, No. 12, December, 1994

Craig, R.F. Knappett, J.A. (2012) Craigs's soil mechanics Eight edition. Spon Press London and New York 2012

Duncan, J.M. and Wright, S-G. (2005) *Soil Strength and Slope Stability* New Jersey; John Wiley & Sons, Inc

Eskstrand, D. and Nylander, P. (2013) *Probabilistic approach to Slope Stability – Assessing Safety, Impact from Underlaying Structures and Clay Properties in Pre Constructed Areas.* Master thesis Chalmers University of Technology Department of Civil and Environmental Engineering Gothenburg

Gregersen, O (1981) The quick clay landslide in Rissa, Norway. The sliding process and discussion of failure modes NGI, Publication No. 135, Oslo 1981.

Griffiths, D.V and Fenton, G.A. (2007) Review of Probability Theory, Random Variables, and Random Fields Springer Vienna New York

Griffiths, D.V and Fenton, G.A. (2007) Probabilistic methods in geotechnical engineering, SpringerWienNewYork

Griffiths, D.V and Fenton, G.A. (2004) Probabilistic slope stability analysis by finite elements. JOURNAL OF GEOTECHNICAL AND GEOENVIRONMENTAL ENGINEERING © ASCE / MAY 2004 / 507

ISO (2012) *Geotechnical investigation and testing -- Field testing -- Part 1: Electrical cone and piezocone penetration test* ISO 22476-1:2012.

Janbu, N. (1954). Stability analysis of slopes with dimensionless parameters. Doctorial Thesis. Cambridge Massachusetts.

Jones, A. L., Kramer, S.L, Arduino, P. (2002) Estimation of uncertainty in Geotechnical properties for performance-based earthquake engineering. University of Washington.

Kornbrekke, A. H. (2012) Skråningsstabilitet ved Rein Kirke med utgangspunkt i resultater fra sherbrooke blokkprøver Fakultet for ingeniørsvetenskap og teknologi Institutt for bygg, anlegg og transport Faggruppe for Geoteknikk NTNU Trondheim 2012 (In Norwegian).

Kulhawy, F.H. (1992). On evaluation of static soil properties Stability and performance of slopes and embankments II (GSP 31) American Society of Civil Engineers, New York

Lacasse S. and Nadim, F (1997) Uncertainties in characterising soil properties Norwegian Geotechnical Institute Oslo, Norway

Long, M. El Hadj, N. Hagberg, K. (2009) *Quality of conventional fixed piston samples of Norwegian soft clay* ASCE Journal of Geotechnical and Geoenvironmental Engineering, 135 (2): 185-198

Lunne, T. Berre, T., Andersen, K.H. Strandvik, S. Sjursen, M. (2006) *Effects of sample disturbance and consolidation procedures on measures shear strength of soft marine Norwegian clays*, Canadian Geotechnical Journal, Vol. 43, No. 7, pp. 726-759

Madsen, H. O. and Egeland, T. (1989) Structural Reliability: Models and Applications. International Statistical Review / Revue Internationale de Statistique, Vol 57, No. 3 (Dec., 1989), pp. 185-203

Multiconsult (2012) *Tolkning av nye grunnundersøkelser. Bestemmelse av designparamere.* Internprosjekt nr. 1 2011 Sund Rissa, Rapportnummer 414792-2 Multiconsult

Müller, R. (2013) *Probabilistic stability analysis of embankments founded on clay* Doctorial ThesisDivision of Soil and Rock Mechanics Department of Civil and Architectural Engineering Royal Institute of Technology Stockholm, 2013

Nadim, F.(2007) Tools and strategies for dealing with uncertainty in geotechnics. International centre for geohazards/ Norwegian Geotechnical Institute, Oslo, Norway.

NIFS A (2012) *Naturefareprosjektet: Kvikkleireworkshop En nasjonal satsing på sikkerhet I kvikkleireområder* Teknologidagene, Trondheim 2012. Rapport 33 2012

NIFS B (2012). Probabilistiske analyser av grunnundersøkelser I sensitive leiromåder Rapport nr.73/2012

Nelson, S (2012) Mass movements Prof. Stephen A. Nelson Tulane University [Retrieved 2014-01-20] Accessible at:

http://www.tulane.edu/~sanelson/eens1110/massmovements.htm

NGI (2009 A) *Rv 717 Sund-Bradden. Tolkning av grundundersøkelser, karakteristiske materialparametre,* Rapport 20091264-00-38-R, NGI

NGI (2009 B) *Rv 717 Sund-Bradden Stabilitetsberegninger* 20091264-00-53-R 9. oktober 2009 Oslo

NGI (2013) *Effekt av progressive bruddutvikling fo utbygging I områder med kvikkleire A4 Sannsynlighetsanalyse* Dokumentnr: 20092128-00-7-R

NGU (2010) *Geofysiske målinger for løsmassekartlegging i Rissa, Sør-Trønderlag,* Rapport 2010.045, NGU

NGU (2011) *Morfologi og skredkartlegging i Botn, Rissa, Sør-Trønderlag,* Rapport 2011.037, NGU

NGU (2012) *Resistivitetsmålinger for løsmassekartlegging ved Rein kirke i Rissa, Sør-Trønderlag,* Rapport 2012.018, NGU

NPRA (2013) Veg- og gateutformning Håndbok 017. Vegdirektoratet Oslo 2013

NPRA (2011). Geoteknikk I vegbygging Håndbok 016. Vegdirektoratet Oslo 2010

Paice, G. M. (1997). Finite element analysis of stochastic soils. PhD. thesis, Univ. of Manchester, Manchester, U.K.

PLAXIS (2011) *PLAXIS Material Models Manual 2011* Plaxis BV. www.plaxis.nl

Peck, RB. (1969). Advantages and limitations of the observational method in applied soil mechanics Géotechnique Volumne 19 Issue 2, 01 June 1969 p. 171-287

Phoon, K-K., Kulhawy, F. H. (1999) Characterization of geotechnical variability Canadian Geotechnical Journal 36(4)

Sandven, R. (1990). *Strength and deformation properties of fine grained soils obtained from piezocone tests* Dr. dissertation Institutt for geoteknikk, Norges tekniske høgskole, Universitetet I Trondheim

Schweckendiek, T. (2006) *Structural Reliability Applied To Deep Excavations-Coupling Reliability Methods With Finite Elements* Section Hydraulic and Geotechnical Engineering Delft University of Technology

SINTEF-Multiconsult (2012) *Detektering av kvikkleire fra like sonderingsmetoder* NIFS delpakke 6

Solberg, I-L. (2007) Geological, geomorphological and geophysical investigations of areas prone to clay slides: Examples from Buvika, Mid Norway. PhD thesis NTNU 2007 Trondheim

Snedecor, G.W. and Cochran, W.G. (1980) *Statistical methods.* University of Iowa Press, p.135-137.

Statens vegvesen (2010), *Håndbok 016 –Geoteknikk I vegbygging* 6. utgave Vegdirektoratet Oslo 2010

Stevens, W. J. (2009) *What is Bayesian statistics?* Hayward Medicalo Communications, a division of Hayward Group Ltd. NPR09/1108.

Sällfors, G. (2009), *Geoteknik Jordmateriallära Jordmekanik* Gothenburg 2009 (In Swedish)

Thakur, V. Jostad, H.P. Kornbrekke, H.A. and Degago, S.A. (2014 A) *How well do we understand the undrained strain softening response in soft sensitive clays?* Chapter 23 in the book *Landslides in Sensitive Clays* pp 291-303.

Thakur, V. Oset, F.Viklund, M.Strand, S-A. Gjelsvik, V. Christensen, S. Fauskerud, O A. (2014 B) *En omforent anbefaling for bruk av anisotropifaktorer i prosjektering i norske leirer* Naturfareprosjektet: Delprosjekt 6 Kvikkleire Rapport nr. 14/2014.

Thoft-Christensen, P. Baker, M.J. (1984) *Structural Reliability Theory and Its Applications* Springer-Verlag Berlin Heidelberg, New York 1982

Vannmarcke, E. (1977), Probabilistic modeling of soil profiles. Journal of the Geotechnical Engineering Division, ASCE, 103(11) 1977

Vanmarcke, E. (1980), *Probabilistic Stability Analysis of Earth Slopes* Engineering Geology, 16(1980) p.29-50

Low, F. and Xu, B. (2006) *Probabilistic stability analyses of embankment based on Finite-Element Method* JOURNAL OF GEOTECHNICAL AND GEOENVIRONMENTAL ENGINEERING © ASCE / NOVEMBER 2006 132: 1444-1454

Zhang, L. Tang, W.H, Zhang, L. and Zheng, J. (2004) *Reducing Uncertainty of Prediction from Empirical Correlations* Journal of Geotechnical and Geoenvironmental Engineering, ASCE 130(5) p.526-534

Zhang, J, Tang, W.H. (2009) *Bayesian Framework for Characterizing Geotechnical Model Uncertainty* Journal of Geotechnical and Geoenvironmental Engineering, ASCE 135(7), 932-940.

Maps

NGU (2014). *Løsmmasser Nasjonal løsmassedatabase* http://geo.ngu.no/kart/losmasse/ (2014-02-04)

NPRA (2012). *Map made for the ground investigations for Fv.717 at Rein Kirke Sund-Bradden.*

NVE (2014). *Skredatlas* www.skredatlas.nve.no (2014-02-04)

10 Appendices

Appendix 1 Benchmark Case 1

Landslide Stability Calculations

Geometry

H=	12.917	m
L_{MAX} =	50.0	m
D1=	8.75	m
α =	14.801	degrees

Calculations for N

d1= 0.677

N1= 7.3

Calculations for N

d1= 0.677

N1= 6.1

Geometry

H=	12.917	m
L_{MIN} =	30.0	m
D1=	8.75	m
α =	24.669	degrees

N mean	6.70
N STDEV	0.258

Water Level

HHW=	11.5	9.42
HW=	11	8.92
MW=	10	7.92
LW=	9	6.92
LLW=	8.5	6.42

Water Levels

mean (LW)	6.92	m
Z·σ =	0.500	m

Stdev = 0.2146

Safety Factors for Slip Surface

Iteration	pW	W	Pd	pSTDEV CU Hi	pSTDEV CU Lo
1	0.769	7.285	133.815	0.343	0.828
2	0.785	7.311	133.558	0.869	0.293
3	0.595	7.037	136.297	0.000	0.236
9998	0.302	6.657	140.098	0.786	0.517
9999	0.379	6.763	139.039	0.704	0.025
10000	0.749	7.252	134.148	0.543	0.868
		Mean	137.528		
		Std.dev	4.9939343		

Probabilities of Landslide

Iteration run	P (F1<1) [%]
1	0.0898
2	0.032
3	0.3160
4	0.0295
5	0.033
6	0.0363
7	0.0318
8	0.0296
9	0.0337
44	0.0317
45	0.0369
46	0.0351
47	0.0314
48	0.0294
49	0.0305
50	0.029
51	0.0325
Mean	0.0378

	N	Cu	Pd
μ	6.886	25.116	137.528
σ	0.149060435	1.269181672	4.9939343
Variance	0.022219013	1.610822116	24.939379
Variance %	0.32 %	6.41 %	18.13 %

	μ	σ	β
m	0.2304	0.192375024	1.1976045
F	1.259	0.0830	3.1221092

Material properties

ϒ =	16.0	kN/m^3
ϒw =	10.0	kN/m^3

Cu

Cu,average	25	kPa
VAR	10 %	%
Culow	18.7999	
Cuhi	31.4001	
STDEV Cu	6.3001	

pCu	STDEV Cu Hi	STDEV Cu Lo	Cu Up	Cu Lo	Cu	pSTDEV Lo
0.925	2.16336	5.219	27.263	19.881	23.572	0.6087
0.061	5.47732	1.844	30.577	23.256	26.917	0.0176
0.651	0.00156	1.488	25.102	23.612	24.357	0.2963
0.024	4.95286	3.260	30.053	21.840	25.947	0.1680
0.606	4.43690	0.157	29.537	24.943	27.240	0.1135
0.638	3.42240	5.468	28.522	19.632	24.077	0.7780
		MEAN	28.253	21.978	25.116	
				Std.dev	1.26918167	

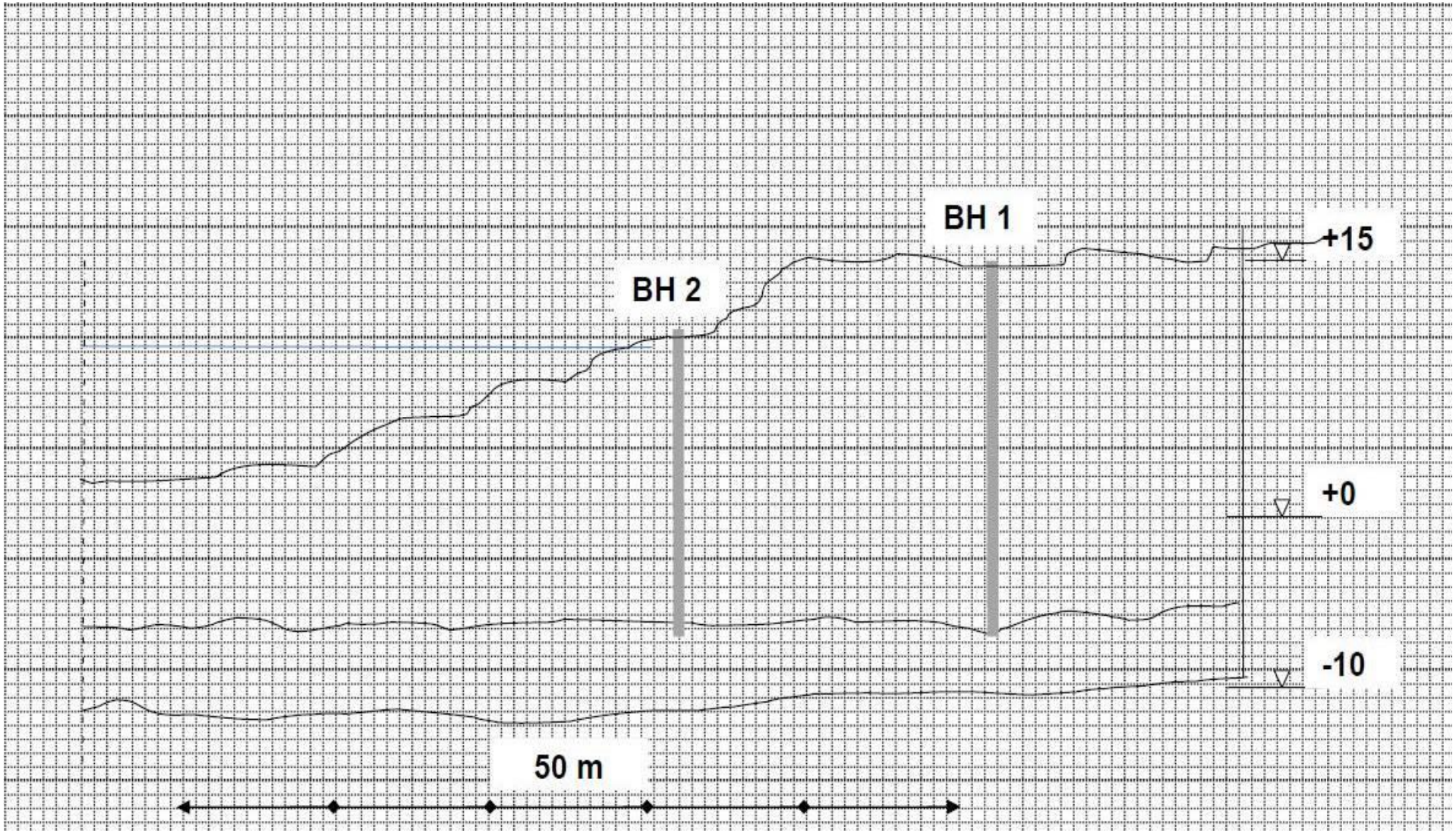
BH 1
BH 2
+15
+0
-10
50 m

STDEV N Lo	N Lo	pSTED Hi	STDEV N Hi	N Hi	N	F
0.157	6.543	0.2638	0.0679	6.964	6.754	1.190
0.005	6.695	0.6459	0.1663	7.346	7.021	1.415
0.076	6.624	0.7759	0.1998	7.476	7.050	1.260
0.043	6.657	0.2096	0.0540	6.910	6.783	1.256
0.029	6.671	0.0645	0.0166	6.764	6.718	1.316
0.200	6.500	0.2635	0.0678	6.963	6.732	1.208
				Mean	6.886	1.257437911
				Std.dev	0.14906	0.037882912
					0.022219	
					Mean	1.259
Safety margin	ln(F)=	0.230389204			**Stdev**	0.0830
		2.776256774			**P (F<1)**	0.089780166427%

Shear strength – *c*

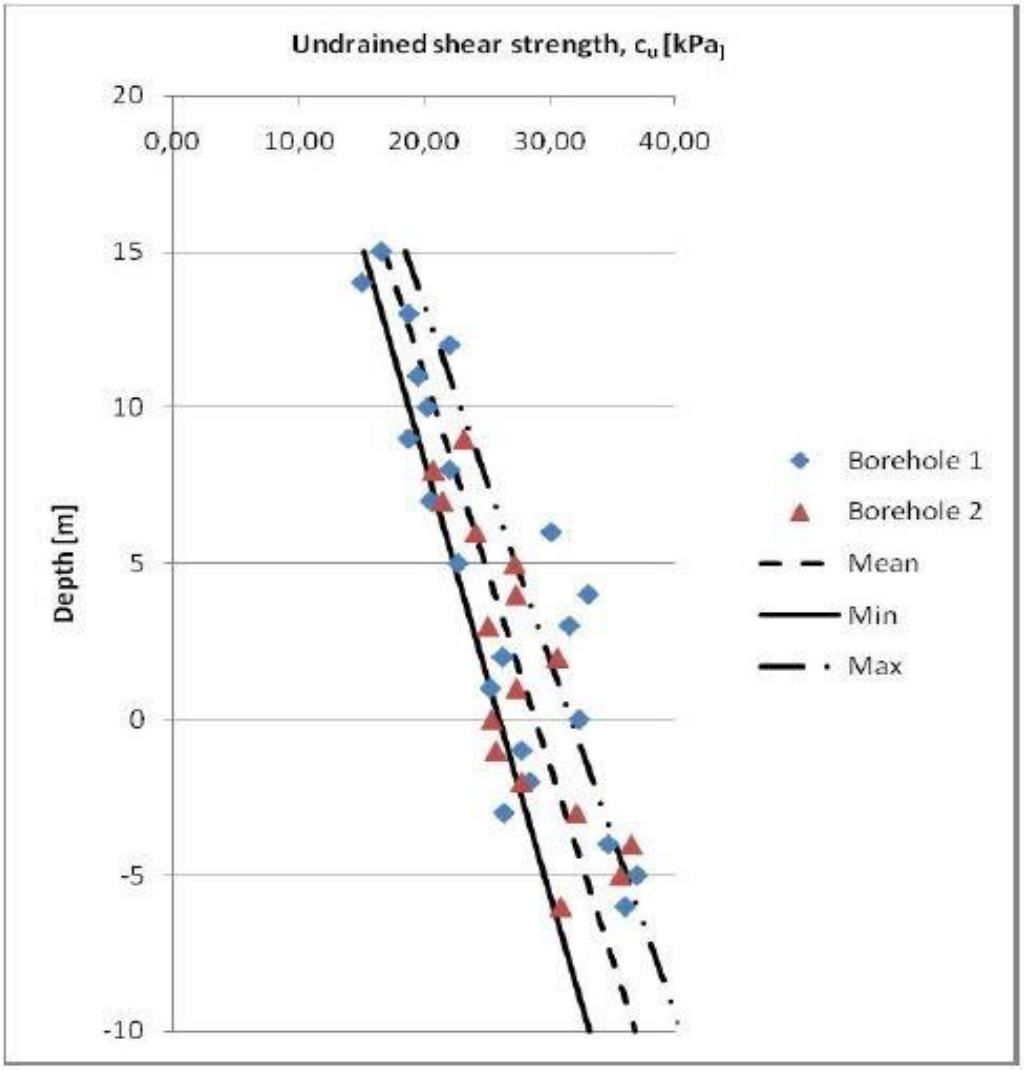

$c_{u,averaqge}$= 25 kPa ; V_{cu}=10%

$c_u \pm \sigma$ captures approx 70% of values

Appendix 2 CPTU

This is taken directly from Helene Kornbrekke's master's thesis and CPTU calculations made by Multiconsult.

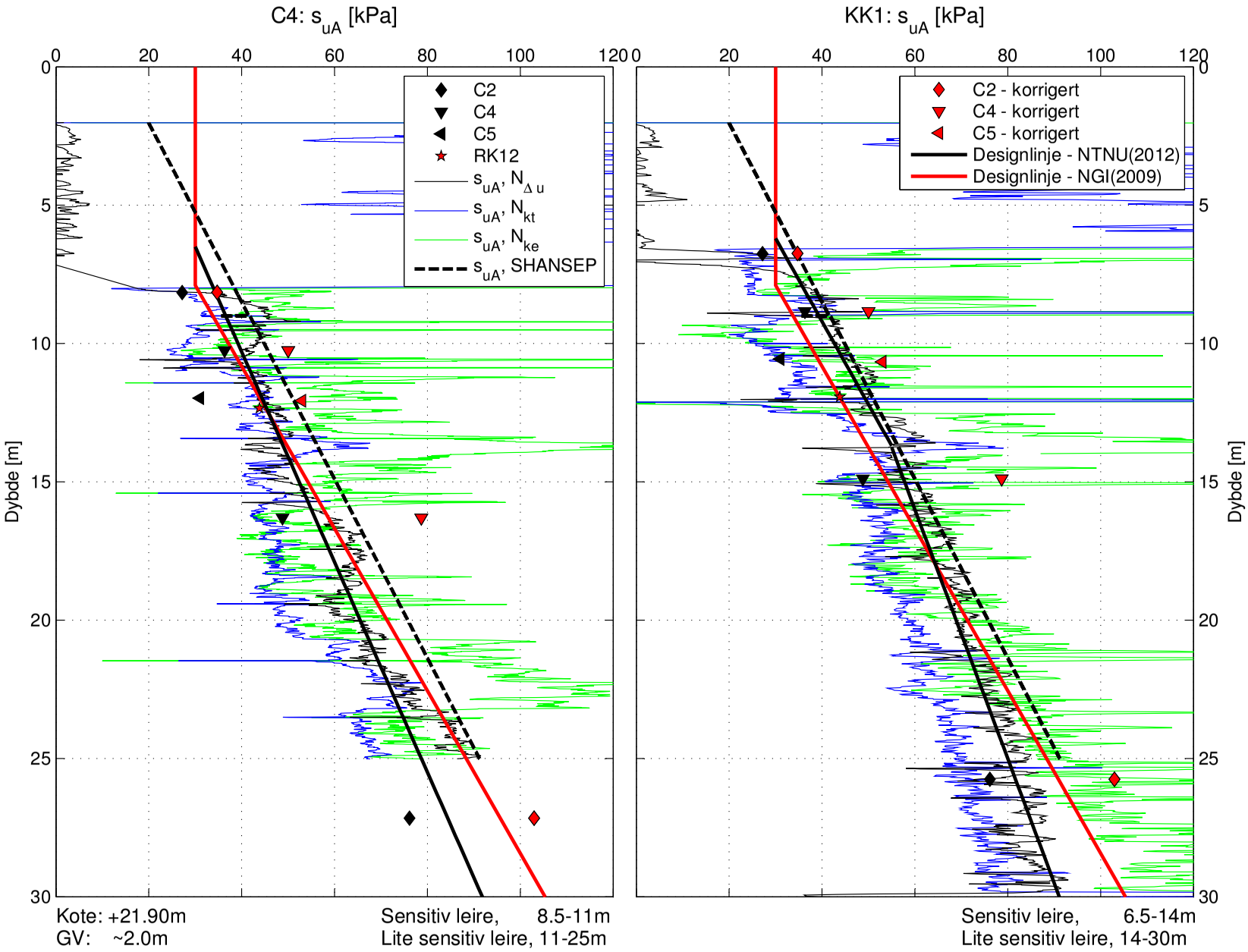
C4: s_uA [kPa]
KK1: s_uA [kPa]
Dybde [m]
C2
C4
C5
RK12
s_uA, N_Δ u
s_uA, N_kt
s_uA, N_ke
s_uA, SHANSEP
C2 - korrigert
C4 - korrigert
C5 - korrigert
Designlinje - NTNU(2012)
Designlinje - NGI(2009)
Kote: +21.90m
GV: ~2.0m
Sensitiv leire, 8.5-11m
Lite sensitiv leire, 11-25m
Sensitiv leire, 6.5-14m
Lite sensitiv leire, 14-30m

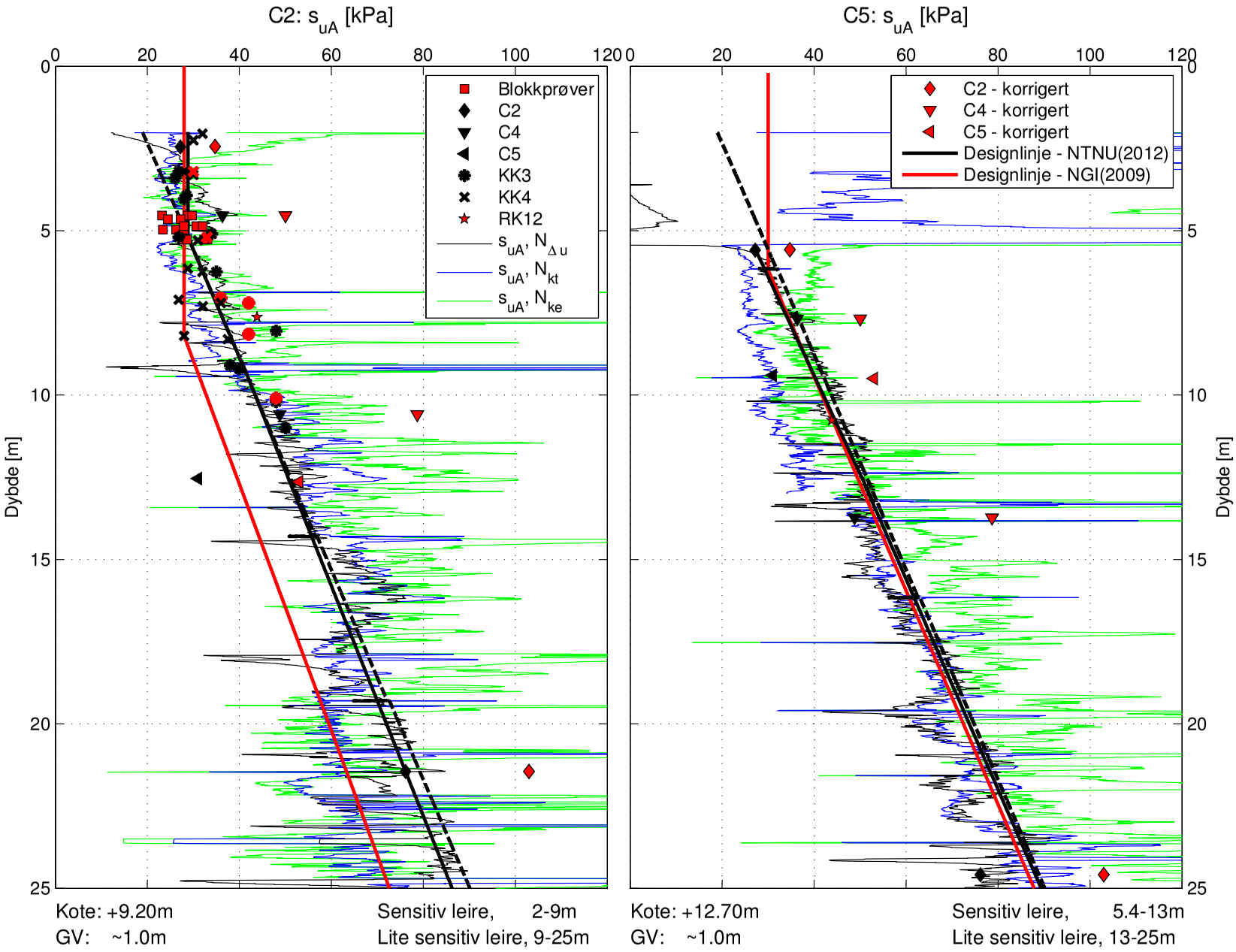
C2: s uA [kPa]
C5: s uA [kPa]
Dybde [m]
Blokkprøver
C2
C4
C5
KK3
KK4
RK12
s uA, N Δ u
s uA, N kt
s uA, N ke
C2 - korrigert
C4 - korrigert
C5 - korrigert
Designlinje - NTNU(2012)
Designlinje - NGI(2009)
Kote: +9.20m
GV: ~1.0m
Sensitiv leire, 2-9m
Lite sensitiv leire, 9-25m
Kote: +12.70m
GV: ~1.0m
Sensitiv leire, 5.4-13m
Lite sensitiv leire, 13-25m

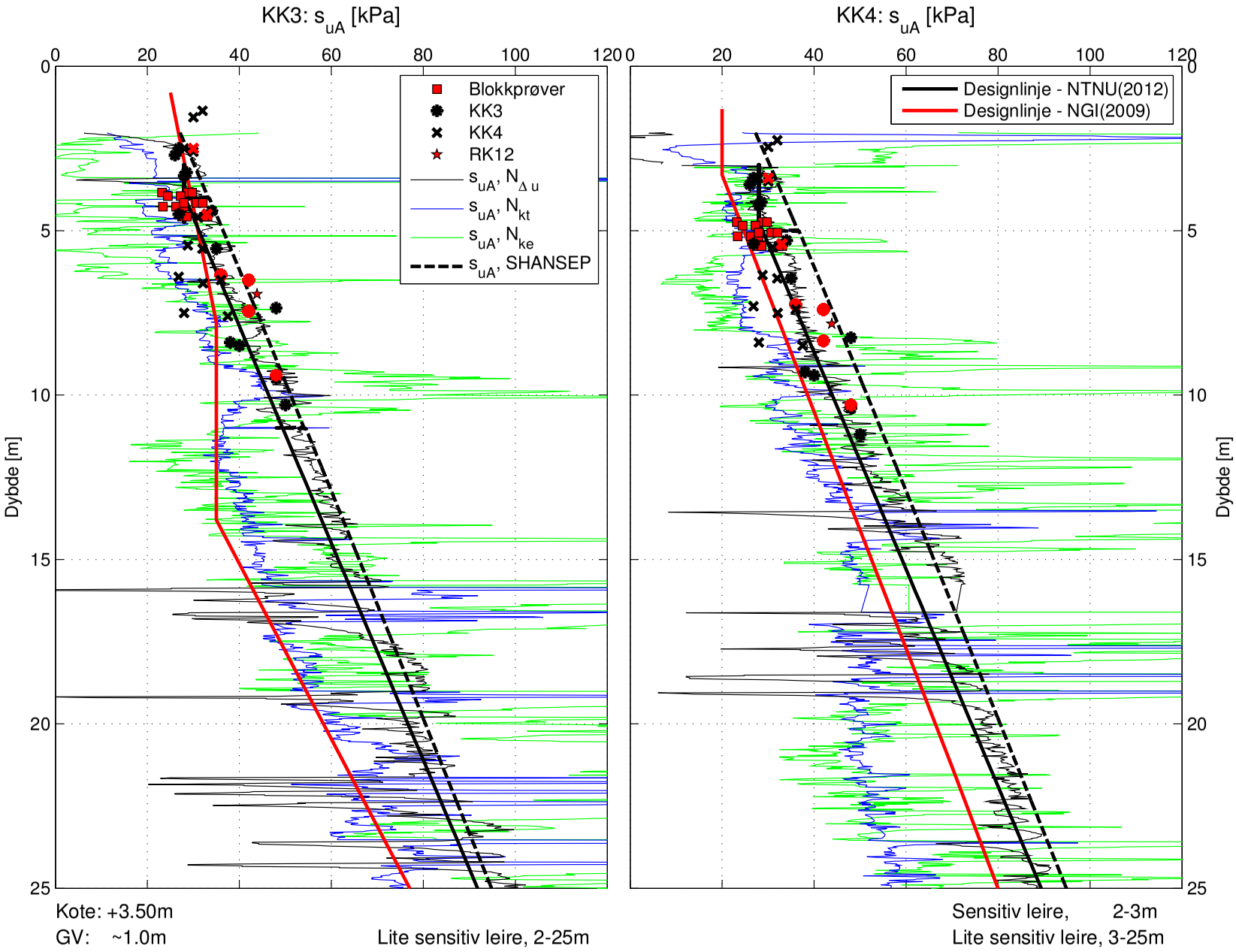
KK3: s_{uA} [kPa]
KK4: s_{uA} [kPa]
0
20
40
60
80
100
120
5
10
15
20
25
Dybde [m]
Blokkprøver
KK3
KK4
RK12
s_{uA}, $N_{\Delta u}$
s_{uA}, N_{kt}
s_{uA}, N_{ke}
s_{uA}, SHANSEP
Designlinje - NTNU(2012)
Designlinje - NGI(2009)
Kote: +3.50m
GV: ~1.0m
Lite sensitiv leire, 2-25m
Sensitiv leire, 2-3m
Lite sensitiv leire, 3-25m

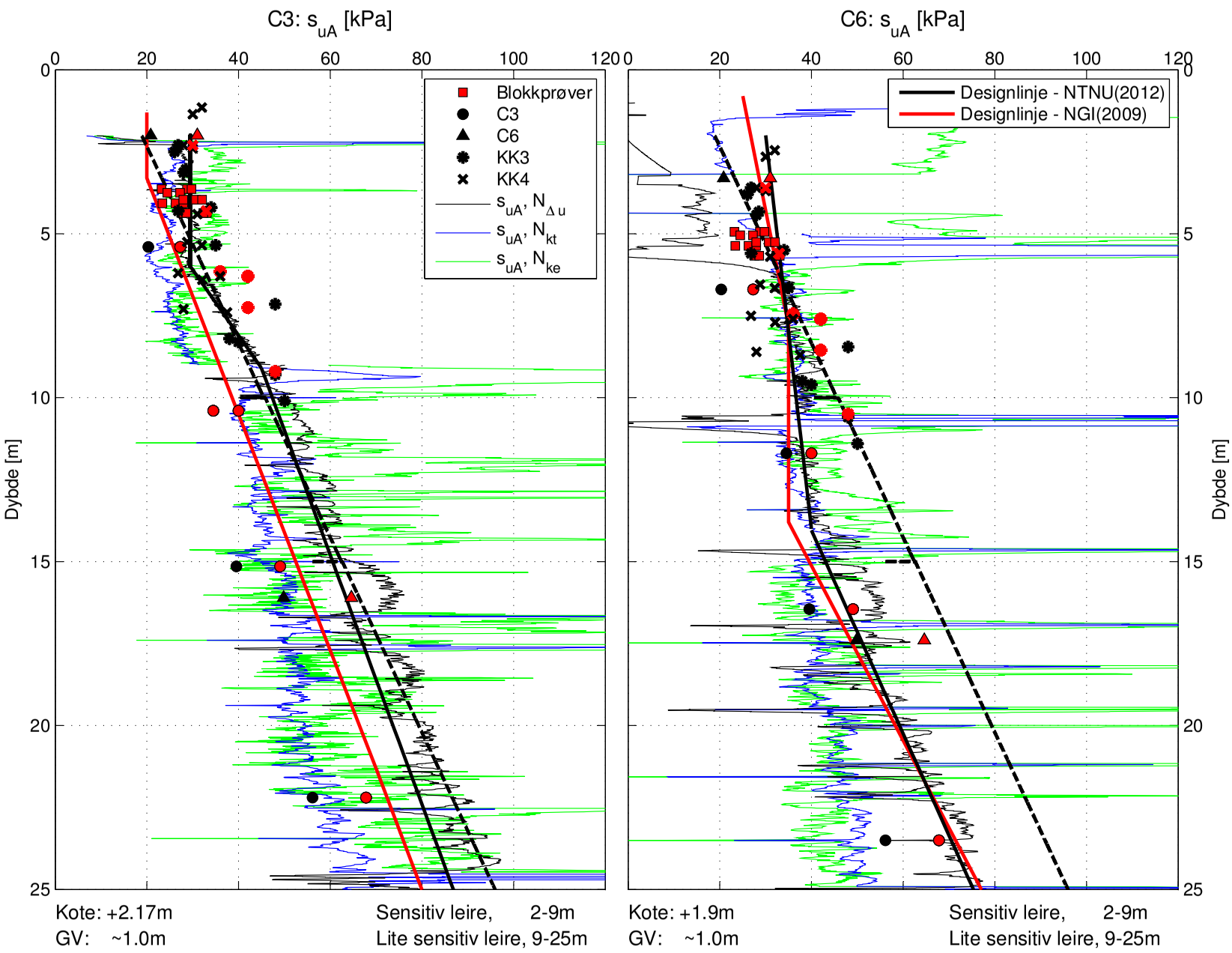
C3: s_{uA} [kPa]
C6: s_{uA} [kPa]
0
20
40
60
80
100
120
5
10
15
20
25
Dybde [m]
Blokkprøver
C3
C6
KK3
KK4
s_{uA}, $N_{\Delta u}$
s_{uA}, N_{kt}
s_{uA}, N_{ke}
Designlinje - NTNU(2012)
Designlinje - NGI(2009)
Kote: +2.17m
GV: ~1.0m
Sensitiv leire, 2-9m
Lite sensitiv leire, 9-25m
Kote: +1.9m
GV: ~1.0m
Sensitiv leire, 2-9m
Lite sensitiv leire, 9-25m

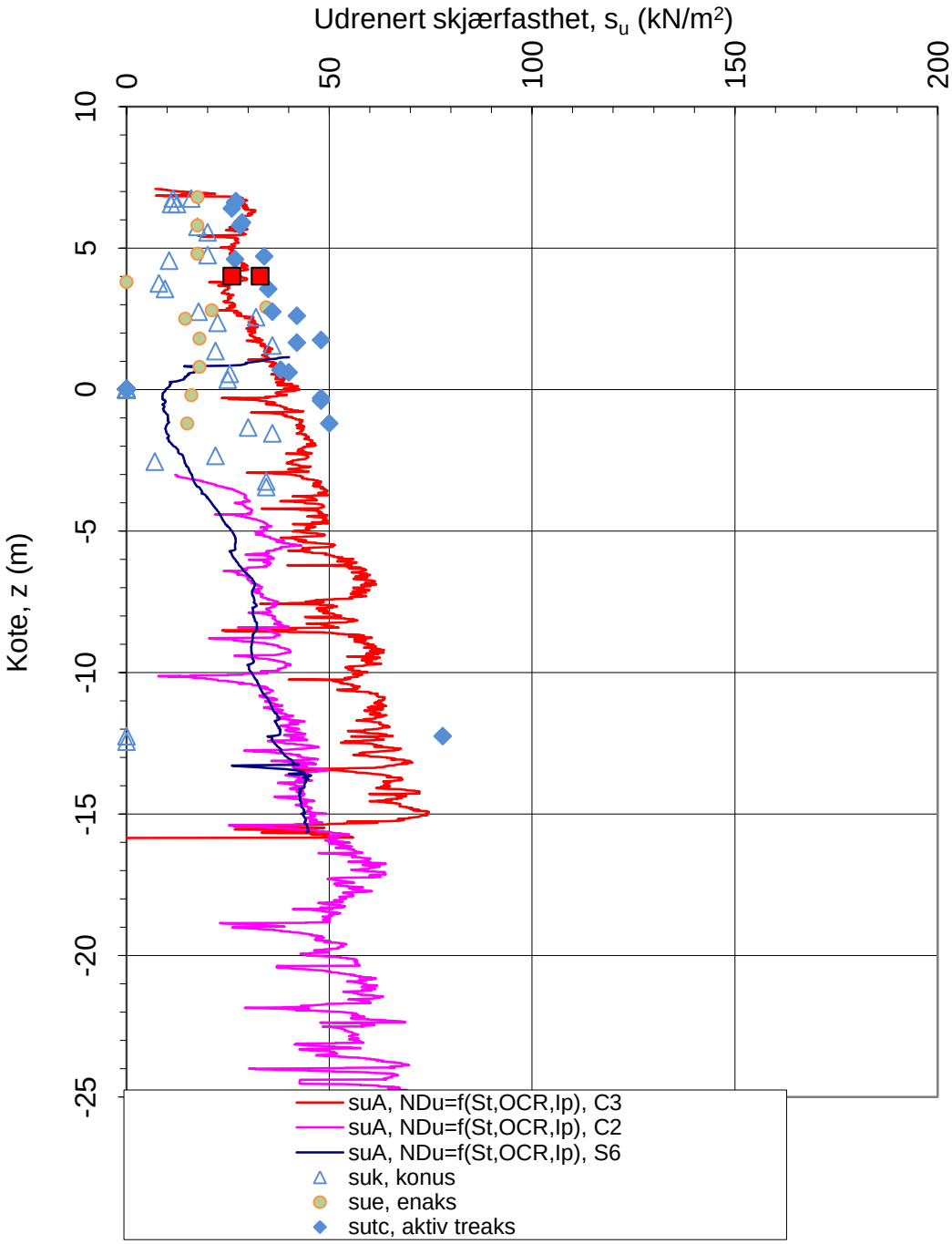

Sensitivitetsvalg: **S_t > 15**

N_{Du}: **$(9,8-4,5 \log OCR+0,0 I_p)$**

Oppdragsgiver: **Statens Vegvesen**		Oppdrag: **414792**		Tegningens filnavn: CPTU_SIGMA_Profil 3
Aktiv udrenert skjærfasthet s_{uA}, N_{Du} - S_t, I_p, OCR-korrelerte verdier.				
CPTU id.:	Profil 3 samplott	**Sonder:**	4454, 20759	
MULTICONSULT AS	Dato: 25.01.2012	Tegnet: rols	Kontrollert:	Godkjent:
	Oppdrag nr.: 414792	Tegning nr.: 53.8	Versjon: 22.05.2011	Revisjon: 1

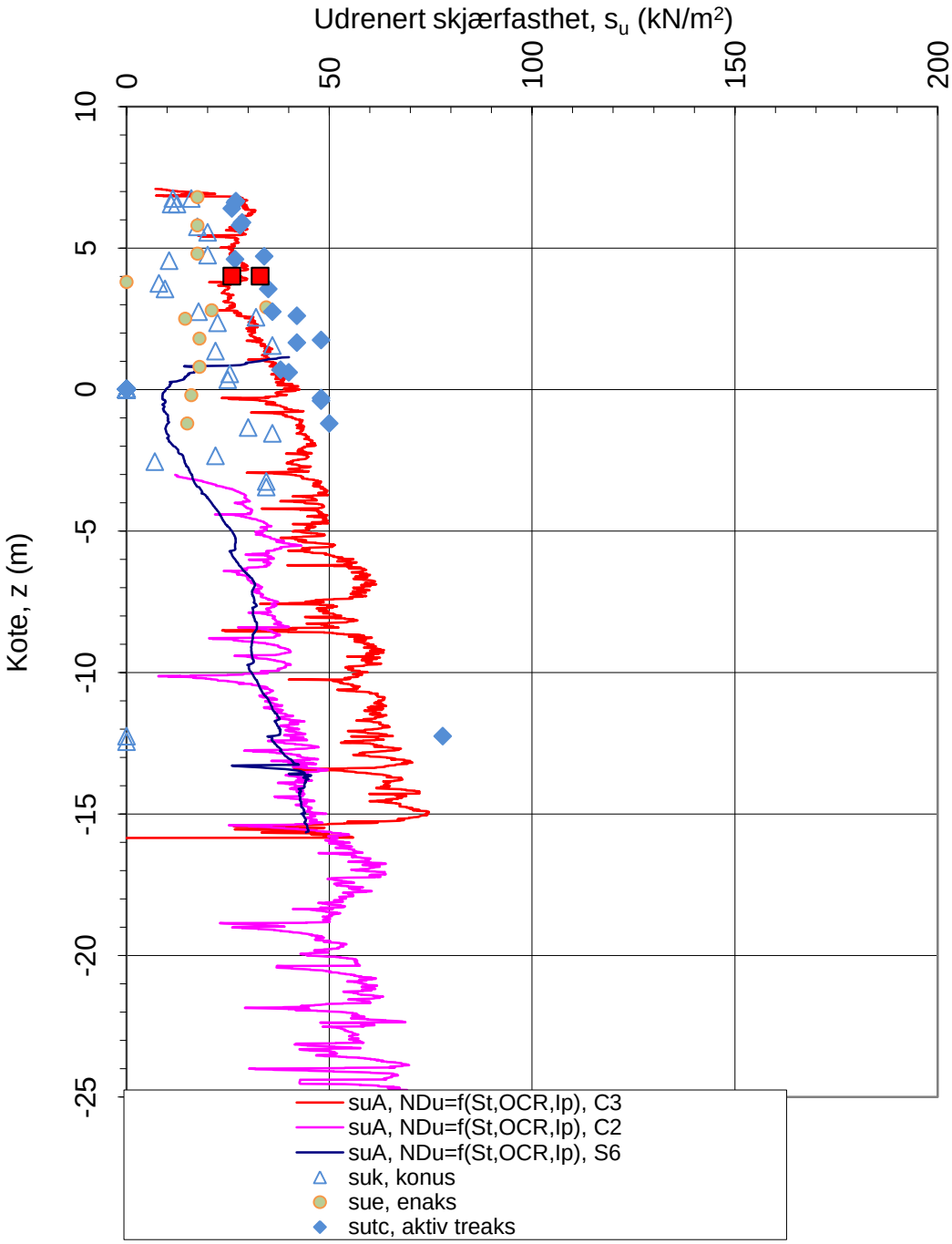

Sensitivitetsvalg: **S_t > 15**

N_{Du}: **$(9,8-4,5 \log OCR+0,0 I_p)$**

Oppdragsgiver: **Statens Vegvesen**		Oppdrag: **414792**		Tegningens filnavn: CPTU_SIGMA_Profil 3
Aktiv udrenert skjærfasthet s_{uA}, N_{Du} - S_t, I_p, OCR-korrelerte verdier.				
CPTU id.:	Profil 3 samplott	**Sonder:**	4454, 20759	
MULTICONSULT AS	Dato: 25.01.2012	Tegnet: rols	Kontrollert:	Godkjent:
	Oppdrag nr.: 414792	Tegning nr.: 53.8	Versjon: 22.05.2011	Revisjon: 1

Appendix 3 Triaxial Tests

This is taken directly from Helene Kornbrekke's master's thesis

Sund, Rissa
Blokkprøve, CIUa001

Dybde: 3.96 m
Prøvetakingsdato og -utstyr: 30.11.11, Sherbrooke pøvetaker, 250 mm × 350 mm
Åpning av blokkprøven: 19.01.12
Forsøksdato: 20.01.12
Tøyningshastighet: 3.0 %/time

$\sigma`_{vo}$	= 46.64kPa	$\sigma`_c$	= 100 kPa
w	= 35.88 %	OCR	= 2.17
γ	= 19.5 kN/m^3		
ΔV	= 5.13 cm^3	tan ϕ	= 0.54
ε_v	= 2.21 %	ϕ	= 28.4 ^{o}
$\Delta e/e_o$	= 0.04	a	= 15 kPa
s_u	= 30.65 kPa	D	= -0.03
ε_f	= 1.75 %	S_f	= 0.91
E_0	= 5.7 MPa	M_f	= 1.13

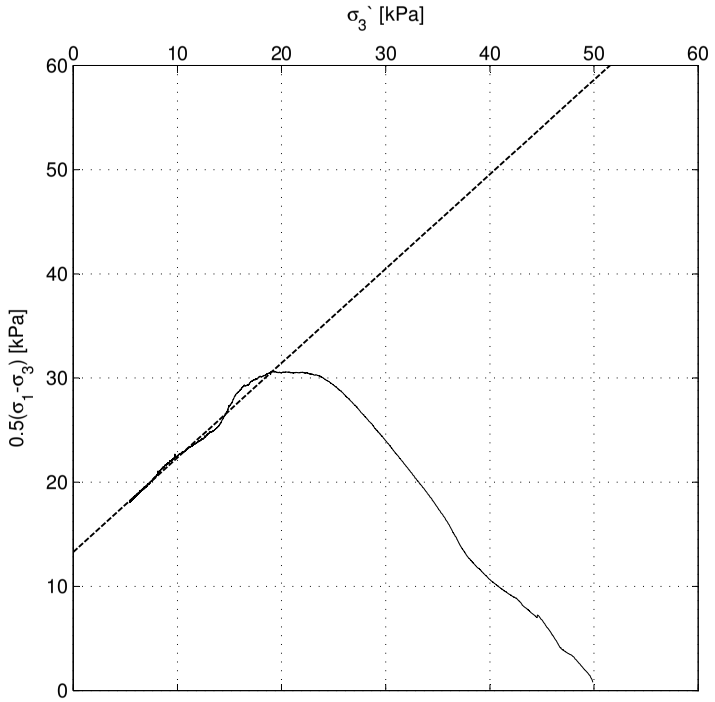

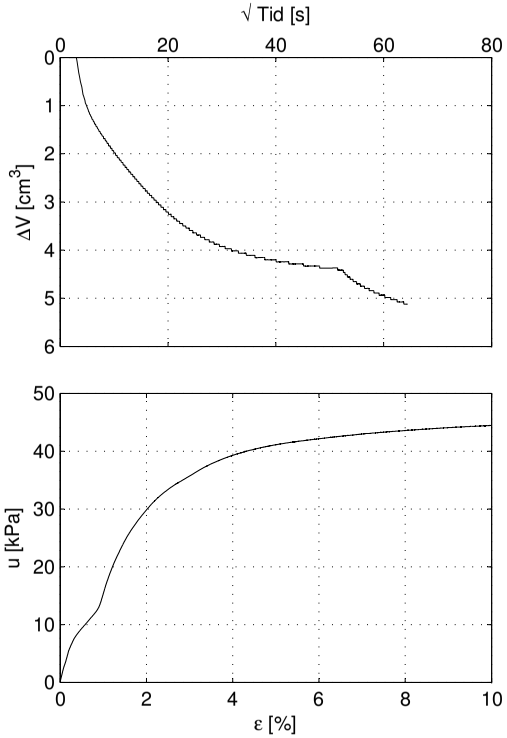

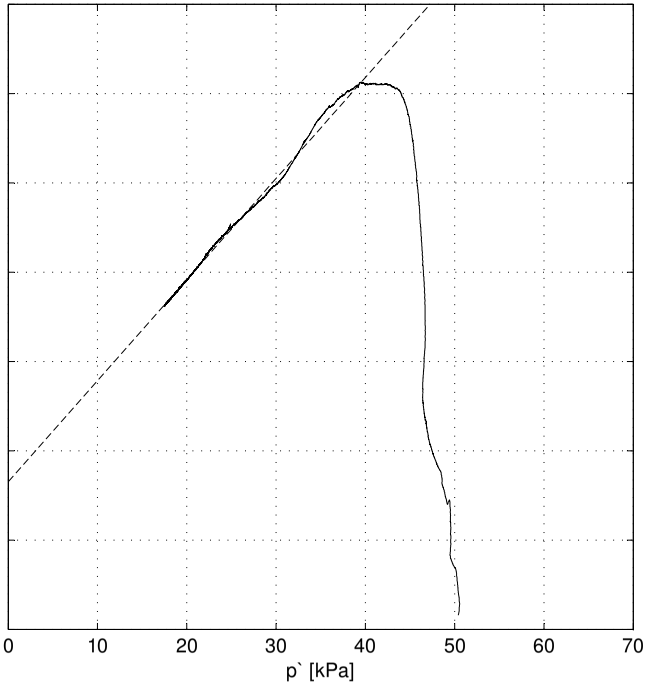

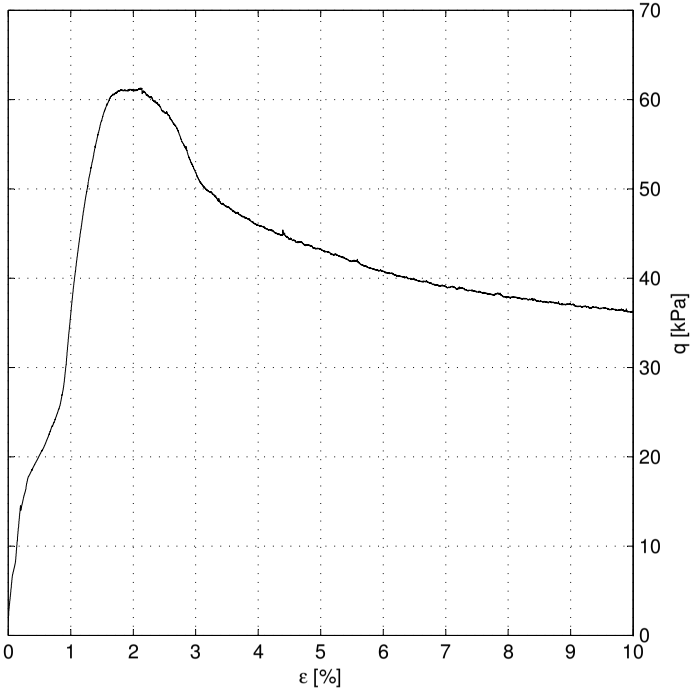

Sund, Rissa
Blokkprøve, CAUa102

Dybde: 3.96 m
Prøvetakingsdato og -utstyr: 30.11.11, Sherbrooke pøvetaker, 250 mm × 350 mm
Åpnning av blokkprøven: 19.01.12
Testingsdato: 24.02.12
Tøyningshastighet: 1.20 %/time (Utført med baktrykk av Multiconsult Trondheim)

$\sigma`_{vo}$	= 45.64kPa	$\sigma`_c$	= 100 kPa
w	= 34.80 %	OCR	= 2.22
γ	= 19.1 kN/m^3		
ΔV	= 3.63 cm^3	tan ϕ	= 0.59
ε_v	= 1.56 %	ϕ	= 30.8 ^{o}
$\Delta e/e_o$	= 0.03	a	= 8 kPa
s_u	= 27.95 kPa	D	= -0.04
ε_f	= 0.73 %	S_f	= 1.05
E_0	= 11.3 MPa	M_f	= 1.23

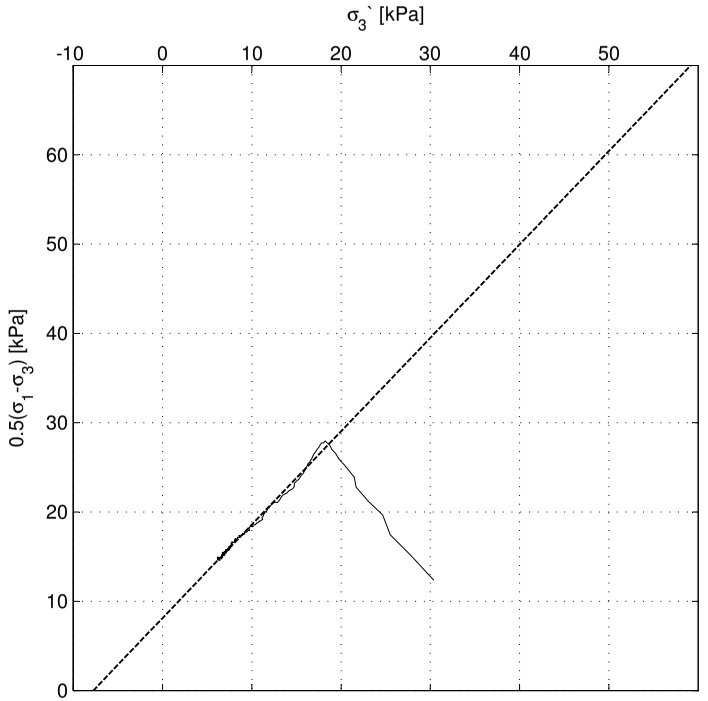

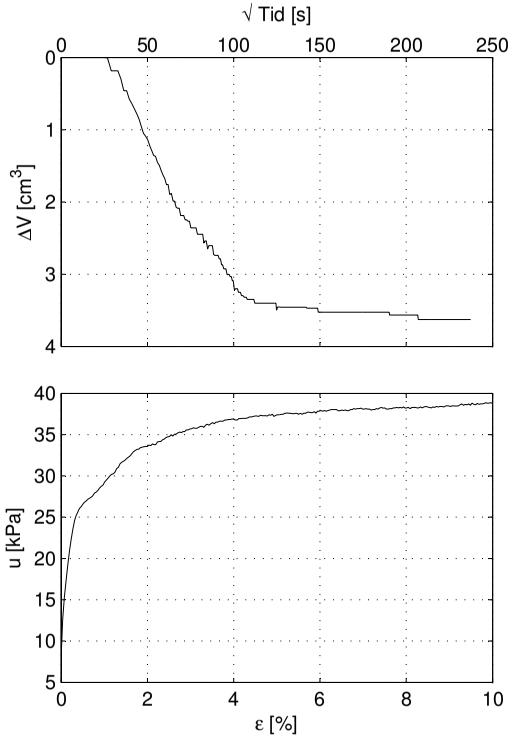

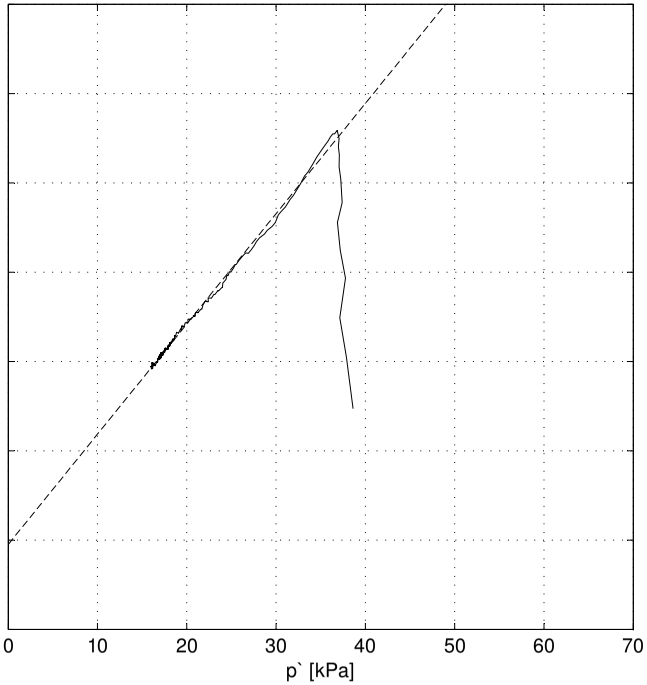

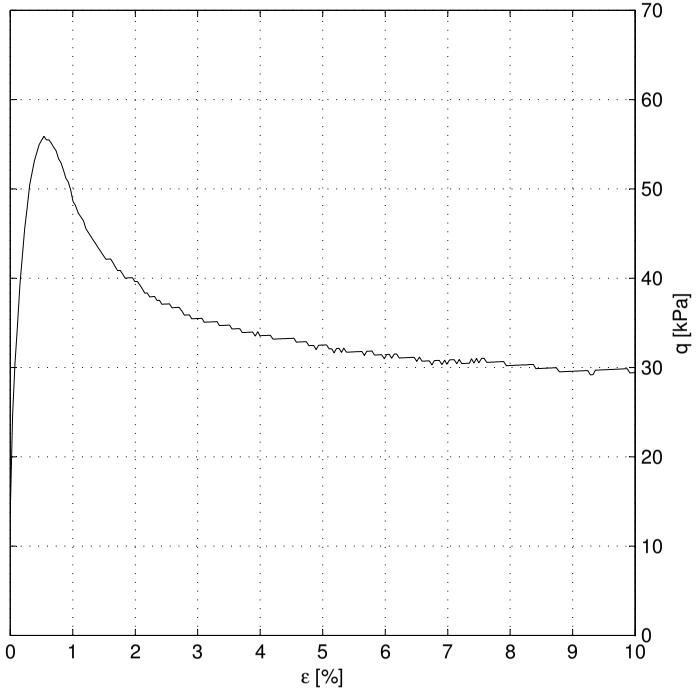

Sund, Rissa
Blokkprøve, CAUa003

Dybde: 3.96 m
Prøvetakingsdato og -utstyr: 30.11.11, Sherbrooke pøvetaker, 250 mm × 350 mm
Åpning av blokkprøven: 19.01.12
Forsøksdato: 26.01.12
Tøyningshastighet: 3.0 %/time

$\sigma`_{vo}$	= 45.64kPa	$\sigma`_c$	= 100 kPa
w	= 37.29 %	OCR	= 2.23
γ	= 19.5 kN/m^3		
ΔV	= 5.16 cm^3	tan ϕ	= 0.43
ε_v	= 2.23 %	ϕ	= 23.4 ^{o}
$\Delta e/e_o$	= 0.04	a	= 23 kPa
s_u	= 32.02 kPa	D	= -0.15
ε_f	= 1.42 %	S_f	= 0.66
E_0	= 6.6 MPa	M_f	= 0.92

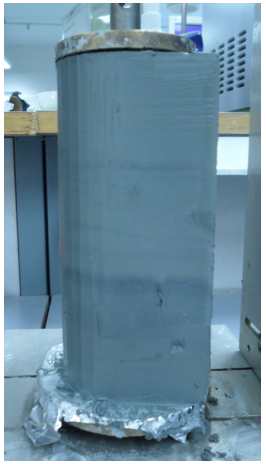

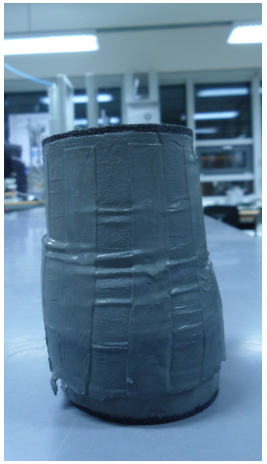

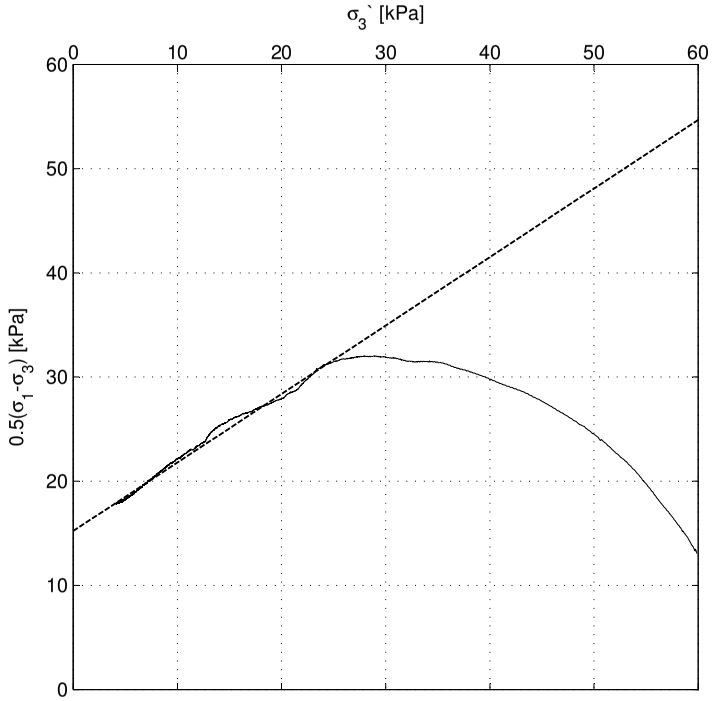

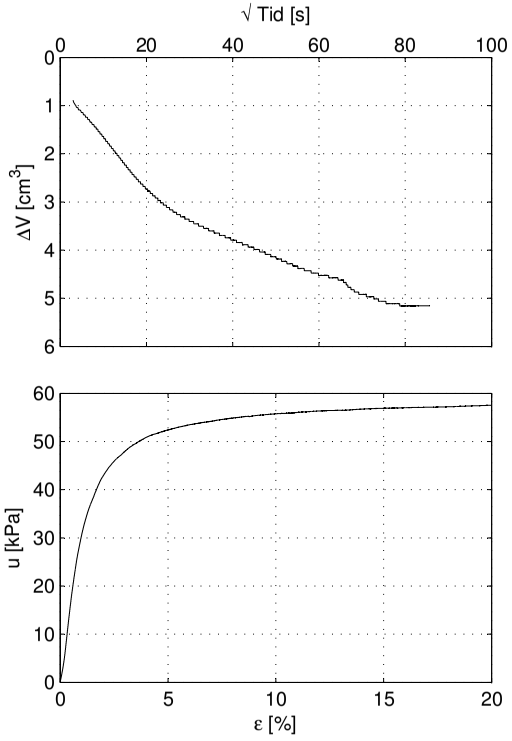

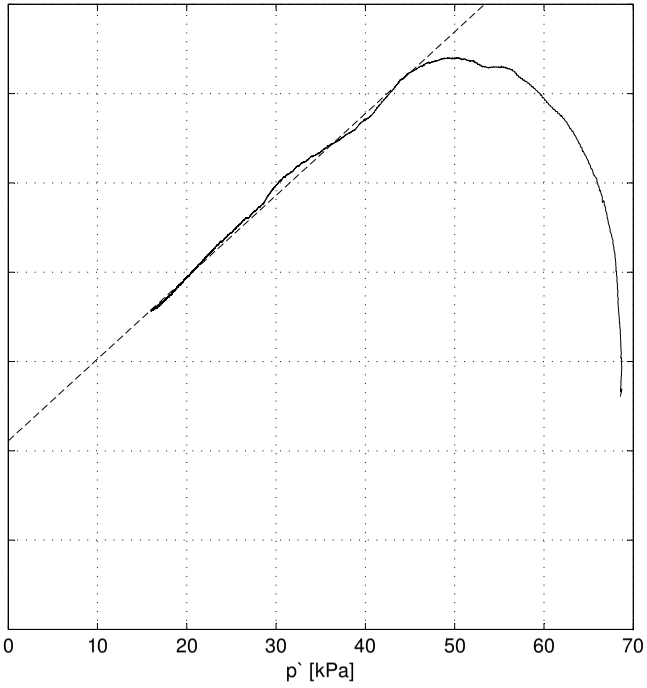

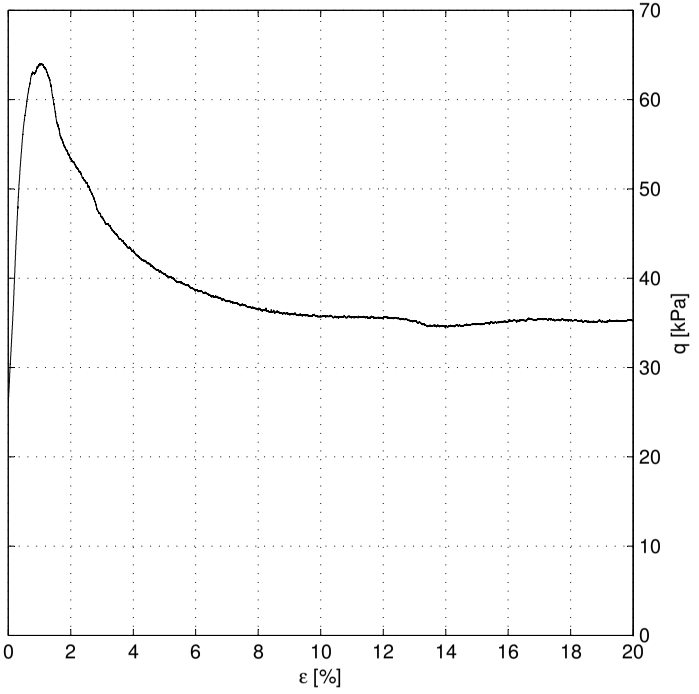

Sund, Rissa
Blokkprøve, CAUa004

Dybde: 4.07 m
Prøvetakingsdato og -utstyr: 30.11.11, Sherbrooke pøvetaker, 250 mm × 350 mm
Åpning av blokkprøven: 19.01.12
Forsøksdato: 02.02.12
Tøyningshastighet: 0.60 %/time

$\sigma`_{vo}$	= 46.63kPa	$\sigma`_c$	= 100 kPa
w	= 36.28 %	OCR	= 2.20
γ	= 19.8 kN/m^3		
ΔV	= 4.45 cm^3	tan ϕ	= 0.56
ε_v	= 1.92 %	ϕ	= 29.3 ^{o}
$\Delta e/e_o$	= 0.04	a	= 16 kPa
s_u	= 27.65 kPa	D	= -0.04
ε_f	= 1.80 %	S_f	= 0.96
E_0	= 5.2 MPa	M_f	= 1.17

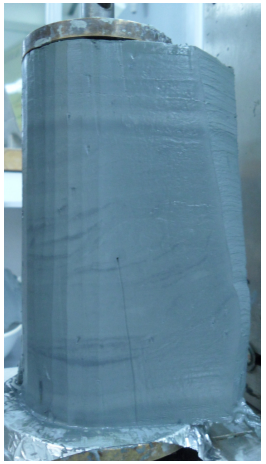

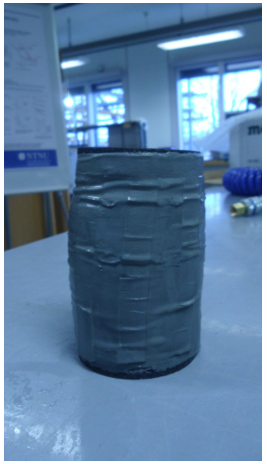

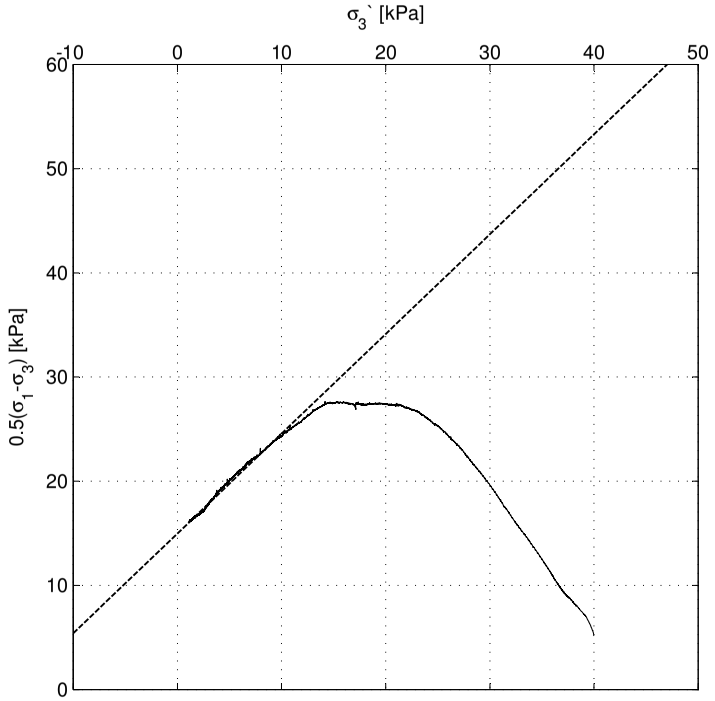

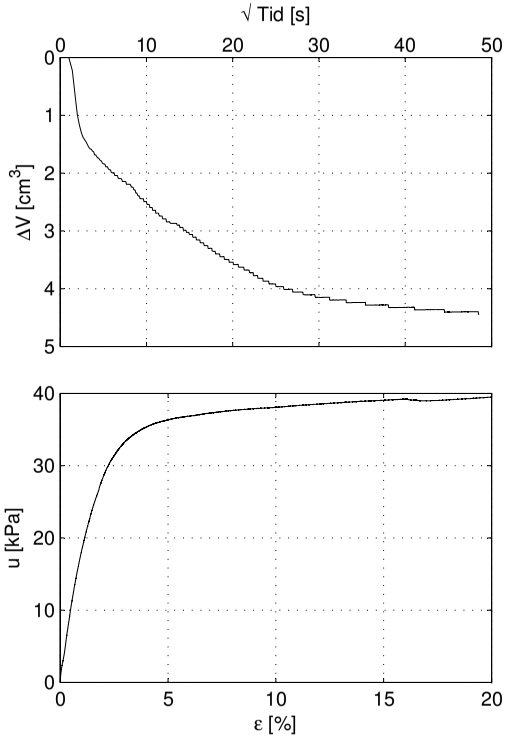

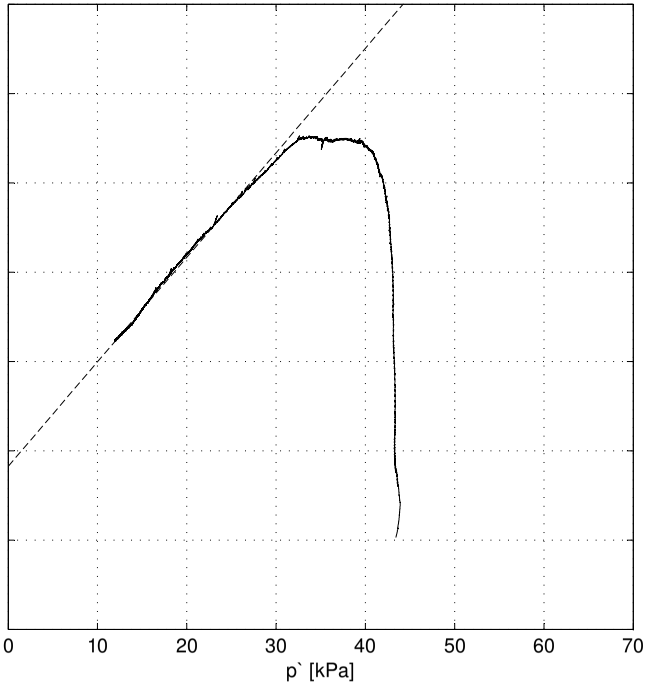

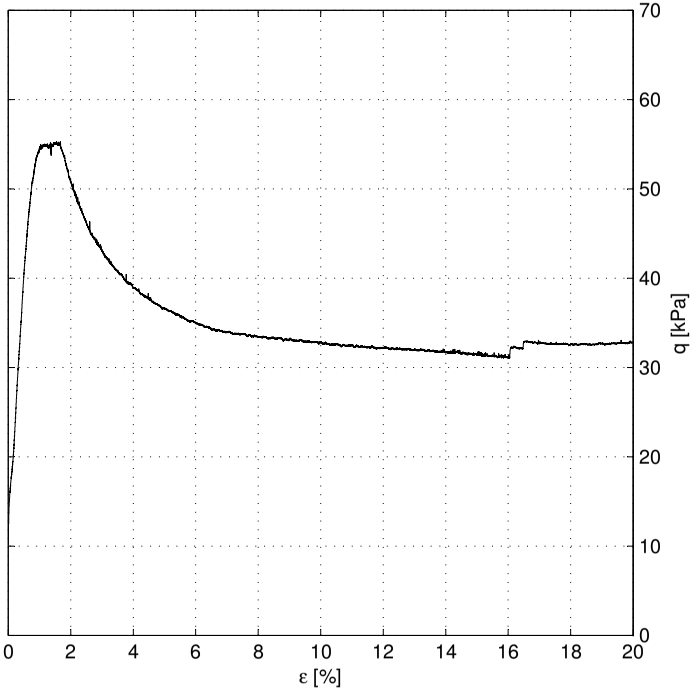

Sund, Rissa
Blokkprøve, CAUa005

Dybde: 4.07 m
Prøvetakingsdato og -utstyr: 30.11.11, Sherbrooke pøvetaker, 250 mm × 350 mm
Åpning av blokkprøven: 19.01.12
Forsøksdato: 03.02.12
Tøyningshastighet: 0.30 %/time

$\sigma`_{vo}$	= 46.63kPa	$\sigma`_c$	= 100 kPa
w	= 36.49 %	OCR	= 2.20
γ	= 19.8 kN/m^3		
ΔV	= 3.45 cm^3	tan ϕ	= 0.69
ε_v	= 1.49 %	ϕ	= 34.4 ^{o}
$\Delta e/e_o$	= 0.03	a	= 10 kPa
s_u	= 26.24 kPa	D	= -0.05
ε_f	= 1.61 %	S_f	= 1.30
E_0	= 5.2 MPa	M_f	= 1.40

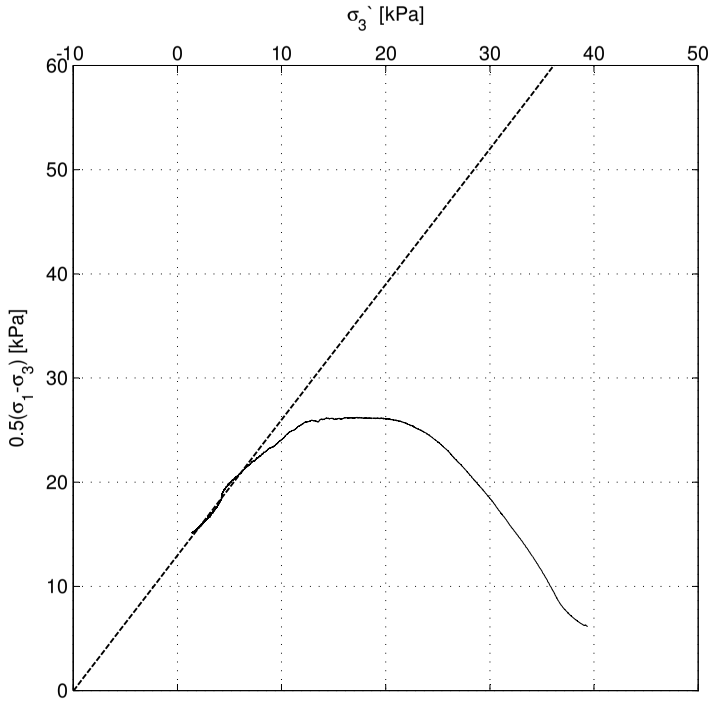

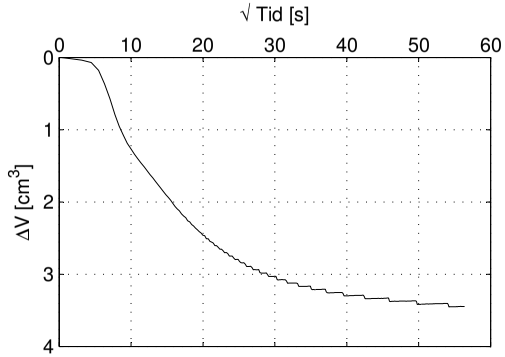

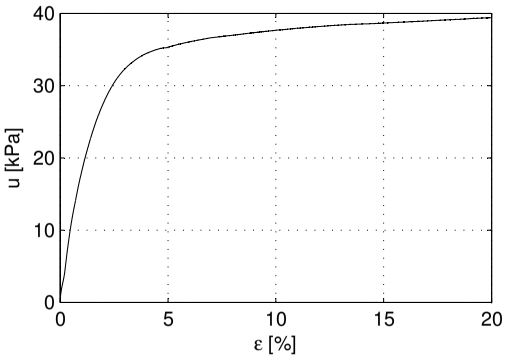

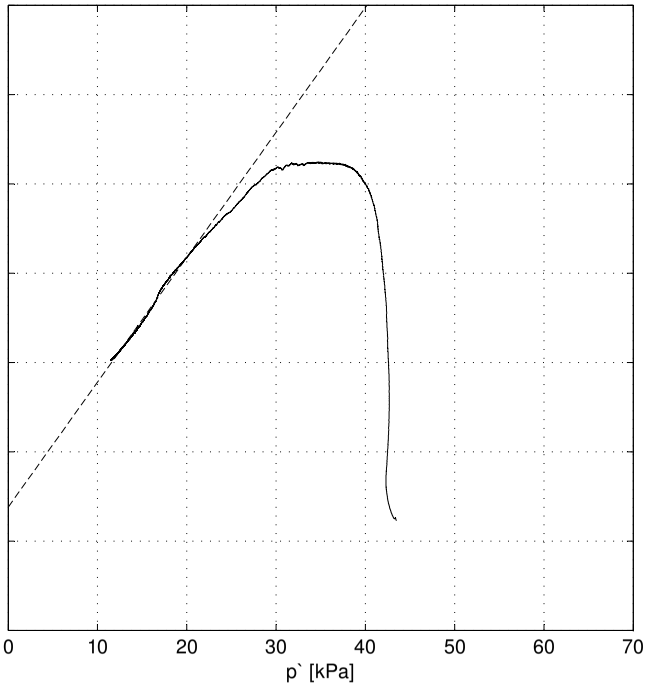

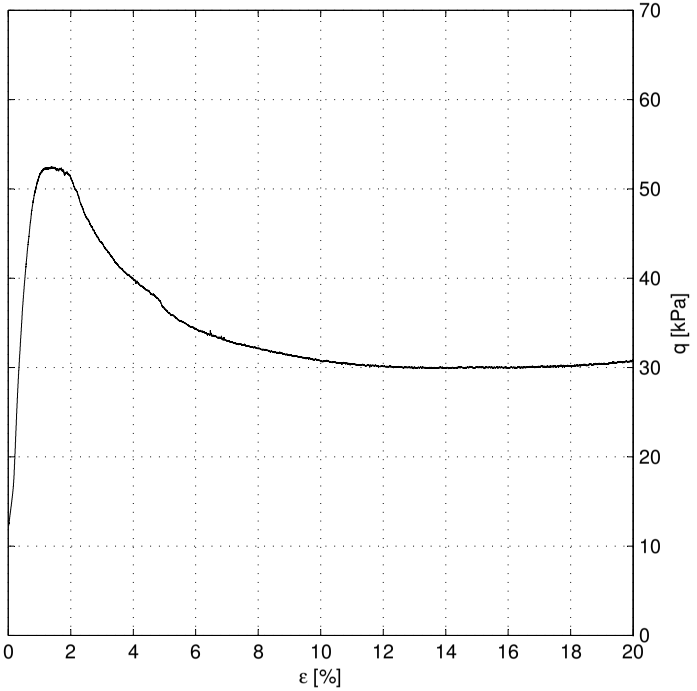

Sund, Rissa
Blokkprøve, CAUa006

Dybde: 4.07 m
Prøvetakingsdato og -utstyr: 30.11.11, Sherbrooke pøvetaker, 250 mm × 350 mm
Åpning av blokkprøven: 19.01.12
Forsøksdato: 08.02.12
Tøyningshastighet: 1.0 %/time

$\sigma`_{vo}$	= 46.63kPa	$\sigma`_c$	= 100 kPa
w	= 35.75 %	OCR	= 2.20
γ	= 19.8 kN/m^3		
ΔV	= 3.26 cm^3	tan ϕ	= 0.46
ε_v	= 1.40 %	ϕ	= 24.5 ^{o}
$\Delta e/e_o$	= 0.03	a	= 21 kPa
s_u	= 27.85 kPa	D	= 0.00
ε_f	= 1.51 %	S_f	= 0.71
E_0	= 4.7 MPa	M_f	= 0.97

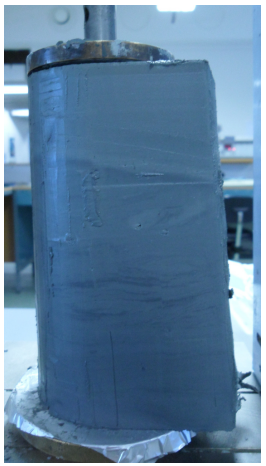

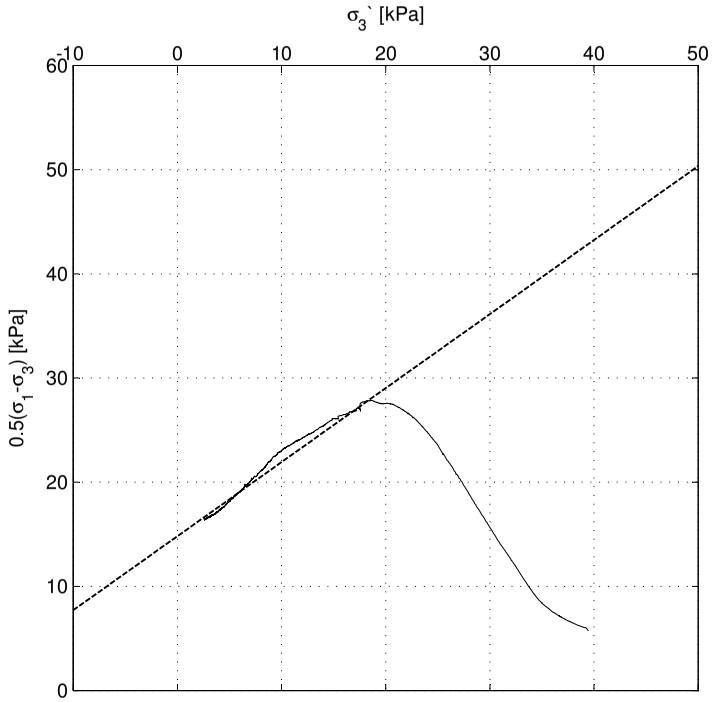

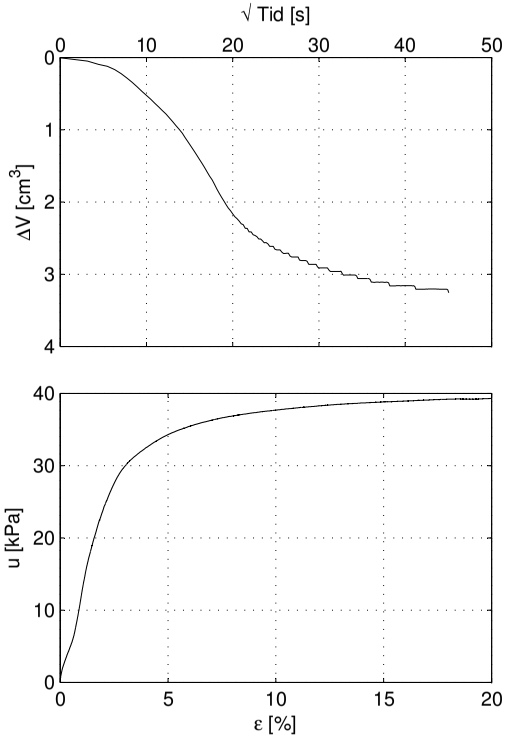

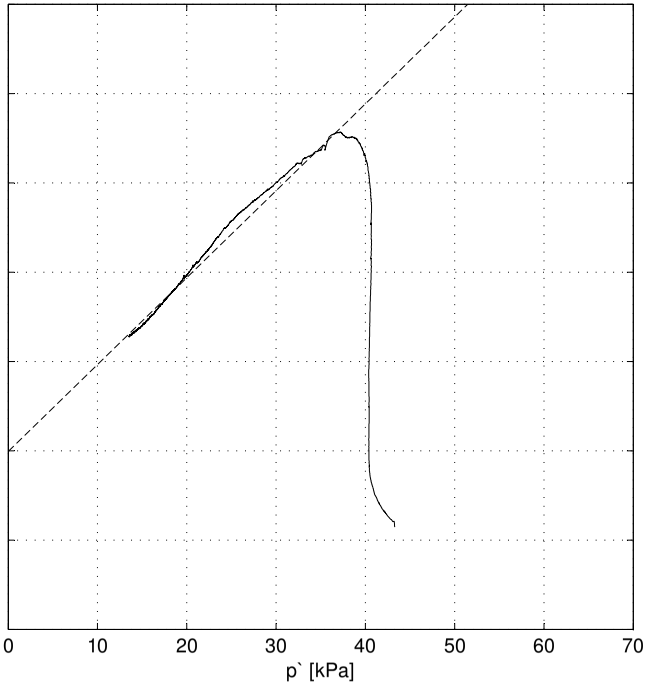

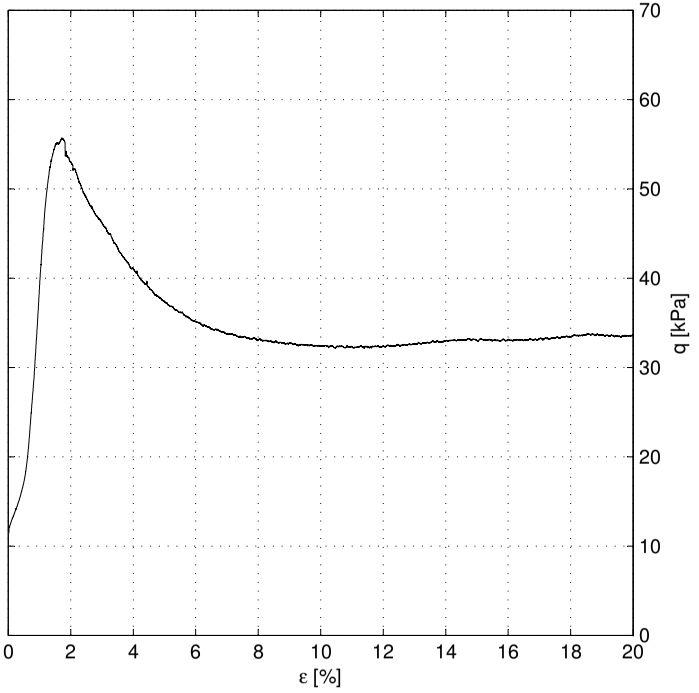

Sund, Rissa
Blokkprøve, CAUa007

Dybde: 4.07 m
Prøvetakingsdato og -utstyr: 30.11.11, Sherbrooke pøvetaker, 250 mm × 350 mm
Åpning av blokkprøven: 19.01.12
Forsøksdato: 09.02.12
Tøyningshastighet: 0.1 %/time

σ'_{vo}	= 46.63kPa	σ'_c	= 100 kPa
w	= 36.00 %	OCR	= 2.20
γ	= 19.8 kN/m^3		
ΔV	= 4.31 cm^3	tan ϕ	= 0.51
ε_v	= 1.86 %	ϕ	= 26.9 ^{o}
$\Delta e/e_o$	= 0.03	a	= 10 kPa
s_u	= 23.39 kPa	D	= -0.06
ε_f	= 1.21 %	S_f	= 0.82
E_0	= 5.4 MPa	M_f	= 1.06

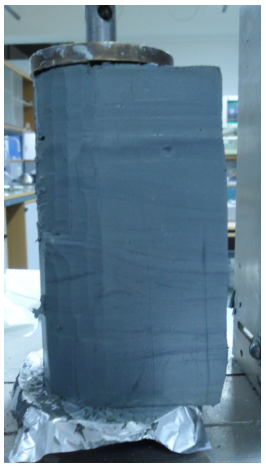

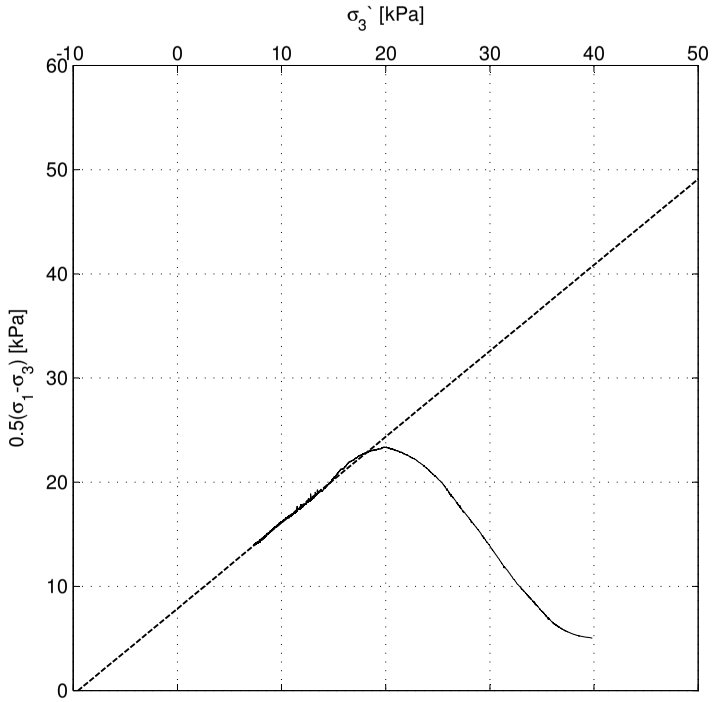

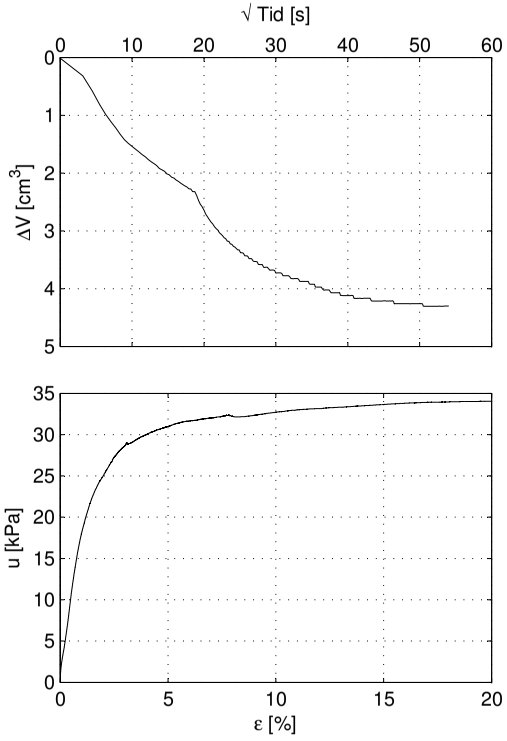

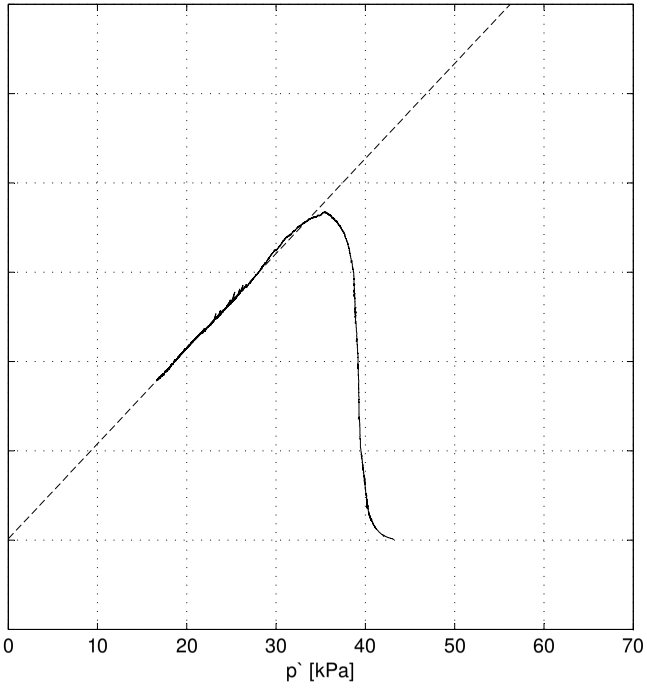

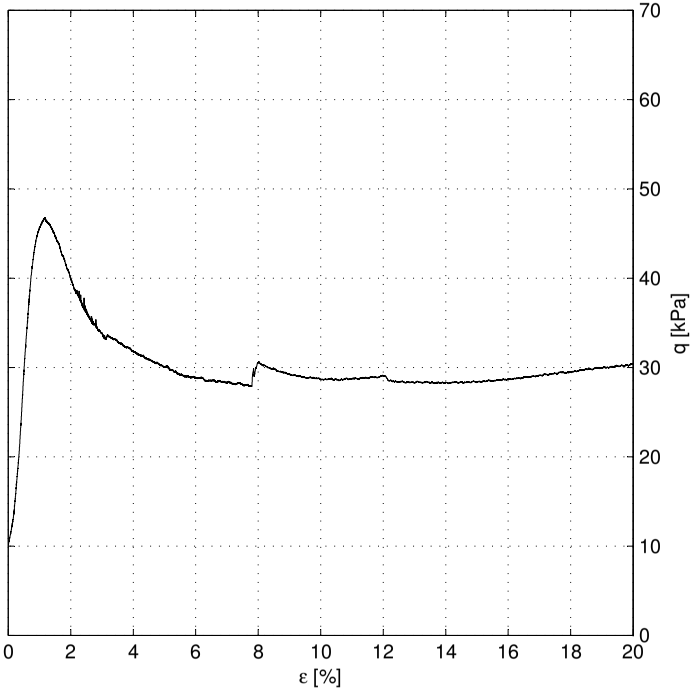

Sund, Rissa
Blokkprøve, CAUa008

Dybde: 3.64 m
Prøvetakingsdato og -utstyr: 30.11.11, Sherbrooke pøvetaker, 250 mm × 350 mm
Åpning av blokkprøven: 13.02.12
Forsøksdato: 13.02.12
Tøyningshastighet: 1.5 %/time

$\sigma`_{vo}$	= 42.76kPa	$\sigma`_c$	= 100 kPa
w	= 31.28 %	OCR	= 2.29
γ	= 19.5 kN/m^3		
ΔV	= 3.12 cm^3	tan ϕ	= 0.47
ε_v	= 1.35 %	ϕ	= 25.2 ^{o}
$\Delta e/e_o$	= 0.02	a	= 19 kPa
s_u	= 28.73 kPa	D	= 0.01
ε_f	= 1.40 %	S_f	= 0.74
E_0	= 6.6 MPa	M_f	= 0.99

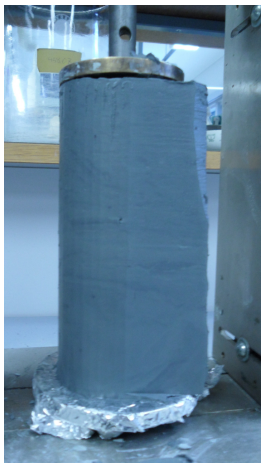

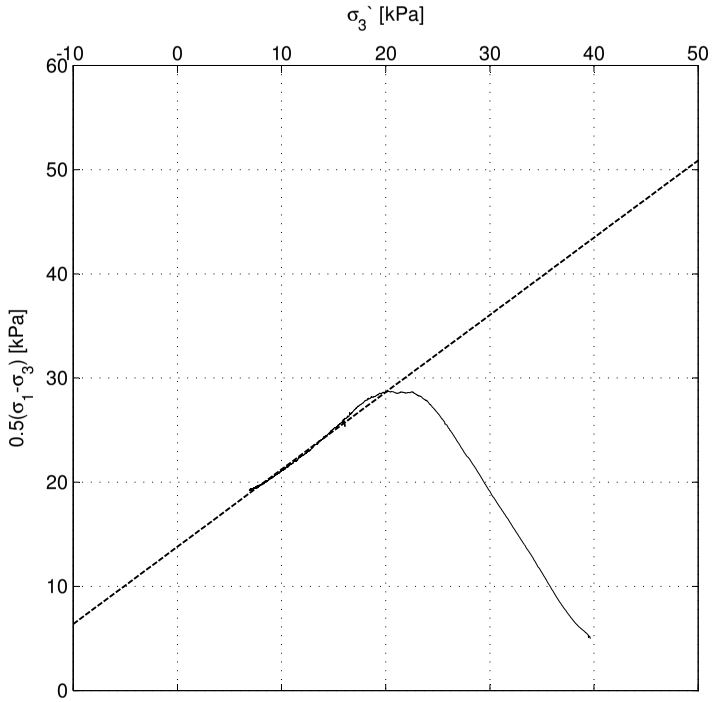

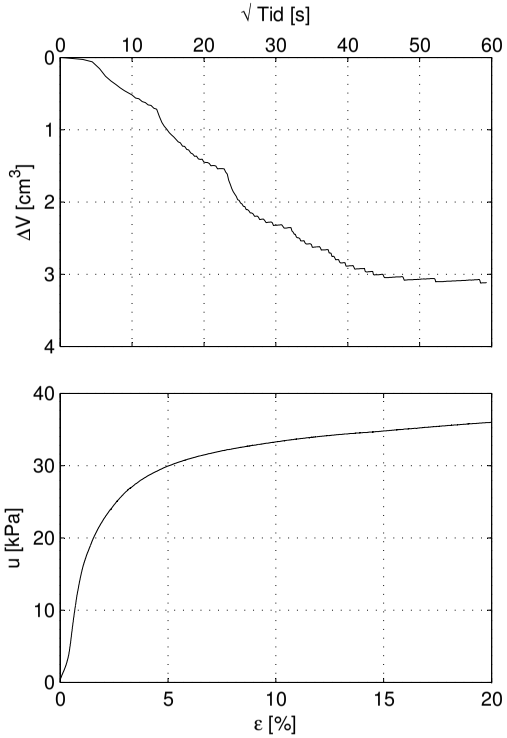

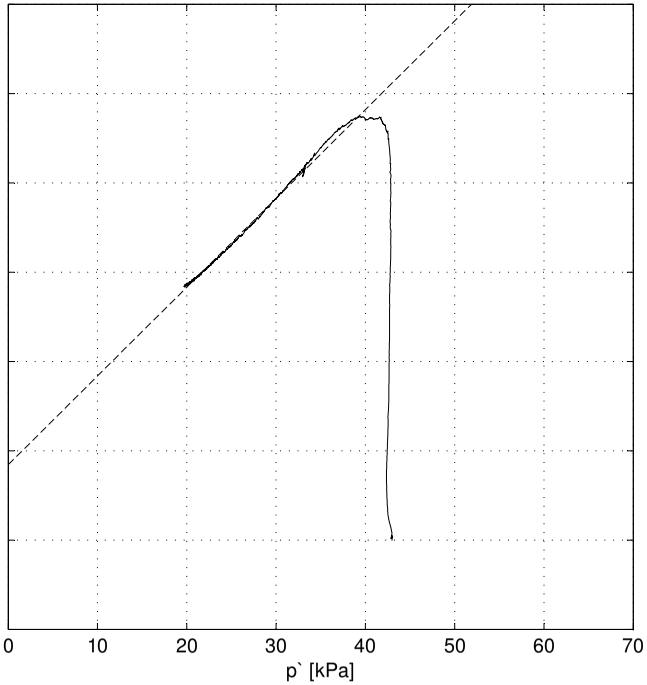

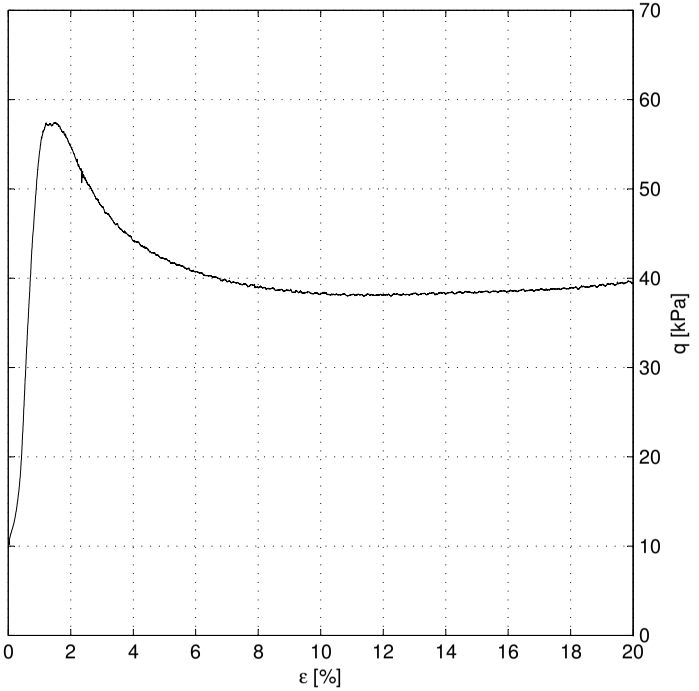

Sund, Rissa
Blokkprøve, CAUa009

Dybde: 3.75 m
Prøvetakingsdato og -utstyr: 30.11.11, Sherbrooke pøvetaker, 250 mm × 350 mm
Åpning av blokkprøven: 13.02.12
Forsøksdato: 15.02.12
Tøyningshastighet: 3.0 %/time

$\sigma`_{vo}$	= 43.75kPa	$\sigma`_c$	= 100 kPa
w	= 34.07 %	OCR	= 2.26
γ	= 19.3 kN/m^3		
ΔV	= 3.28 cm^3	tan ϕ	= 0.43
ε_v	= 1.41 %	ϕ	= 23.1 ^{o}
$\Delta e/e_o$	= 0.02	a	= 22 kPa
s_u	= 27.24 kPa	D	= -0.01
ε_f	= 1.07 %	S_f	= 0.64
E_0	= 7.1 MPa	M_f	= 0.90

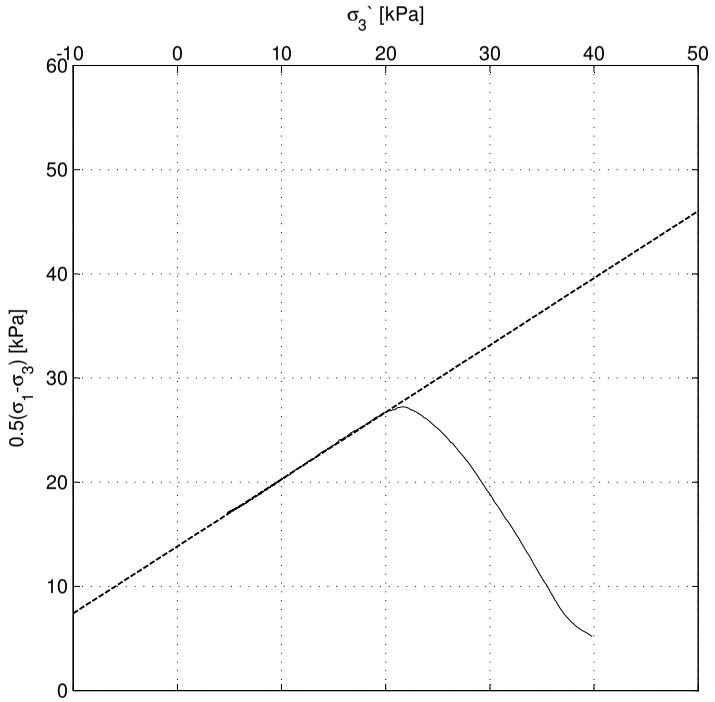

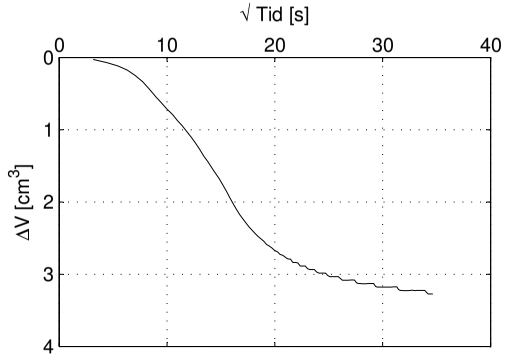

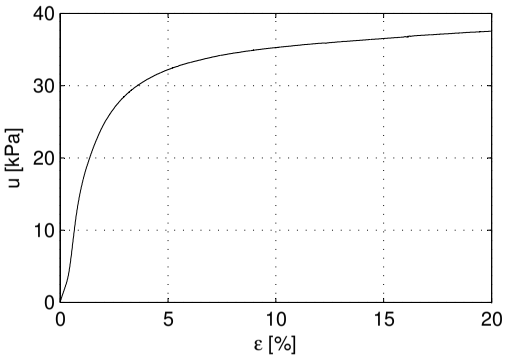

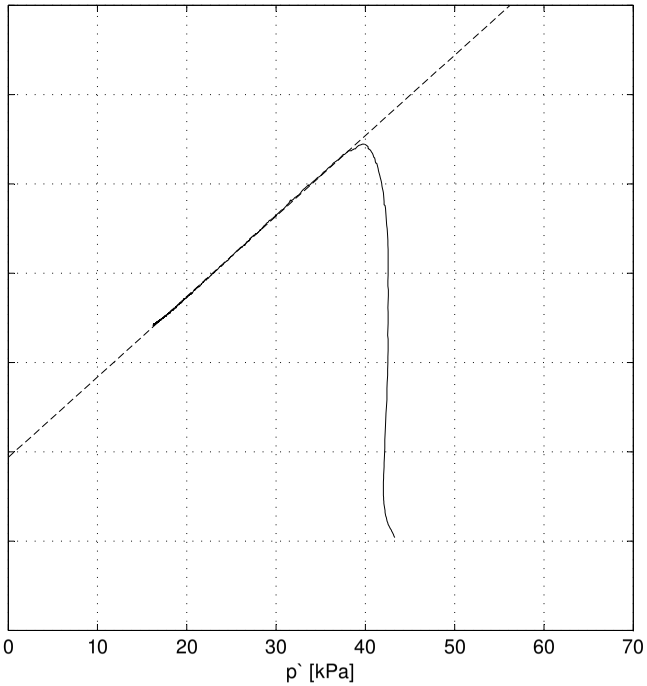

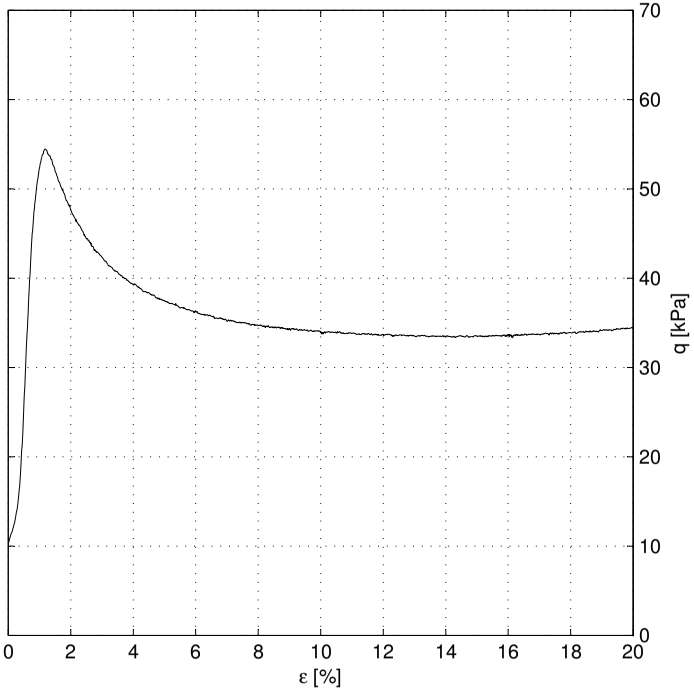

Sund, Rissa
Blokkprøve, CAUa010

Dybde: 3.64 m
Prøvetakingsdato og -utstyr: 30.11.11, Sherbrooke pøvetaker, 250 mm × 350 mm
Åpning av blokkprøven: 13.02.12
Forsøksdato: 17.02.12
Tøyningshastighet: 0.30 %/time

$\sigma`_{vo}$	= 42.76kPa	$\sigma_c`$	= 100 kPa
w	= 32.08 %	OCR	= 2.29
γ	= 19.4 kN/m^3		
ΔV	= 4.01 cm^3	tan ϕ	= 0.48
ε_v	= 1.73 %	ϕ	= 25.7 ^{o}
$\Delta e/e_o$	= 0.03	a	= 12 kPa
s_u	= 23.19 kPa	D	= -0.09
ε_f	= 1.22 %	S_f	= 0.77
E_0	= 5.4 MPa	M_f	= 1.02

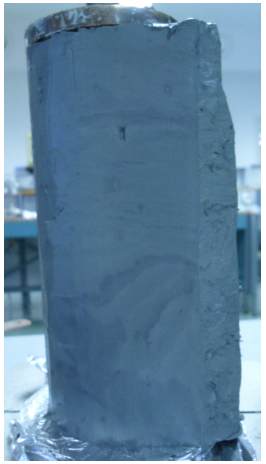

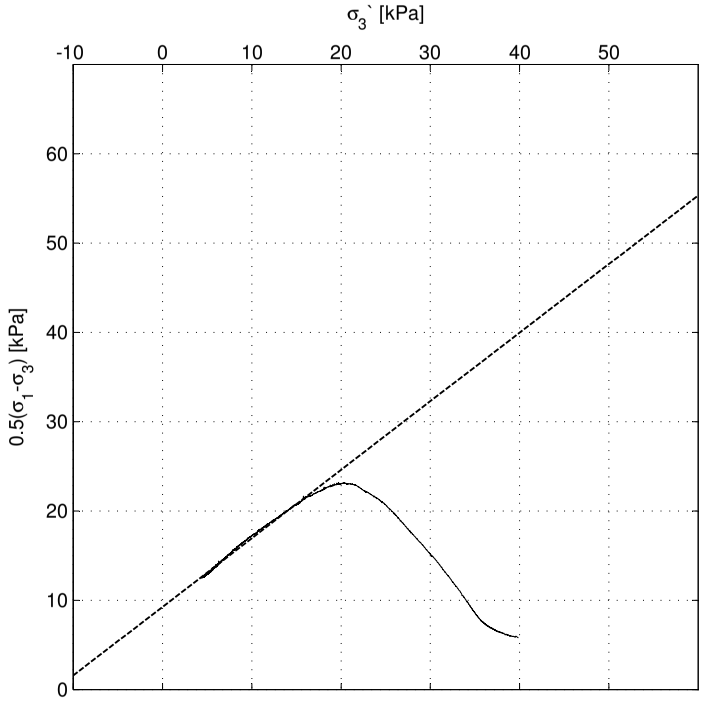

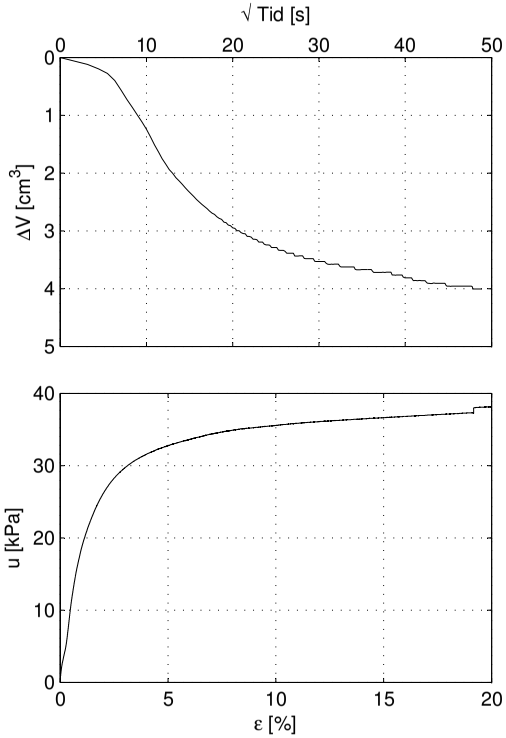

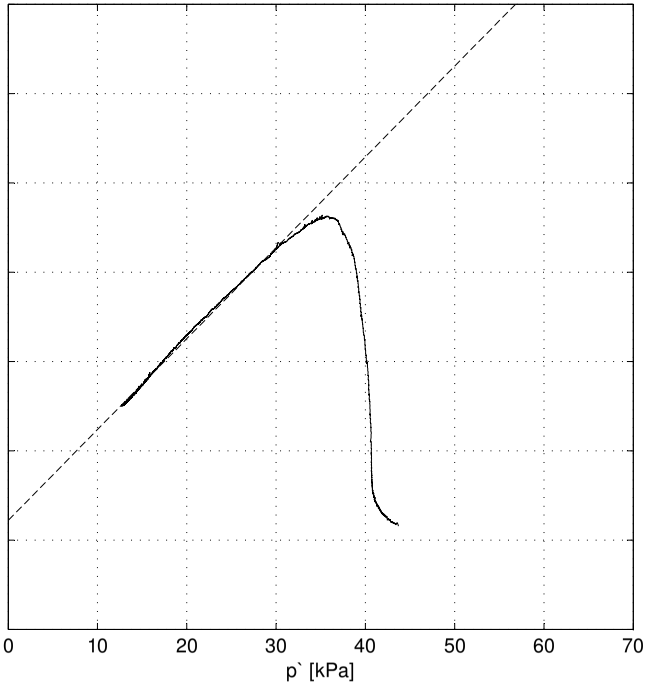

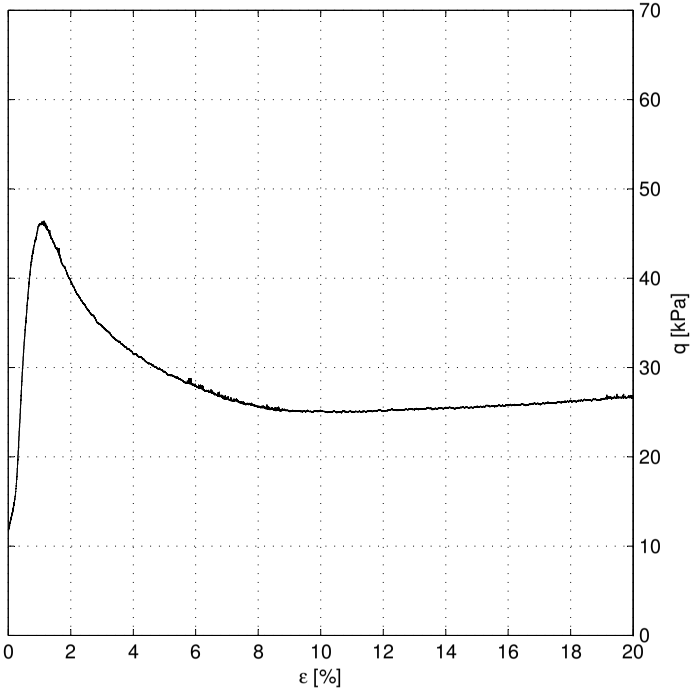

Sund, Rissa
Blokkprøve, CAUa011

Dybde: 3.64 m
Prøvetakingsdato og -utstyr: 30.11.11, Sherbrooke pøvetaker, 250 mm × 350 mm
Åpning av blokkprøven: 13.02.12
Forsøksdato: 20.02.12
Tøyningshastighet: 4.50 %/time

$\sigma`_{vo}$	= 42.76kPa	$\sigma`_c$	= 100 kPa
w	= 35.37 %	OCR	= 2.29
γ	= 19.4 kN/m^3		
ΔV	= 3.64 cm^3	tan ϕ	= 0.41
ε_v	= 1.57 %	ϕ	= 22.3 ^{o}
$\Delta e/e_o$	= 0.03	a	= 25 kPa
s_u	= 29.74 kPa	D	= 0.01
ε_f	= 0.96 %	S_f	= 0.61
E_0	= 7.4 MPa	M_f	= 0.87

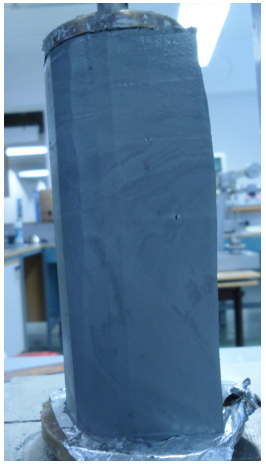

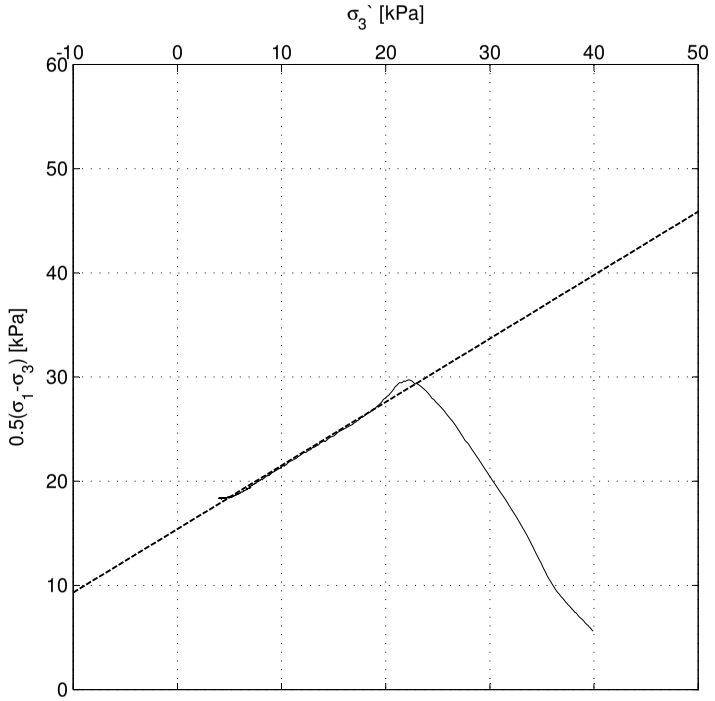

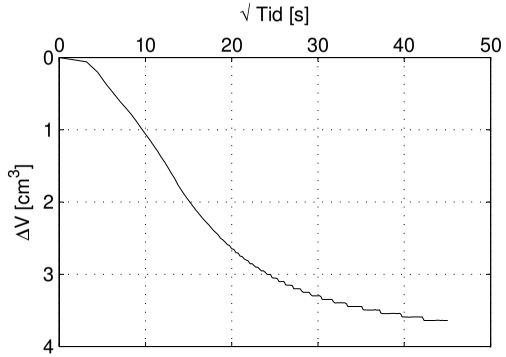

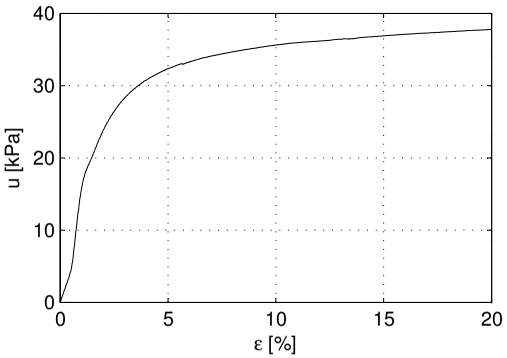

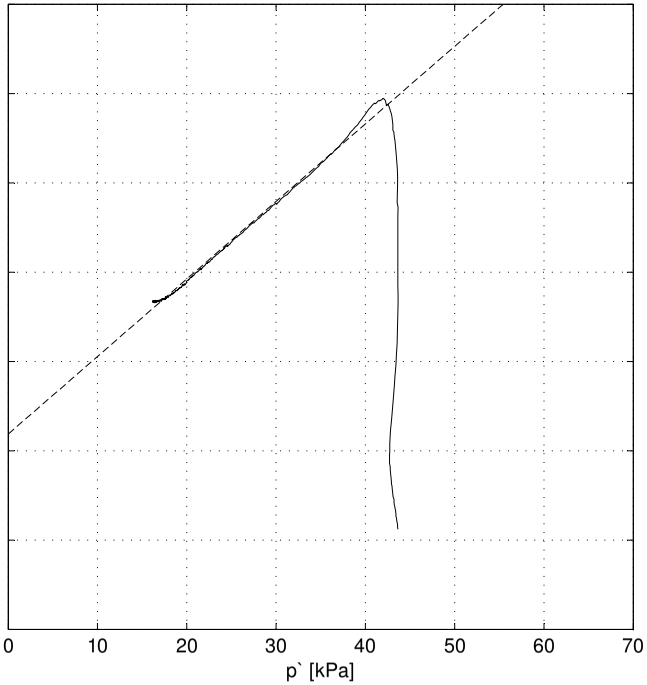

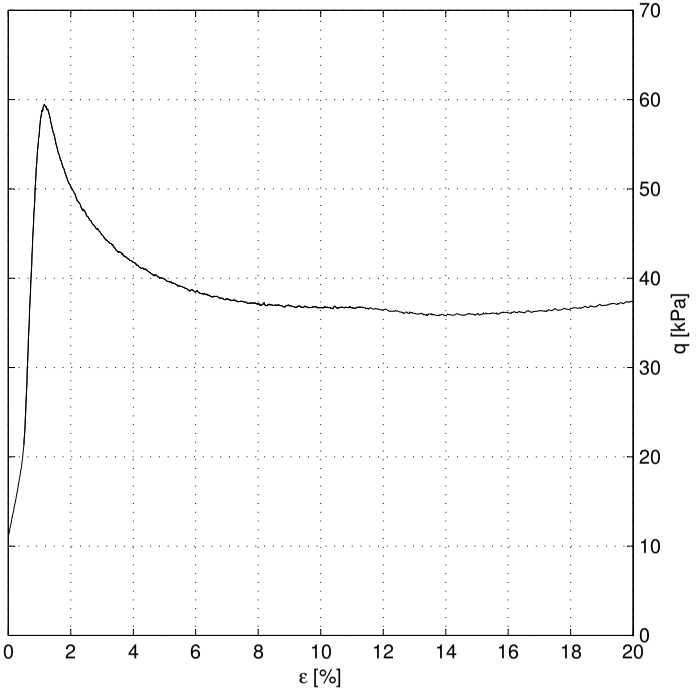

Sund, Rissa
Blokkprøve, CAUa012

Dybde: 3.75 m
Prøvetakingsdato og -utstyr: 30.11.11, Sherbrooke pøvetaker, 250 mm × 350 mm
Åpning av blokkprøven: 13.02.12
Forsøksdato: 22.02.12
Tøyningshastighet: 0.10 %/time

$\sigma`_{vo}$	= 4.75kPa	$\sigma`_c$	= 100 kPa
w	= 32.44 %	OCR	= 2.26
γ	= 19.3 kN/m^3		
ΔV	= 4.87 cm^3	tan ϕ	= 0.49
ε_v	= 2.10 %	ϕ	= 26.1 ^{o}
$\Delta e/e_o$	= 0.04	a	= 15 kPa
s_u	= 18.26 kPa	D	= -0.34
ε_f	= 1.69 %	S_f	= 0.79
E_0	= 3.3 MPa	M_f	= 1.05

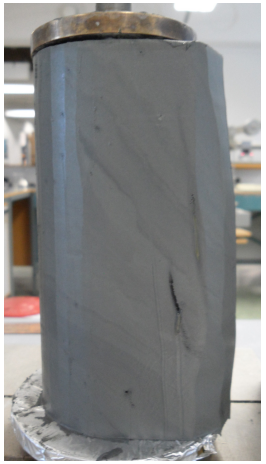

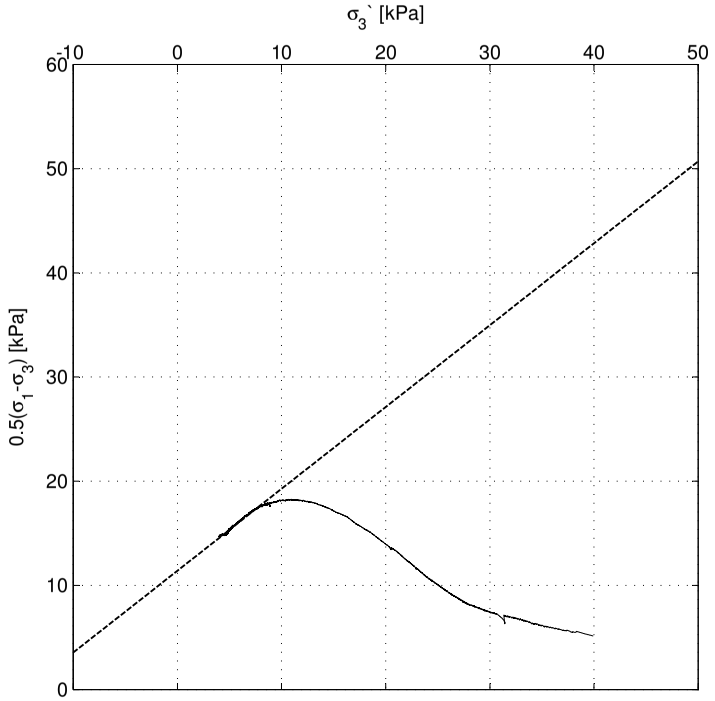

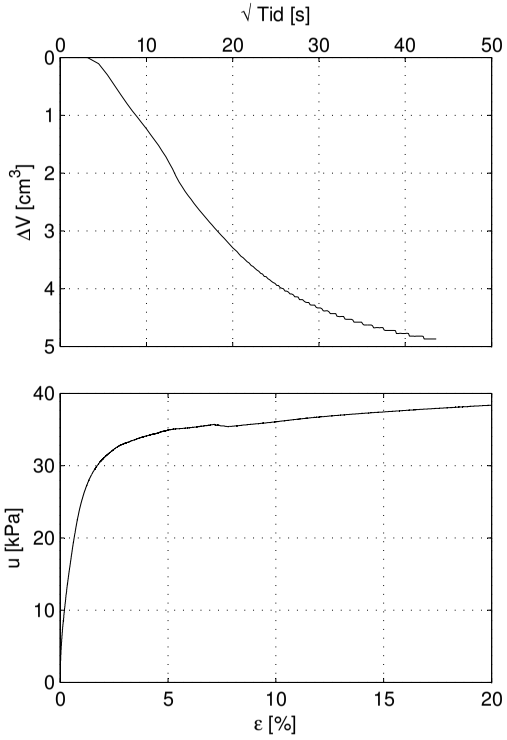

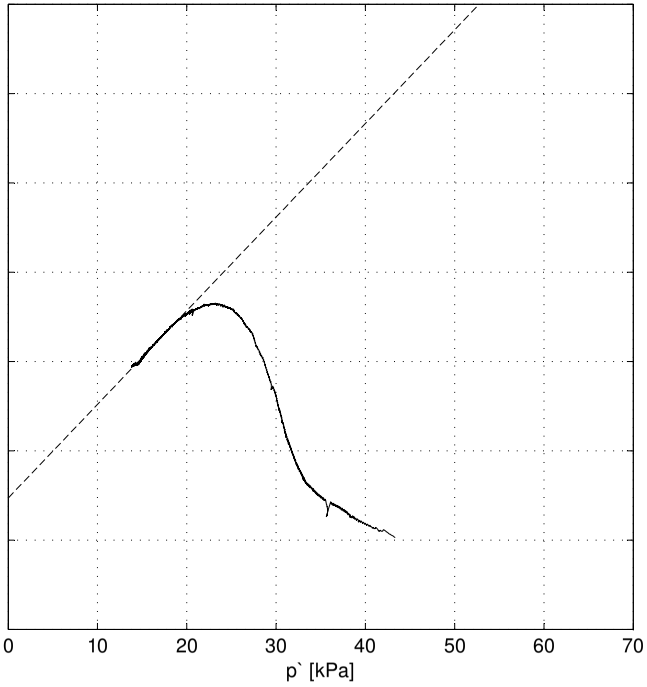

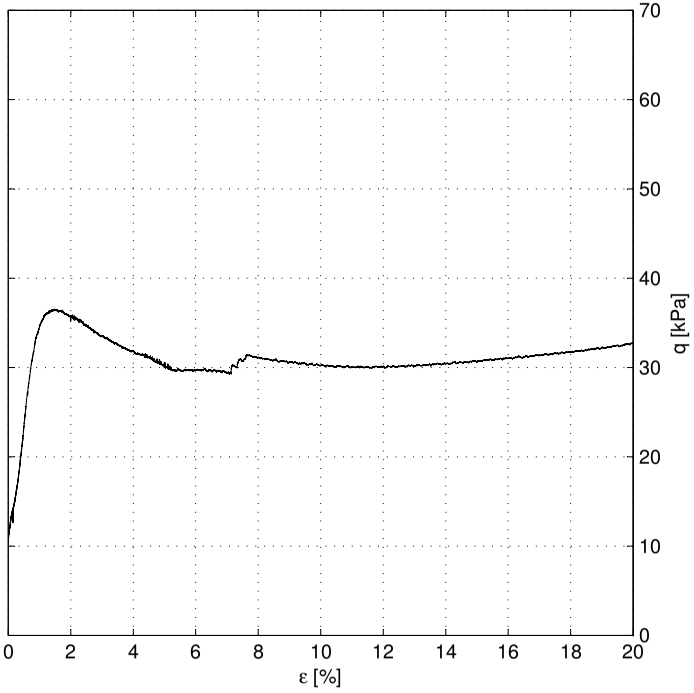

Sund, Rissa
Blokkprøve, CAUa013

Dybde: 3.75 m
Prøvetakingsdato og -utstyr: 30.11.11, Sherbrooke pøvetaker, 250 mm × 350 mm
Åpning av blokkprøven: 13.02.12
Forsøksdato: 26.02.12
Tøyningshastighet: 0.10 %/time

$\sigma`_{vo}$	= 43.75kPa	$\sigma`_c$	= 100 kPa
w	= 32.74 %	OCR	= 2.26
γ	= 19.3 kN/m^3		
ΔV	= 4.08 cm^3	tan ϕ	= 0.42
ε_v	= 1.76 %	ϕ	= 22.6 ^{o}
$\Delta e/e_o$	= 0.03	a	= 22 kPa
s_u	= 24.46 kPa	D	= -0.07
ε_f	= 1.17 %	S_f	= 0.62
E_0	= 6.9 MPa	M_f	= 0.88

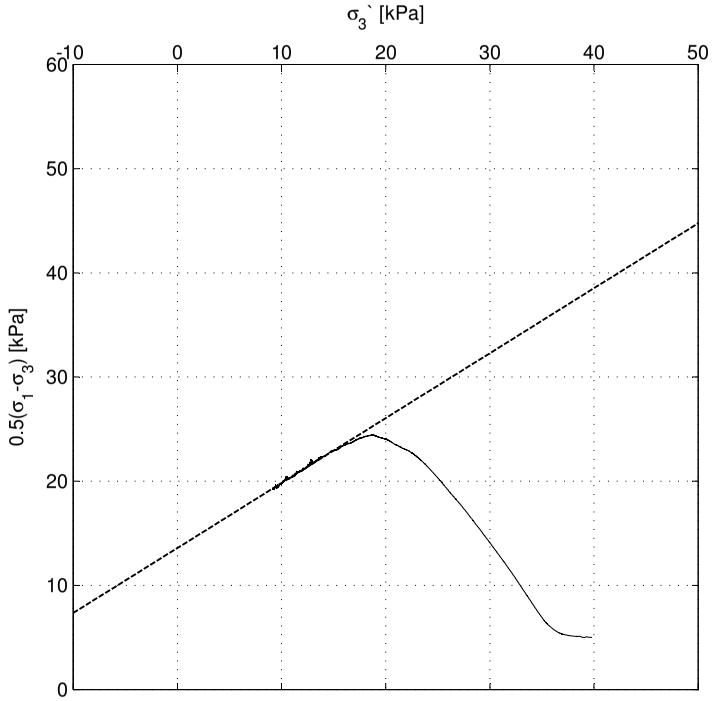

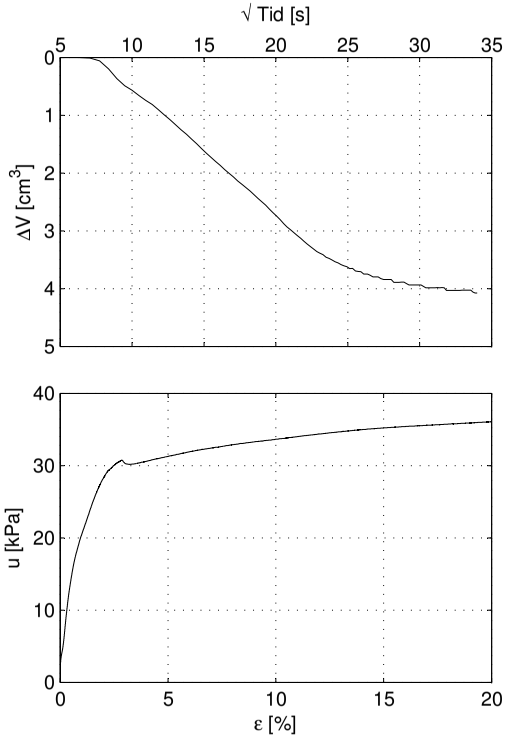

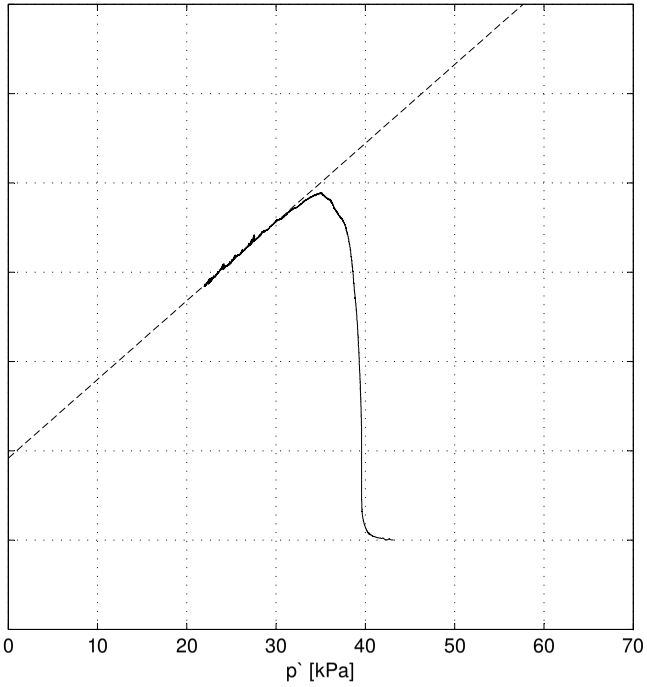

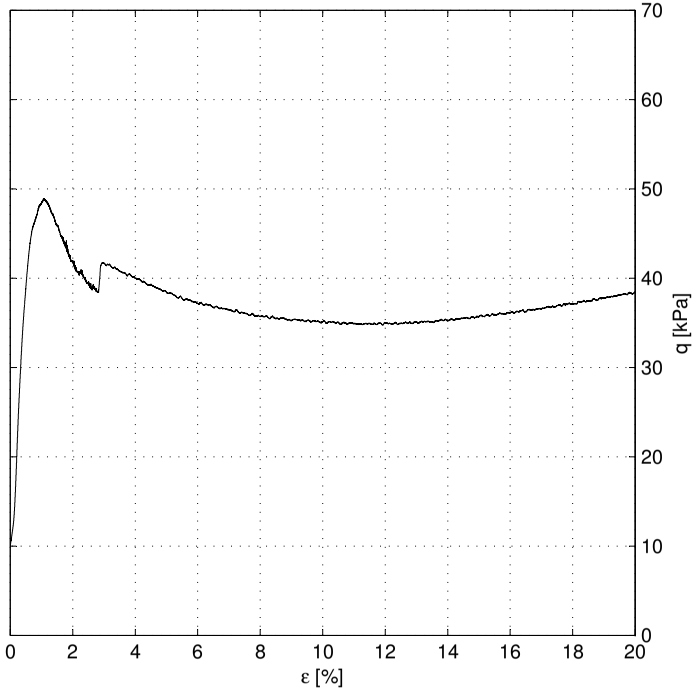

Sund, Rissa
Blokkprøve, CAUa014

Dybde: 3.75 m
Prøvetakingsdato og -utstyr: 30.11.11, Sherbrooke pøvetaker, 250 mm × 350 mm
Åpning av blokkprøven: 13.02.12
Forsøksdato: 02.03.12
Tøyningshastighet: 0.01 %/time

$\sigma`_{vo}$	= 43.75kPa	$\sigma`_c$	= 100 kPa
w	= 37.36 %	OCR	= 2.26
γ	= 19.3 kN/m^3		
ΔV	= 4.40 cm^3	tan ϕ	= 0.55
ε_v	= 1.90 %	ϕ	= 28.8 ^{o}
$\Delta e/e_o$	= 0.04	a	= 10 kPa
s_u	= 13.72 kPa	D	= -1.34
ε_f	= 0.29 %	S_f	= 0.93
E_0	= 14.7 MPa	M_f	= 1.15

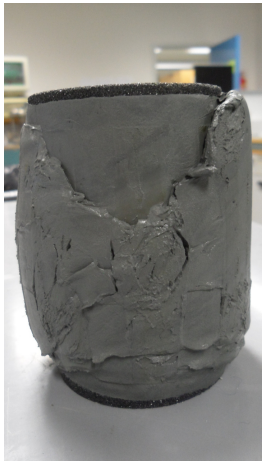

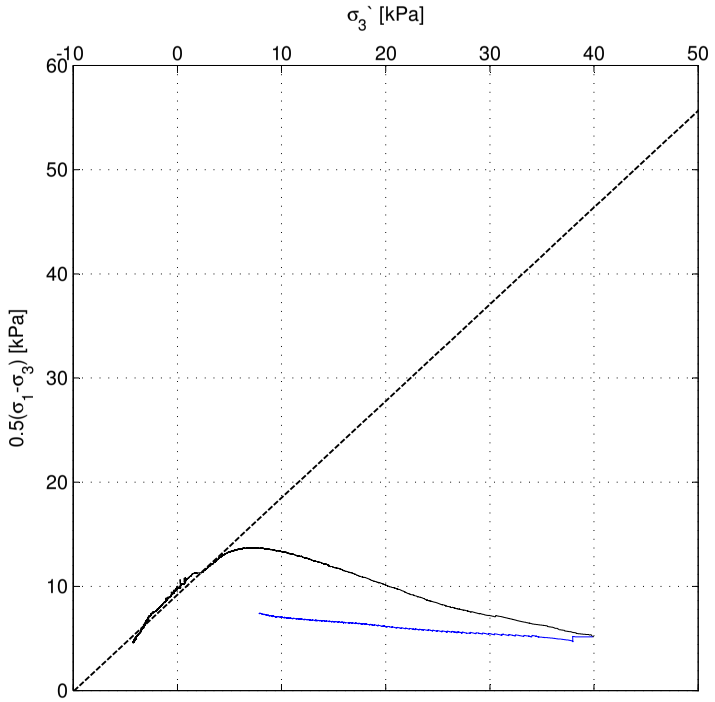

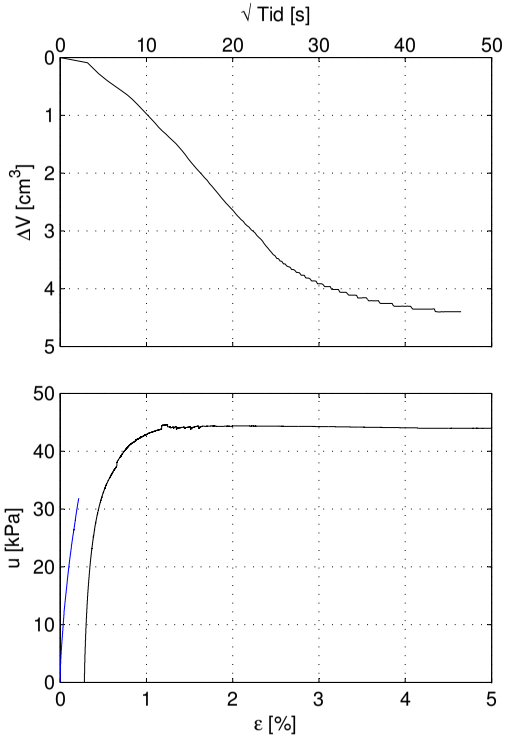

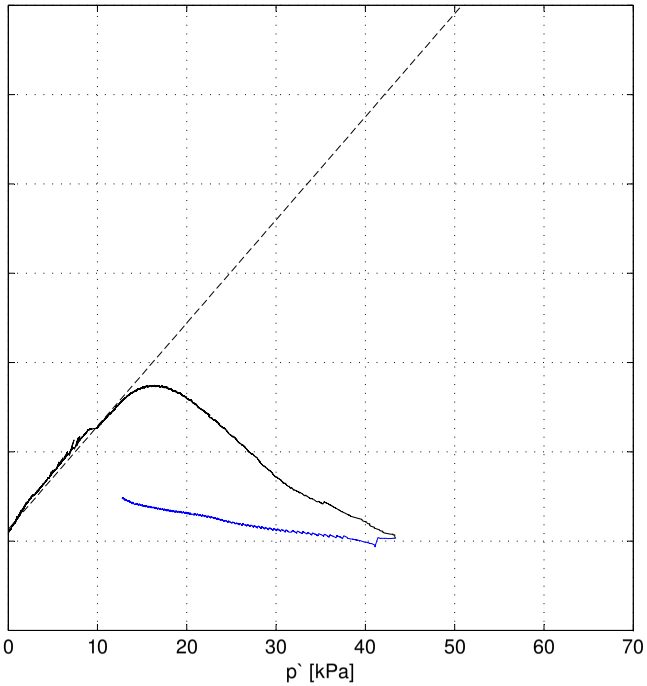

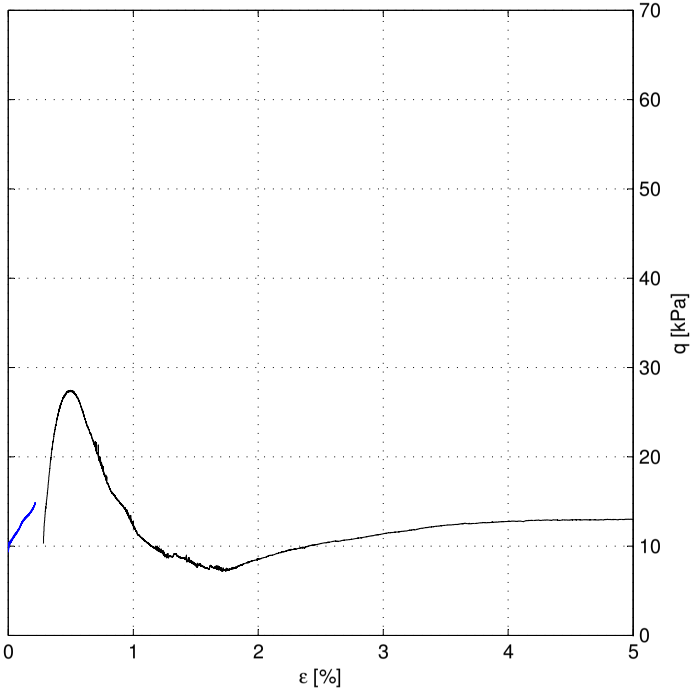

Sund, Rissa
Blokkprøve, CAUa015

Dybde: 4.37 m
Prøvetakingsdato og -utstyr: 30.11.11, Sherbrooke pøvetaker, 250 mm × 350 mm
Åpning av blokkprøven: 12.03.12
Forsøksdato: 12.03.12
Tøyningshastighet: 3.0 %/time

$\sigma`_{vo}$	= 49.33kPa	$\sigma`_c$	= 100 kPa
w	= 37.70 %	OCR	= 2.14
γ	= 19.3 kN/m^3		
ΔV	= 3.44 cm^3	tan ϕ	= 0.56
ε_v	= 1.48 %	ϕ	= 29.1 ^{o}
$\Delta e/e_o$	= 0.03	a	= 15 kPa
s_u	= 33.08 kPa	D	= 0.02
ε_f	= 1.35 %	S_f	= 0.95
E_0	= 6.4 MPa	M_f	= 1.17

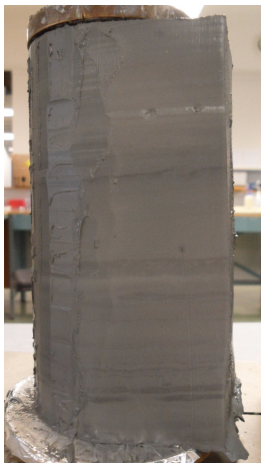

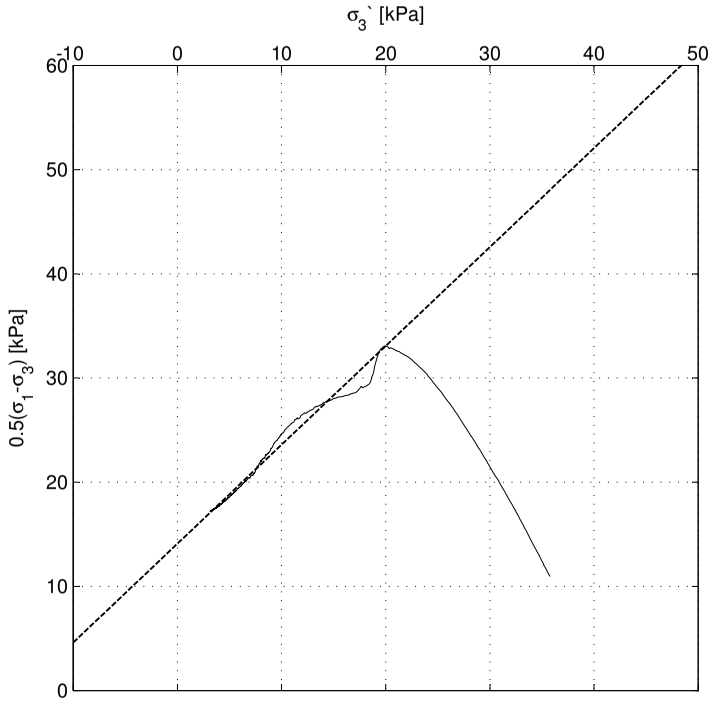

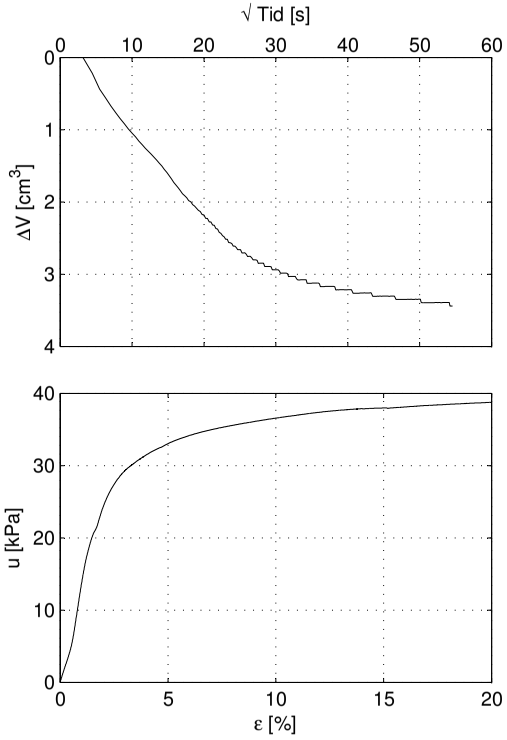

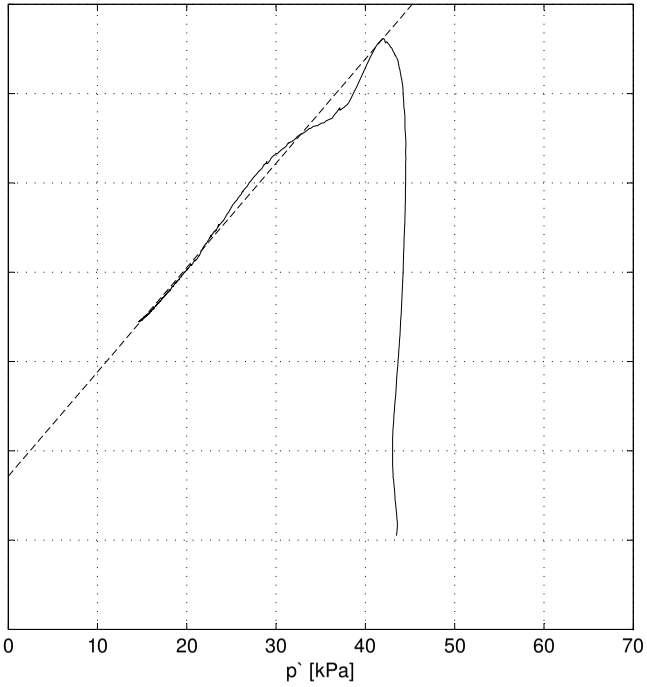

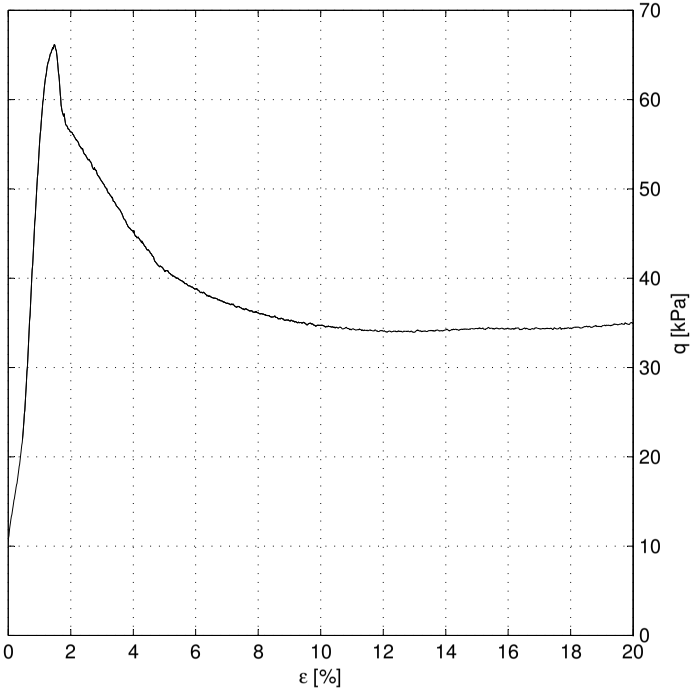

Sund, Rissa
Blokkprøve, CAUa016

Dybde: 4.37 m
Prøvetakingsdato og -utstyr: 30.11.11, Sherbrooke pøvetaker, 250 mm × 350 mm
Åpning av blokkprøven: 12.03.12
Forsøksdato: 13.03.12
Tøyningshastighet: 1.0 %/time

$\sigma`_{vo}$	= 49.33kPa	$\sigma`_c$	= 100 kPa
w	= 37.51 %	OCR	= 2.14
γ	= 19.3 kN/m^3		
ΔV	= 4.63 cm^3	tan ϕ	= 0.62
ε_v	= 2.00 %	ϕ	= 31.6 ^{o}
$\Delta e/e_o$	= 0.04	a	= 14 kPa
s_u	= 32.32 kPa	D	= -0.01
ε_f	= 1.47 %	S_f	= 1.10
E_0	= 6.3 MPa	M_f	= 1.28

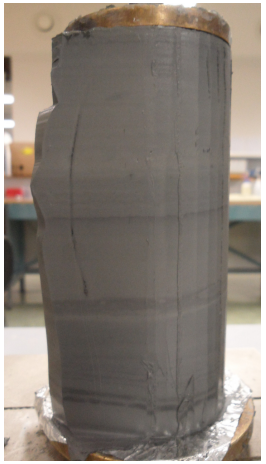

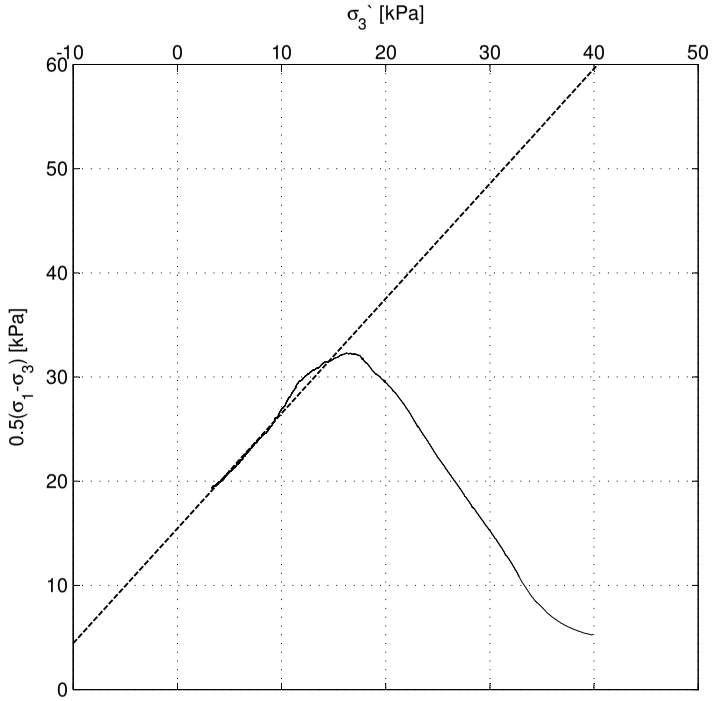

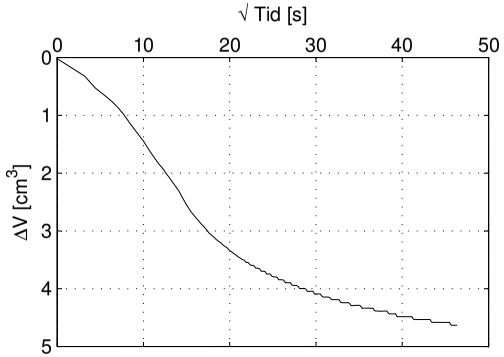

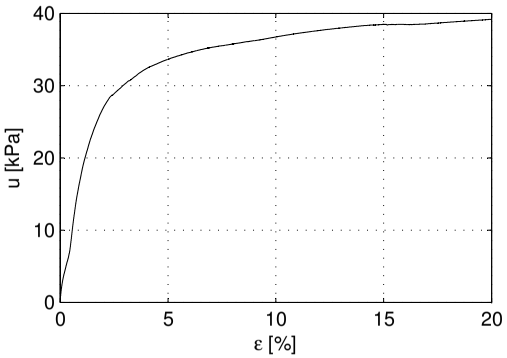

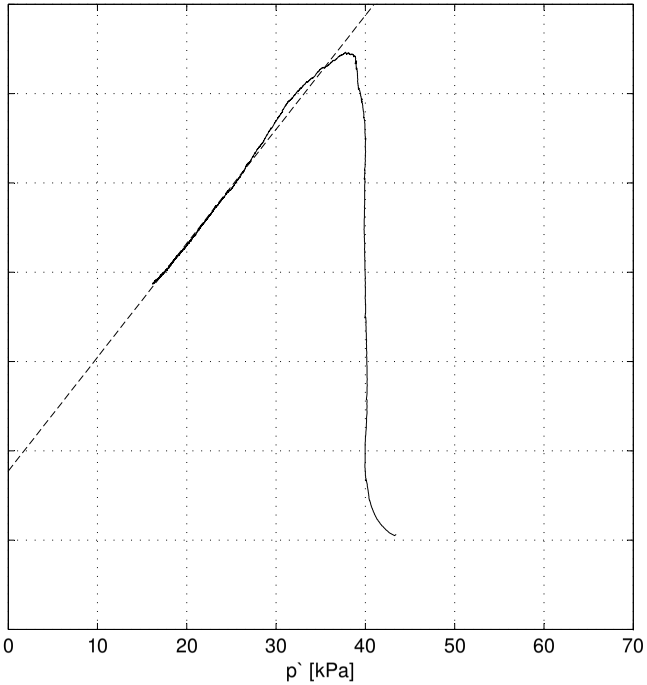

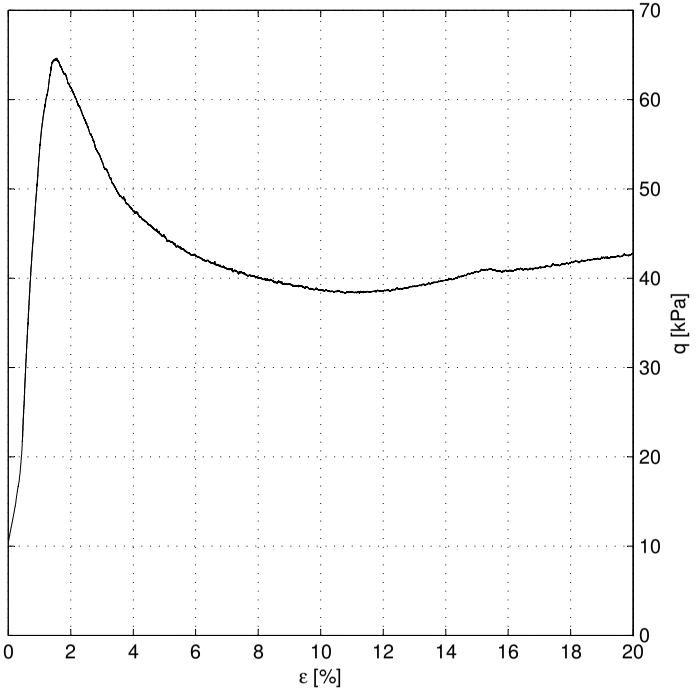

Sund, Rissa
Blokkprøve, CAUa017

Dybde: 4.37 m
Prøvetakingsdato og -utstyr: 30.11.11, Sherbrooke pøvetaker, 250 mm × 350 mm
Åpning av blokkprøven: 12.03.12
Forsøksdato: 14.03.12
Tøyningshastighet: 0.10 %/time

$\sigma`_{vo}$	= 49.33kPa	$\sigma`_c$	= 100 kPa
w	= 37.36 %	OCR	= 2.14
γ	= 19.3 kN/m^3		
ΔV	= 3.54 cm^3	tan ϕ	= 0.60
ε_v	= 1.52 %	ϕ	= 31.1 ^{o}
$\Delta e/e_o$	= 0.03	a	= 14 kPa
s_u	= 27.57 kPa	D	= -0.05
ε_f	= 1.01 %	S_f	= 1.07
E_0	= 7.8 MPa	M_f	= 1.25

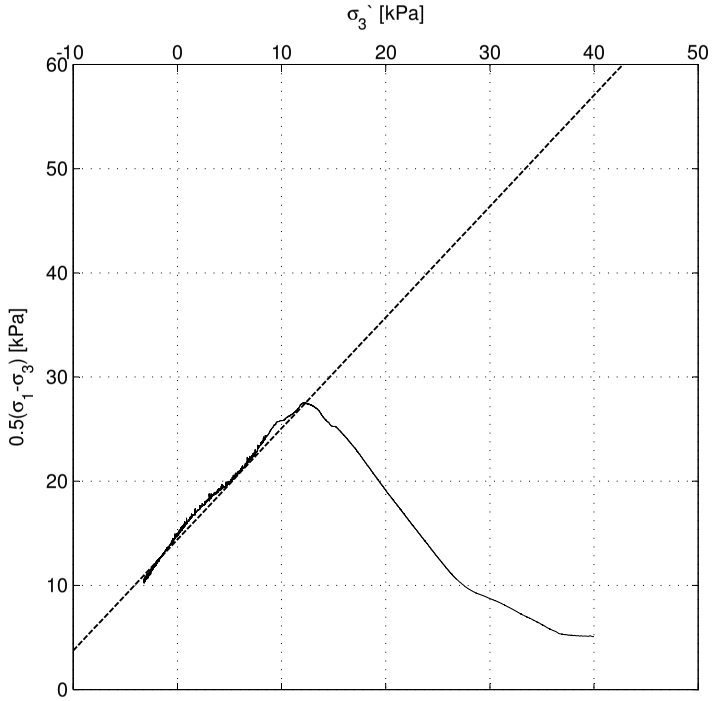

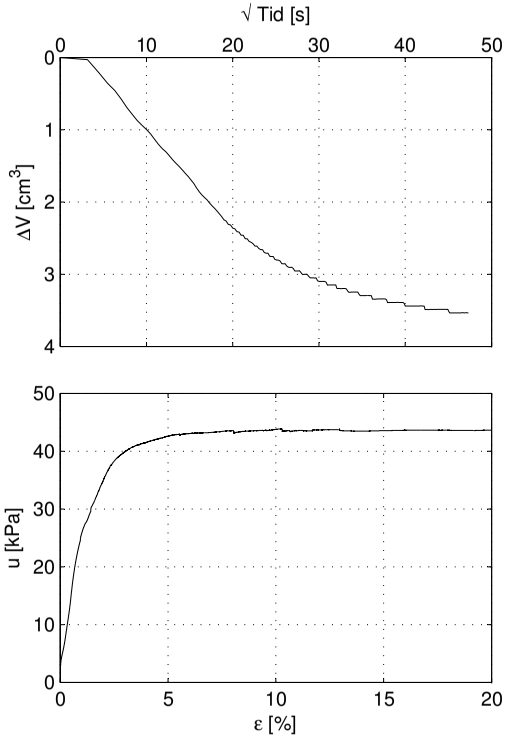

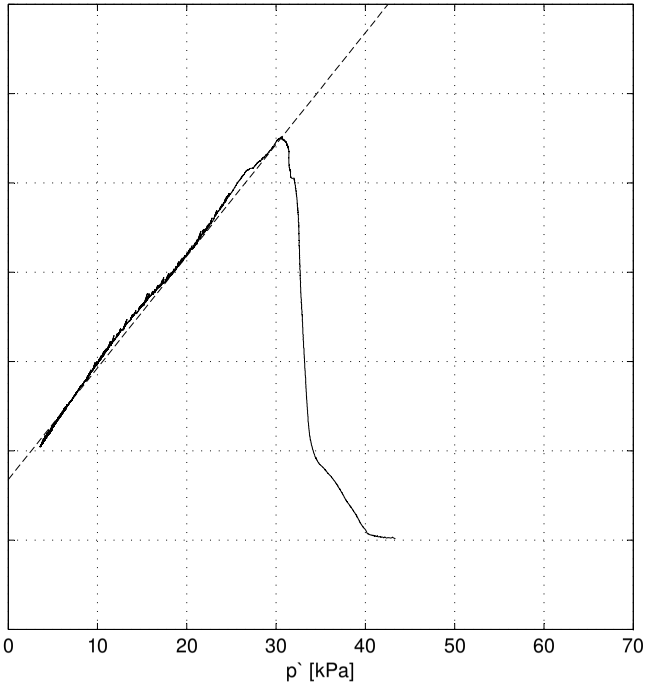

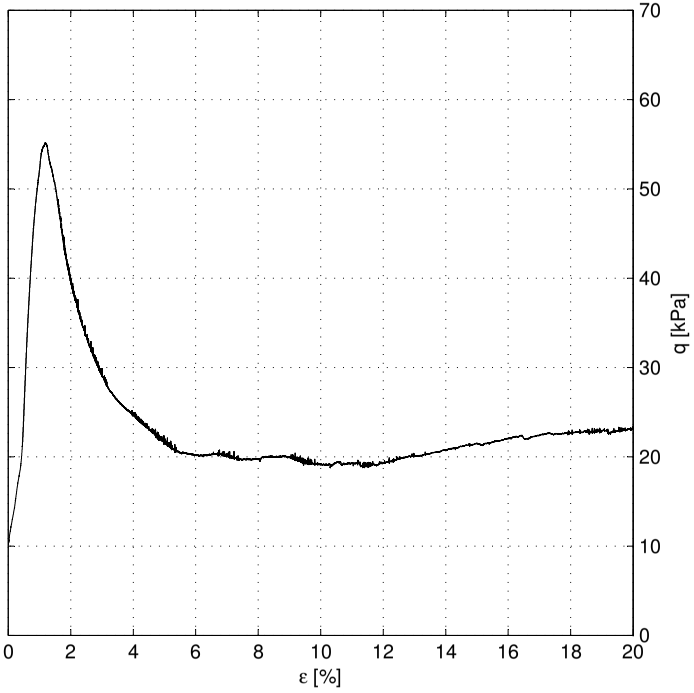

Sund, Rissa
Blokkprøve, CAUa018

Dybde: 4.37 m
Prøvetakingsdato og -utstyr: 30.11.11, Sherbrooke pøvetaker, 250 mm × 350 mm
Åpning av blokkprøven: 12.03.12
Forsøksdato: 21.03.12
Tøyningshastighet: 0.30 %/time

σ'_{vo}	= 49.33kPa	σ'_c	= 100 kPa
w_{vo}	= 35.45 %	OCR	= 2.14
γ	= 19.3 kN/m^3		
ΔV	= 4.00 cm^3	tan ϕ	= 0.63
ε_v	= 1.73 %	ϕ	= 32.1 ^{o}
$\Delta e/e_o$	= 0.03	a	= 11 kPa
s_u	= 28.58 kPa	D	= 0.04
ε_f	= 0.93 %	S_f	= 1.14
E_0	= 7.3 MPa	M_f	= 1.30

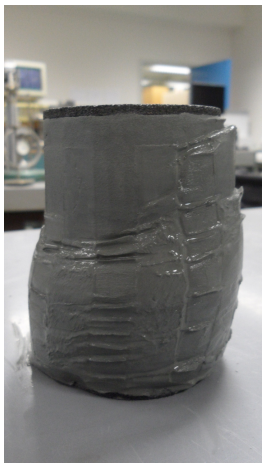

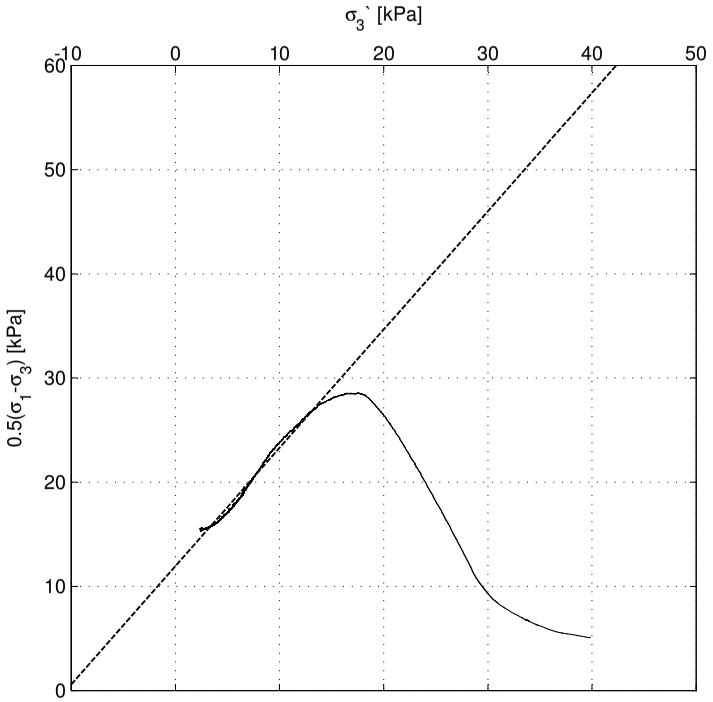

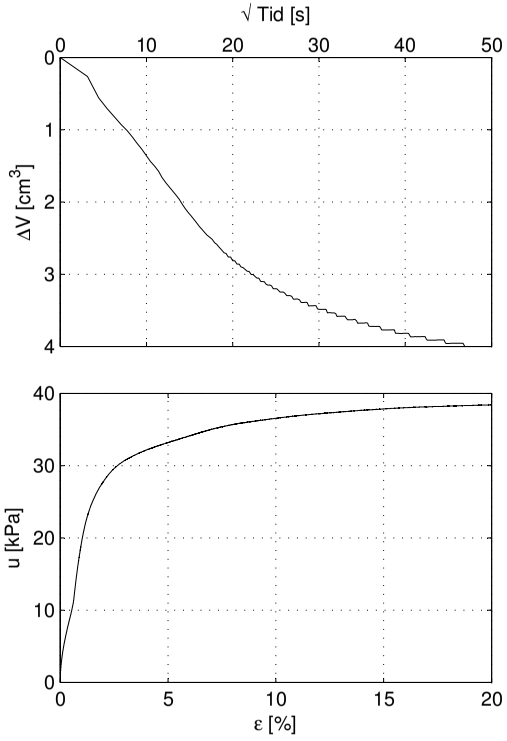

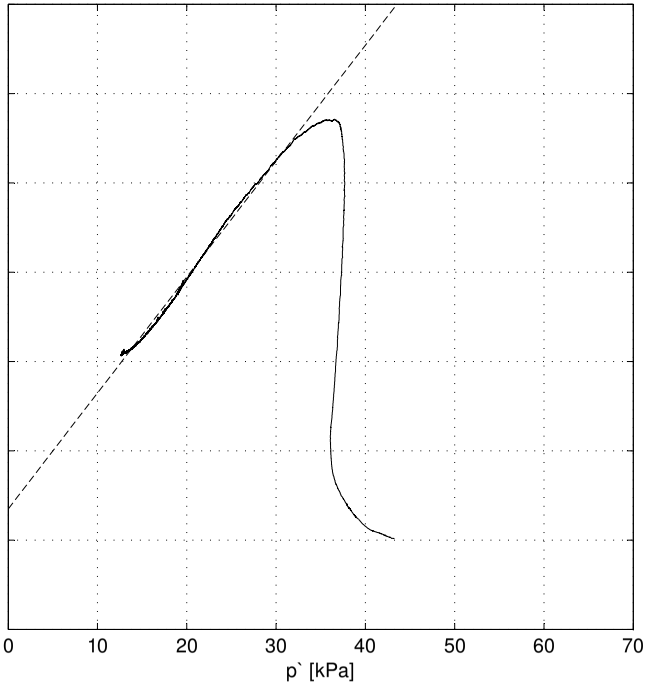

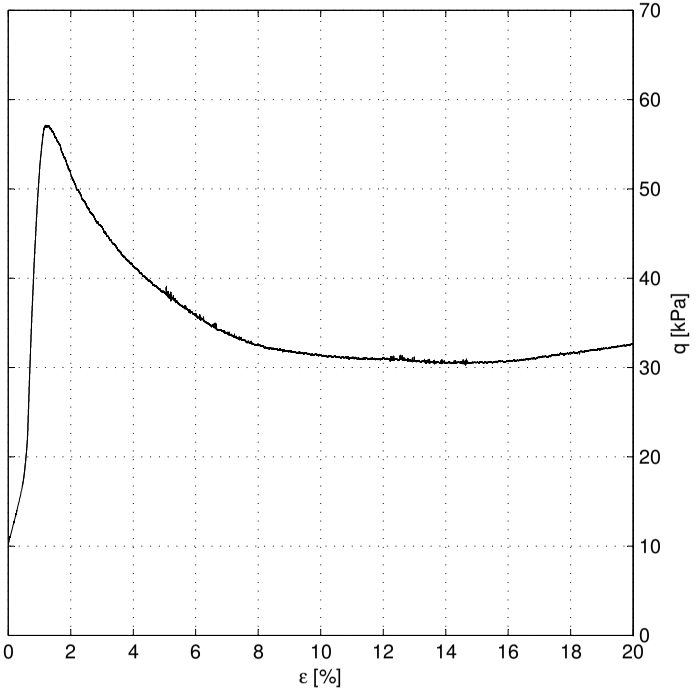

Sund, Rissa
Blokkprøve, CAUp101

Dybde: 3.96 m
Prøvetakingsdato og -utstyr: 30.11.11, Sherbrooke pøvetaker, 250 mm × 350 mm
Åpning av blokkprøven: 19.01.12
Forsøksdato: 20.01.12
Tøyningshastighet: -1.20 %/time (Utført med baktrykk av Multiconsult Trondheim)

$\sigma`_{vo}$ = 45.64kPa $\sigma`_c$ = 100 kPa
w = 33.80 % OCR = 2.22
γ = 19.2 kN/m^3

ΔV = 5.88 cm^3
ε_v = 2.53 %
$\Delta e/e_o$ = 0.05

s_u = 9.44 kPa
ε_f = 1.21 %
E_0 = 2.0 MPa

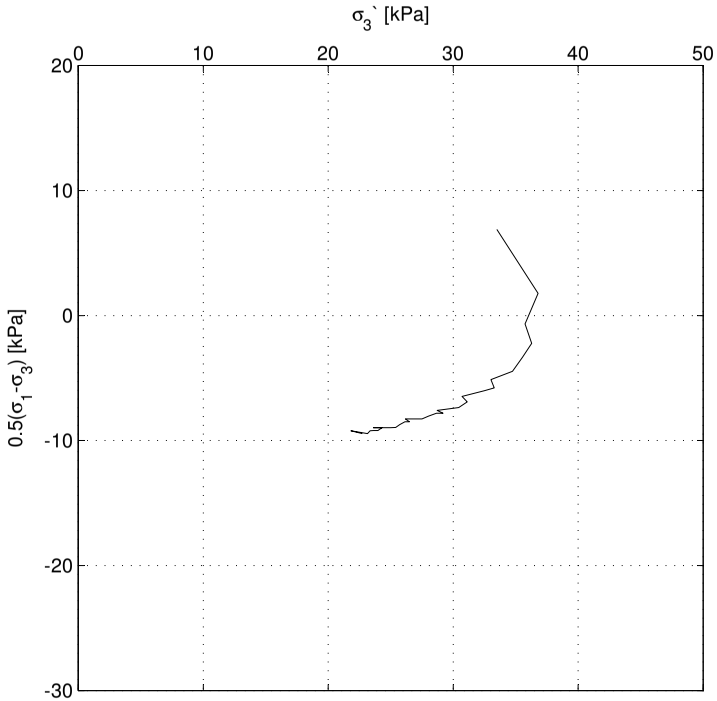

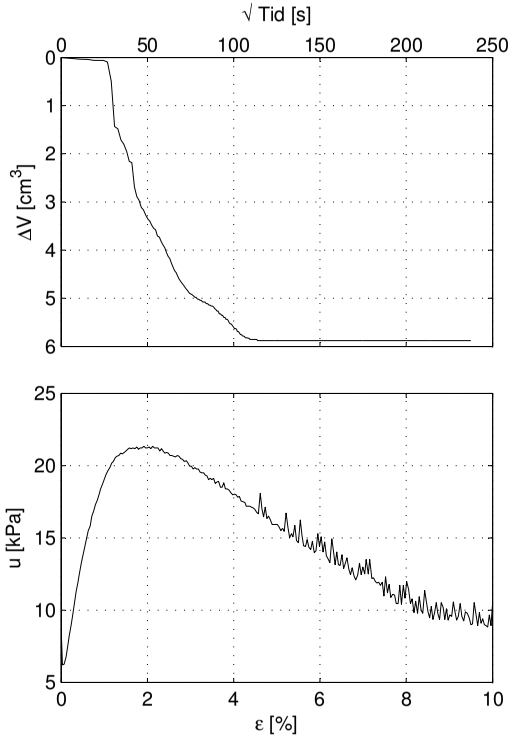

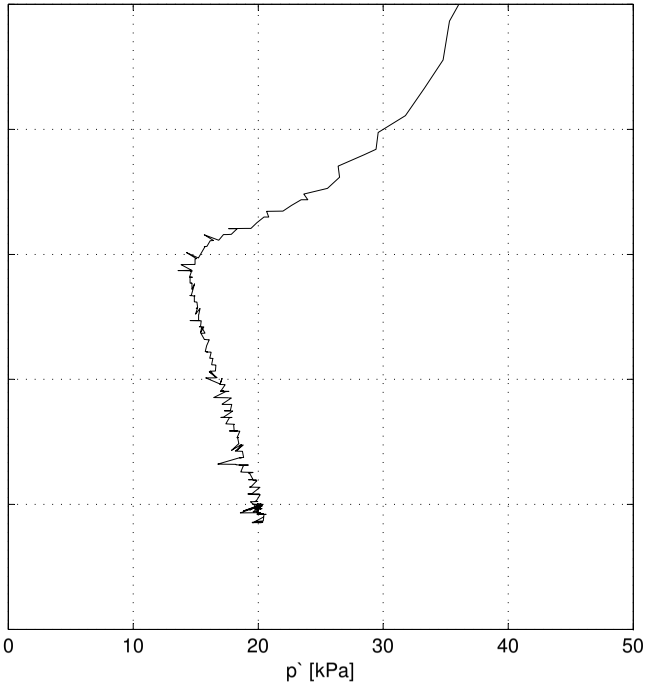

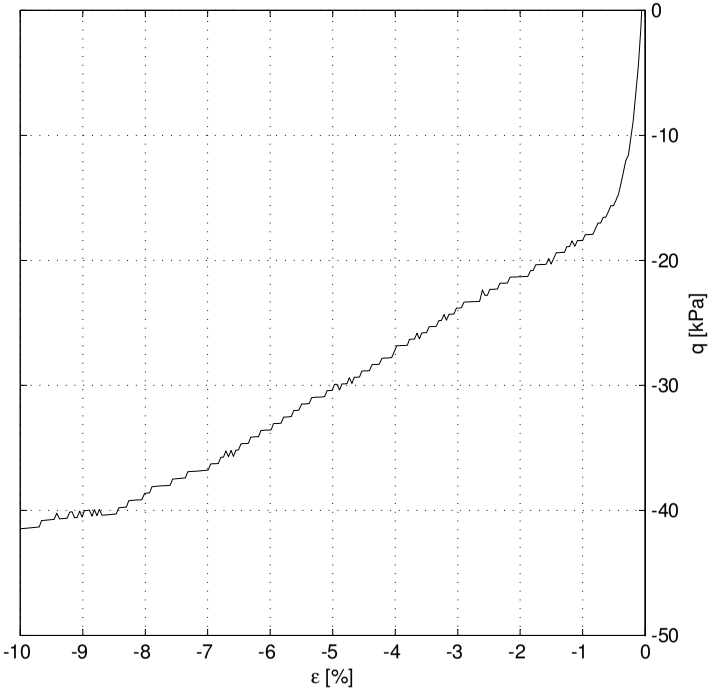

Sund, Rissa
Blokkprøve, CAUp103

Dybde: 4.07 m
Prøvetakingsdato og -utstyr: 30.11.11, Sherbrooke pøvetaker, 250 mm × 350 mm
Åpning av blokkprøven: 13.02.12
Forsøksdato: 06.02.12
Tøyningshastighet: -1.20 %/time (Utført med baktrykk av Multiconsult Trondheim)

$\sigma`_{vo}$ = 46.63kPa $\sigma`_c$ = 100 kPa
w = 33.40 % OCR = 2.20
γ = 19.2 kN/m^3

ΔV = 3.77 cm^3
ε_v = 1.63 %
$\Delta e/e_o$ = 0.03

s_u = 10.21 kPa
ε_f = 0.58 %
E_0 = 17.0 MPa

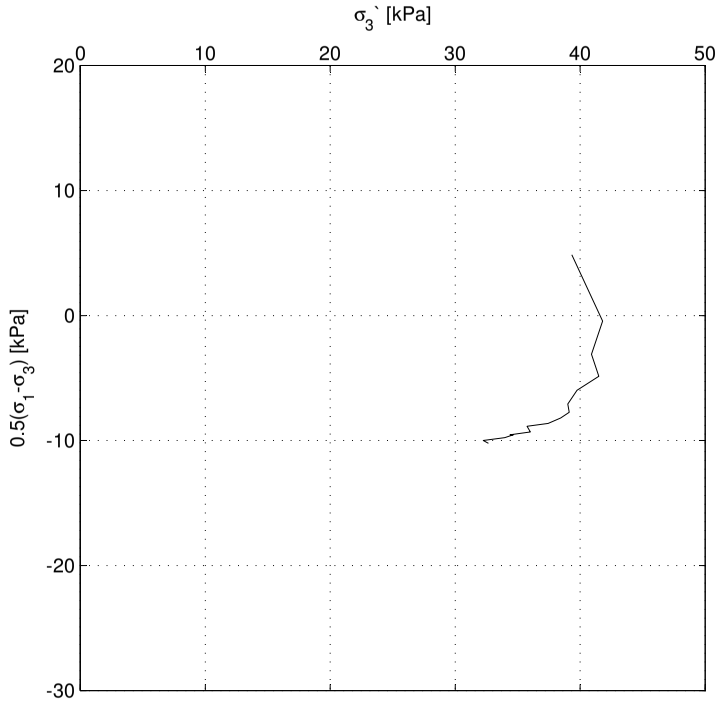

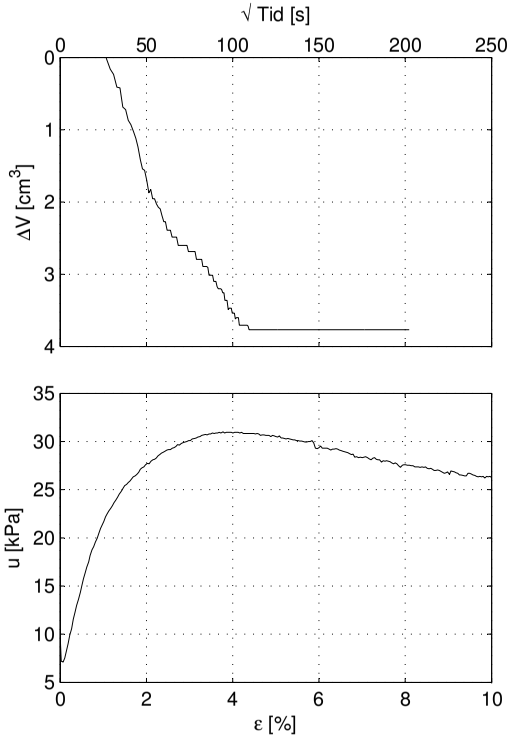

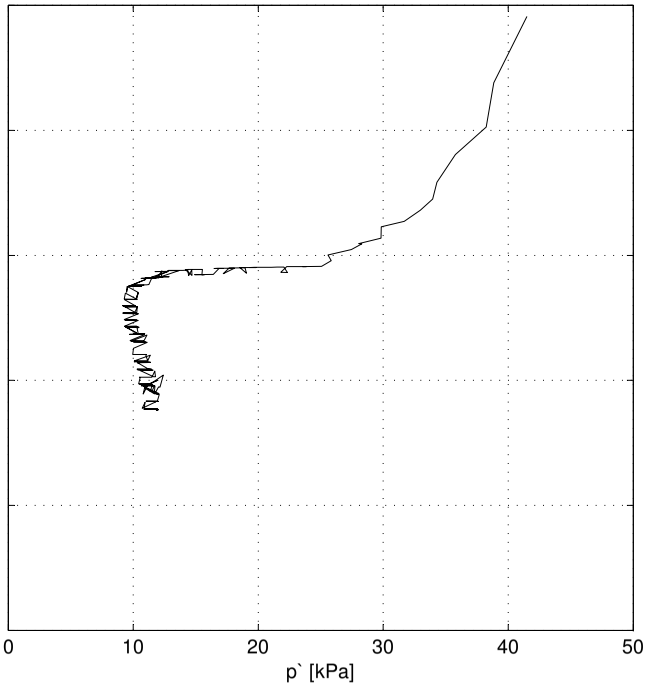

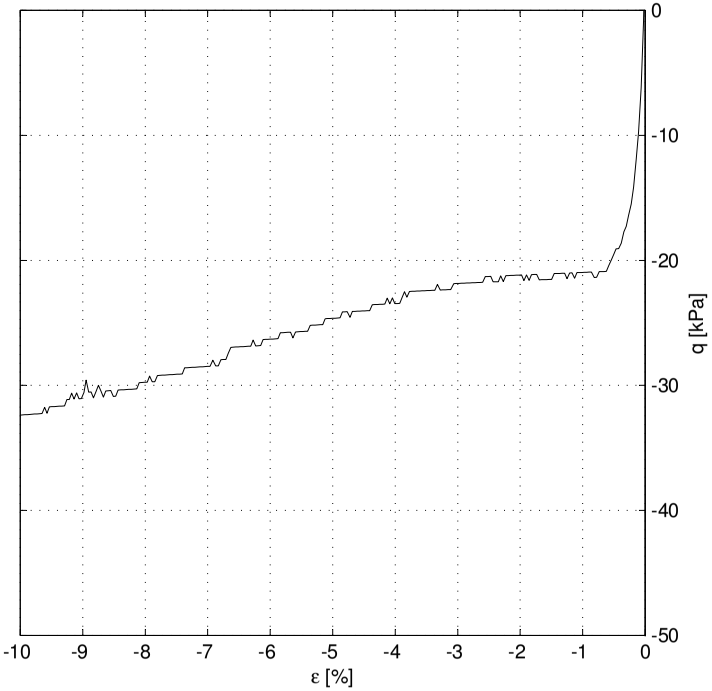

Sund, Rissa
Blokkprøve, CAUp104

Dybde: 3.96 m
Prøvetakingsdato og -utstyr: 30.11.11, Sherbrooke pøvetaker, 250 mm × 350 mm
Åpning av blokkprøven: 13.02.12
Forsøksdato: 26.02.12
Tøyningshastighet: -1.20 %/time (Utført med baktrykk av Multiconsult Trondheim)

$\sigma`_{vo}$ = 42.94kPa $\sigma`_c$ = 100 kPa
w = 26.59 % OCR = 2.28
γ = 19.4 kN/m^3

ΔV = 3.44 cm^3
ε_v = 1.48 %
$\Delta e/e_o$ = 0.02

s_u = 10.28 kPa
ε_f = 1.35 %
E_0 = 13.1 MPa

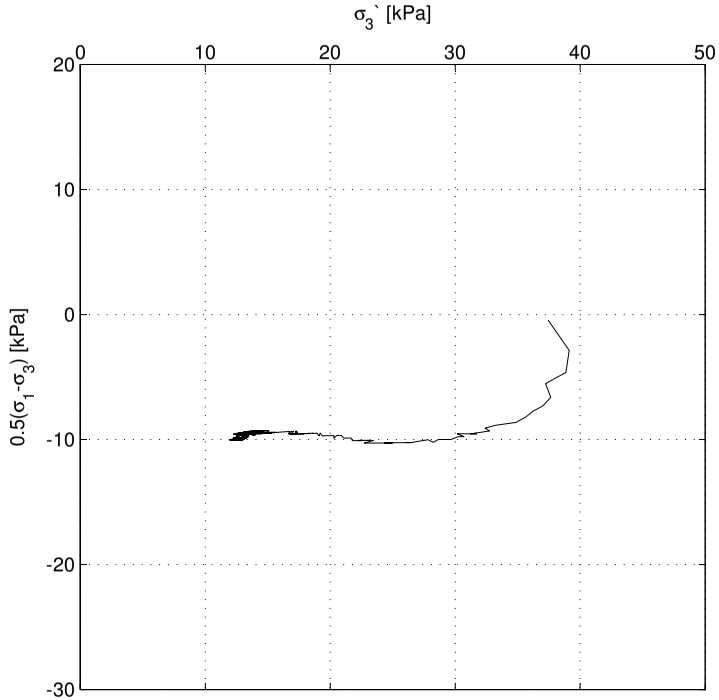

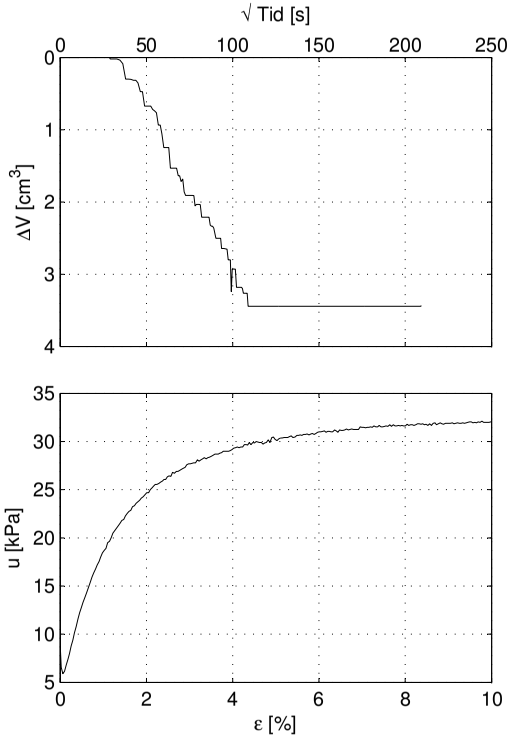

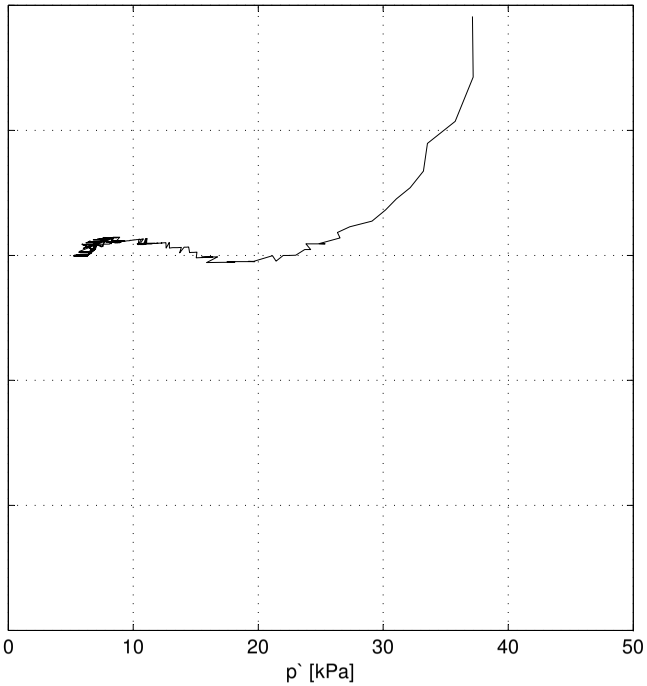

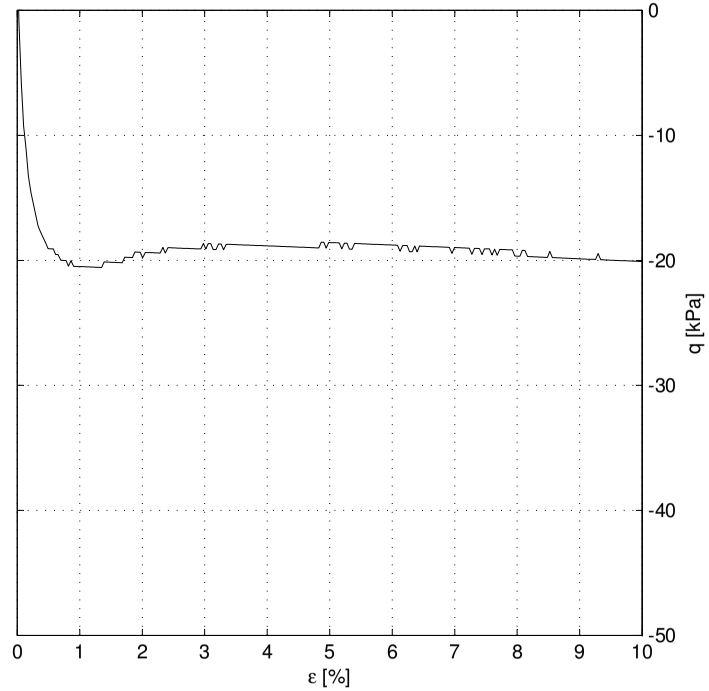

Sund, Rissa
Blokkprøve, CAUp105

Dybde: 3.75 m
Prøvetakingsdato og -utstyr: 30.11.11, Sherbrooke pøvetaker, 250 mm × 350 mm
Åpning av blokkprøven: 13.02.12
Forsøksdato: 28.02.12
Tøyningshastighet: -1.20 %/time (Utført med baktrykk av Multiconsult Trondheim)

$\sigma`_{vo}$ = 43.75kPa $\sigma`_c$ = 100 kPa
w = 32.46 % OCR = 2.26
γ = 19.2 kN/m^3

ΔV = 4.94 cm^3
ε_v = 2.13 %
$\Delta e/e_o$ = 0.04

s_u = 9.83 kPa
ε_f = 0.84 %
E_0 = 14.9 MPa

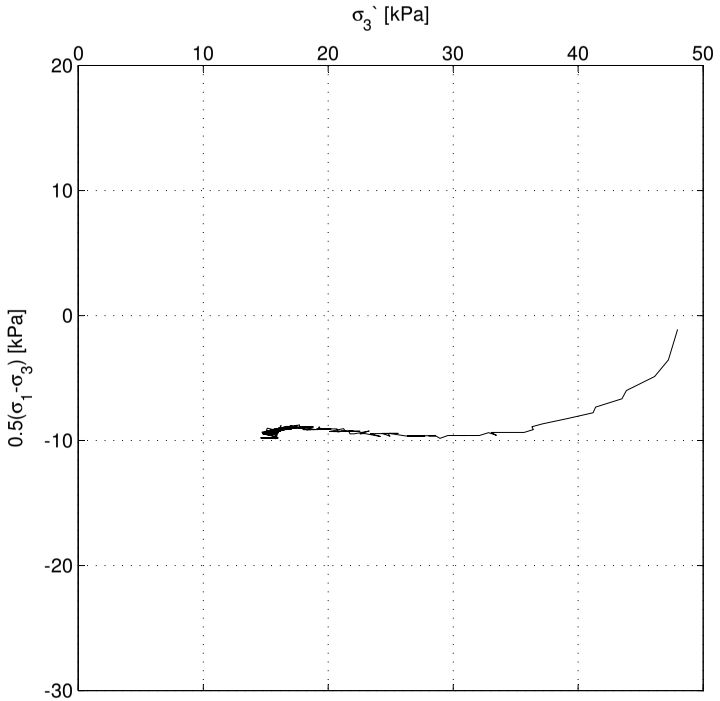

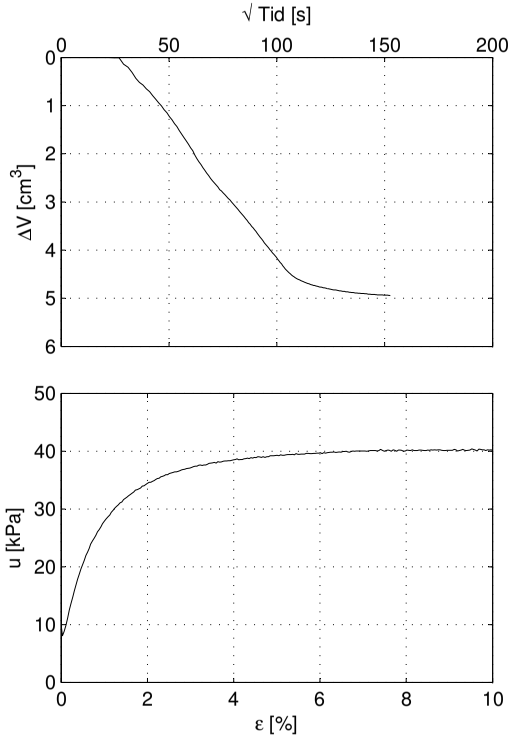

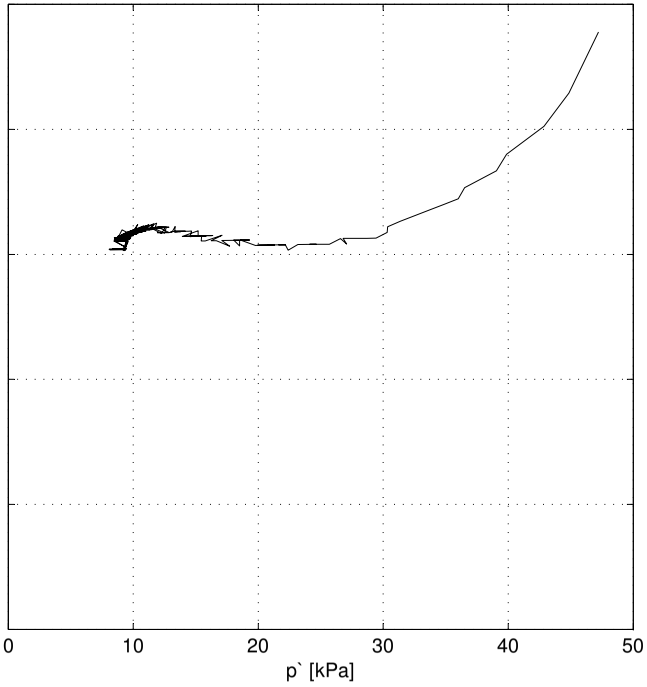

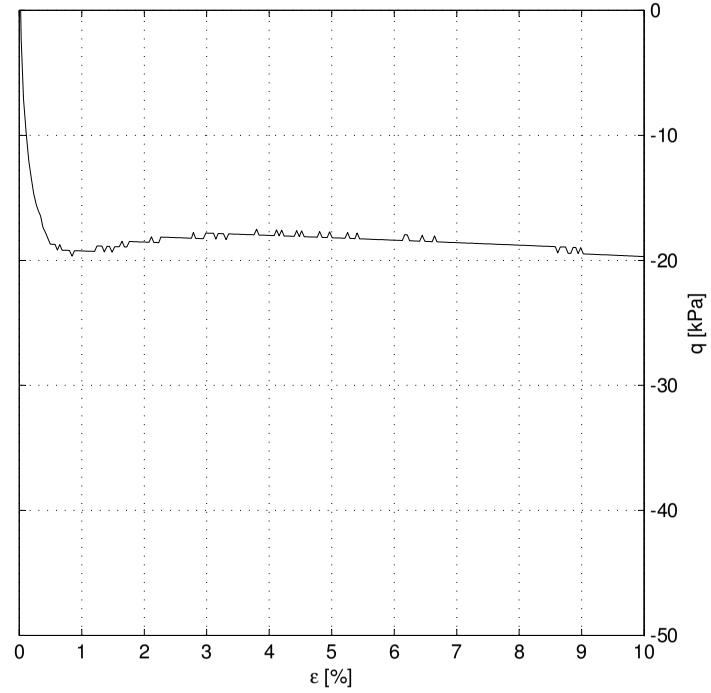

Sund, Rissa
Blokkprøve, CAUp106

Dybde: 4.37 m
Prøvetakingsdato og -utstyr: 30.11.11, Sherbrooke pøvetaker, 250 mm × 350 mm
Åpning av blokkprøven: 12.03.12
Forsøksdato: 26.02.12
Tøyningshastighet: -2.40 %/time (Utført med baktrykk av Multiconsult Trondheim)

$\sigma`_{vo}$ = 49.33kPa $\sigma`_c$ = 100 kPa
w = 37.11 % OCR = 2.14
γ = 19.0 kN/m^3

ΔV = 4.36 cm^3
ε_v = 1.88 %
$\Delta e/e_o$ = 0.03

s_u = 11.22 kPa
ε_f = 9.32 %
E_0 = 5.3 MPa

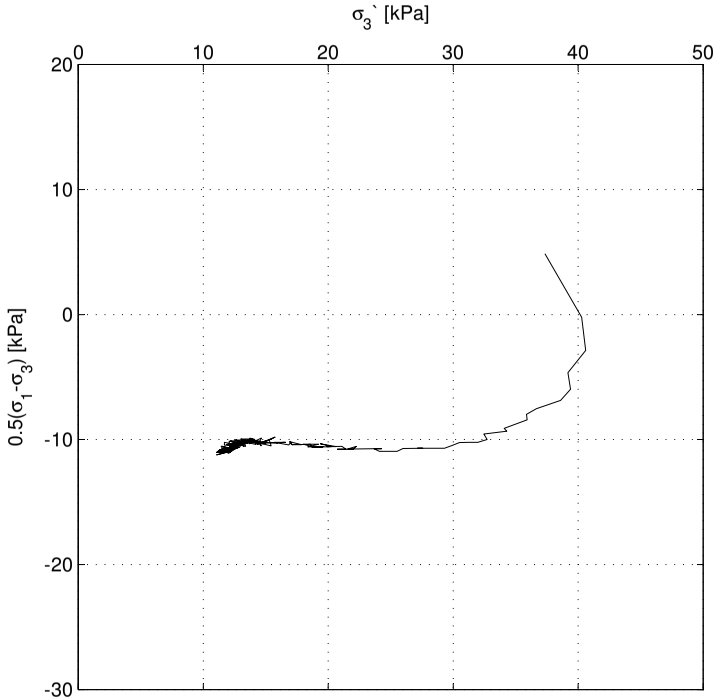

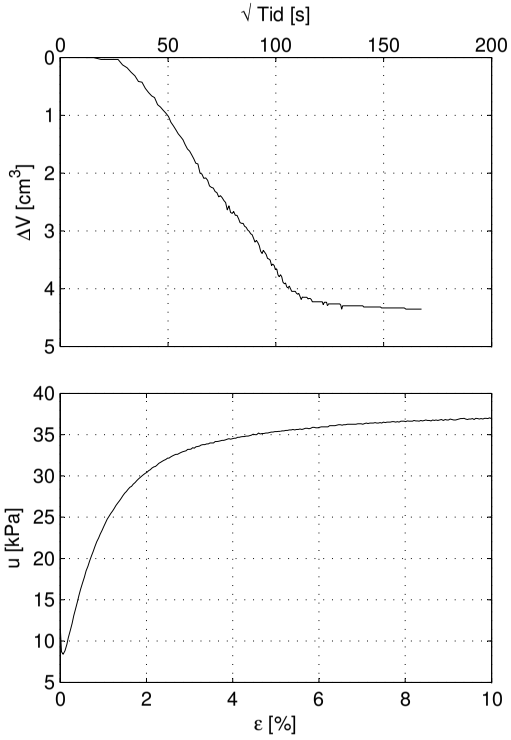

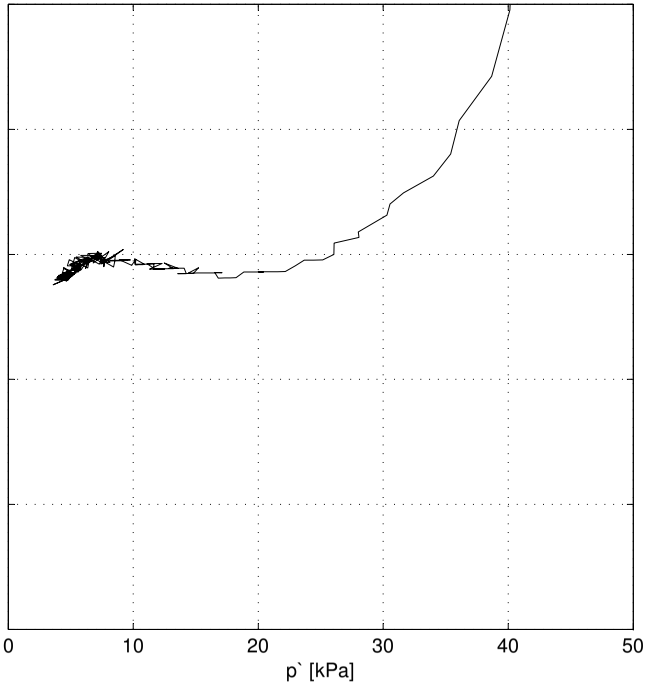

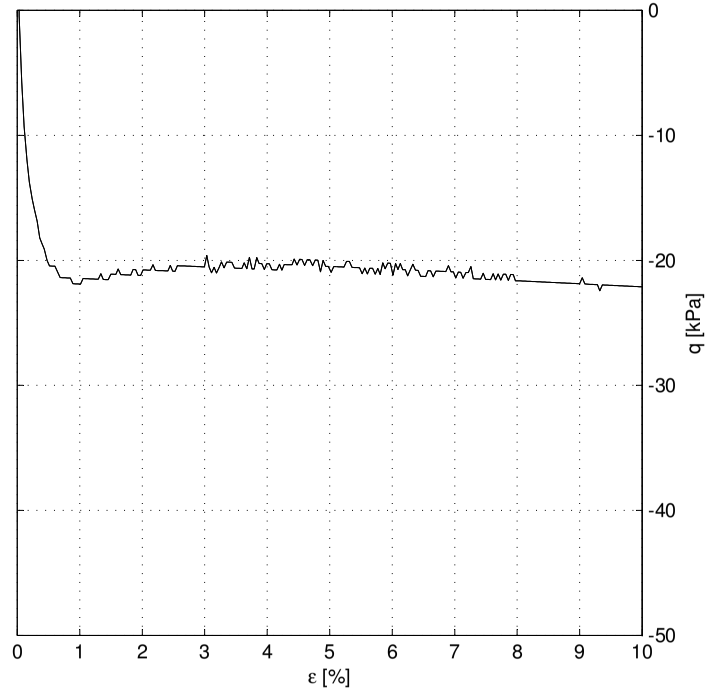

Sund,Rissa
Blokkprøver, dybde 3.50-4.59m

Prøvetakingsdato og -utstyr: 30.11.11, Sherbrooke pøvetaker, 250 mm × 350 mm
Åpningsdato: 19.01.11 - 3.85m, 13.02.12 - 3.50m, 12.03.12 - 4.20m

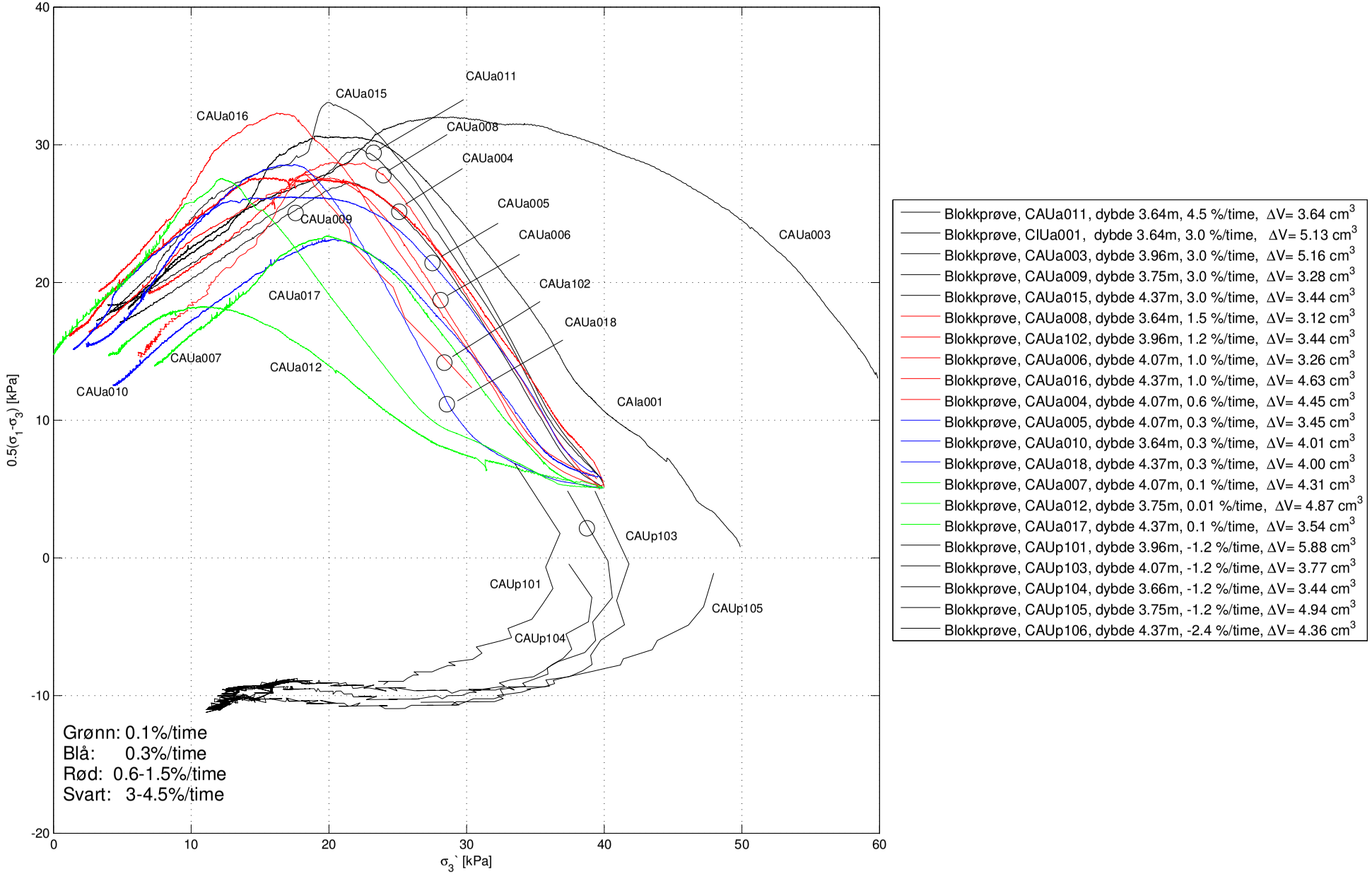

- Blokkprøve, CAUa011, dybde 3.64m, 4.5 %/time, ΔV= 3.64 cm^3
- Blokkprøve, CIUa001, dybde 3.64m, 3.0 %/time, ΔV= 5.13 cm^3
- Blokkprøve, CAUa003, dybde 3.96m, 3.0 %/time, ΔV= 5.16 cm^3
- Blokkprøve, CAUa009, dybde 3.75m, 3.0 %/time, ΔV= 3.28 cm^3
- Blokkprøve, CAUa015, dybde 4.37m, 3.0 %/time, ΔV= 3.44 cm^3
- Blokkprøve, CAUa008, dybde 3.64m, 1.5 %/time, ΔV= 3.12 cm^3
- Blokkprøve, CAUa102, dybde 3.96m, 1.2 %/time, ΔV= 3.44 cm^3
- Blokkprøve, CAUa006, dybde 4.07m, 1.0 %/time, ΔV= 3.26 cm^3
- Blokkprøve, CAUa016, dybde 4.37m, 1.0 %/time, ΔV= 4.63 cm^3
- Blokkprøve, CAUa004, dybde 4.07m, 0.6 %/time, ΔV= 4.45 cm^3
- Blokkprøve, CAUa005, dybde 4.07m, 0.3 %/time, ΔV= 3.45 cm^3
- Blokkprøve, CAUa010, dybde 3.64m, 0.3 %/time, ΔV= 4.01 cm^3
- Blokkprøve, CAUa018, dybde 4.37m, 0.3 %/time, ΔV= 4.00 cm^3
- Blokkprøve, CAUa007, dybde 4.07m, 0.1 %/time, ΔV= 4.31 cm^3
- Blokkprøve, CAUa012, dybde 3.75m, 0.01 %/time, ΔV= 4.87 cm^3
- Blokkprøve, CAUa017, dybde 4.37m, 0.1 %/time, ΔV= 3.54 cm^3
- Blokkprøve, CAUp101, dybde 3.96m, -1.2 %/time, ΔV= 5.88 cm^3
- Blokkprøve, CAUp103, dybde 4.07m, -1.2 %/time, ΔV= 3.77 cm^3
- Blokkprøve, CAUp104, dybde 3.66m, -1.2 %/time, ΔV= 3.44 cm^3
- Blokkprøve, CAUp105, dybde 3.75m, -1.2 %/time, ΔV= 4.94 cm^3
- Blokkprøve, CAUp106, dybde 4.37m, -2.4 %/time, ΔV= 4.36 cm^3

Sund,Rissa
Blokkprøver, dybde 3.50-4.59m

Prøvetakingsdato og -utstyr: 30.11.11, Sherbrooke pøvetaker, 250 mm × 350 mm
Åpningsdato: 19.01.11 - 3.85m, 13.02.12 - 3.50m, 12.03.12 - 4.20m

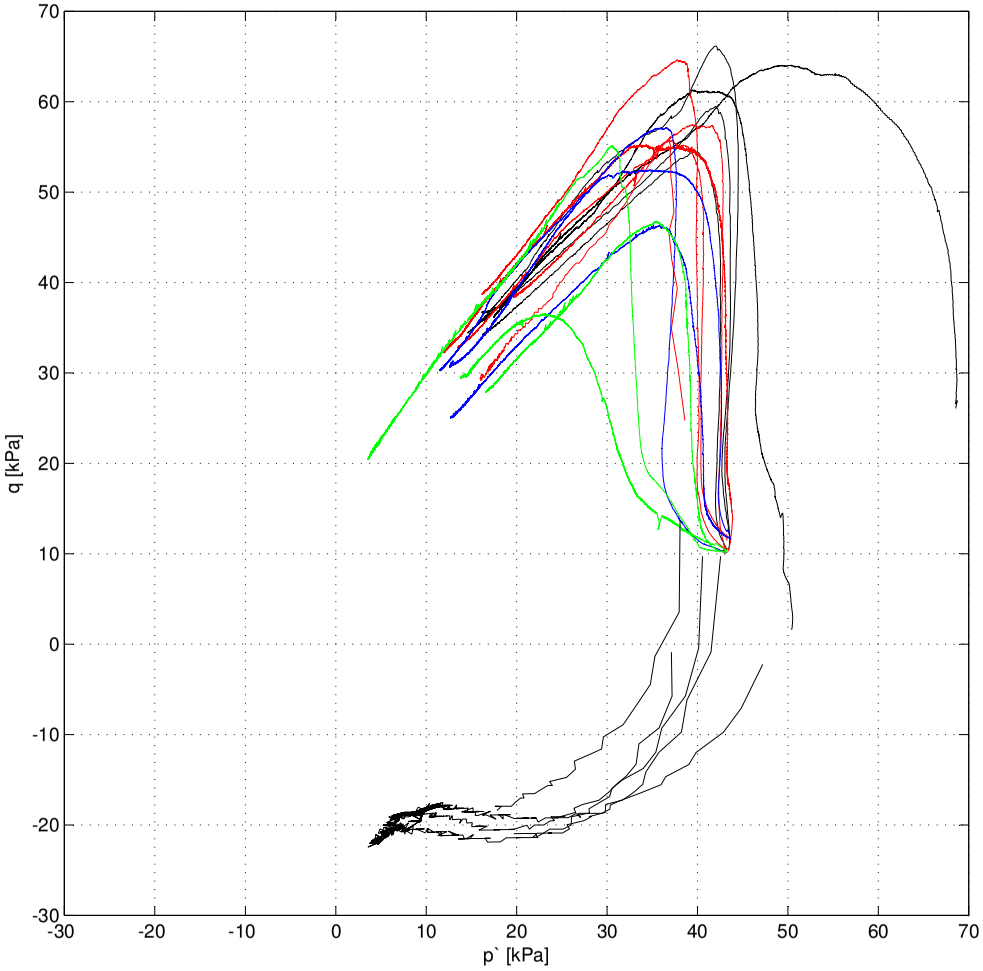

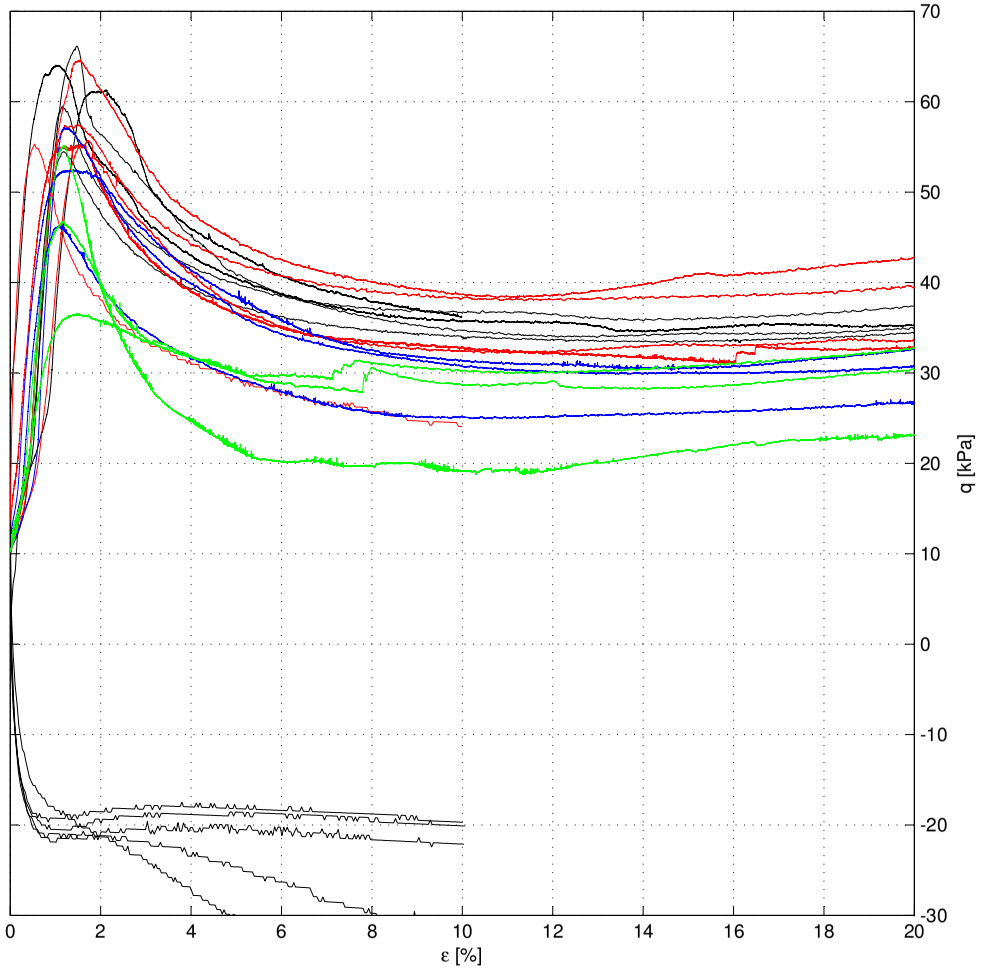

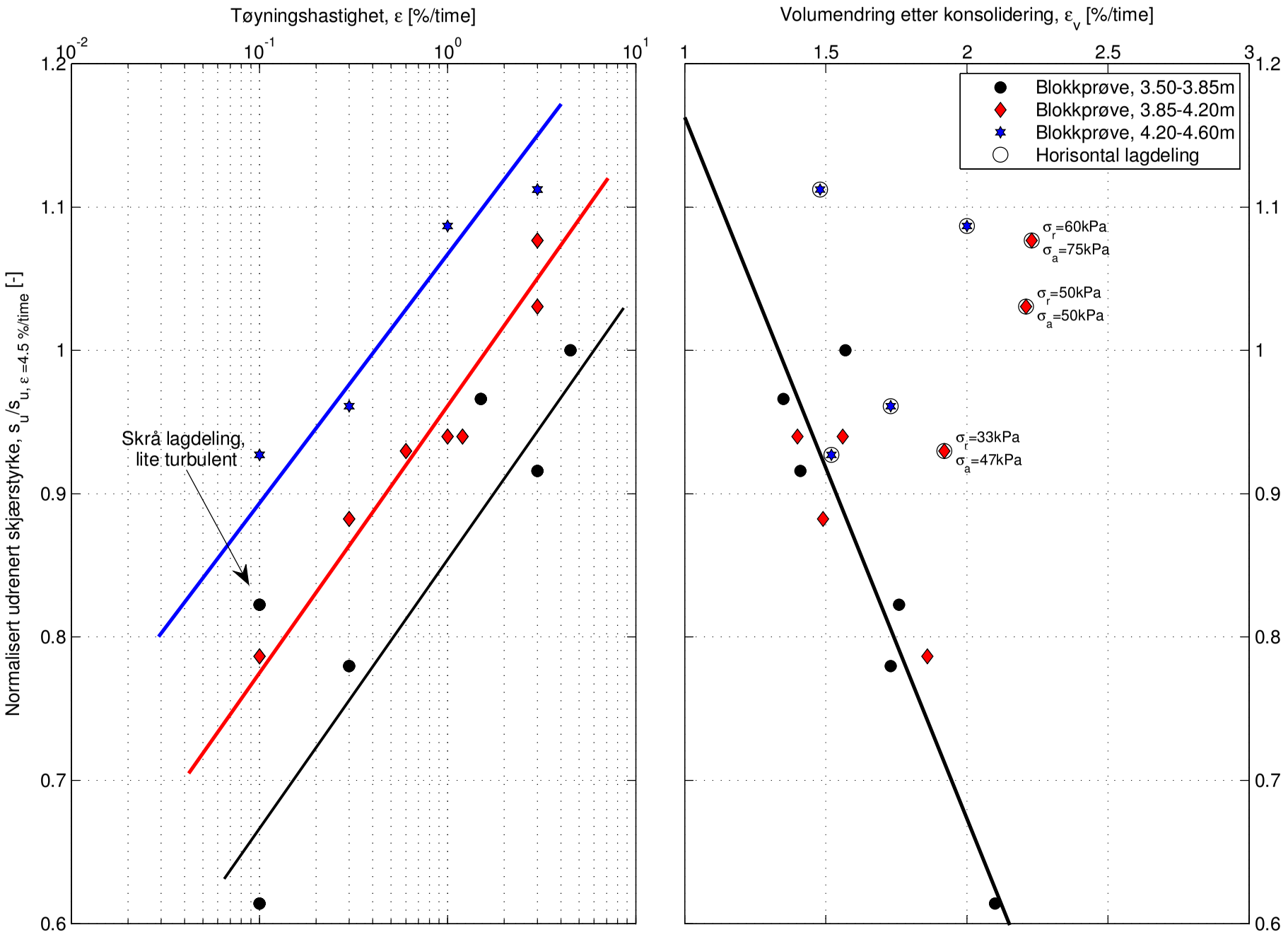
Tøyningshastighet, ε [%/time]
Volumendring etter konsolidering, ε_v [%/time]
Normalisert udrenert skjærstyrke, $s_u/s_{u,\ \varepsilon=4.5\ \%/time}$ [-]
Skrå lagdeling, lite turbulent
Blokkprøve, 3.50-3.85m
Blokkprøve, 3.85-4.20m
Blokkprøve, 4.20-4.60m
Horisontal lagdeling
σ_r=60kPa
σ_a=75kPa
σ_r=50kPa
σ_a=50kPa
σ_r=33kPa
σ_a=47kPa

Sund,Rissa
54 mm sylinderprøver, C3 og C6, dybde 3.0-23.0m og 2.0-18.0m

Prøvetakingsdato: 05.10.11
Åpningsdato: 25.11.11 - 05.01.12

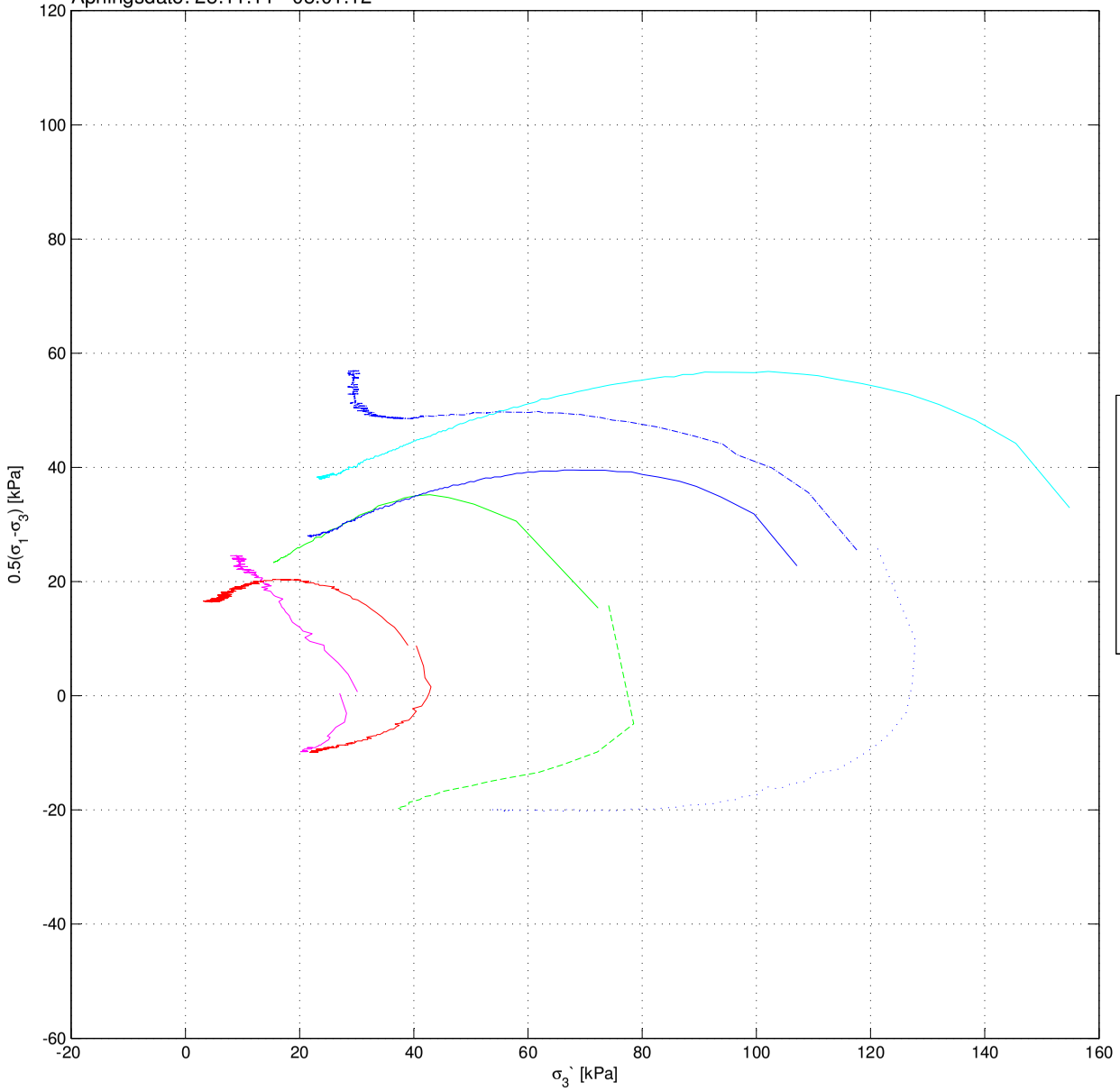

- 54 mm, C6, CAUa, dybde 3.30m, 1.2%/time, ΔV=3.4cm^3
- 54 mm, C6, CAUp, dybde 3.4m, -1.2%/time, ΔV=2.3cm^3
- 54 mm, C3, CAUa, dybde 5.4m, 0.5%/time, ΔV=8.2cm^3
- 54 mm, C3, CAUp, dybde 5.6m, -0.5%/time, ΔV=10,0cm^3
- 54 mm, C3, CAUa, dybde 10.4m, 5.0%/time, ΔV=7.0cm^3
- 54 mm, C3, CAUp, dybde 10.6m, -5.0%/time, ΔV=8.5cm^3
- 54 mm, C3, CAUa, dybde 15.15m, 1.2%/time, ΔV=14.2cm^3
- 54 mm, C6, CAUa, dybde 17.4m, 1.2%/time, ΔV=14.1cm^3
- 54 mm, C6, CAUp, dybde 17.7m, -1.2%/time, ΔV=12.2cm^3
- 54 mm, C3, CAUa, dybde 22.2m, 1.2%/time, ΔV=13.9cm^3

Sund,Rissa
54 mm sylinderprøver, C3 og C6, dybde 3.0-23.0m og 2.0-18.0m

Prøvetakingsdato: 05.10.11
Åpningsdato: 25.11.11 - 05.01.12

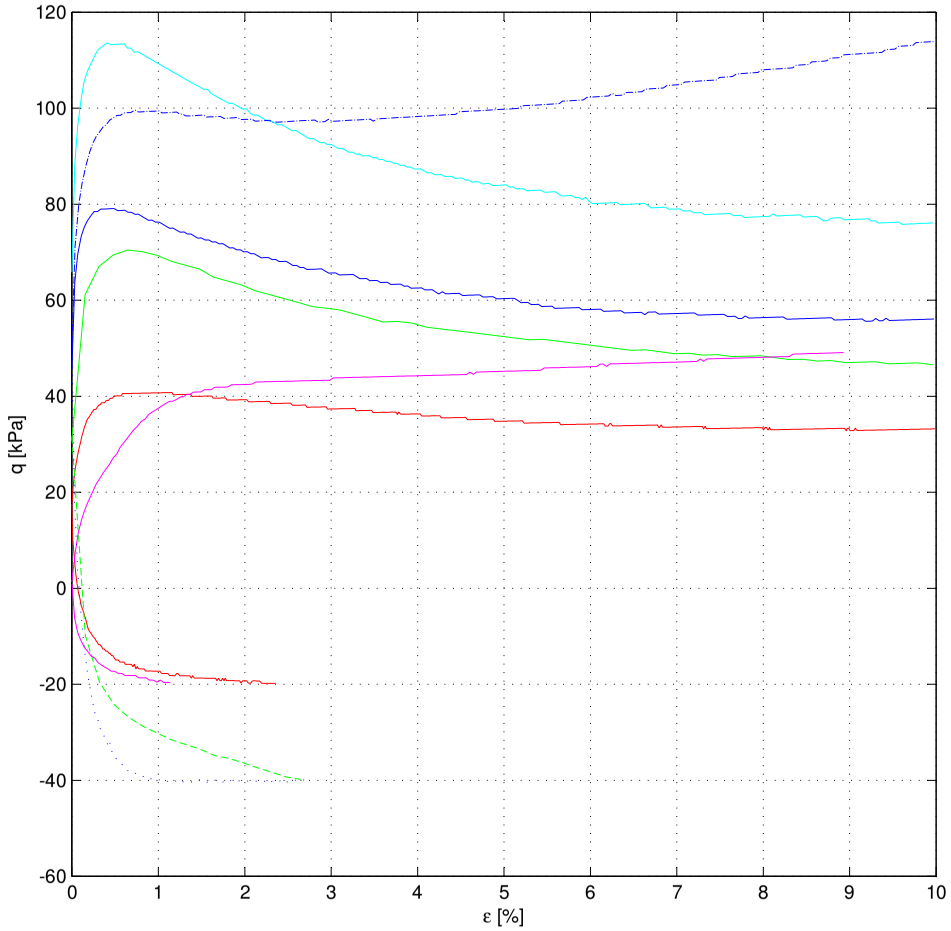

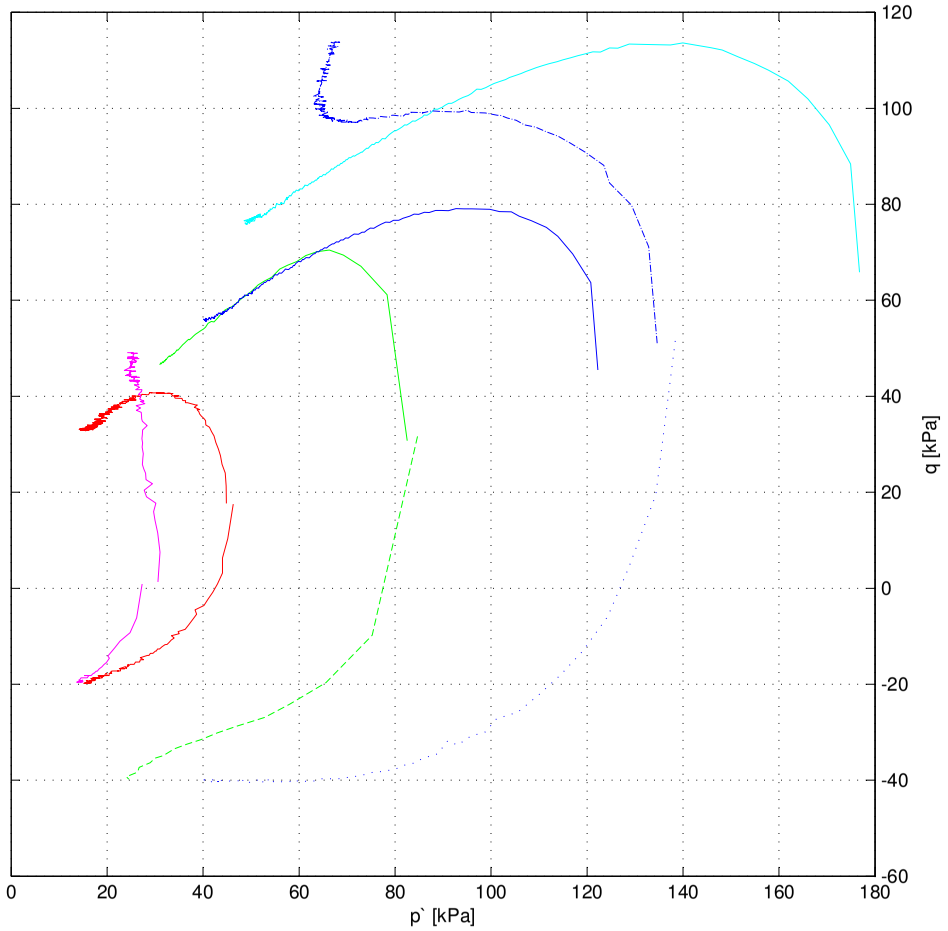

Sund,Rissa
54 mm sylinderprøver, C3 og C6, dybde 3.0-23.0m og 2.0-18.0m

Prøvetakingsdato: 05.10.11
Åpningsdato: 25.11.11 - 05.01.12

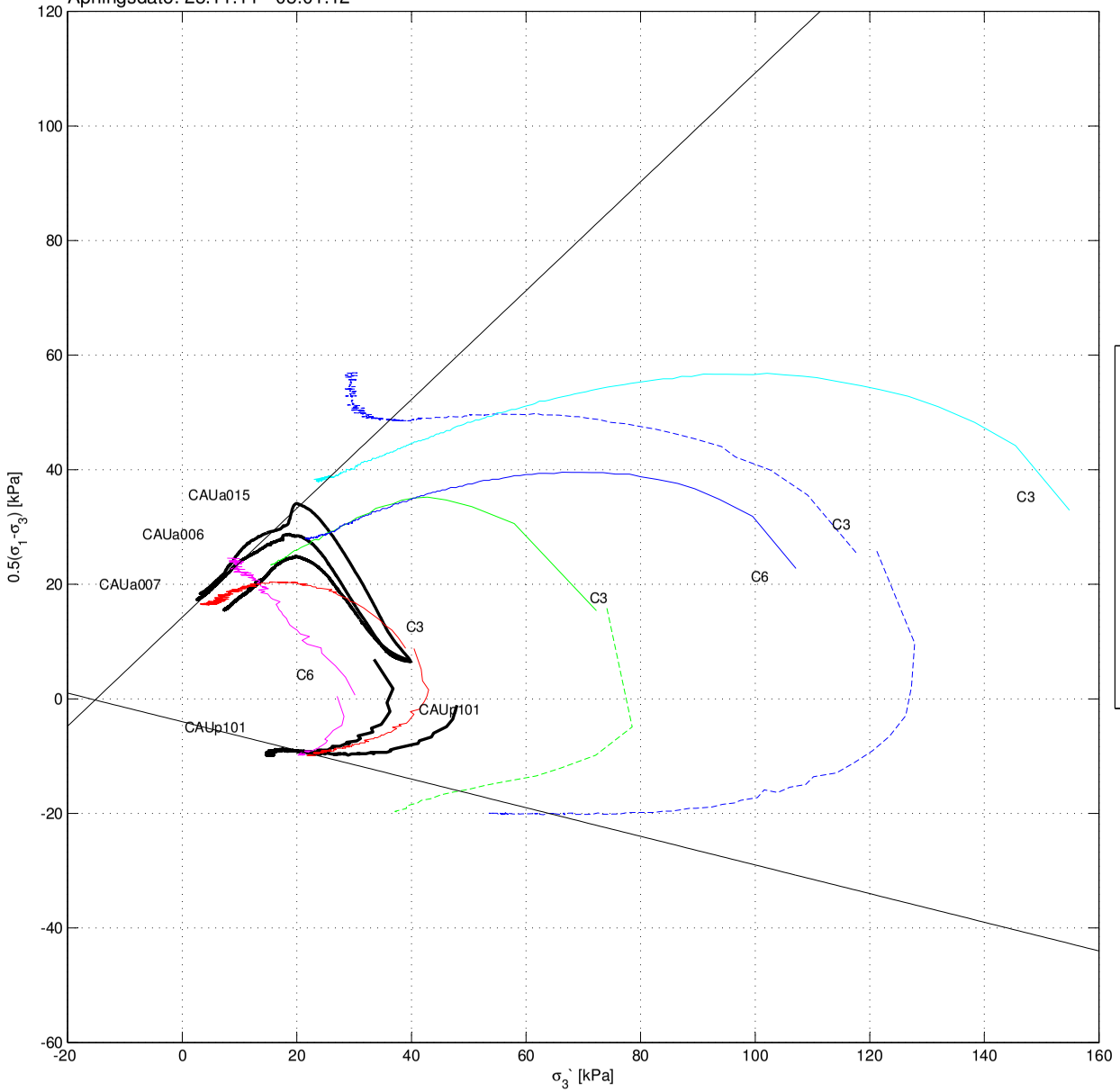

tan ϕ = 0.56
ϕ = 29.2 °
a = 15 kPa

- Blokkprøve, CAUa015, dybde 4.37m, 3.0 %/time, ΔV= 3.44 cm^3
- Blokkprøve, CAUa006, dybde 4.07m, 1.0 %/time, ΔV= 3.26 cm^3
- Blokkprøve, CAUa007, dybde 4.07m, 0.1 %/time, ΔV= 4.31 cm^3
- Blokkprøve, CAUp101, dybde 3.96m, -1.2 %/time, ΔV= 5.88 cm^3
- Blokkprøve, CAUp105, dybde 3.75m, -1.2 %/time, ΔV= 4.94 cm^3
- 54 mm, C6, CAUa, dybde 3.30m, 1.2%/time, ΔV=3.4cm^3
- 54 mm, C6, CAUp, dybde 3.4m, -1.2%/time, ΔV=2.3cm^3
- 54 mm, C3, CAUa, dybde 5.4m, 0.5%/time, ΔV=8.2cm^3
- 54 mm, C3, CAUp, dybde 5.6m, -0.5%/time, ΔV=10,0cm^3
- 54 mm, C3, CAUa, dybde 10.4m, 5.0%/time, ΔV=7.0cm^3
- 54 mm, C3, CAUp, dybde 10.6m, -5.0%/time, ΔV=8.5cm^3
- 54 mm, C3, CAUa, dybde 15.15m, 1.2%/time, ΔV=14.2cm^3
- 54 mm, C6, CAUa, dybde 17.4m, 1.2%/time, ΔV=14.1cm^3
- 54 mm, C6, CAUp, dybde 17.7m, -1.2%/time, ΔV=12.2cm^3
- 54 mm, C3, CAUa, dybde 22.2m, 1.2%/time, ΔV=13.9cm^3

Appendix 4 Triaxial Tests

This is taken directly from Helene Kornbrekke's master's thesis

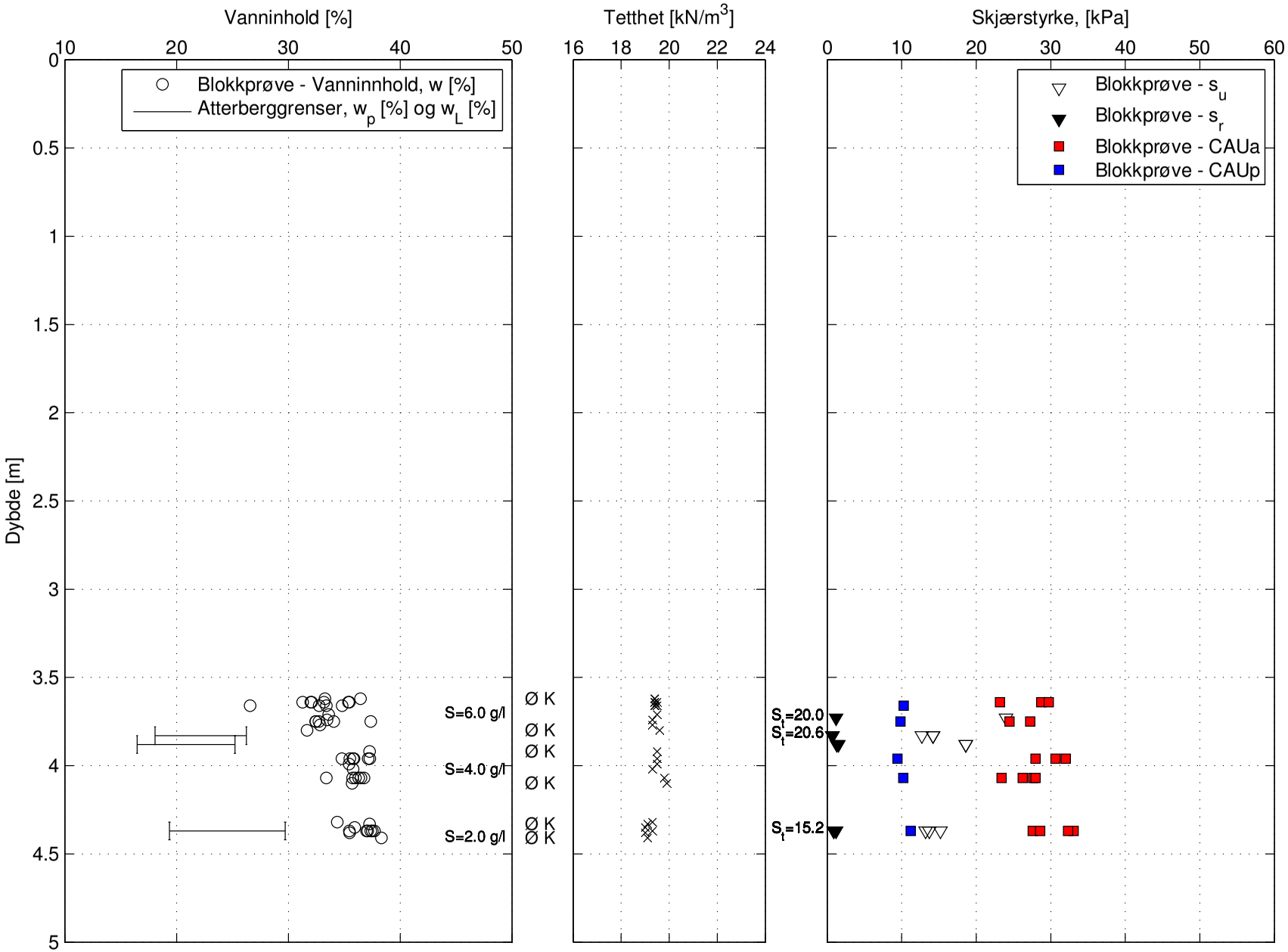

Borpunkt C3/C6

Prøvetype: 250 mm

Kote: +2.2m
GV: ~1.0m
Koordinater:

K - Korngraderingsanalyse
S - Saltinnhold [g/l]
S_t - Sensitivitet
Ø - Ødometer forsøk

Utført av: NTNU (H. A. Kornbrekke), 2012

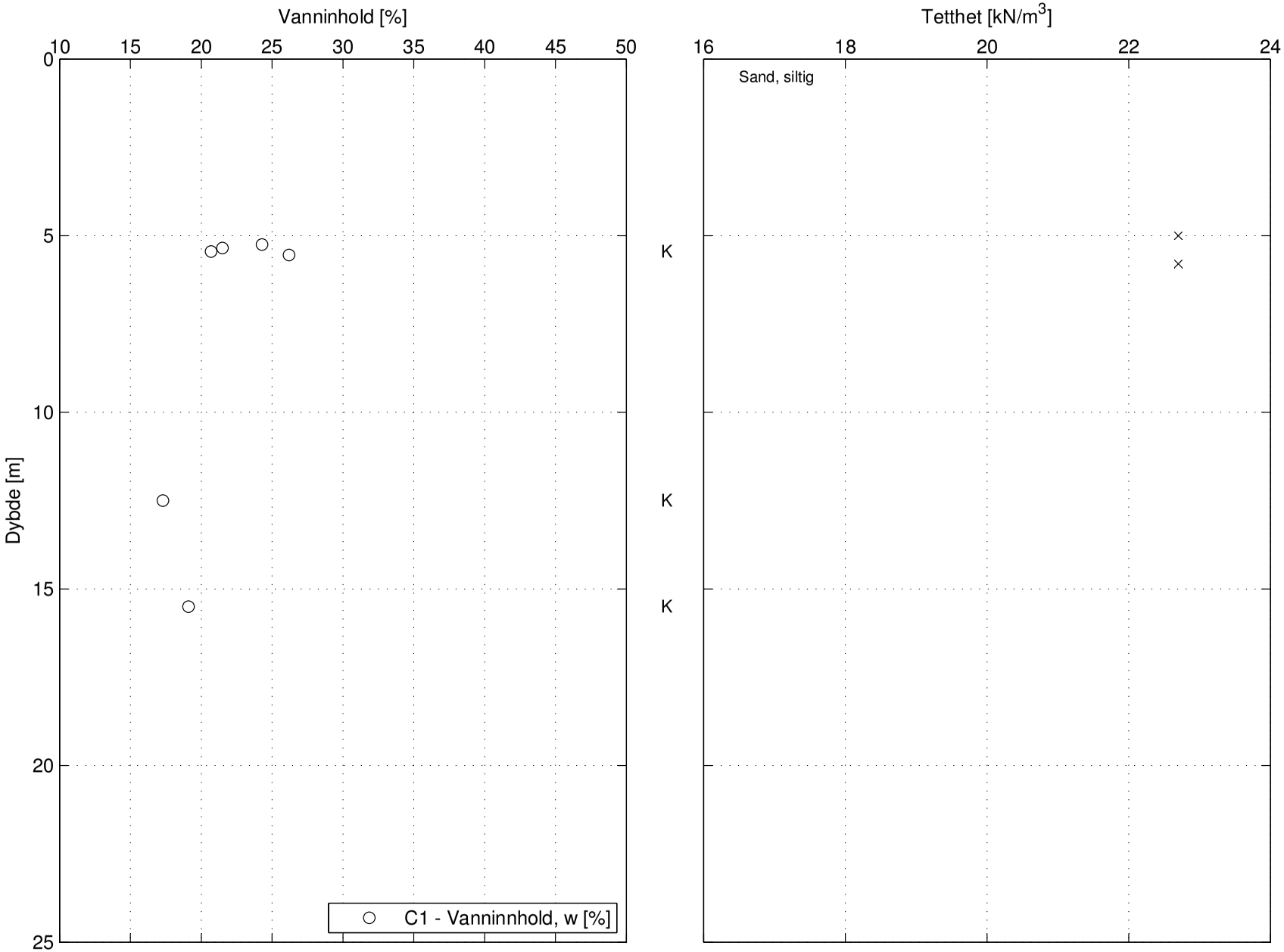

Borpunkt C1

Prøvetype: 54 mm

Kote: +25.14m
GV: ~3.3 m
Koordinater: Ø546115.00 N7048853.01

Utført av: Geo-Vest Haugland, 2011

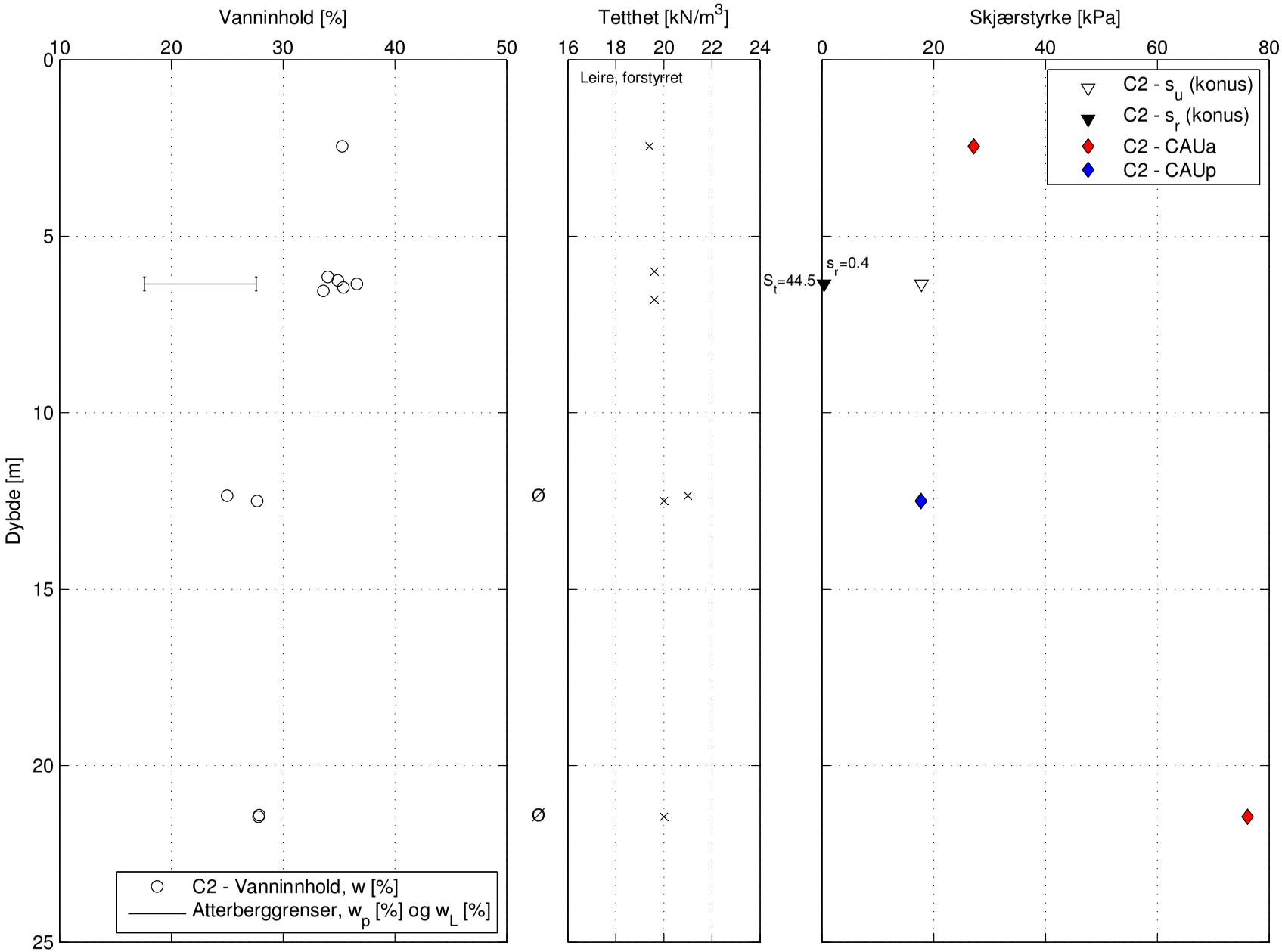

Borpunkt C2

Prøvetype: 54 mm

Kote: +9.1m
GV: ~2.0m
Koordinater: Ø546186.99 N7048828.00

K - Korngraderingsanalyse
S_t - Sensitivitet
Ø - Ødometer forsøk

Utført av: Geo-Vest Haugland, 2011

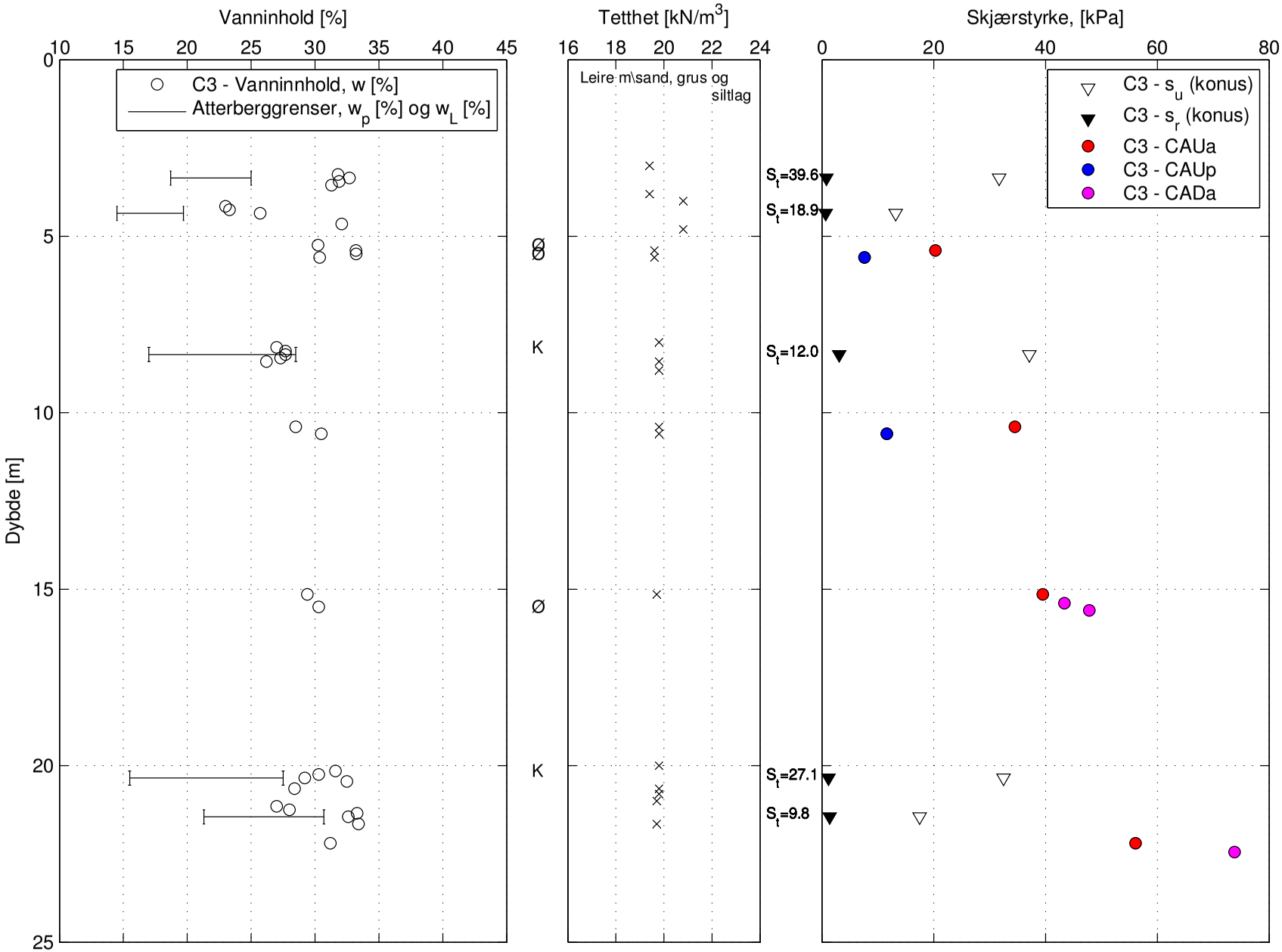

Borpunkt C3

Prøvetype: 54 mm

Kote: +2.17m
GV: ~1.0m
Koordinater: Ø546238.43 N7048812.01

K - Korngraderingsanalyse
S_t - Sensitivitet
Ø - Ødometer forsøk

Utført av: Geo-Vest Haugland, 2011

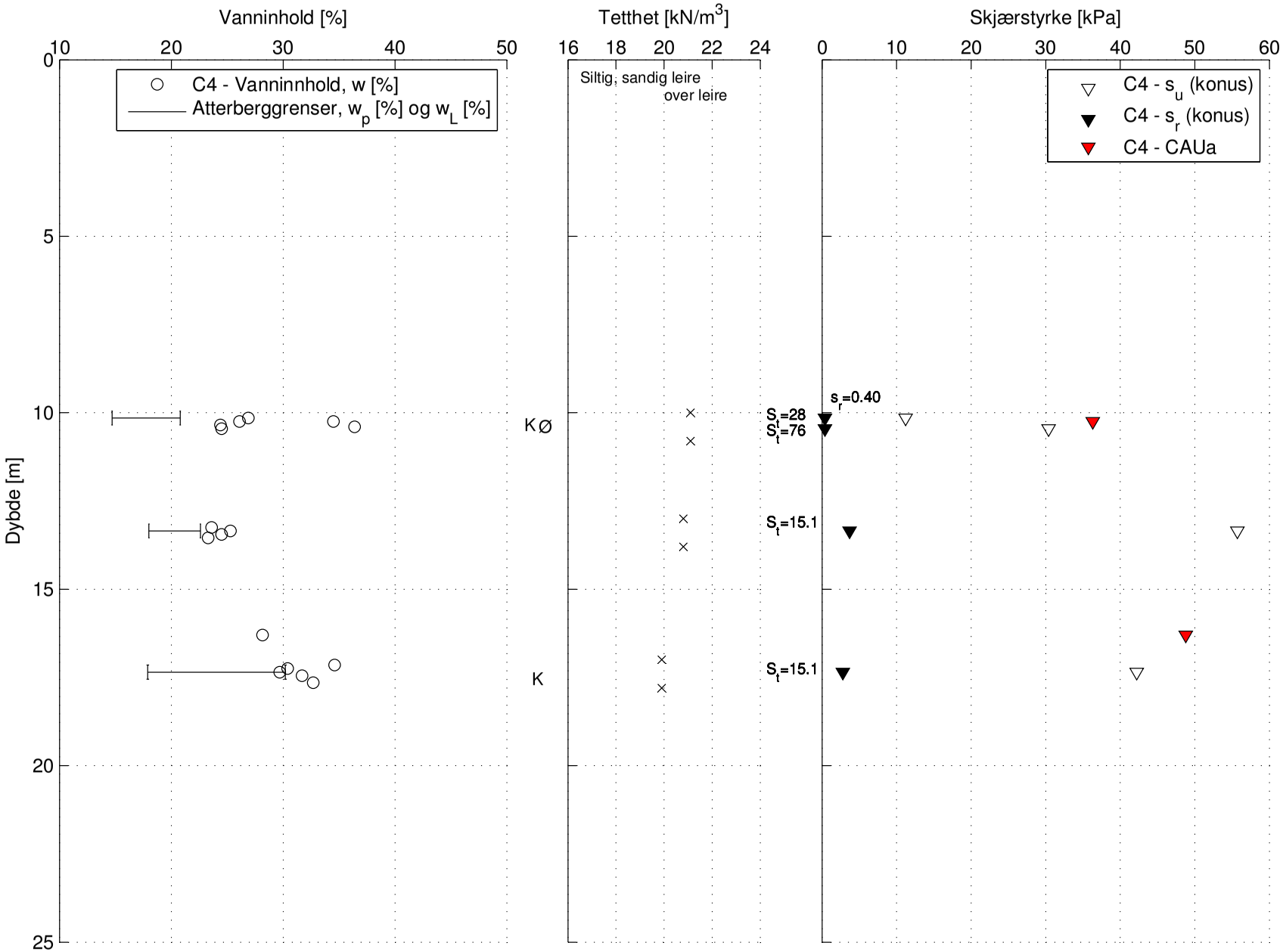

Borhull C4

Prøvetype: 54 mm

Kote: +21.9m
GV: ~2.0m
Koordinater: Ø546084.06 N7048775.07

K - Korngraderingsanalyse
S_t - Sensitivitet
Ø - Ødometer forsøk

Utført av: Geo-Vest Haugland, 2011

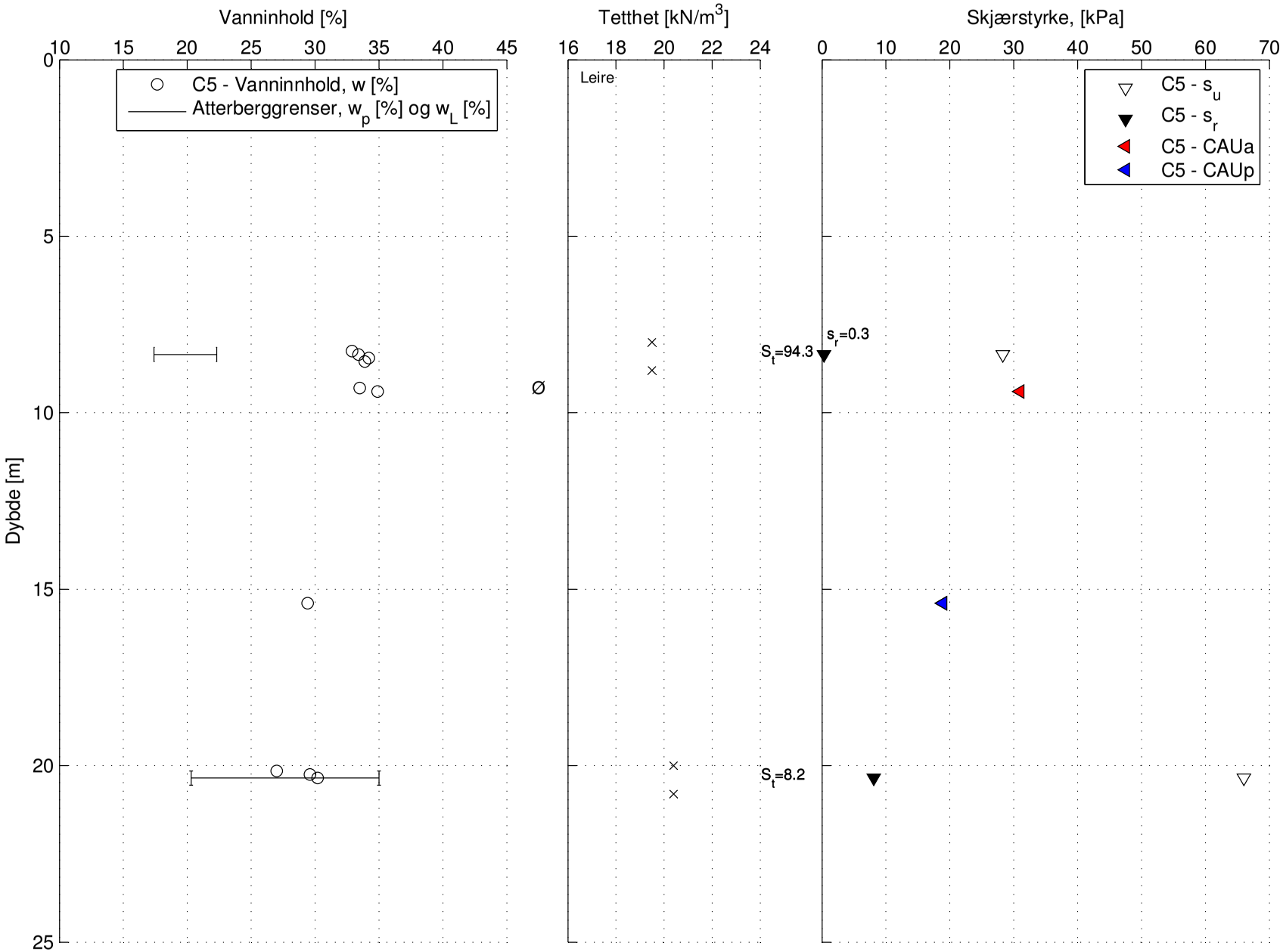

Borhull C5

Prøvetype: 54 mm

Kote: +12.7m
GV: ~1.0m
Koordinater: Ø546148.05 N7048747.57

K - Korngraderingsanalyse
S_t - Sensitivitet
Ø - Ødometer forsøk

Utført av: Geo-Vest Haugland, 2011

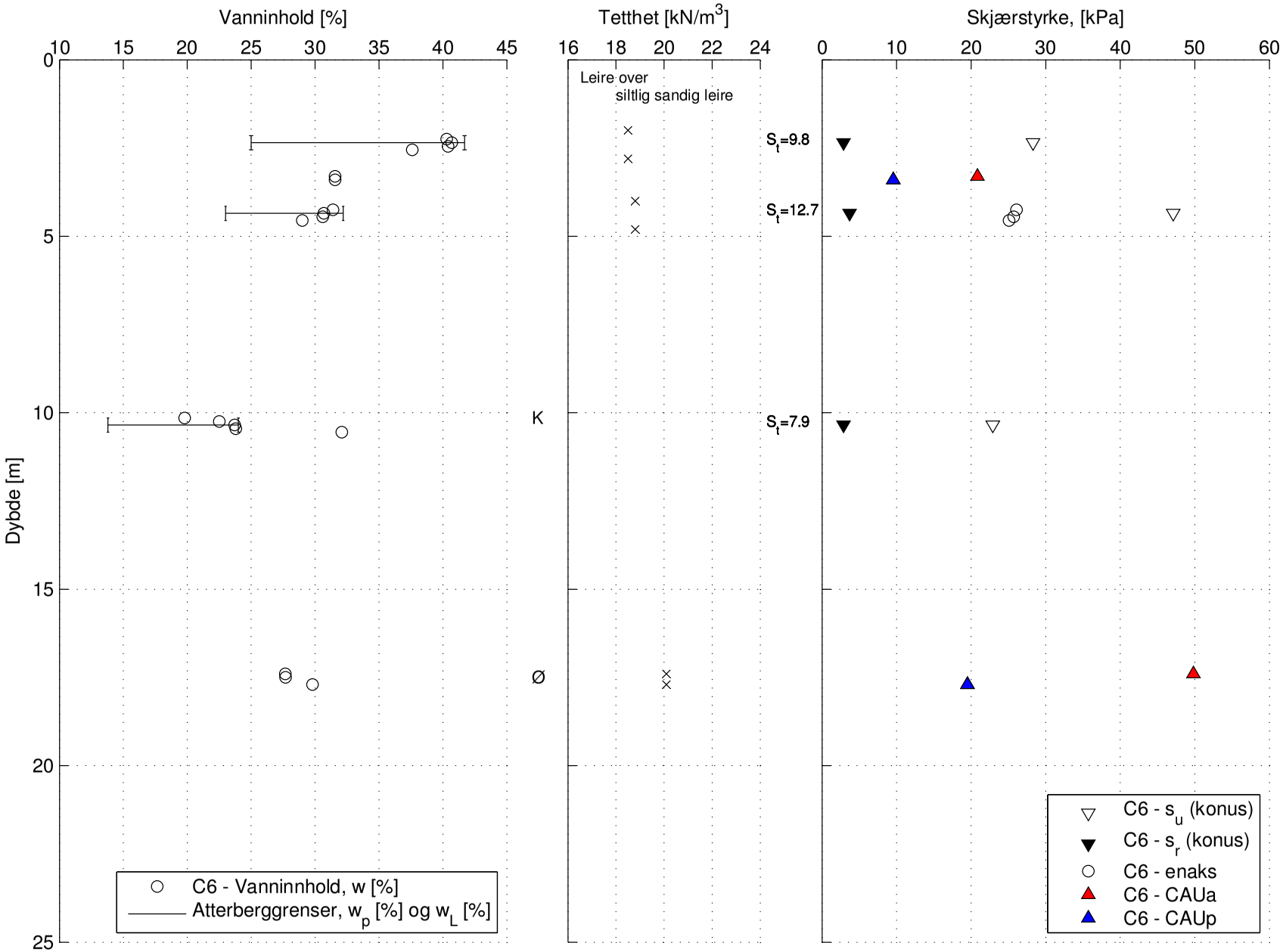

Borhull C6

Prøvetype: 54 mm

Kote: +1.89m
GV: ~1.0m
Koordinater: Ø546249.52 N7048688.79

K - Korngraderingsanalyse
S_t - Sensitivitet
Ø - Ødometer forsøk

Utført av: Geo-Vest Haugland, 2011

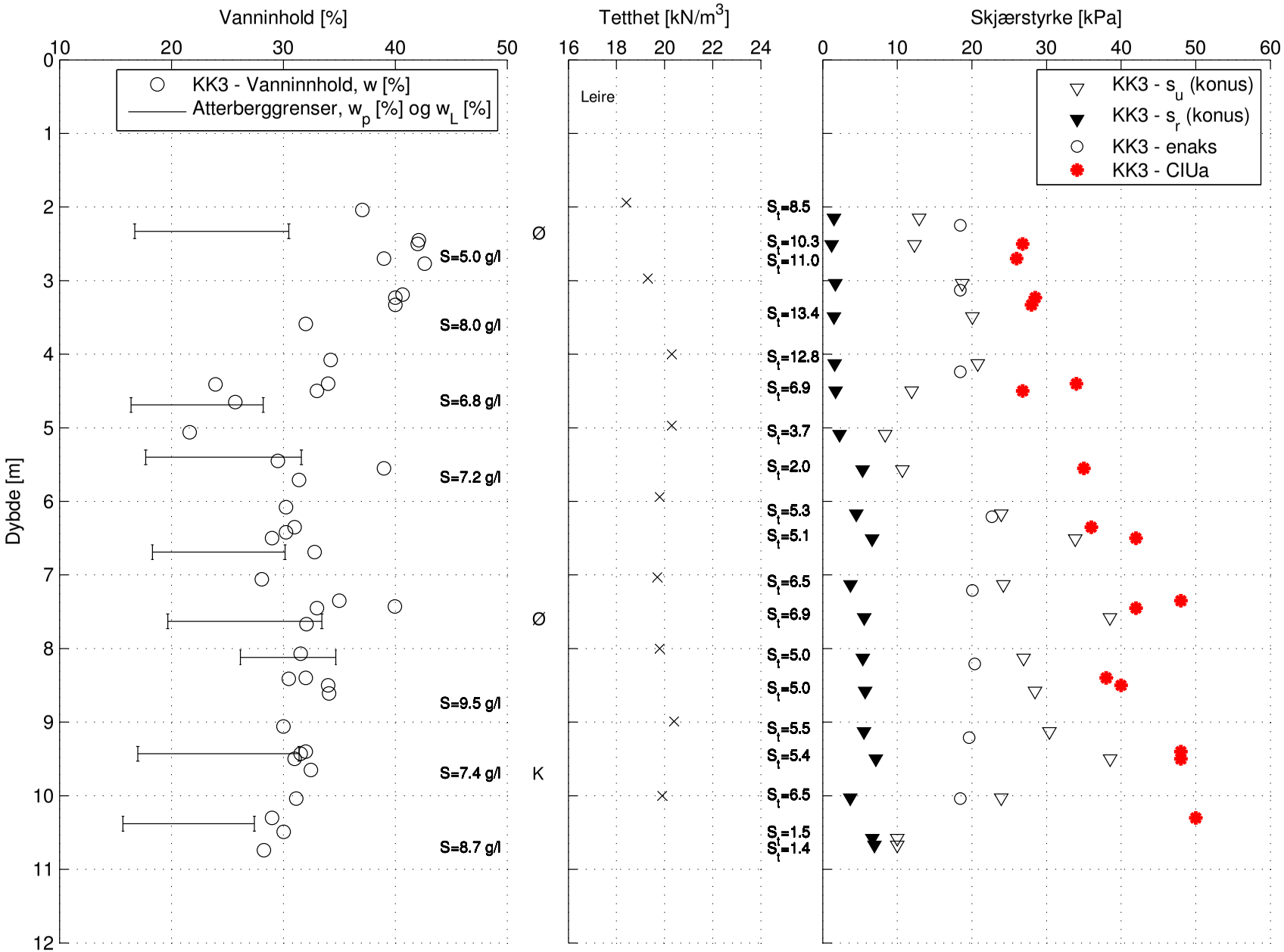

Borhull KK3

Prøvetype: 54 mm

Kote: +3.5m
GV: ~1.0m
Koordinater: Ø546191 N7048732

K - Korngraderingsanalyse
S - Saltinnhold [g/l]
S_t - Sensitivitet
Ø - Ødometer forsøk

Utført av: NTNU (K. Kåsin), 2010

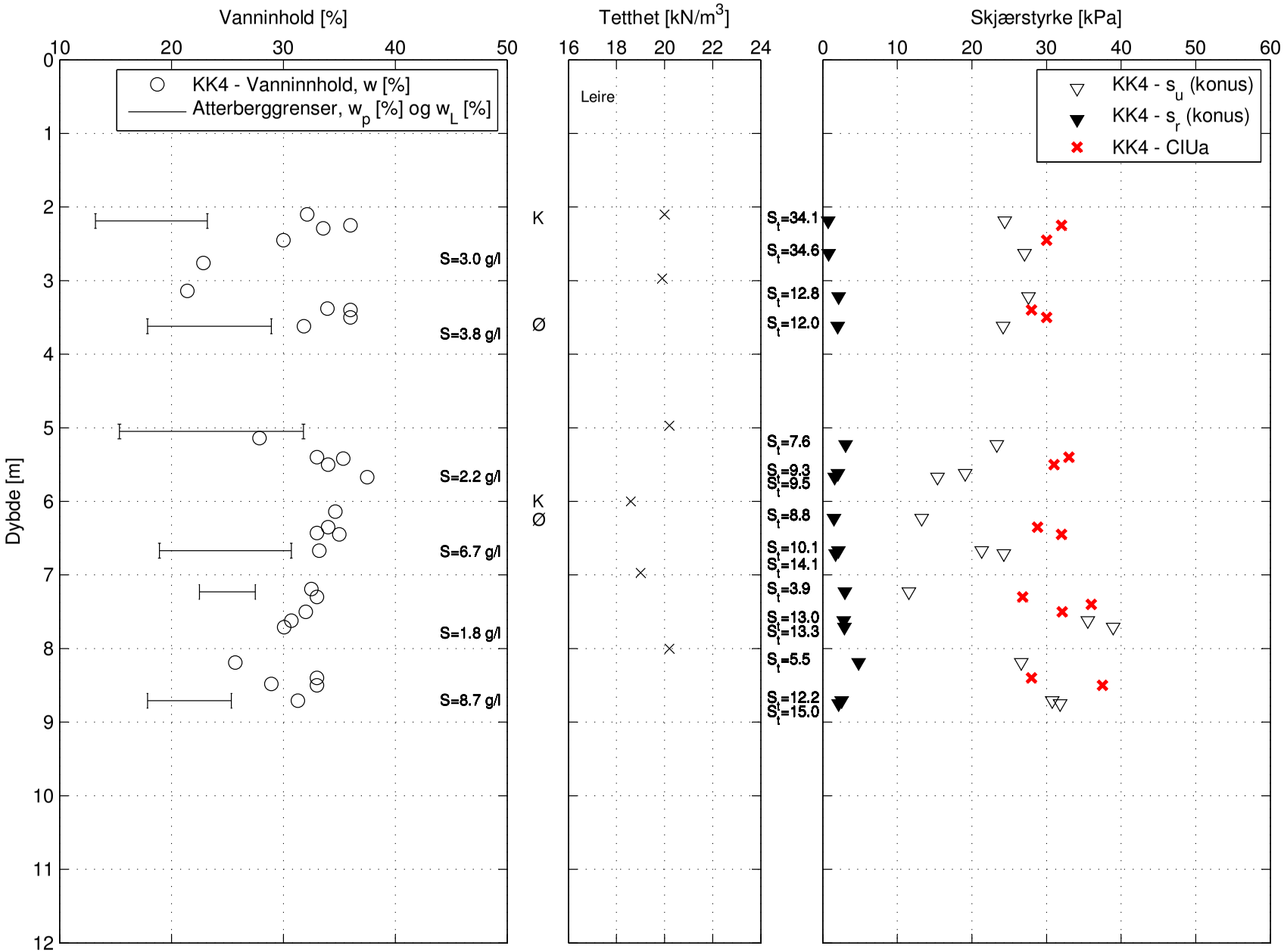

Borpunkt KK4

Prøvetype: 73 mm

Kote: +3.5m
GV: ~1m
Koordinater: Ø546213 N7048809

K - Korngraderingsanalyse
S - Saltinnhold [g/l]
S_t - Sensitivitet
Ø - Ødometer forsøk

Utført av: NTNU (K. Kåsin), 2010

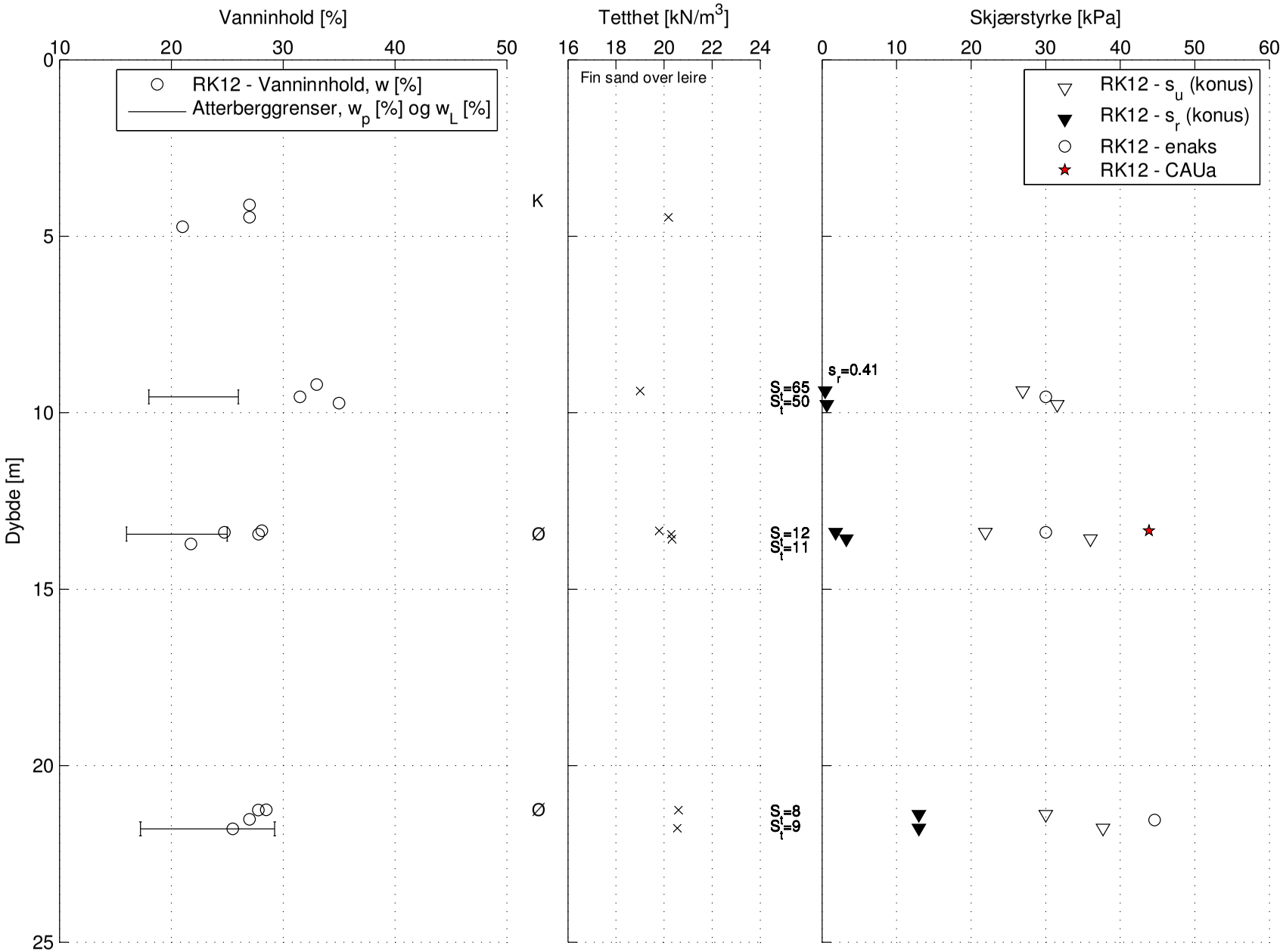

Borhull RK12

Prøvetype: 72 mm

Kote: +21.9m
GV: ~1.0m
Koordinater: Ø546084.24 N7048775.33

K - Korngraderingsanalyse
S_t - Sensitivitet
Ø - Ødometer forsøk

Utført av: NGI, 2009

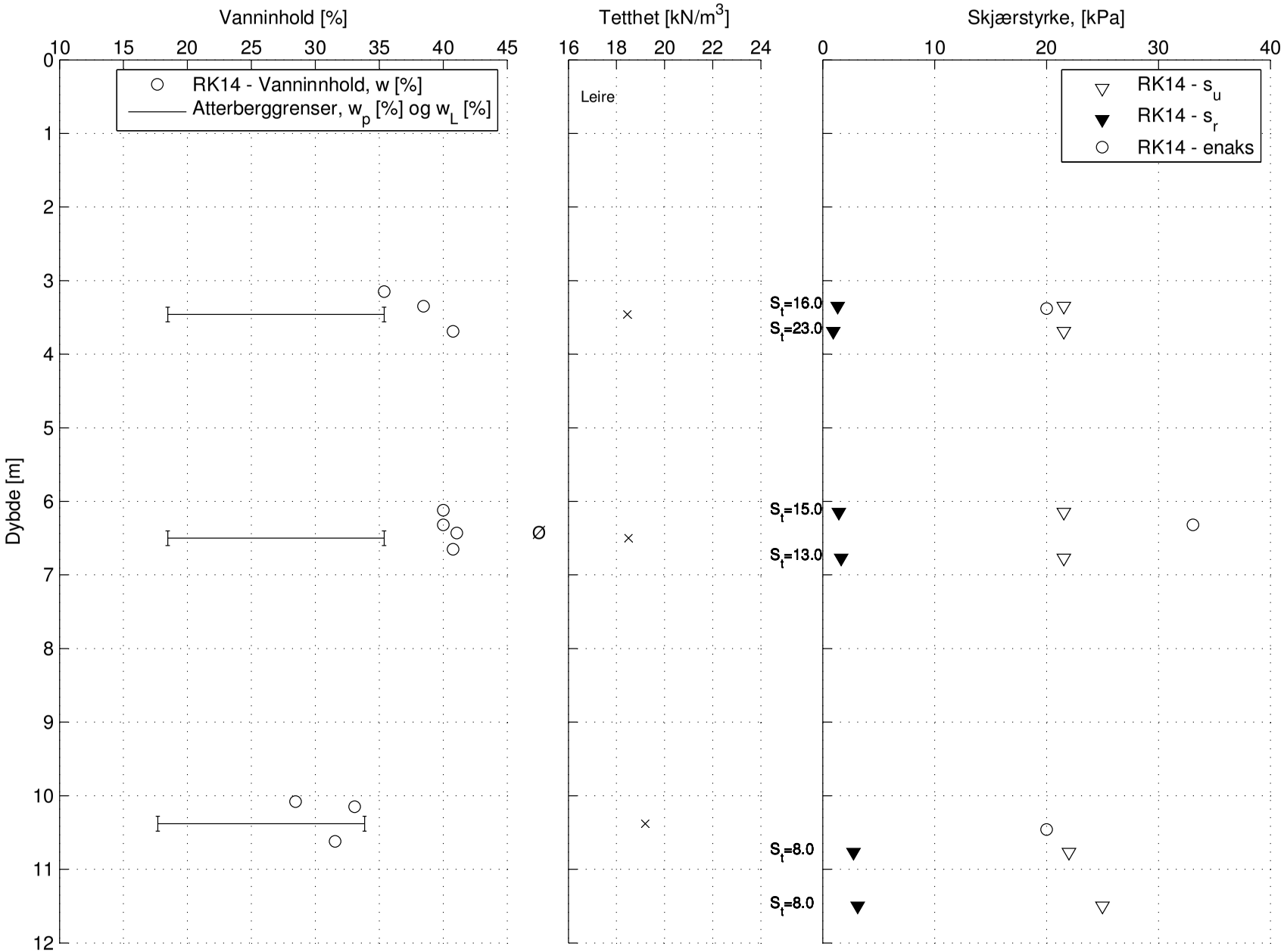

Borhull RK14

Prøvetype: 72 mm

Kote: +2.7m

GV: ~1.0m

Koordinater: Ø546216.00 N7048719.00

K - Korngraderingsanalyse

S_t - Sensitivitet

Ø - Ødometer forsøk

Utført av: NGI, 2009

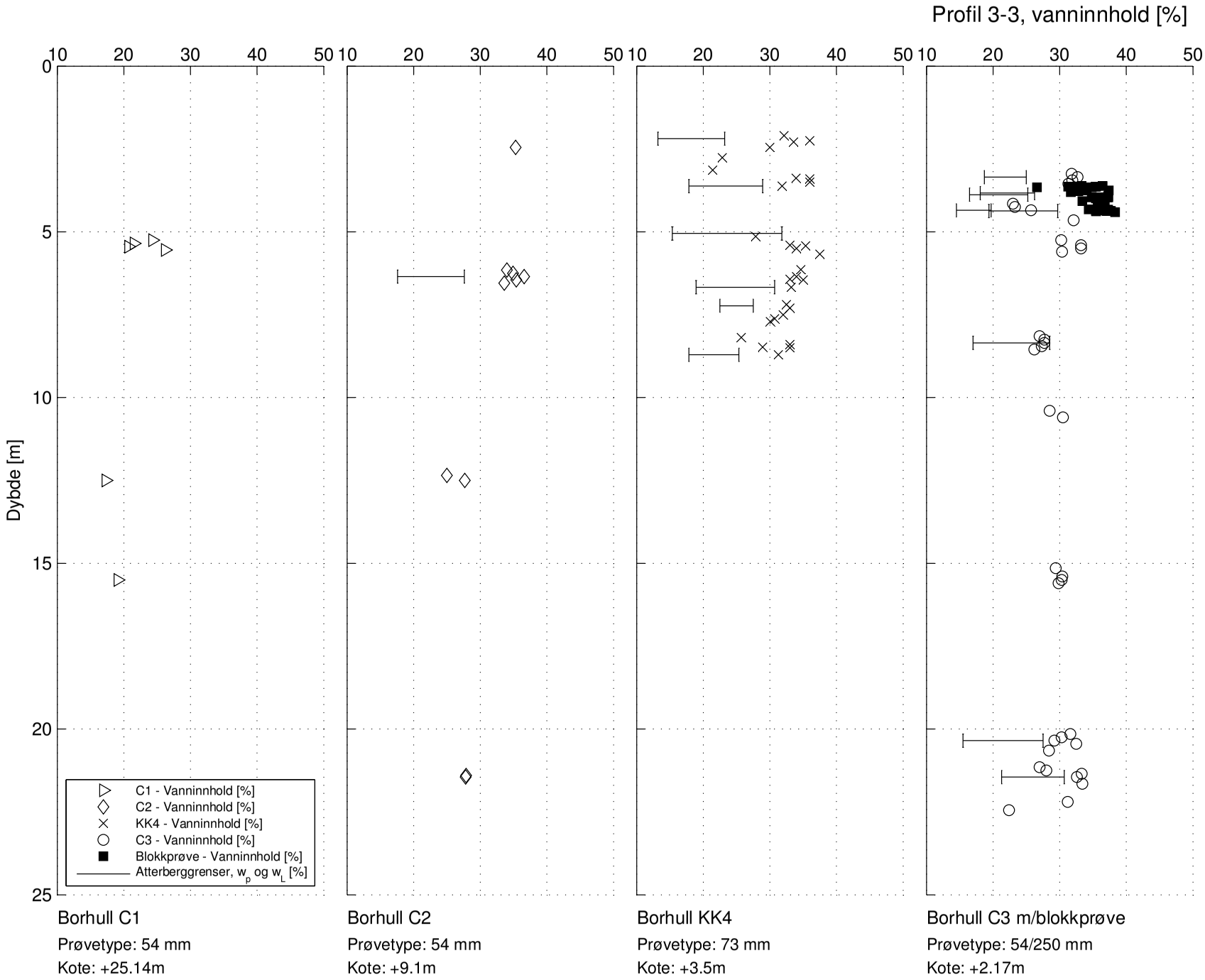
Profil 3-3, vanninnhold [%]
Dybde [m]
C1 - Vanninnhold [%]
C2 - Vanninnhold [%]
KK4 - Vanninnhold [%]
C3 - Vanninnhold [%]
Blokkprøve - Vanninnhold [%]
Atterberggrenser, w_p og w_L [%]
Borhull C1
Prøvetype: 54 mm
Kote: +25.14m
Borhull C2
Prøvetype: 54 mm
Kote: +9.1m
Borhull KK4
Prøvetype: 73 mm
Kote: +3.5m
Borhull C3 m/blokkprøve
Prøvetype: 54/250 mm
Kote: +2.17m

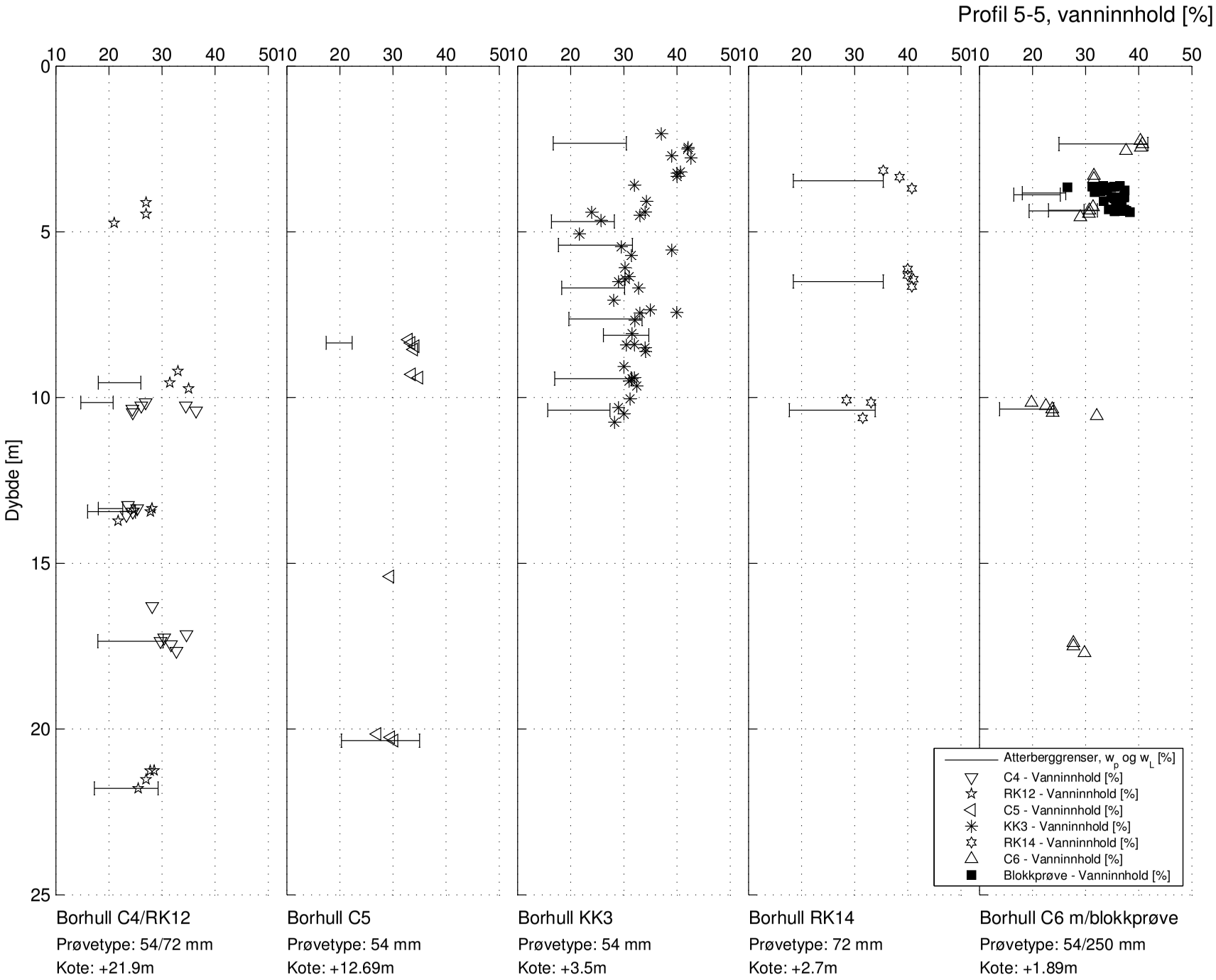
Profil 5-5, vanninnhold [%]
Dybde [m]
Atterberggrenser, w_p og w_L [%]
C4 - Vanninnhold [%]
RK12 - Vanninnhold [%]
C5 - Vanninnhold [%]
KK3 - Vanninnhold [%]
RK14 - Vanninnhold [%]
C6 - Vanninnhold [%]
Blokkprøve - Vanninnhold [%]
Borhull C4/RK12
Prøvetype: 54/72 mm
Kote: +21.9m
Borhull C5
Prøvetype: 54 mm
Kote: +12.69m
Borhull KK3
Prøvetype: 54 mm
Kote: +3.5m
Borhull RK14
Prøvetype: 72 mm
Kote: +2.7m
Borhull C6 m/blokkprøve
Prøvetype: 54/250 mm
Kote: +1.89m

Profil 3-3, skjærstyrke [kPa]

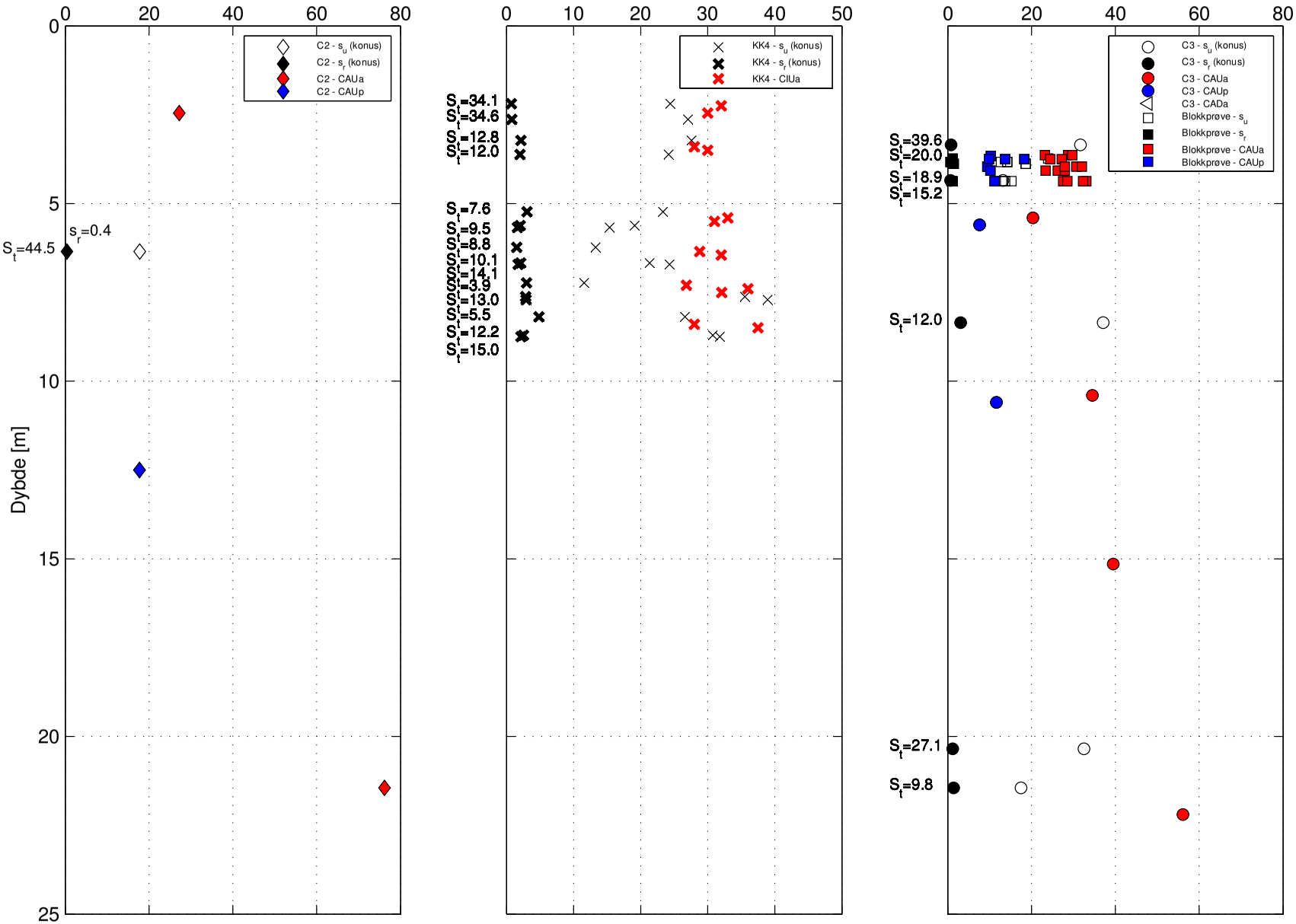

Borpunkt C2
Prøvetype: 54 mm
Kote: +9.1m

Borpunkt KK4
Prøvetype: 73 mm
Kote: +3.5m

Borpunkt C3 m/blokkprøve
Prøvetype: 54/250 mm
Kote: +2.17m

Profil 5-5, skjærstyrke [kPa]

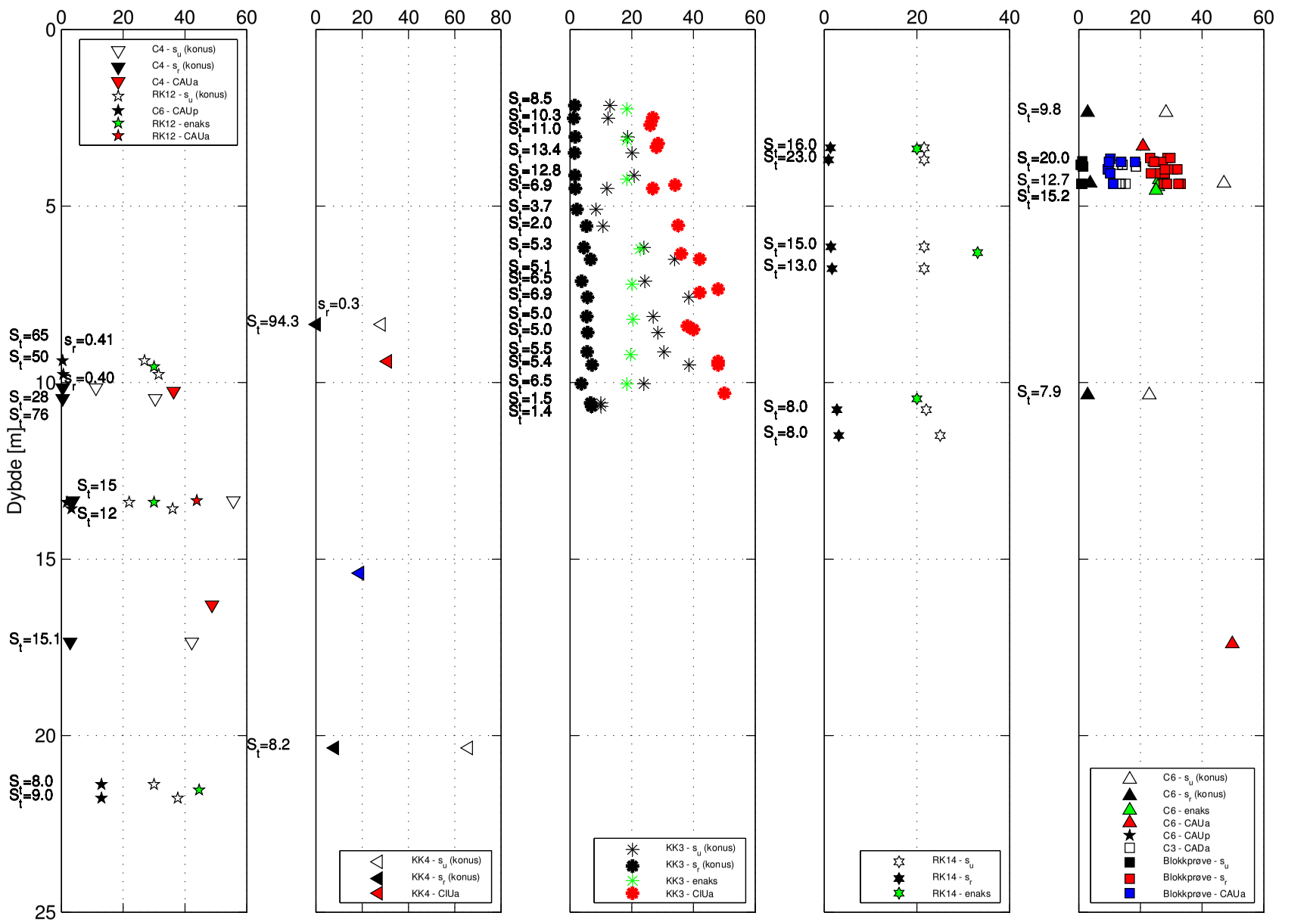

Borpunkt C4/RK12
Prøvetype: 54/72 mm
Kote: +21.9m

Borpunkt C5
Prøvetype: 54 mm
Kote: +12.69m

Borpunkt KK3
Prøvetype: 54 mm
Kote: +3.5m

Borpunkt RK14
Prøvetype: 72 mm
Kote: +2.7m

Borpunkt C6 m/blokkprøve
Prøvetype: 54/250 mm
Kote: +1.89m

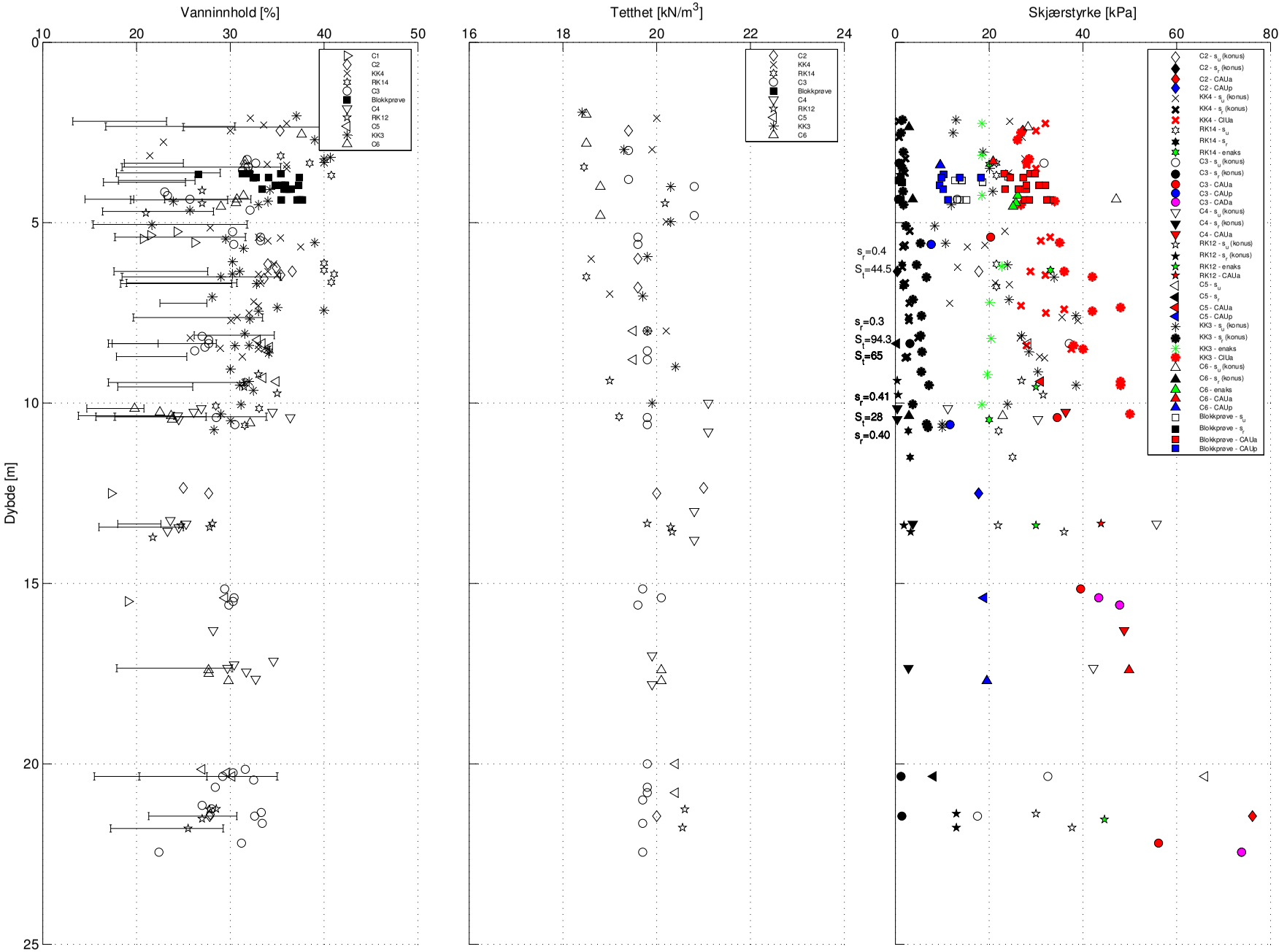

Borhull C1	Borhull C2	Borhull KK4	Borhull RK14	Borhull C3 m/blokkprøve	Borhull C4/RK12	Borhull C5	Borhull KK3	Borhull C6
Prøvetype: 54 mm	Prøvetype: 54 mm	Prøvetype: 73 mm	Prøvetype: 72 mm	Prøvetype: 54/250 mm	Prøvetype: 54/72 mm	Prøvetype: 54 mm	Prøvetype: 54 mm	Prøvetype: 54 mm
Kote: +25.14m	Kote: +9.1m	Kote: +3.5m	Kote: +2.7m	Kote: +2.2m	Kote: +21.9m	Kote: +12.69m	Kote: +3.5m	Kote: +1.89m